Condition Assessment of Concrete Bridge Girders Using Modal Testing – A Preliminary Study

By

NIRAJKUMAR N. CHALISHAJAR

October 2009

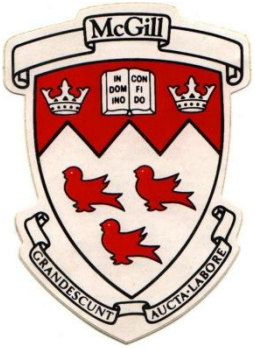

Department of Civil Engineering and Applied Mechanics

McGill University

Montreal, Quebec, Canada

A Thesis submitted to the Department of Civil Engineering and Applied Mechanics in partial fulfillment of the requirements for the degree of Master of Engineering

Abstract

This thesis deals with vibration frequency evaluation using non-destructive modal testing of beam-type structures. The current state of Canada`s bridges is reviewed for its present condition and urgent needs. The basic modes of deterioration in concrete bridges, namely, corrosion of reinforcing steel and freezing and thawing cycles were also reviewed. Bridge inspection fundamentals are discussed summarily. In addition, a summary of the available research on modal testing is presented.

Five reinforced concrete beams were tested in this preliminary research program to study the effect of progressive cracking at increasing load levels on the changes in their natural frequencies. Analysis of the results shows that the natural frequency is related to the changes in the structural stiffness of the beam, and the level of damage. The results from this preliminary investigation show that vibration testing is a useful tool for studying the existing health of a structural system.

Sommaire

L'auteur présente une étude préliminaire de la faisabilité d'utiliser des techniques d'analyse modale dans les poutres en béton armé comme méthode non-destructive d'évaluation de leur résistance.

Un survol de l'état de détérioration des ponts au Canada permet d'abord d'établir les besoins les plus urgents. La thèse résume ensuite l'état des connaissances sur les modes de détérioration les plus communs dans les ponts en béton, soit la corrosion des aciers d'armature et les effets cycliques des conditions saisonnières de gel et dégel. Un résumé des étapes de base de l'inspection des ponts est également suivi d'une revue sommaire de la recherche sur les méthodes d'analyse modale.

L'aspect expérimental de la recherche comprend des tests de mesures modales sur cinq spécimens de poutres en béton armé afin d'évaluer les variations de la fréquence naturelles des spécimens en fonction de leur état de fissuration induite par des surcharges. L'analyse des résultats indique clairement que la fréquence naturelle est réduite par les changements de rigidité des poutres selon le niveau d'endommagement. Les résultats de cette étude préliminaire indiquent que les méthodes vibrationnelles sont utiles pour évaluer la condition structurale des composants.

ACKNOWLEDGEMENT

The author would like express his deep sense of sincere and profound gratitude to his supervisor Professor M. S. Mirza, Professor Emeritus, Department of Civil Engineering Mechanics, McGill University, Canada for his excellent guidance, constant encouragement throughout the research program, resulting in the development and publication of this work. Despite of his busy schedule, he has taken enough pain to conduct stimulating discussions of several basic concepts and to sharpen the ideas and results of this thesis. The constant encouragement, moral support and inspiration he offered were fundamental to the completion of the research program.

The author is extremely grateful to Dr. William Cook for his invaluable assistance and guidance with the operation of testing equipment and software in the Jamieson Structural Laboratory during the testing.

The author acknowledges his thanks to Messrs Ronald Sheppard and Marek Przykorski for their technical help in preparing and testing the specimens.

The author would like to take opportunity to thank Professor D. Mitchell, Past Chair of the Department of Civil Engineering and Applied Mechanics, for providing concrete for the casting for the test specimens.

The author would like to sincerely thank Professor G. McClure for French translation of the abstract.

The financial assistance through a Research Assistantship, and McGill Principal's Graduation Fellowship were very helpful to complete this M.Eng. program. These are gratefully acknowledged.

Finally, the author would like to express his love and appreciation to his beloved parents, Niranjanaben and Navinchandra Chalishajar, elder brother Dimplekumar Chalishajar, and little son, Ayush, who were the great sources of strength during this time. He would like to thank to his wife, Kinnary, without whose understanding and support this thesis would not be possible. Their wholehearted blessing, love, moral support and patience were the inspiration and determination to perform and to succeed in life.

Table of Contents

1. Introduction 1
   1.1 Overview 1
   1.2 Classification of damage and damage identification methods 4
   1.3 Terminology 5
   1.4 Objectives 6
   1.5 Outline 7
2. Bridges and Canada 9
   2.1 Introduction 9
   2.2 Aging of Canadian infrastructures 9
   2.3 Average age of Canadian bridges 13
   2.4 Government Investment 15
   2.5 FCM Survey 18
   2.6 Investment Trend 19
   2.7 Importance of Maintenance 20
3. Deterioration Modes in Concrete Bridges 22
   3.1 Introduction 22
   3.2 Freezing and thawing cyclic attack 26
      3.2.1 Mechanism 27
      3.2.2 Effect of de-icing salt 29
      3.2.3 Effect of coarse aggregates 31
      3.2.4 Factors influences frost resistance 32
   3.3 Reinforcement corrosion 36
      3.3.1 Passivation 36
      3.3.2 Corrosion of reinforcement 37
      3.3.4 Effect/ consequences of corrosion 41
      3.3.5 Types of corrosion 42
   3.4 Concrete defects 53
      3.4.1 Scaling 53
      3.4.2 Delamination 55
      3.4.3 Spalling 57
      3.4.4 Cracking 58
4. Bridge Inspection 63
   4.1 Importance and need for bridge inspection 63
   4.2 Related documents 64
   4.3 Non-destructive testing (NDT) 65

4.4 Fundamental aspects of bridge inspection 68
4.5 Areas to be inspected 78
5. Modal Testing 82
5.1 Introduction 82
5.2 Type of modal test 87
5.2.1 Forced vibration tests (FVT) 87
5.2.2 Ambient vibration test (AVT) 89
5.3 Effect of structural damage on natural frequency 91
5.4 Factors affecting the natural frequency for damage detection 94
5.5 Suggested guidelines 95
5.6 Application 96
5.7 Advantages 97
5.8 Limitations 97
5.9 Comparisons with other wave-based NDT methods 98
6. Literature Review – Modal Testing 101
7. Experimental Work 124
7.1 Introduction 124
7.2 Description of test beams 124
7.3 Test set-up and instrumentation 126
7.3.1 Load test 126
7.3.2 Frequency measurement 129
7.4 Instrumentation 129
7.5 Problem faced and modification made during the experiment 130
7.6 Test results and discussion 132
7.7 Summary and discussion of results 161
8. Summary and Conclusions 165
References 169
Appendix A 185
Design of Beam 185
Appendix B 190
Cracking and Ultimate Load 190
Appendix C 196
Frequency Calculations 196
Appendix D 198

Photographs – Cracking Pattern..... 198
Appendix E 224
Experimental Frequencies..... 224

List of Figures

Figure 2.1 Average infrastructure age 10
Figure 2.2 Age by asset types 11
Figure 2.3 Distribution of time of new transportation infrastructure construction 12
Figure 2.4 Average age of bridges by province, 2007 14
Figure 2.5 Average age of bridges as a percent of useful life by province, 2007 14
Figure 2.6 Average age of brides at different level of government 15
Figure 2.7 Investment in transportation by all level of government 16
Figure 2.8 Investment in roads and bridges by all level of government 17
Figure 2.9 Average breakdown of investment between new construction and renovations, 1992-1997, by level of government 19
Figure 2.10 Qualitative deterioration – time relationship for different levels of maintenance 21
Figure 2.11 de Sitter's time deterioration curve 21
Figure 3.1 Factors affecting on bridges during their service life 23
Figure 3.2 Causes of deterioration of reinforced-concrete structures 25
Figure 3.3 Cause of spalling 26
Figure 3.4 Depression of freezing point due to surface energy 27
Figure 3.5 Pore size distribution 28
Figure 3.6 Distribution of tensile strain in concrete experiencing thermal shock at the surface due to the effects of chlorides 30
Figure 3.7 Scaling due to variation in the timing of freezing of layers:
(a) intermediate layer is initially frozen; 31
(b) outer layer freezes later, causing scaling 31
Figure 3.8 Pop-out due to non-frost resistant aggregates 32
Figure 3.9 Effect of w/c ratio on relative weight loss during a severe frost attack 35
Figure 3.10 (a) Anodic and cathodic reaction as the corrosion of steel in concrete 38
(b) Volumetric expansion as a result of oxidation of metallic iron 38
Figure 3.10 (c) Expansive corrosion products on steel in chloride contaminated concrete 39
Figure 3.11 Schematic representation of corrosion rate of steel in different concretes and exposure conditions 40

Figure 3.12 Structural consequences of corrosion in reinforced concrete structures 41
Figure 3.13 Ingress of the carbonated zone to the reinforcement 43
Figure 3.14 Rate of carbonation 44
Figure 3.15 The critical chloride content according to CEB recommendations 49
Figure 3.16 Schematic of the D_{app} for chloride as a function of time and type of cement for Portland cement, 30% fly ash (PFA) and 70% ground granulated blast furnace slag (GGBS) exposed to a marine environment 51
Figure 3.17 Types of scaling 54
Figure 4.1 Special lifting equipments 74
Figure 4.2 (a) Scuba diving for under water inspection, 75
(b) Underwater photography 76
Figure 5.1 Detection procedure 86
Figure 5.2 Different types of forced excitation methods 88
Figure 6.1 Model plate-girder bridge 108
Figure 6.2 Top view, cross-section, elevation of Z24 110
Figure 6.3 Alamosa Canyon Bridge 111
Figure 6.4 Schematic of plate-girder test bridge 112
Figure 6.5 (a) Accelerometers mounted on a U.S. Grant cable stay 113
(b) The partially completed U.S. Grant Bridge 113
Figure 6.6 (a) Side view of Romeo Bridge 114
(b) Maximum settlement of 59.2 cm at the northern abutment during the first damage scenario 115
Figure 6.7 Millennium Bridge, London 116
Figure 6.8 Aerial view of I–80 Fly over Bridge 117
Figure 6.9 I-215 Curved Girder Bridge 118
Figure 6.10 Holway Road Bridge 119
Figure 6.11 5th South viaduct, Salt Lake City 120
Figure 6.12 Roebling suspension bridge 121
Figure 6.13 Alfred Zampa Memorial Bridge 122
Figure 7.1 Geometry and cross-section of test beam 125
Figure 7.2 Schematic diagram for test set-up 128
Figure 7.3 Schematic diagram for instrumentation 130

Figure 7.4 Load – frequency curve for test beam 1 134
Figure 7.5 Load – steel strain curve for test beam 1 135

Figrue 7.6 Load – mid-span deflection curve for beam 2 139
Figure 7.7 Load – steel strain curves for beam – 2 140
Figure 7.8 Load – frequency relationships for beam 2 141
Figure 7.9 Load – steel strain curves for beam 3 146
Figure 7.10 Load – frequency relationships for beam 3 147
Figure 7.11 load – mid-span deflection curve for beam 3 148
Figure 7.12 Load-mid-span deflection curve for beam – 4 152
Figure 7.13 Load-frequency relationships for beam – 4 153
Figure 7.14 Load- mid-span deflection curve for beam – 5 157
Figure 7.15 Load-steel stain curves for beam 158
Figure 7.16 Load-frequency relationships for beam 5 159

List of Tables

Table 2.1 Bridges in different provinces and territories in Canada 12

Table 2.2 Federal investment 17

Table 2.3 Provinces/Territorial/Local investment 18

Table 3.1 Exposure classes with recommendation for freeze-thaw attack with or without de-icing agents 34

Table 3.2 Variation of air content with aggregate size 36

Table 3.3 Threshold chloride content values reported by various codes/researchers 48

Table 3.4 Concrete deterioration with time 61

Table 4.1 Summary of nondestructive testing methods for evaluating bridge conditions 79

Table 7.1 Test results for beam 1 133

Table 7.2 Percentage decrease in natural frequency and stiffness at each loading stage for beam 1 134

Table 7.3 Test result for beam 2 138

Table 7.4 Percentage decrease in natural frequency and stiffness at each loading stage for beam 2 139

Table 7.5 Test result for beam 3 144

Table 7.6 Percentage decrease in natural frequency and stiffness at each loading stage for beam 3 145

Table 7.7 Test result for beam 4 151

Table 7.8 Percentage decrease in natural frequency and stiffness at each loading stage for beam 4 152

Table 7.9 Test result for beam 5 156

Table 7.10 Percentage decrease in natural frequency and stiffness at each loading stage for beam 5 157

Table 7.11 summary of decrease in frequency with increase in damage in five beams 162

Table 7.12 Summary evaluation of stiffness for beams with applied load removed; under self-weight of beam only 164

1. Introduction

1.1 Overview

Bridges enable movement of people and goods, and form a "life line" for society's economy. Majority of the bridges in Canada were constructed between 1950 and mid 1972s. Bridges are often subjected to severe loading conditions, harsh environmental conditions and even natural disasters. This results in deterioration of the bridge structures with time. A considerable percentage of bridges in Canada and the United States are structurally or functionally deficient mostly due to deferred maintenance. This reduces the safety, serviceability and service life resulting in increased risk of injuries and fatalities, besides considerably higher maintenance, repair and rehabilitation costs. Several national codes and standard have introduced the concept of a minimum service life. However, design for durability is still based on "deem-to-satisfy rules". Some limiting values are specified for concrete grade, cement content, water/cement ratio, air content, concrete cover thickness, and structural crack width. There is no provision in current design standard to consider this type of time-dependent loading, which results in increasing the rate of deterioration which leads to loss of functional and structural damage before reaching the expected useful life. (According to current Canadian Highway Bridge Design Code (CSA S6-2006), bridges are designed for expected minimum service life of 75 years.) In practice, several bridges suffer a significant level of deterioration when they reach about half of their life span and need strengthening, rehabilitation, or replacement, using the limited maintenance budgets.

To overcome this situation, presently four basic design options are available to the structural engineer to ensure satisfactory performance of the structure throughout the expected service life; this can be achieved by providing adequate load-bearing structure, incorporating redundancy in the basic structure, by making provision for sacrificial defensive mechanisms in the structure, and by installing appropriate monitoring systems to provide warning about changes in the structural condition caused by the various forms of deterioration over time (Armer 1988). Out of these four options, the last one is related principally to the assessment of present state of the structure and prediction of the residual service life. Monitoring of bridges is useful not only to the owner/user, but also to the designer/engineer. It can lead to savings in maintenance costs and provides more options for repair and rehabilitation since several defects can be detected at an earlier stage of damage. Goltermann et al. (2002) demonstrated reduction in maintenance or repair cost by about 25 – 40% through permanent health monitoring of bridges subjected to chloride-induced corrosion. Monitoring of existing old structure can also help with determination of the balance of the service life of the structure before it needs costly rehabilitation. It provides useful information to the designer for improving future design procedures. Thus, continuous monitoring and proper assessment of bridges can help bridge owners and engineers to determine the risk involved at different stages of the service life, and to plan the required maintenance and rehabilitation program to keep the structures in a functional condition until the end of the expected life span with minimum cost for routine maintenance.

After collapse of Silver Bridge in 1967, the National Bridge Inspection Standards (NBIS) require inspecting the bridges every two years. The 1992 ISTEA (International Surface Transportation Efficiency Act) mandates the use of a quantitative computerized bridge management system by 1996 (Prine 1995). This needs quantitative bridge inspection methods that help to detect the defect at early stage of deterioration so that timely decision can be taken before the damage worsens considerably, requiring costly rehabilitation. In Canada and U.S., presently visual inspection is used most commonly for evaluation of condition of bridges. In special cases, local NDT is adopted for health monitoring. However, visual inspection has some limitations which lead to wrong condition assessment. Federal Highway Administration reported that over 56% of bridges in U.S. inspected through visual-based inspections were not correct, whatever was the factor: inspector's experience, or bridge type and condition (Phares, 2001). Local NDE methods require knowing the location of the damage in advance (Chapter 4). It requires more advanced NDT techniques for detailed damage identification. Therefore, there is a strong need to develop advanced diagnostic methods (rational and scientific methodologies) for more precise bridge inspection and evaluation of bridges. Modal testing, the vibration based identification test method, has the possibility to overcome this limitations. It does not need to know the location of damage in advance. Sensors not need be placed in vicinity of the damage locating; also, a limited numbers of sensors are often sufficient to detect, locate and quantify the damage.

1.2 Classification of damage and damage identification methods

The effects of damage on the structure can be linear or non-linear. In linear damage conditions, the structure that responded in a linear-elastic fashion initially behaves in linear elastic after introduction of damage. The modal properties of a structure alter with the changes in the shape and overall condition of the structures and material properties, and the overall structural response can be determined by solving linear equation of motion. The scenario is different in the nonlinear case. The structure, that responds in a linear-elastic fashion initially, responds in a non-linear manner after occurrence of the damage. The example of non-linear damage includes formation of fatigue cracks, loose connection that rattle and others.

Rytter (1993) has classified four stages for non-destructive evaluation of damage in the structure:

Level 1: Damage detection – Determination of present of damage in the structure

Level 2: Damage localization – Level 1 plus determination of the location of the damage

Level 3: Damage Quantification – Level 2 plus quantification of the severity of damage

Level 4: Residual service life – Level 3 plus evaluation of impact of the damage in the structure, along with estimation of the remaining service life of the structure

1.3 Terminology

The following basic terminology is used throughout the thesis.

Damage/deterioration: Any changes introduced in the structure that adversely affect the normal mechanical, physical and chemical properties of the concrete, and affect the current or future performance of the structure.

Maintenance: Work needed to preserve the required load carrying capacity of the bridge and also for safety of people using the bridges, or passing under them.

Repair implies keeping the structure in good shape, or in proper working condition. It is concerned mainly with local damages to the structural members or equipments rather than the complete structure.

Rehabilitation refers to repair work considerable larger and costlier than the routine maintenance work, required basically to bring the bridge structure to its original service condition. It is concerned principally with the entire bridge structure.

Replacement refers to reconstruction of complete structure, or a major part of it, since the costs and/or extent of repairs can be well beyond the acceptable rehabilitation costs and/or technical limits; it is normally costlier to repair/rehabilitate such a structure and it is simpler and less costly to replace the structure.

Bridge failures: the complete structure, or a major component, fails to perform its intended function for which it is originally constructed.

Structurally deficient bridges include those structures whose main load-carrying elements are in poor or unacceptable condition due to deterioration or damage.

Functionally deficient bridge includes those whose geometry does not match the current standard/code geometry requirements e.g. shoulder width, number of bridge lanes, clearance to vehicle, trains, ships, etc. It is generally the result of changing traffic demands and changes in the design and operating standards. It also includes the case of insufficiency of waterway opening, causing unacceptable disturbance.

1.4 Objectives

The thesis examines the age, present condition and the available maintenance funding along with the principal modes of deterioration in concrete bridges. The importance and the need for inspection using non-destructive testing and specific needs in a structure are reviewed summarily. A brief state-of-the-art of modal testing is also presented.

The main objective of this work was to study the more advanced non-destructive test techniques for condition assessment of large beam type civil engineering structures, such as bridges. The preliminary tests were conducted as a combination of static and dynamic tests to study the effect of cumulative damage on modal parameters, particularly the natural frequency and to check the practicality of implementation of modal testing in the field for large scale structures.

1.5 Outline

The thesis is divided mainly into three parts: the state of the art report, literature review and the experimental work. The different chapters in this thesis mainly deal with following.

- **Chapter 2** discusses the state of Canada's bridges. It focuses mainly on their aging, and the useful life of bridges, along with the investments by different level of governments, to upgrade the transportation infrastructure to a minimum acceptable level, current investment trends, and the importance of timely maintenance or defer maintenance.
- **Chapter 3** outlines the common concrete defects which occur in concrete bridges and the related causes, including environmental and other related conditions.
- **Chapter 4** deals with bridge inspection, with a brief review of the guidelines. It summarizes the fundamental aspects of bridge inspection and the importance of non-destructive testing techniques.
- **Chapter 5** reviews the basics of modal testing. It deals with basic theory, types of vibration tests, effect of damage on modal parameters – natural frequency, factors affecting modal parameters, applications, advantages and limitations of frequency-based vibration testing for detection of damage.

- **Chapter 6** summarizes a case study on modal testing. It reviews existing literature summarily, and focuses mainly on the case studies of large scale of structures.
- **Chapter 7** presents the experimental work conducted. It deals primarily with modal testing, and its applicability in field.
- **Chapter 8** summarized the thesis along with some conclusions.
- **Appendices A to D** summarize calculations related to the beam design, frequency evaluation, cracking and ultimate load, and stiffness evaluation.
- **Appendices E and F** present photographs showing the severity of damage induced by static loading, along with the relevant experimental frequency charts.

2. Bridges and Canada

2.1 Introduction

Canadian infrastructure assets are deteriorating at accelerating rate. In recent years, the condition of Canada's infrastructure has become a major issue for both governments and the public. Dickson Bridge, Montreal was decommissioned just after useful life of only 34 years. In 2000 an overpass over Souvenir Boulevard in Laval, Quebec collapsed during construction resulting in one death and two injuries. Just after six years de La Concorde overpass collapsed in Laval, after a useful service life of 34 years, killing five persons, including one pregnant woman and also caused serious injuries of six individuals.

2.2 Aging of Canadian infrastructures

In 2003, the Civil Infrastructure System Technology Road Map (CIS-TRM) noted that 31% of Canadian infrastructures were between the ages of 40 to 80 years while another 28% of Canada's infrastructures were more than 80 years old. Miller (2004) reported that Canada's half of the civil infrastructures including roads and bridges will reach the end of their useful service life in less than 20 years. Gagnon, M. et al. (2008) studied the aging of roads and highways, sewer systems, wastewater treatment facilities, water supply systems, and bridges owned by governments over the past 45 years, from 1962 to 2007. The study revealed that Canada's infrastructure is aging and the average age of infrastructure increased substantially between 1973 and 1999. Their average age remained stable until 2002, and then started declining since 2003 (Figure 2.1).

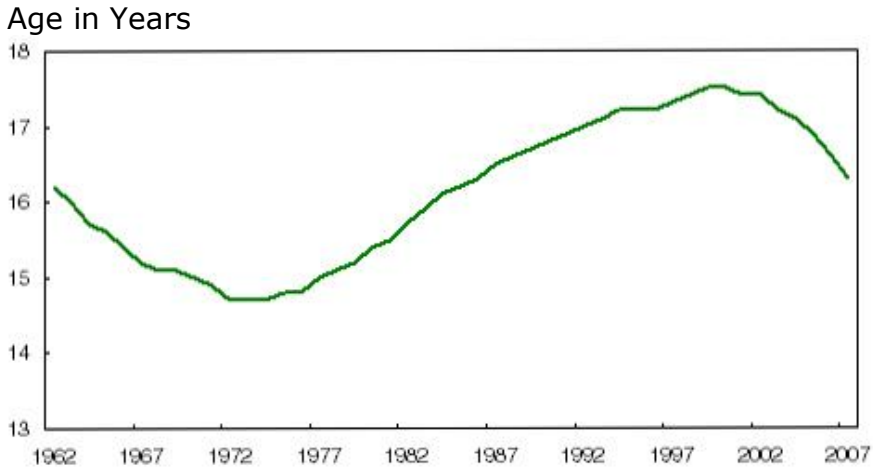

Figure 2.1 Average infrastructure age (Infrastructure Canada 2008)

According to "The Daily" February 13, 2008, the average age of Canada's public infrastructures has dropped to 16.3 years in 2007 from its peak of 17.5 in 2000. But, this reduction in the average age is a result of investment made in the construction of new infrastructures facilities. It does not mean that each physical asset is younger, or in a better condition, or it meets the current standards. Figure 2.2 demonstrate the average age of each infrastructure service.

The average age seem to be confusing with current condition of infrastructures. At first, it appears that Canada's infrastructure is younger, but it is important to note that in this study, the average age has not been defined in technical term and is not the actual age of the infrastructure. It is defined by economists and for analytical purpose they have used a complex formula to estimate the age of public assets. The key factor used in estimating the average age is **the amount of investment** in public infrastructure. The other variables used are the survival function, the year of investment, and gross capital stock at the end of year. Thus, it shows that the amount of investment made in infrastructure rather than its

actual age. For example, average age of Prince-Edward Island bridges decreased from 21.6 to 6.5 years between 1993 and 1996 due to construction of Confederation Bridge, costing 1.0 billion Canadian dollars.

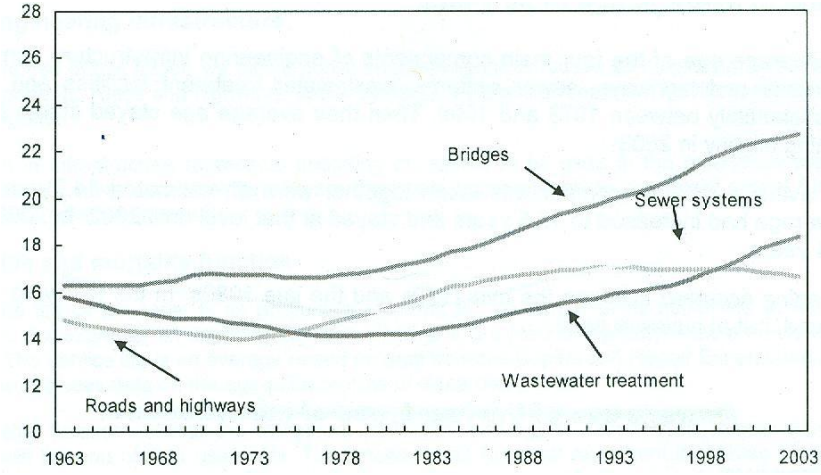

Figure 2.2 Age by Asset types (Gaudreault et al, 2006)

All levels of government (federal, provincial, and municipal) have made significant amounts of investment over the years. The gross stock in bridge amounted to $23.93 billion in 2007 and represented about 8% of the total public assets owned by the federal, provincial, territorial, regional and municipal governments in 2007. Table-2.1 describes the bridge stock and their condition assessment rating system used by concerned agency at different Provinces and Territories in Canada.

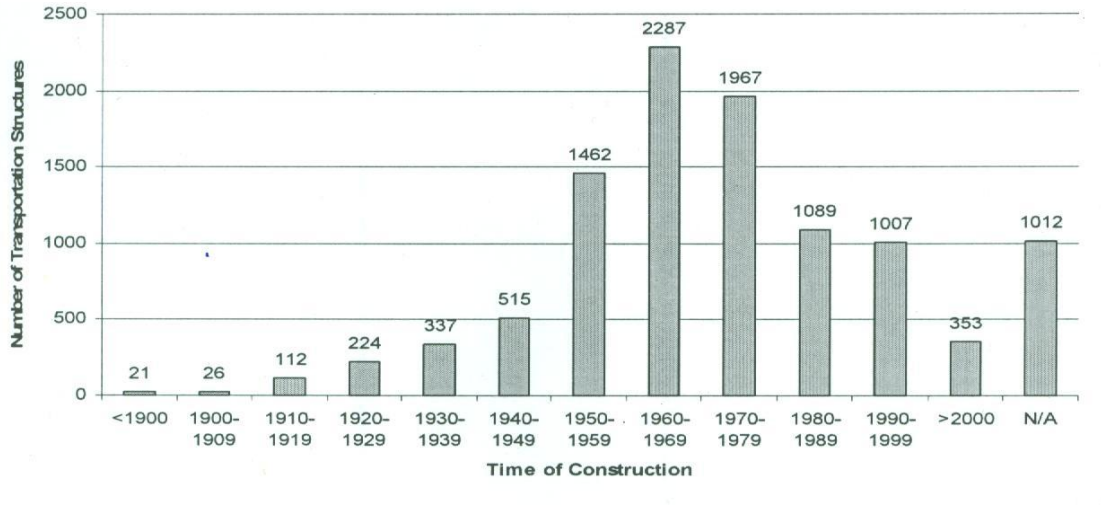

Figure 2.3 Distribution of time of new transportation infrastructure construction (Hammad et al., 2007)

Table 2.1 Bridges in different Provinces and Territories in Canada (Hammad et al., 2007)

Province	**No. of Bridges P: Provincial M: Municipal**	**Condition Rating system**	**Distribution by Material Type**	**Agency Responsible of BMS**
Alberta	9,800 (M) 4,100 (P)	9	N.A.	Department of Infrastructure and Transportation
British Columbia	20,000	5	N.A.	Ministry of Transportation
Manitoba	1200 (P)	5	N.A.	Department of Infrastructure and Transportation
New Brunswick	N.A.	N.A.	N.A.	Department of Transportation
Newfoundland and Labrador	N.A.	N.A.	N.A.	Department of Transportation
Nova Scotia	4000 (P)	4	Timber: 60% Concrete: 20% Steel: 20%	Department of Transportation and Public Works
Ontario	3000 (P)	4	N.A.	Ministry of Transportation
Quebec	4300 (P) 4400 (M)	5	Timber: 0.3% Concrete: 75.8% Steel: 16.7% Other: 7.2%	Ministry of Transportation
Saskatchewan	820 (P) 2200 (M)	4	N.A.	Department of Highway and Transportation
Prince Edward Island	200	4	Timber: 50% Concrete: 25% Steel: 25%	Department of Transportation and Public works

2.3 Average age of Canadian bridges

Most bridges across Canada were built between 1950's and 1970's (Figure 3.3). Over 40% of the bridges across Canada are over 50 years old (Bisby et al., 2004) and a significant percentage of them are structurally or functionally deficient. They are considered deficient by the present standards mainly due to aging increased traffic loads, deterioration and more stringent bridge design codes (Daniel et al., 2008). According to the current standards, bridges are designed for the minimum expected service life of 75 years with only routine maintenance. But, the effective durability and lifespan of bridges is continuously decreasing as a result of aging, climate changes, defects, deterioration and damage. This affects safety, serviceability and functionality of bridges. Consequently, many bridges require extensive and expensive rehabilitation only after service life of 20-30 years. In Canada, about 40% of the bridges are over 40 years old with rehabilitation costs estimated at $10 billion (Lounis 1999). It is estimated that one-third to one-half of the projected rehabilitation costs in North America are allocated for rehabilitation of bridge deck deterioration (Lounis et al., 1999, and Lounis 2007).

Based on the level of investment, the investment year, the survival function, and the year-end gross capital stock, the average age of bridges and overpasses was noted to increase by 3.2 years from 21.3 in 1985 to 24.5 in 2007. Between 2001 and 2007, the average age of the bridges increased by 0.8 years, because the gross stock grew by only 0.4% a year on average. Figure 2.4 present the average age of bridges by province.

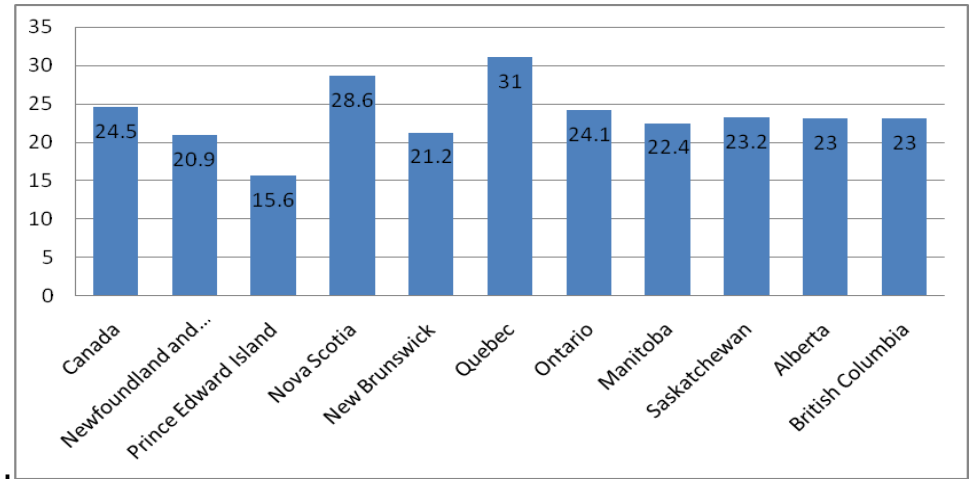

Figure 2.4 Average age of bridges by province, 2007
(Statistics Canada 2008)

Bridges in Canada have a mean service life of 43.3 years, which implies that Canada's bridges have passed 57% of their useful life. Figure 2.5 illustrates the useful life of bridges by different provinces in 2007. By 2007, bridges and overpasses in Quebec had passed 72% of their useful life, the highest ratio in Canada, compared with 57% nationally. Between 2001 and 2007, the gross capital stock for bridges in Quebec declined 1.3% a year on average, compared with a 0.4% gain nationally.

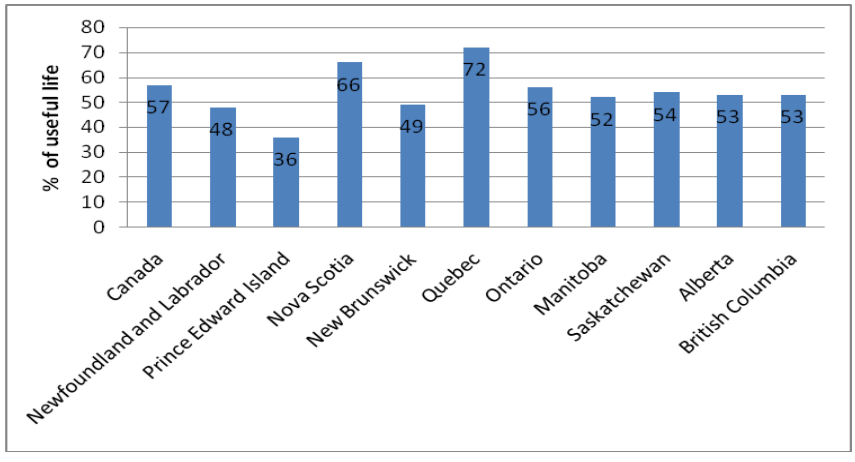

Figure 2.5 Average age of bridges as a percent of useful life by province, 2007
(Statistics Canada 2008)

Figure 2.6 shows the average age of bridges owned by the different level of governments; it demonstrates that provincial bridges were primarily responsible for the aging of the total bridge stock. In 2003, federal bridges accounted for only 3% of the total stock, and had passed 57% of useful life and were 26.4 years old, while the provincial bridges had passed 53% of useful life. The municipal bridges were comparatively younger. They were 19 years old, and had passed only 41% of their useful life and made up 39% of bridge infrastructure stock in 2003 (The Daily, January 30, 2006). It does not necessarily imply that each physical asset is younger, or in a better condition, or that a greater proportion of assets meets the specific quality standards.

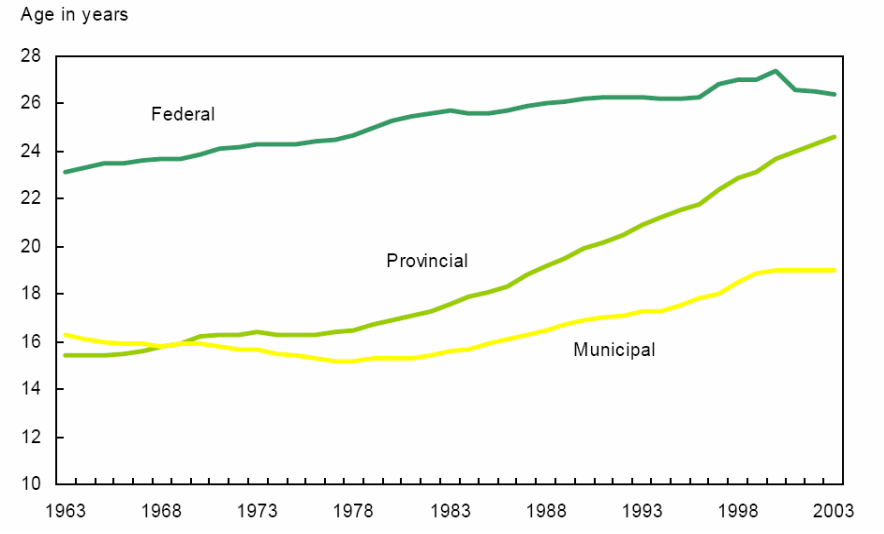

Figure 2.6 Average age of bridges at different level of government (Gaudreault et al, 2006)

2.4 Government Investment

The 2006 Annual Report of Transportation in Canada reviews the government spending on transportation, which includes air, marine, rail, road and bridges, transit and others. Up to 2000-01, the average total gross transportation

investment by all levels of government was around $18 billion. This investment increased to $24.2 billion in the fiscal year 2005-06, which is about 26% higher than the 2002-03 investment of about $19.1 billion. Figure 2.7 shows the investments made by all level of government from 1996-97 to 2005-06.

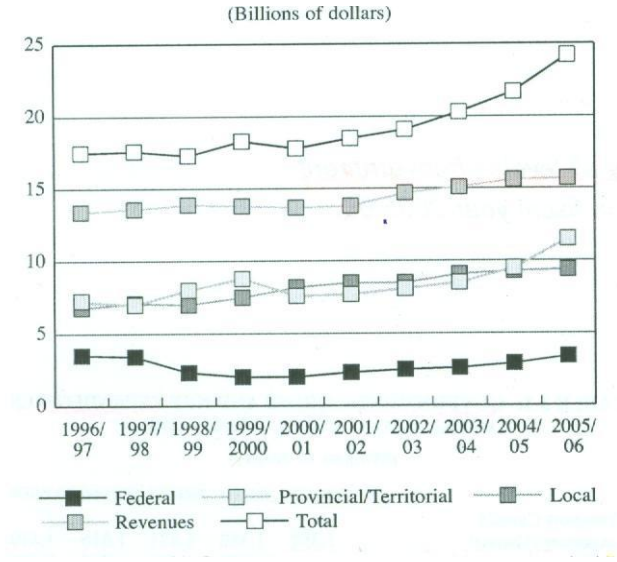

Figure 2.7 Investment in transportation by all level of government
(Transportation in Canada, 2006 Annual Report)

For the period 1996-97 to 2005-06, the investment by local government increased every year except for a slight decline in 1998-99. The provincial/territorial investment fell to $7.6 billion in 2000-01 from previous year's $8.8 billion, before reaching a peak of about $12 billion in 2005-06. The contribution of the Federal Government is comparatively low compared with the local and provincial investment. The federal investment increased steadily to $3.4 billion in 2005-06 and then fell to $2.0 billion in 1999-2000 and 2000-01 from $3.5 billion in 1996-97. From 2002-03 to 2005-06 local, provincial and federal government raised their contribution by 0.3%, or $31.8 million, 21.2% or $2.0 billion and 15.0% or $442.1 million to $ 3.4 billion, respectively. The federal operating, maintenance

and capital investment towards roads and bridges fell to $147 million in 2003-04 from $193 million in 2002-03 and then steadily increased to $184 million in 2006-07. Against the net investment of $24.2 billion in transportation by all level of government in year 2005-06, $17.5 billion was spent towards roads and bridges. This is just about 35% of the actual need of $50.2 billion, according to FCM survey (FCM 2007).

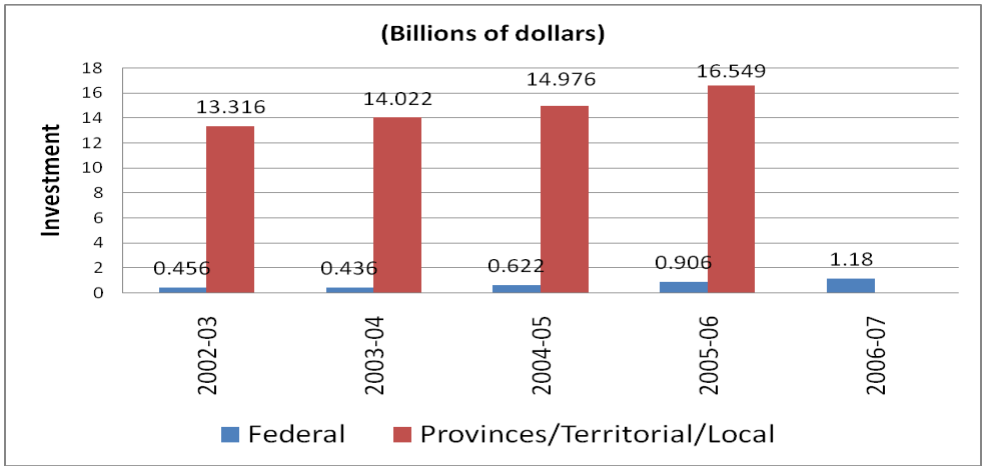

Figure 2.8 Investment in roads and bridges by all level of government.
(Data adapted from Transportation in Canada, 2006 Annual Report)

Table 2.2 Federal investment (Millions of dollars)
(Data adapted from Transportation in Canada, 2006 Annual Report)

	2002-03	2003-04	2004-05	2005-06	2006-07
Roads and Bridges	456	436	622	906	1180
Total Investment	2516	2640	2940	3382	3543

Table 2.3 Provinces/Territorial/Local investment (Billions of dollars)
(Data adapted from Transportation in Canada, 2006 Annual Report)

	2002-03	2003-04	2004-05	2005-06	2006-07
Roads and Bridges	13.3	14.0	15.0	16.6	N/A
Total Investment	16.6	17.6	18.8	20.8	N/A

Figure 2.8 demonstrate the investment by different level of governments towards roads and bridges. It reveals that federal contribution is increasing towards roads and bridges but it is still only a small part compared to provincial and local government contributions. Table 2.2 and 2.3 present the investment by different level of governments compared to total investment in transportation.

2.5 FCM Survey

In collaboration with McGill University, the Federation of Canadian Municipalities (FCM) undertook a survey of Canada's five type of municipal infrastructure: Water and wastewater systems, **transportation,** transit, waste disposal, and cultural, social, community and recreational facilities during the fall of 2007. The transportation infrastructure included paved roads, unpaved roads, sidewalks, curbs, bicycle paths, **bridges**, **overpasses**, and road cleaning and snow removal equipment and facilities. The aim of the survey was to determine the needs to maintain and upgrade the existing deteriorating assets and to evaluate the demand for new infrastructure facilities. The average cost to upgrade the transportation infrastructure facilities was forecast $11.4 billion in 1996 (FCM-McGill Survey 1996). The results of the 2007 survey estimated that $21.7 billion

is needed to maintain and upgrade the existing deteriorated transportation infrastructure, while another $28.5 billion is needed for new transportation infrastructure facilities.

2.6 Investment Trend

Recent data for investment trends in new construction, and maintenance and renovation are not available. However, data for the five year period, between 1992 to 1997 shows that major share of total investment goes to construction of new infrastructure compared to maintenance and renovation. Figure 2.9 shows that the average breakdown of investment between new construction and renovations, made by all level of government for 1992-1997 periods. This reveals the current wrong practice: “Design, Build and Forget” (Mirza 2007).

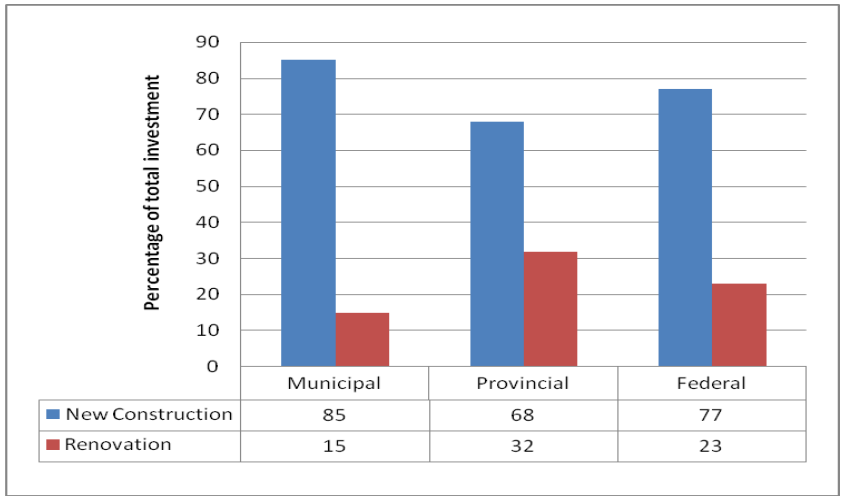

Figure 2.9 Average breakdown of investment between new construction and renovations, 1992-1997, by level of government (Adapted from Gaudreault et al., 2006)

2.7 Importance of Maintenance

A majority of transportation infrastructure assets, especially highways, roads, bridges and overpasses were constructed during the period from 1962 to the mid 1970's (Figure 2.6). From mid 1970's to 2003, the government investment in new infrastructure, as well as in maintenance, repair and rehabilitation of the existing deteriorating infrastructure decreased. Consequently, there is a continuing increase in the average age of bridge infrastructure (Figure 2.2) that results in an accelerated rate and extent of deterioration.

Figures 2.10 and 2.11 illustrate the important of a regular maintenance program by the deterioration-time curve. Mirza (2004) developed the qualitative performance versus time curve for four different level of maintenance: 0, 0.5, 1.0 and 2.0% (Figure 2.10). It can be noted that with increasing level of maintenance, the performance level of the service increases significantly along with the service life of the structure. In case of zero maintenance, the deterioration could reach beyond the repair or rehabilitate stage, and the structure may need costly replacement before reaching the anticipated service life.

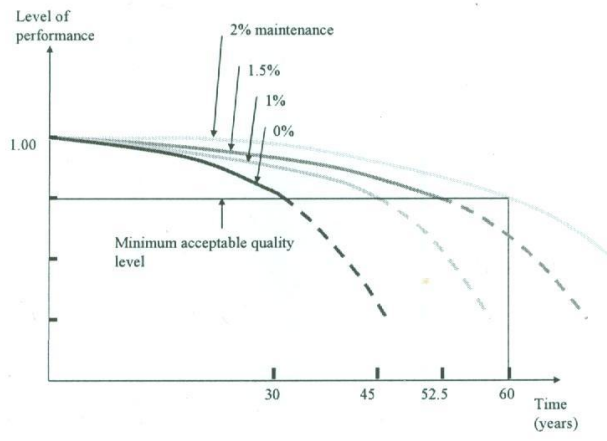

Figure 2.10 Qualitative deterioration – time relationship for different levels of maintenance (Mirza 2004)

In de Sitter's opinion (Figure 2.11), $1 spent in phase A for correctly designing and construction of structure is as effective as $5 spent in phase B, $25 in phase C or $125 in phase D. Excellent quality control during phase A (design and construction) and regular maintenance during phase B, where initiation of deterioration may occur, can prevent or significantly delay the starting of phase C, where increasing deterioration manifests. The costs involve in phase A and B are not significant compared with costs involved in phase C. The system would need major repair, or rehabilitation at considerably higher costs in phase C. In the absence of these actions, the system would enter phase D with a significantly accelerated deterioration rate. In some cases, it may be possible to salvage the structure and replace it by many times the original cost of the structure, along with the related socio-economic and environmental costs.

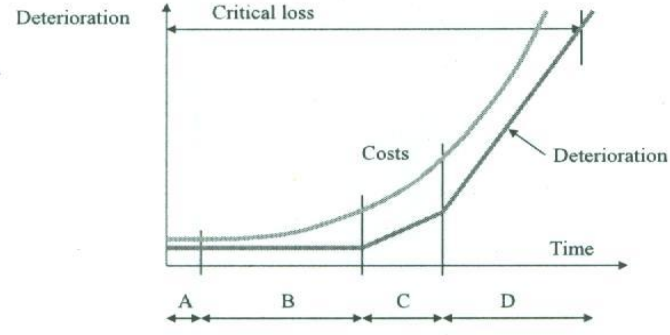

Phase A – Design and construction stage
Phase B – Initiation of deterioration
Phase C – Increasing deterioration
Phase D – Accelerated deterioration requiring replacement

Figure 2.11 de Sitter's deterioration-time curve (CEB 1992)

3. Deterioration Modes in Concrete Bridges

3.1 Introduction

Bridge structures are designed for a comparatively long service life (75 years in Canada). Therefore it is desirable to ascertain durability of materials to ensure a long service life for the structure with regular routine maintenance. Concrete is the most versatile, economical and durable material compared with several others in construction industry. Therefore, when concrete was first used as construction material in bridge construction in the early 20th century, it was generally assumed that it would be durable, requiring minimum maintenance. A sufficient amount of cement would prevent the concrete from damage. It was also assumed that everlasting protecting layer would prevent the embedded reinforcement from corrosion. But, since the 1980's, rapid deterioration of concrete bridges has become a serious and costly problem all over the world, including developed countries, such as the U.S.A., Canada, and the U.K. (Gaal et al. 2005). It has been observed that reinforced concrete bridges around the world are deteriorating at faster rate than originally predicted at the time of construction. A majority of the bridges have suffered from serious levels of deterioration when they reached only half of the service life (Ahlskog 1990).

According to the 2006 statistics, the Federal Highway Administration (FHWA) noted that about 12.6% of bridges, of the 607,363 bridges in U.S.A. were structurally deficient. From about 600,000 bridges, about 150 to 200 bridges could collapse partially or fully at any time (Gaal et al. 2005). It was estimated that more than $188 billion would be needed for repairing them (AOL India

News, 2007). In North America, more than 40% of highway bridges are found deteriorating (Hassanain 2003). Significant percentages of over 40% of bridges across Canada are structurally or functionally deficient and they need costly rehabilitation and replacement (Lounis 2007). It is estimated that about one third to one half of the total projected cost of rehabilitation are spent on rehabilitation of the bridge decks only (Lounis 2005 and 2007). In France, about 50% of more than about 20,000 bridges require repair. In Hungary, about 45% of main highway bridges and about 60% of secondary highway bridges need urgent repair. In Poland, about 50% of bridges are in service for more than 60 years and about 20% are structurally deficient and functionally obsolete.

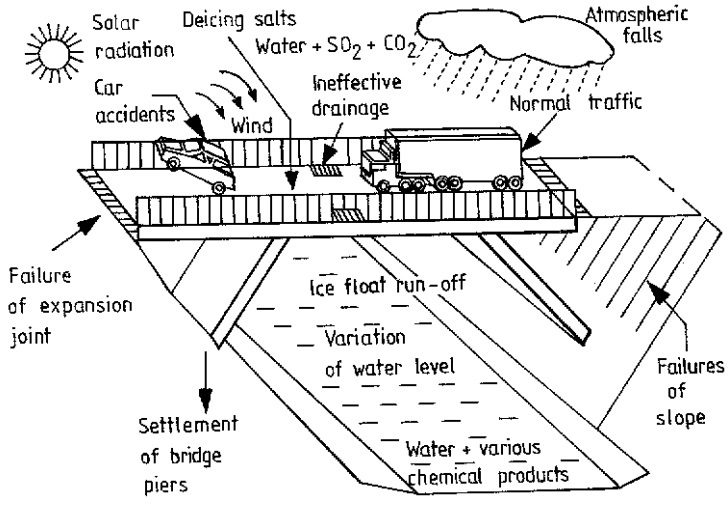

Figure 3.1 Factors affecting on Bridges during their service life (Radomski 2002)

Bridges are usually subjected to the worst exposure conditions during their service life, such as frequent wetting-drying cycles, temperature changes, freezing and thawing cycles, and increasing live load with time (Figure 3.1). It is commonly known that horizontal surfaces are more susceptible to deterioration

than the vertical faces; alternate wetting and drying cycle are more dangerous than continuously submerged condition; and freezing and thawing cycles constitute a more severe exposure condition than a constant freezing. According to the current standard, a minimum 75 mm thick concrete cover is needed to protect the structure against corrosion in marine environment. A majority of the bridges were constructed long ago and they do not satisfy the requirements of the current standards. However, the present code of practice has prescriptive provisions for durability.

There are various causes for degradation of concrete bridges. According to the 1988 TRB Report, the factors that affect the deterioration of concrete bridges include: "poor design details; construction deficiencies; lack of maintenance; temperature variation; chemical attack; reactive aggregates and high alkali cement; moisture absorption; wear and abrasion; shrinkage and flexure forces; collision damage; scour; shock waves; overstress; fire damage; foundation movement; and corrosion of steel reinforcement." Figure 3.2 shows some common causes of degradation of concrete bridges that lead to premature deterioration of bridge structures.

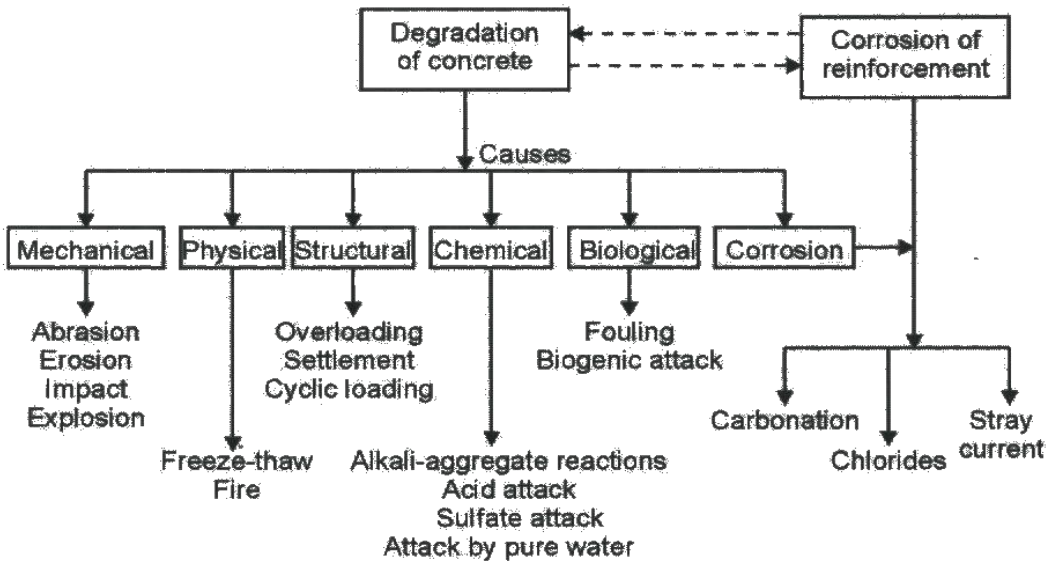

Figure 3.2 Causes of deterioration of reinforced-concrete structures
(Elsener et al., 2004)

The main manifestation of concrete bridge deterioration includes cracking, spalling, scaling, rust staining, surface disintegration (wear and abrasion), efflorescence, and exudation. Out of these scaling, delamination, spalling and cracking are the most common defects that can result in concrete bridges.

As mentioned before, there are several reasons for deterioration of concrete structure; however, the two main reasons that are accepted worldwide are corrosion of steel reinforcement, and freeze-thaw cyclic attack in cold regions. Therefore, only these two causes are discussed briefly here. Figure 3.3 demonstrates the percentage of various causes responsible for damage in concrete structures.

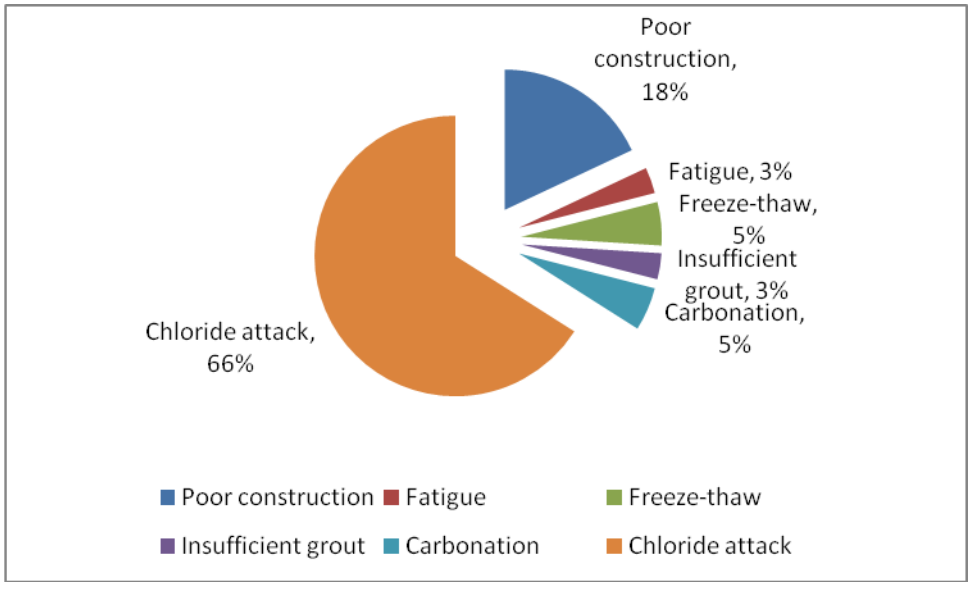

Figure 3.3 Cause of spalling (Gaal et al. 2002)

3.2 Freezing and thawing cyclic attack

Freezing and thawing damage in concrete occurs mainly due to the expansion involved when water is converted into ice, and due to the differential temperature co-efficient. When the temperature falls below 0° C, the water in the concrete pores freezes; transition of water to ice increases the volume by about 9%. When concrete pores are saturated above critical value, about 80-90%; it generates tensile stress.

The freezing of the pore water is a gradual process. It depends on microstructure of concrete (Figure 3.4) and also on environmental conditions, such as the degree of saturation of water, number of freezing and thawing cycles, rate of freezing and the minimum temperature reached. Freezing begins from the outer layers and larger pore sizes to the inner layers and smaller pores of concrete, depending on further temperature drop.

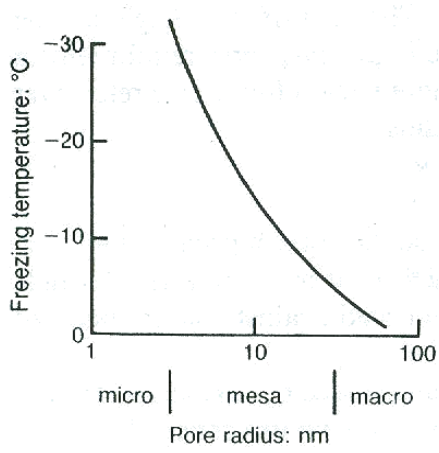

Figure 3.4 Depression of freezing point due to surface energy (CEB 1992)

Beddoe et al (1988 and 1990) described the relationship between the freezing temperature of pore water and the pore sizes for saturated Portland cement paste as follows.

Pore size	**Freezing Temperature**
0.1 mm	0 to -10° C
0.1 to 0.01mm	-20° C to -30°C
< 10 nm (gel water)	< -35° C

3.2.1 Mechanism

The rate of transport mechanism is influenced by the pore size distribution in the hydrated cement paste (hcp). According to their origin and characteristics, the pores are categorized as compaction pores, air pores, capillary pores or gel pores (Figure 3.5). Freezing action occurs in capillary pores. Gel pores are too small (pores < 10nm), therefore, freezing cannot occur in gel pores until temperature drops below -35° C (Mehta et al, 1993). Free water in pores larger than 0.1 mm

freezes between 0° to – 10° C; water in pores between 0.1 and 0.01 mm freezes between -20° and -30° C.

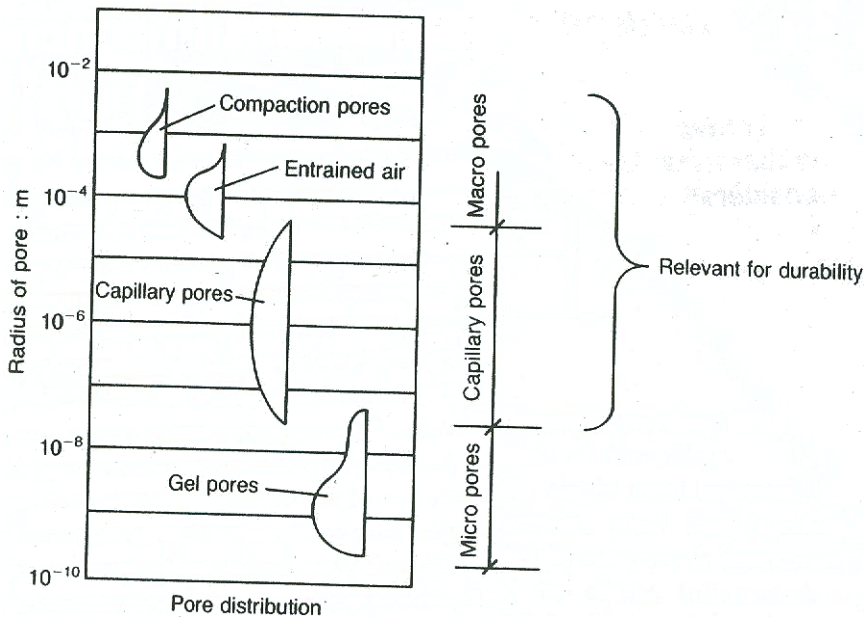

Figure 3.5 Pore size distribution (CEB 1992)

Frost damage is explained in the literature by three main mechanisms (Elsener 2004):

1. As already mentioned, water first freezes inside the capillary pores. The increase in volume due to formation of ice crystal exerts internal pressure on the surrounding paste. This pressure can only be released if there are empty (non-water saturated) pores available in vicinity and it depends on the pore size and the distance to empty pores for the frozen water to travel. The pressure increases with decreasing pore size and increasing distance.
2. Concentration of ions, dissolved in the part of the pore water that is not yet frozen, increases in the gel pores with the freezing of water in capillary pores. This develops difference in concentration between

capillary pores and gel pores that causes the water to move from gel pores in the capillary pores and to increase internal pressure.

3. As mentioned above, water or vapour transports from small pores to ice, already formed in larger pores where it freezes. Thus, there is an increase in the volume of ice and consequently an increase in the pressure. This type of mechanism is relatively slow and more important for longer freezing periods.

3.2.2 Effect of de-icing salt

De-icing salt is the most commonly used material to melt the snow from the roadway and keep it open for traffic movement in cold regions. The application of calcium and sodium chloride as de-icing salt is a detrimental factor. The effect of freeze thaw damage alone is not as serious as those due to combination of frost –thaw cycles, along with the use of de-icing salt. This can be explained as follows:

1. **Degree of saturation**

   The use of de-icing salt lowers the freezing temperature. But simultaneously it also increases the water saturation in the concrete due to the hygroscopic effect.

2. **Thermal shock**

   The presence of de-icing salts decreases the temperature at outer layer of concrete during thawing of the ice. Temperature changes (increases) with increasing distance from the concrete surface. Significant temperature difference (thermal shock) is developed between the outer and the

intermediate concrete layers. This causes internal stresses and finally results in cracking of the outer layers of the concrete (Figure 3.6).

3. As mentioned in (2) above, on application of de-icing salt, the temperature decreases at the concrete surface and this decrease increases with increasing distance from the surface. Moreover, the content of de-icing salt decreases with increasing distance from surface. As a consequences of both these effects (Figure 3.7), the outer concrete layers and intermediate concrete layer freeze at different times. This may case tensile stress between two layers and result in scaling of the concrete.
4. The use of chloride as de-icing salt can result in corrosion of the steel reinforcement (section 3.3). The use of other de-icing agent may result in a chemical attack on the concrete. The chemical effects on concrete are not covered here; the CEB Design Guide (1992) deals with them briefly.

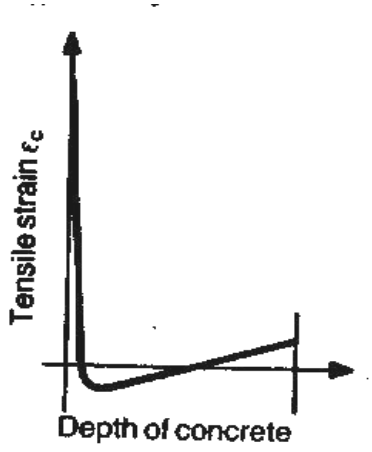

Figure 3.6 Distribution of tensile strain in concrete experiencing thermal shock at the surface due to the effects of chlorides (CEB Design Guide, 1992)

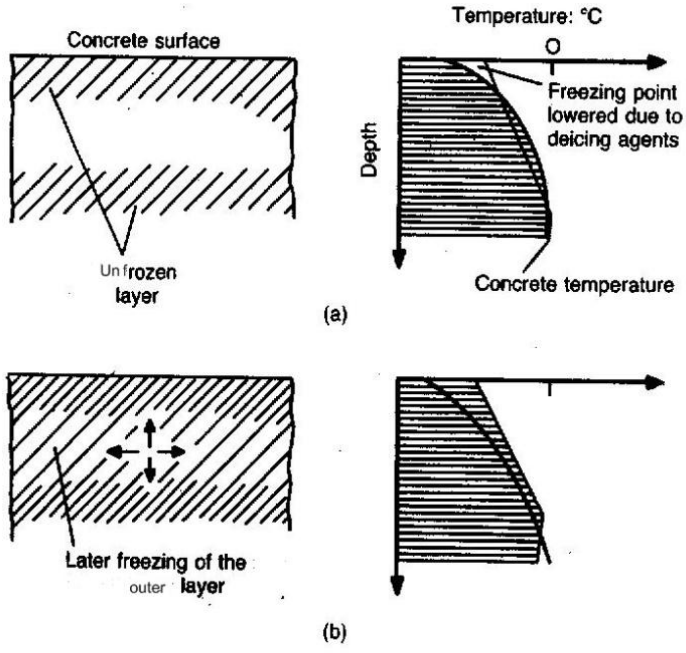

Figure 3.7 Scaling due to variation in the timing of freezing of layers: (a) intermediate layer is initially frozen; (b) outer layer freezes later, causing scaling (Adapted from CEB Design Guide, 1992)

3.2.3 Effect of coarse aggregates

The coarse aggregates used as concrete ingredients in concrete mixtures may sometimes not be resistant to frost attack. They absorb water and as a rule, when water freezes it expands in volume. This may result in either spalling or micro-cracking of the cement paste (Figure 3.8) and the aggregate such as sandstone, being more permeability gets fractured when water freezes in its pores.

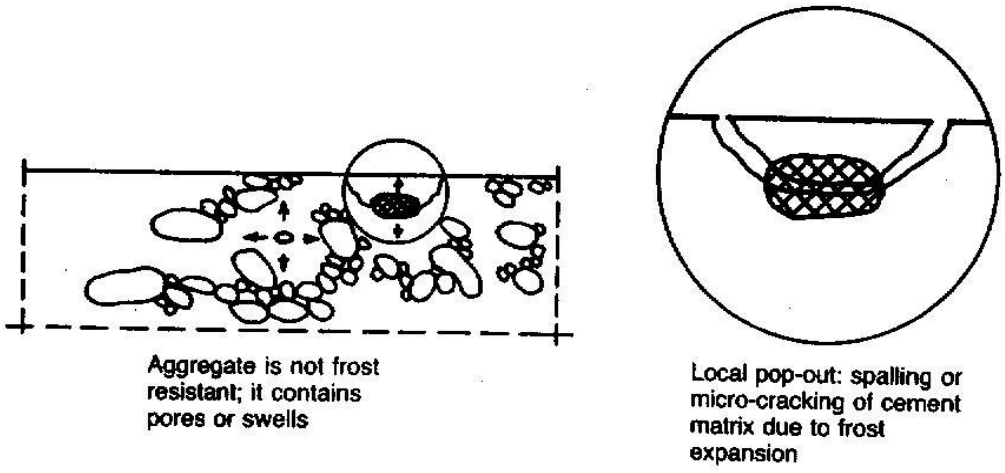

Figure 3.8 Pop-out due to non-frost resistant aggregates
(CEB Design Guide, 1992)

3.2.4 Factors influences frost resistance

1. Degree of saturation

The frost resistance of concrete is highly influenced by its degree of saturation. The critical degree of saturation can be defined as the limiting value of water content in the concrete pores that is required to cause damage by frost attack. In general, 80-90% of water content, depending up on the type of concrete, is assumed to be a critical value. The concrete is capable of withstanding a significant number of freezing and thawing cycles below the critical limit, and it can get damaged by only a fewer freezing and thawing cycles above this critical value. The critical degree of saturation depends on the age of concrete, pore size distribution, environmental conditions, the rate of cooling, frequency of freezing and thawing cycles, and drying out between freezing and thawing cycle. A sufficient numbers of pores, not filled with water, allow the expansion of water and prevent damage from frost attack.

2. Effect of air entrainment:

Air entrainment is inclusion of artificial air pores (bubbles) that are added to concrete mix through air entrainment. They are not filled with water even in the case of fully saturated concrete and provide space for expansion of water forming ice, and thus they prevent generation of internal pressure. In the case of a severe frost attack, air entrainment can reduce the relative weight loss by 10-20% compare to concrete with same mix but without air entrainment. However, the use of air entrainment reduces the compressive strength of the concrete. An increase in the air entrainment content by one percent reduces the compressive strength of concrete by about five percent. Therefore, to obtain the same strength, it is required to use the concrete with comparatively lower w/c ratio.

Air entrainment is effective only if it is provided in a sufficient quantity. Below this limit, it will not solve the purpose effectively. For effective freeze-thaw resistance, the limiting distance between bubbles required should not be more than 0.1-0.2 mm and the volume of air entrainment should be between 4-7%, depending on the concrete volume (Neville 1987). The European Standard EN 206 (2000) proposed protection against the freeze-thaw attack with recommendations for maximum w/c, minimum cement content and minimum strength for each class of attack; this is reproduced in Table 3.1 for completeness.

Table 3.1 Exposure classes with recommendation for freeze-thaw attack with or without de-icing agents (Adapted from European Standard EN 206, 2000)

Class designation	Description of the environment	Informative examples where exposure class may occur	Minimum w/c	Minimum cement content (kg/m^3)	Minimum air content (%)
XF1	Moderate water saturation, without de-icing agent	Vertical concrete surfaces exposed to rain and freezing.	0.55	300	-
XF2	Moderate water saturation, with de-icing agent	Vertical concrete surface of road structures exposed to freezing and airborne de-icing agents.	0.55	300	4.0
XF3	High water saturation , without de-icing agent	Horizontal concrete surfaces exposed to rain and freezing	0.50	320	4.0
XF4	High water saturation, with de-icing agent or seawater	Road and bridges decks exposed to de-icing agents. Concrete surfaces exposed to direct spray containing de-icing agents and freezing. Splash zone of marine structures exposed to freezing.	0.45	340	4.0

3. Environmental condition

Ambient environmental conditions are another governing factor for frost resistance. In case of nearly saturated concrete, even slight drying out of the concrete between two successive freezing cycles provide sufficient space for water to expand and release the resulting internal pressure. This can increase the frost resistance considerably without depending on the w/c ratio and the air content.

4. W/c ratio and cement content

The w/c ratio and the cement content also influence the frost resistance. Dense concrete with low w/c ratio and higher cement content increase the resistance to frost attack as shown in Figure 3.9.

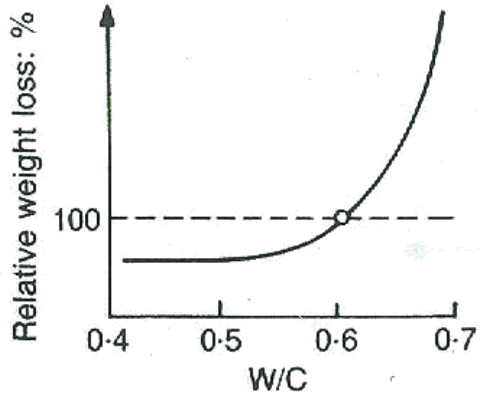

Figure 3.9 Effect of w/c ratio on relative weight loss during a severe frost attack (CEB Design Guide, 1992)

The damage caused by the freezing and thawing attack is a gradual process and not the result of a single cycle. However, this is a cumulative effect that leads to scaling, cracking or spalling of the concrete over period of time.

5. Effect of aggregate size on the air content

The air content required depends on the volume of frozen water to be accommodated. However, the average air content required is approximately 9 percent of the cement paste volume. According to this, concrete with a maximum aggregate size of 20 mm, the air content required is about 5 percent of the concrete volume. Concrete with lower maximum aggregate size have higher cement paste volumes; consequently higher air content is required. The converse is also true for larger aggregate size. Table 3.2 provides typical values of air content for various maximum size of aggregate.

Table 3.2 Variation of air content with aggregate size (Richardson 2002)

Maximum nominal upper aggregate size (mm)	Recommended air content	
	BS 5328: Part I: 1997 (Mean total air content %)	National Annex to IS/EN 206-1: 2002 (Minimum air content %)
10	7.5	5.5
14	6.5	4.5
20	5.5	3.5
40	4.5	3.0

3.3 Reinforcement corrosion

3.3.1 Passivation

Steel embedded in the concrete is protected against corrosion by the passive layer of oxides on the steel rebar surface. This passivation is due to high pH value of concrete. During hydration of cement, the value of pH in the pore solution can be

between 13.0 and 13.8; due to this high pH, a thin layer of oxides is formed on surface of ordinary reinforcement embedded in the concrete. This passive film is only a few nanometres thick and composed of hydrated iron oxides. It provides protection against corrosion to reinforced steel. The carbonation of concrete, ingress of chloride ions or leaching out of alkalis by streaming water through leaky construction joints, or poor drainage system can destroy this passive film, either locally or over large surface area. When the pH of concrete drops below 9 at the reinforcement surface, or chloride concentration exceeds the chloride threshold value; the protective layer is lost. The chloride concentration of 0.6 to 0.9 kg/m^3 in concrete, or 300 – 1200 g/litre in the pore fluid is reported to be critical value to destroy the passive film.

3.3.2 Corrosion of reinforcement

Corrosion of reinforcing steel is an electrochemical process. It consists of an anode, a cathode and an electrolyte (concrete pore water solution) (Figure 3.10a). Once the passive film over the steel surface is destroyed, the iron ion gets oxidized and forms ferrous ions (Fe^{2+}) (anodic process).

$$Fe \rightarrow Fe^{2+} + 2e^-$$

The electrons released from the anode flow through the steel rebar to the cathode. At the cathode, the surplus electrons in the steel combine with water and oxygen and form hydroxyl ions $(OH)^-$

$$2e^- + \tfrac{1}{2} O_2 + H_2O \rightarrow 2(OH)^-$$

Fe^{2+} at the anode react with $(OH)^-$ at the cathode and produce ferrous hydroxide $Fe(OH)_2$.

$$Fe^{2+} + (OH)^{-} \rightarrow Fe(OH)_2$$

This $Fe(OH)_2$ gets converted into $Fe_2O_3.H_2O$ (ordinary red-brown rust) and $Fe_3O_4 \cdot H_2O$ (green hydrated magnetite) before forming final rust product of Fe_2O_3 (black magnetite).

$$4\ Fe(OH)_2 + O_2 \rightarrow Fe_2O_3.H_2O + 2H_2O$$

$$6\ Fe(OH)_2 + O_2 \rightarrow 2\ Fe_3O_4 \cdot H_2O + 4\ H_2O$$

$$Fe_3O_4 \cdot H_2O \rightarrow Fe_3O_4 + H_2O$$

The rust has a volume about 4 to 6 times higher than the metallic iron, depending on the availability of oxygen and composition of the rust products (Figure 3.10b). This increase in volume causes expansion of concrete, exerts pressure and often leads to delamination and spalling of the concrete at the location of poor quality of concrete covers or at the location of the most aggressive microclimate. Figure 3.10c shows the expansive corrosion products on steel cause cracking.

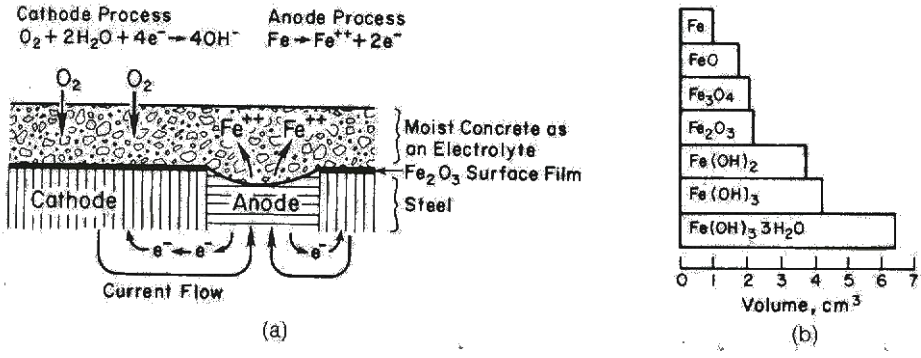

Figure 3.10 (a) Anodic and cathodic reaction as the corrosion of steel in concrete
(b) Volumetric expansion as a result of oxidation of metallic iron
(Mehta, 1991)

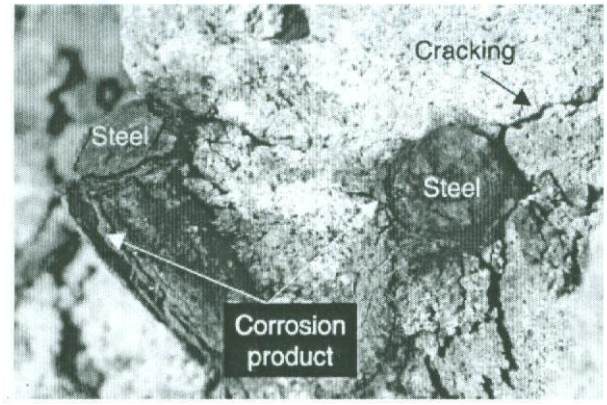

Figure 3.10 (c) Expansive corrosion products on steel in chloride contaminated concrete (Glass et al. 2000b)

Rust is a water containing product and only oxygen is consumed during corrosion process. Therefore, corrosion cannot occur in dry concrete in which moisture is not available for the electrolytic process, as well as in fully water saturated concrete in which oxygen cannot penetrate into the concrete, even though the passive film is totally lost. This means that oxygen and moisture are two most influencing parameters for corrosion and corrosion process is only possible in the presence of both oxygen and moisture. Therefore, the highest corrosion rate is observed at the concrete surface exposed to maximum wetting and drying conditions. Figure 3.11 shows the corrosion rate of steel embedded in carbonated or chloride-contaminated concrete, with respect to exposure condition involving humidity.

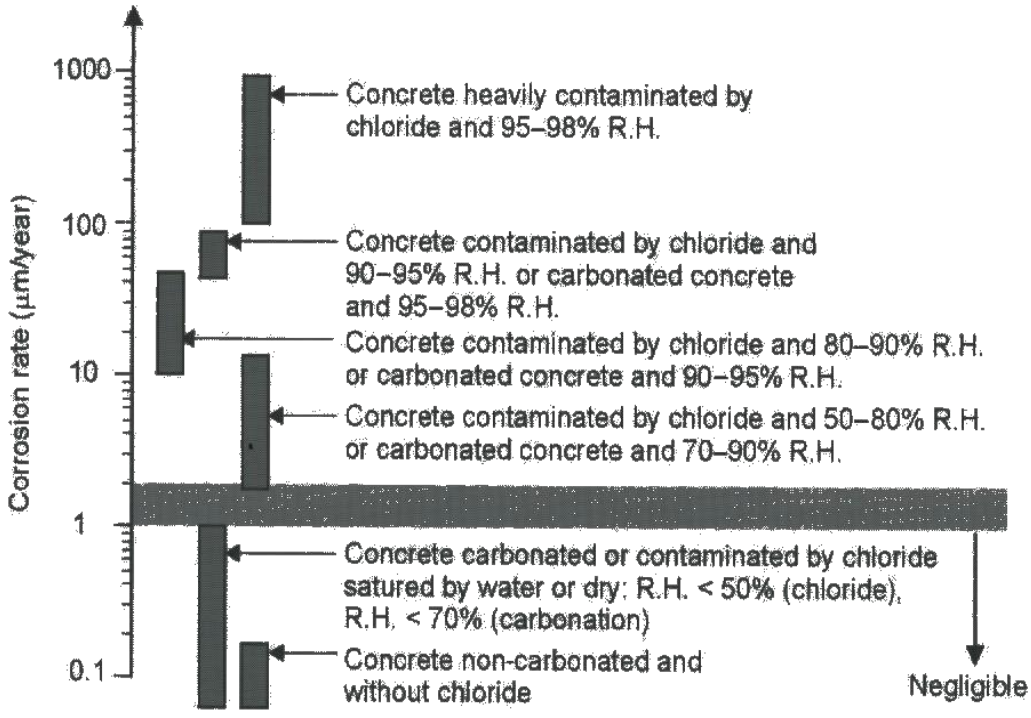

Figure 3.11 Schematic representation of corrosion rate of steel in different concretes and exposure conditions (Elsener et al, 2003)

3.3.3 Manifestation

The distress due to corrosion is manifested as reduction in the cross-sectional area of reinforcement, reduction of bond strength at the steel-concrete interface after a slight initial increase, damage to concrete cover and rust spots on the surface. The severity of the damage depends on the size and spacing of the reinforcement as well as on the quality and thickness of concrete cover. The first signs of distress can be a pop-out, or a long thin crack along the direction of reinforcement depending up on type of corrosion – carbonation-induced corrosion, or chloride-induced corrosion.

3.3.4 Effect/ consequences of corrosion

Corrosion does not only affect the serviceability of the structure but also reduces the performance and integrity of the structure. Figure 3.12 shows the structural consequences of corrosion in reinforced concrete structures.

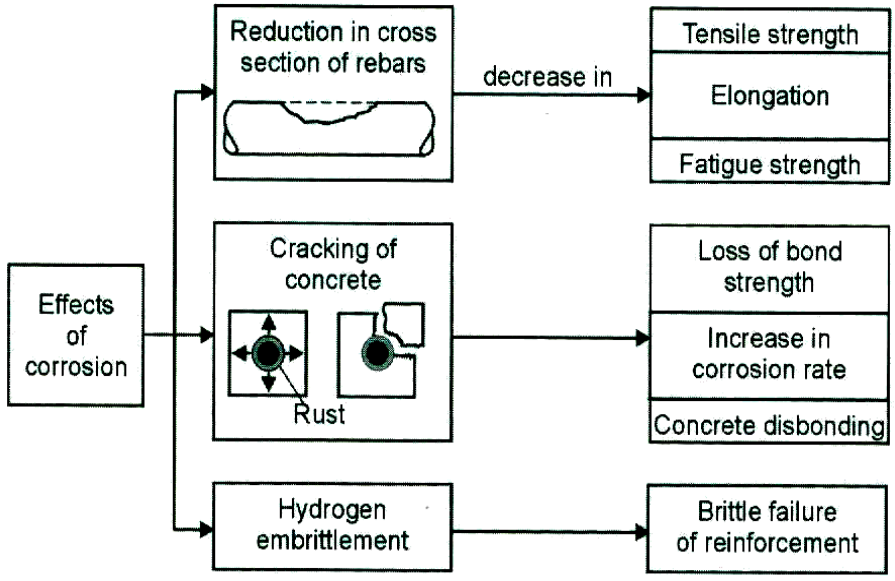

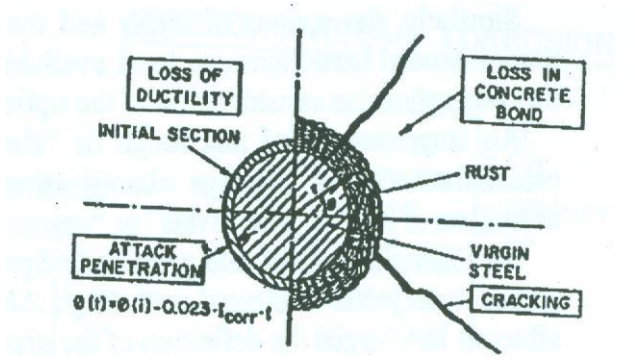

Figure 3.12 Structural consequences of corrosion in reinforced concrete structures (Andrade 1994)

Corrosion reduces the cross-sectional area of the reinforcing steel and concrete (by spalling). The reduction in cross-section areas of steel and concrete lowers

the load bearing capacity of the structural member, ductility, and fatigue strength of the structure. Out of these three, load-bearing capacity is reduced in a roughly linear fashion, while other two decrease substantially with a small reduction in the cross-sectional area. This means that latter two properties (ductility and fatigue strength) are more sensitive to corrosion compared to the load-bearing capacity. Corrosion also reduces the bond strength at the steel rebar-concrete interface.

3.3.5 Types of corrosion

Corrosion is classified in two basic categories: (1) carbonation-induced corrosion, and (2) chloride-induced corrosion. Carbonation-induced corrosion occurs over the entire surface of the steel which is in contact with carbonated concrete. Thus, it causes general corrosion, or uniform corrosion. While, chloride-induced corrosion affects only local area depending up on chloride attack and causes pitting corrosion.

3.3.5.1 Carbonation of concrete

3.3.5.1.1 Mechanism

Concrete is a porous material. Carbon dioxide (CO_2) is always present in atmosphere. Due to the difference in CO_2 concentration between atmosphere and the concrete pores, initially CO_2 diffuses in the concrete and a thin layer of "carbonation front" is developed at the concrete surface. Further penetration of CO_2 depends on the permeability of the concrete and the availability of calcium hydroxide. CO_2 can easily penetrate the carbonation front and it enters the

concrete, where it reacts with $Ca(OH)_2$ already available in the concrete and forms the next layer of the carbonation front. Thus, CO_2 can penetrate progressively into the concrete over time, and finally the carbonation front reaches the reinforcement embedded in concrete (Figure 3.13). The chemical reaction can be described as

$$Ca(OH)_2 + CO_2 \xrightarrow{H2O,NaOH} CaCO_3 + H_2O$$

$Ca(OH)_2$ is mainly responsible for higher pH value of concrete. $Ca(OH)_2$ is consumed during carbonation process. As a result pH of concrete decreases to a value below 9. This leads to breakdown the protective passive layer over the steel bar surface and causes corrosion in the steel reinforcement.

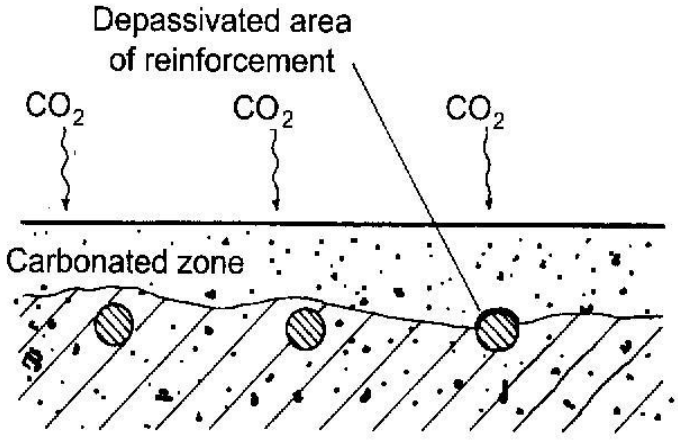

Figure 3.13 Ingress of the carbonated zone to the reinforcement
(Richardson, 2002)

3.3.5.1.2 Effect of carbonation

Carbonation of concrete increases the rate of chloride-induced corrosion. Free chlorides are responsible for the corrosion of chloride-induced corrosion. At the end of carbonation, chlorides bound on the pore walls are released again.

Consequently, the content of chloride in pore water increases and leads to higher risk of corrosion due to chloride.

3.3.5.1.3 Factors affecting carbonation

The primary factors influencing the rate of carbonation includes diffusivity/ permeability of concrete, reserve alkalinity, concentration of CO_2 in atmosphere, and exposure conditions (humidity, temperature etc.). As diffusion of CO_2 is only possible in air filled pores in the concrete, carbonation cannot occur in fully saturated concrete. The rate of carbonation roughly follows the square root time law; increase of carbonation depth with time The depth of carbonation increases with time. The ultimate value decreases with the permeability of the concrete, the amount of carbonizable substance and increasing environmental humidity (Figure 3.14).

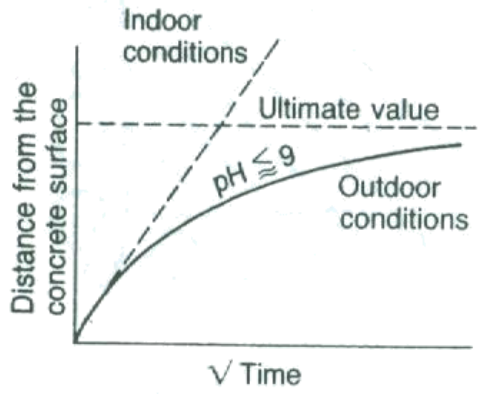

Figure 3.14 Rate of carbonation (CEB 1992)

3.3.5.2 Chloride-induced corrosion

Chloride-induced corrosion is the most damaging cause of corrosion of steel embedded in concrete if sufficient amount of oxygen and moisture is available.

There are two main sources through which chloride ions can introduce in concrete.

1. **Internal source**: Concrete can get chloride ions from within itself; ingredients used in manufacture of concrete such as chloride-contaminated water and coarse aggregates, sand from the sea. Admixtures used in the concrete mix for different purposes may contain chloride ions. In cold region, admixtures, such as calcium chloride are added in concrete for rapid hardening of the concrete.
2. **External sources**: Use of de-icing salt and sea water are the most common external sources of chloride ingress in concrete. Sodium chloride ($NaCl_2$) is the most commonly used de-icing salt in winter to keep the roads and bridges clear from snow. Also, Gaal et al. 2005 noted that surface spalling in California was considerably less before the late 1960's, and it increased significantly after the start of use of chloride-based de-icing salts.

   Sea water contains chloride ions. Therefore, chlorides can penetrate into concrete bridges exposed to the marine environment. Chloride ions penetrate from external sources to the steel surface by capillary attraction and ionic diffusion.

3.3.5.2.1 Causes

Cement has capacity to bind chloride ions on the surface of the pores in the hydrated cement paste. However, there are some chloride ions that are not bound and remain as free ions in the pore solution and are responsible for corrosion of

steel. There is always a dissolution equilibrium between the bound chlorides and the free chloride ions in the pore water. In addition, carbonation of concrete also releases some of the bound chlorides, which increases the concentration of free chloride in the pore water solution and leads to corrosion of steel.

3.3.5.2.2 Ingress of chlorides

As a rough estimate, the rate of penetration of chlorides follows the square root time law. However, the rate of chloride ingress in concrete depends on material and environmental factors that include chloride diffusivity of the concrete, sorptivity of concrete, chloride binding capacity of concrete, w/c ratio, chloride diffusivity of the aggregates, exposure conditions to chloride sources, temperature, carbonation, etc and governed by Fick's second law of diffusion (Equation 3.1) under the assumption that (1) the concentration of the diffusing ion, measured on the surface of the concrete, is constant in time and is equal to C_s($C=C_s$ for x=0 and for any t), (2) the coefficient of diffusion D does not vary in time, (3) the concrete is homogeneous, so that D does not vary through the thickness of the concrete, and (4) it does not initially contain chlorides (C=0 for x>0 and t=0). Chloride concentration decreases with the increasing distance from the concrete surface, as chlorides penetrate into the concrete through the diffusion process. Equation 3.2 is the solution obtained from equation 3.1 for ingress of chlorides.

$$\frac{\partial C}{\partial t} = \mathrm{D}\,\frac{\partial^2 \mathrm{C}}{\partial \mathrm{x}^2} \tag{3.1}$$

$$\frac{C(x,t)}{C_s} = 1 - erf\left(\frac{x}{2\sqrt{Dt}}\right) \tag{3.2}$$

where,

$$\mathrm{erf}(z) = \frac{2}{\sqrt{\pi}} \int_0^z e^{-t^2} dt$$

3.3.5.2.3 Factors influencing chloride-induced corrosion

1. Chloride threshold level (C_{th})

The chloride threshold level can be defined as the critical value of chloride that is required to destroy the passive film and initiate the corrosion process. C_{th} is usually measured as a ratio of the total chloride to cement content of concrete and expressed as percentage of the weight of cement.

The value of chloride threshold concentration depends on many factors, including the concrete quality (w/c ratio, type of cement, proportion of ingredients, etc.), exposure conditions (chloride sources, temperature, moisture content, relative humidity, etc), conditions at the steel-concrete interface, presence of macroscopic voids in the concrete at the steel etc. Glass et al. (2000) reported that the chloride threshold is dependent on the present of microscopic voids present in the concrete at the steel surface. Presently, there is no common agreement on threshold chloride values in the literature, and wide variations are reported (Table 3.3). This may be due to no common threshold chloride content in concrete for initiation of corrosion due to various experimental techniques, the exposure conditions, and "undefined line between potential to corrode and actual progression of steel corrosion".

Table 3.3 – Threshold chloride content values reported by various codes/researchers (Hussain et al., 1996)

Source	Threshold chloride, Percent by weight of cement	
	Free (water soluble)	Total (acid soluble)
ACI 201	0.10 (exposed to chlorides) 0.15 (not exposed to chlorides)	-
ACI 222	-	0.20
BS 8110	-	0.40
Hope and Ip	-	0.10 to 0.20
Everett et al.	-	0.40
Thomas et al.	-	0.50
Page and Havdahl	0.54	1.00
Stratfull	-	0.15

Note: Values specified by ACI and BS are code limits and not necessarily the threshold values for onset of corrosion.

Figure 3.15 presents the relationship between some of the factors (moisture content and the quality of concrete cover) and the CEB critical chloride threshold value. Many highway agencies use a total chloride threshold level of 0.2% by weight of cement, or 0.7 kg/m^3 (Glass et al, 2000). In North America, the critical chloride content typically used is 0.6 kg/m3 to 0.9 kg/m^3 or 0.17% to 0.26 of binding material weight (Lounis et al, 2008).

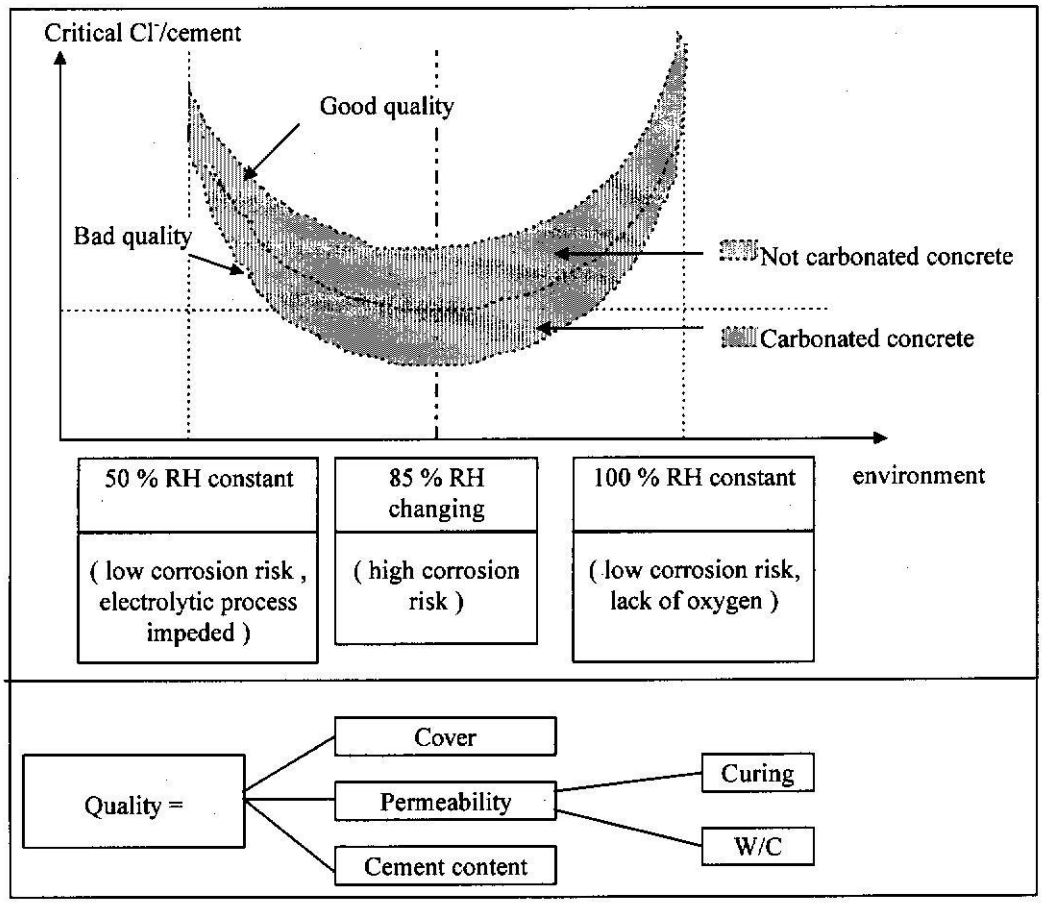

Figure 3.15 The critical chloride content according to CEB recommendations (Liu Y., 1996)

2. Surface chloride content (C_s)

The surface chloride concentration defines the content of chlorides at the concrete surface. Bridge structures are exposed to different chloride concentrations, depending upon the season. The value of C_s depends on the several factors including concrete composition (cement type, chloride binding, absorption, permeability), position of structure and its members, the orientation of its surface and the microclimate, concentration of chloride in the atmosphere, general exposure conditions, such as winds, rain and temperature, and carbonation of concrete. Carbonation releases the bound chlorides. The values of C_s also depend

on cement content and the type of the binder. Higher values of C_s are reported with cement containing fly ash or slag (Bamforth, 1994). In marine environment, relative height and position with respect to mean sea level also affect the C_s value. At higher level, there is strong effect of drying out that leads to higher C_s value. Wetting and drying cycles accumulate chloride on the concrete surface. Therefore, comparatively higher value of C_s can be observed in splash zone. The surfaces exposed to wind and rain wash out the chloride already deposited on surface and thereby reduce the C_s content.

From the analysis of the chloride profile based on field data, it is observed that Cs values increase with age and reaches a quasi-constant concentration in about 5 years (Weyers, 1998 and Bamforth 1993). Moreover, bridges are designed for a long service life of 75 years; therefore, it is practical and reasonable to consider constant value of C_s. However, this is not accepted by all researchers and it is still a matter of considerable debate.

3. Diffusion co-efficient (D)

Diffusion co-efficient is a measure of the diffusion mechanism and total chloride content in the concrete. The chlorides penetrate into the concrete through different transport mechanisms including diffusion, capillary sorption and permeation. Moreover, only free chlorides are responsible for corrosion process. Practically, it is difficult to measure separately free chlorides and bound chloride. Since diffusion is not the only transport mechanism and the total chloride content is not responsible for the corrosion process, the value of diffusion coefficient is not a true value but a value for the apparent diffusion coefficient (D_{app}).

The value of D_{app} does not remain constant. It varies with time, depending on the concrete pore structure, the quality of concrete (w/b ratio, compaction, curing), exposure conditions, such as temperature, and the presence of micro-cracks. Hydration of cement and the reaction of sea water ions with hydration products reduce the pore structures. The type of cement also influences the 'D_{app}' value. The increasing proportion of pozzolanas or blast furnace slag reduces the value of 'D_{app}' significantly. Figure 3.16 presents the apparent diffusion coefficient for chloride (D_{app}) obtained from long-term field tests on concrete of various compositions during marine-splash zone exposure.

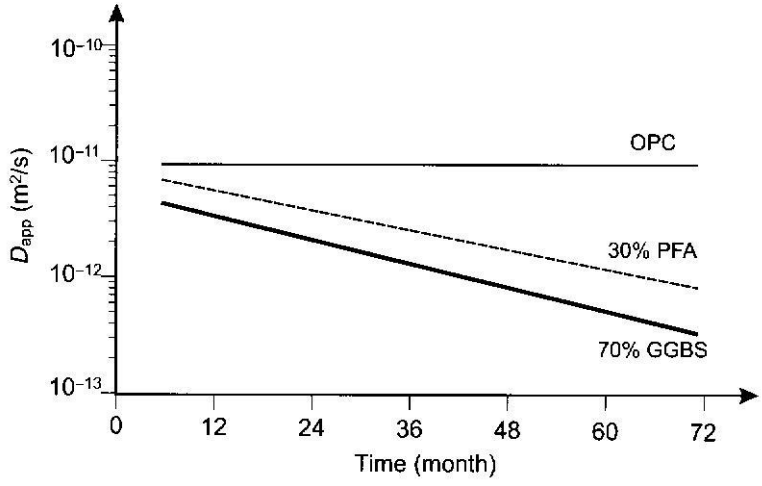

Figure 3.16 Schematic of the D_{app} for chloride as a function of time and type of cement for Portland cement, 30% fly ash (PFA) and 70% ground granulated blast furnace slag (GGBS) exposed to a marine environment (Polder et al., 1995)

In general, the value of the surface chloride content and apparent diffusion coefficient can be estimated by best fitting the experimental data to the equation

$$C(x,t) = C_s \left(1\text{-erf} \frac{x}{2\sqrt{Dapp.t}}\right)$$

where, C(x,t) = total chloride content at depth x after exposure time t

C_s = surface chloride concentration

D_{app} = apparent diffusion coefficient

erf = error function

4. Mathematical model for chloride-induced corrosion

As an essential part of the bridge management systems, it is useful to predict the deterioration of the structure at different stages over its service life; this requires development of a mathematical model relating deterioration with time. It helps decision making authority in scheduling maintenance and rehabilitation programs. However, there is no general agreement on an appropriate durability model. The model presented here is not only the possible model, and many other analytical models have also been developed and can also be applicable, if they meet the general requirements for appropriate durability design.

The diffusion coefficient is a time-dependent variable; only time-dependent diffusion coefficient can give an accurate prediction of the deterioration in a concrete structure. Gaal et al. (2005) describe the time-depended diffusion coefficient, based on Fick's second law of diffusion considering the ongoing hydration of concrete over time, besides considering the age of the structure at which it is first subjected to de-icing salts. They developed the following model which they found to be more reliable than others.

$$C(x,t) = C_i + (C_s - C_i)\,\mathrm{erfc}\,\frac{x}{\sqrt{4\,\frac{D_0}{1-n}\,t_0^n\left[t^{1-n} - t_s^{1-n}\right]}} \qquad t > t_s$$

where, C(x,t) = chloride content at depth x and time t

C_i = initial uniform chloride concentration in the fresh concrete originates from water, binder, and aggregate

C_s = surface chloride concentration at the concrete surface

D_0 = Reference chloride diffusion co-efficient (associated with time t_0)

n = aging co-efficient ($0 < n < 1$)

t_0 = reference period

t = time (age of structure or service life of structure)

t_s = age at which structure exposed to de-icing salt

3.4 Concrete defects

3.4.1 Scaling

Definition: Scaling can be defined as peelings away of mortar or coarse aggregates of the hardened concrete at the surface.

Manifestation: Scaling is a surface defect, observed on the outermost concrete layer. This is a gradual process in which cement mortar and aggregate disintegrate. It starts from outer layer and progresses inwards. Initially, it starts in the form of small patches that merge and extend over time and transform in larger areas. Depending up on the depth of scaling, scaling are classified in three categories (Figure 3.17).

(1) Light scaling: Loss of surface mortar without exposure of coarse aggregate.

(2) Moderate scaling: Loss of surface mortar between 3 to 10 mm depth with exposure of coarse aggregates.

(3) Severe scaling: Loss of surface mortar between 5 -10 mm; in addition, there is complete loss of mortar between 10 to 20 mm around coarse aggregate that result in loosening of coarse aggregate.

Light scaling

Moderate scaling

Severe scaling

Figure 3.17 Types of scaling

Time of appearance: Scaling generally appears at the end of a series of freezing and thawing cycles during the first winter after construction. At this initial stage, generally scaling is in a light form and it can transform into severe scaling after several years.

Causes: Scaling of the concrete surface occurs mainly due to freezing-thawing cycles and the presence of de-icing salt ($NaCl_2$ or $CaCl_2$). Other causes of scaling are:

- use of high water content,
- use of non-air-entrained concrete, improper curing,
- chemical attack, and
- a higher w/c ratio at the concrete surface due to bleeding, resulting in a lower concrete strength at the surface.

The applications of de-icing salt melt the ice on the concrete surface. The energy required for this melting process is drawn from the concrete; this causes a rapid temperature drop (thermal shock) at the surface. The differential temperature between the surface and the internal layer produce tensile stress in concrete, which result in cracking and subsequent scaling. Moreover, the content of de-icing salt decreases with increasing distance from the surface. Above both effects, differential temperature and change in content of de-icing salt result in variation in the time of freezing of the concrete layers. This may result in scaling (Figure 3.7).

Recommended action

Following actions should be taken to prevent scaling

1. Use of lower w/c ratio. Concrete with moderate slump of 75 – 125 mm
2. Use of air-entrained concrete
3. Avoid use of de-icing agent for the first winter and seal the surface with boiled linseed oil.
4. The surface must be finished in time.
5. Provide sufficient curing.

3.4.2 Delamination

Definition: Separation of concrete layer at or near the level of top reinforcement, or above another layer of concrete, or subsurface material.

Manifestation: Delamination is an initial stage before concrete spalls. It may occur in bridge decks, columns, piers, and column caps. This defect can be identified by visual inspection as well as by a hammer strike that produce a

hollow or dull sound on the concrete surface. Occasionally, the noise of traffic vehicles may create problems. In decks covered with asphalt, it difficult to identify the delamination by sound. The NDE techniques can be used to determine the extent and depth of delamination (e.g. chain drag, GPR).

Time of appearance: It can vary depending upon the rate of corrosion, concrete cover thickness, permeability of concrete and the effect of thermal shock due to freezing-thawing cycles.

Causes: This may occur due to corrosion of the steel reinforcement, or ineffective bond between concrete layers, or various environmental effects, or the presence of cracks in the concrete surface.

As mentioned earlier, the bridge deck is subjected to frequent application of de-icing salt and to the marine environment, which constitute the worst exposure conditions. The volume of iron corrosion products, indicted by the ingress of chlorides into the concrete is six times higher than the volume of iron in the steel, depending upon the availability of oxygen; this higher volume exerts expansive pressure in the concrete that may cause cracking and delamination.

Recommended action: Delamination of concrete should be repaired as early as possible otherwise it can turn into large-scale spalling. Epoxy injection is the most common method used for repair this type of deterioration. The same procedure used for repairing of spalling can also be applied for repairing of delamination.

3.4.3 Spalling

Definition: Spalling is a separation or complete detachment of the concrete in the form of fragments from main member.

Manifestation: Spalling is roughly circular or oval shape depression in concrete. It can be seen by visual inspection and occur on any part of the bridge including its deck, columns, pier, abutment, column cap, girder, etc. depending on the exposure condition. Falling of concrete is very dangerous to the traffic passing underneath the bridge.

Causes: Spalling is the next stage of deterioration after delamination. As the delaminating process continues, it results in spalling, because of internal pressure exerted by freezing and thawing cycles, corrosion of reinforcing steel, and the formation of internal cracks that are transformed into spalling over time.

Moisture penetrates into concrete. The volume of water increases by about 9% during freezing. In case of completely saturated condition, there is no more space available for water to expand, which causes a splitting force on concrete and result in cracking. These cracks allow further ingress of moisture which expands again on freezing, and enlarges and propagates the cracks with each freezing and thawing cycle. The process continues over time and results in spalling. Additionally, aggressive agents, such as chlorides, are also transported with water into the concrete. When they reach the reinforcing steel and exceed the threshold level, they destroy the passivating layer on the steel bar which starts corroding; this results in volumetric expansion. This, in turn, produces weak fracture planes and results in spalling of the concrete when subjected to loading.

Recommended action

Falling of spalled concrete is very dangerous for traffic passing underneath the bridge structure. Therefore, precautions are normally taken by fixing wire mesh around the spalled location.

Before commencing any repair work, it is essential to carry out a detailed evaluation to determine the severity and causes of damage. The areas of active steel corrosion and contaminated concrete is normally larger than the area of spalled and delaminated concrete. Therefore, it is not enough to repair only the spalled or delaminated concrete; it is important to remove all of the contaminated concrete, which can be implemented by scarifying with pneumatic hammers. Generally, the scarification process may go up to or beyond the reinforcement. Once this process is completed, it is necessary to clean the entire surface properly by using water or compressed air. Some of the steel rebars need to be replaced depending on the loss of cross-sectional area. If the bar loss is too high, it is preferable to fix a new cage of steel bar to replace the deteriorated steel rebars. This would normally increase the overall cross-section and resistance of the member. It is important that the new concrete added must be well designed, well compacted and cured, and impermeable with sufficient cover thickness to avoid/delay the deterioration again.

3.4.4 Cracking

Definition: A crack is defined as fracture in the concrete. It causes discontinuity without complete separation of member.

Time of appearance: Young concrete is at high risk to cracking. The transition period normally starts about 2 hour after casting and lasts for about 4-16 hours; this period is critical for cracking. Concrete has a low tensile strength and low deformability during this period. The times of appearance of cracks resulting from different forms of deterioration are summarised in Table 3.4.

Causes: Concrete is very weak in tension, therefore cracking can develop whenever the tensile force acting on section exceeds the tensile strength of concrete. The tensile strength capacity of concrete varies with time and the rate of application of tensile force. Tensile force can be caused by shrinkage, temperature changes, structural actions due to the applied loads, corrosion of reinforcement, sulphate and chemical attacks. Table 3.4 summarize the different types of cracks frequently developed in practice.

Plastic settlement cracks are caused due to non-uniform settlement of concrete. This can happen where there is variation in depth of member, or where there is restraint from reinforcement, or from formwork. Due to the gravitational force, concrete particles settle down and replace the mixing water of the concrete. Sometimes, this downward moment is restrained from top reinforcement, or formwork. Concrete above the steel rebars hangs itself over the steel rebar while the concrete below the rebar separate from reinforcement and settle down. This cause voids under the reinforcement and crack may occur.

Plastic shrinkage cracks occur due to rapid evaporation of concrete surface water. Normally, the evaporating water from the concrete surface is compensated by the bleeding water. The rate of evaporation depends on the ambient environmental conditions such as temperature, wind speed and relative humidity.

When the rate of evaporation exceeds the rate of bleeding, reduction in volume (shrinkage) takes place at surface. This reduction in surface volume is restrained by the concrete that is not subjected to volume change, immediately below it, which causes tensile stresses in concrete. As mentioned earlier, younger concrete has low tensile strength, and this situation can lead to cracking.

Temperature cracking: This type of cracking is similar to shrinkage cracking, and is caused by the restraint to the movement during expansion and contraction of the concrete member due to temperature changes. During hydration, heat is generation in concrete. In massive concrete member, it is not possible to transfer all of this heat to the surrounding air from the concrete surface. A temperature gradient develops from the core to the outer concrete surface; this gradient increases with increasing heat at the core and decreasing air temperature. Self-equilibrating stress conditions are developed, with tensile stress in the outer layers and compressive stress in the core. If the tensile stress exceeds the low tensile strength, cracking can occur.

Recommended action: Cracks developed during construction phase are fine and do not influence the structural strength of the concrete but it opens as easy path for moisture and chloride to enter into the concrete and lead to corrosion. Therefore, it is preferable to seal all the cracks using a special mortar or epoxy resins. However, development of crack at early age can be minimized by using good quality impermeable concrete, proper curing, good workmanship, proper compaction and mix design of the concrete.

Table 3.4 Concrete deterioration with time (Mirza CIVE 624 Class-Notes, 2008)

Type of cracking	**Primary causes**	**Secondary causes**	**Possible manifestation**	**Remedial measures**	**Time of appearance**
Plastic settlement	Excessive bleeding	Rapid early drying conditions	Cracking, localized bond loss and/or cover to rebars	Reduce bleeding by air-entrainment, or revibration	15 minutes – 4 hours
Plastic shrinkage	Rapid early drying, inadequate cover	Low rate of bleeding		Improve early curing	2-6 hours
Early thermal contraction	Excessive heat generation, excessive temperature gradients	Rapid cooling	Cracking in-depth, localized loss of cover to rebars	Reduce heat, or insulate	1 day – 4 weeks
Early drying shrinkage	Rapid early drying	Inefficient joints	Crazing and/or cracking, reduced cover to rebars	Improve early curing; pattern concreting	2 days – 6 months
Long-term drying shrinkage	Inefficient joints	Excessive shrinkage, inefficient curing	Surface cracks	Use lower w/c ratio concrete mixtures, improve curing	Several months
Crazing	"Fair-faced" concrete slabs	Impermeable formwork, over-trowelling	Shallow cracking induced by shrinkage of the surface zone	Improving finishing operation and curing	1-14 days
Freezing and thawing cycles	Expansion (9%) upon freezing	Freezing point lowered in smaller pores, and further due to de-icing salts	Scaling due to freezing of different layers at different times. Local pop-out due to spalling or micro-cracking of cement matrix	Air entrainment; drying concrete; avoid frost-action at early age of concrete	Variable

Corrosion of reinforcement	Lack of concrete cover; chloride ingress; carbon dioxide ingress; excessive calcium chloride. Depassivation of steel rebar; decreased pH.	Poor quality concrete. Stray electrical currents	Reduction of rebar cross-section; splitting of concrete cover; cracking and spalling. Loss of bond between concrete and rebar.	Decrease concrete permeability (low w/c ratio, higher cement content, good compaction, and curing). Sufficient thickness and good quality of cover; add pozzolans. Reduce relative humidity of concrete (<60%); drying helpful	Normally about 5 years

4. Bridge Inspection

4.1 Importance and need for bridge inspection

According to current CSA Standard S6 - 2006, bridges should be designed for a minimum service life of 75 years. During their long service life bridges are generally subjected to harsh environments. Significant environmental damages (e.g. corrosion, cracking and other damage) occur before average bridges reach the half of their lifespan which affects the load carrying capacity of the structures. Therefore, it is necessary to inspect, or monitor periodically all of the bridge elements, or components responsible for safety and performance so that an early detection of damage can be made and structure can be updated accordingly.

Bridge inspection is an important part of the bridge maintenance program. It determines the present condition of an entire population of bridges. It yields very important information regarding degree of repair or rehabilitation work to be carried out for each bridge in the system. The detailed evaluation also determines whether further destructive or non-destructive testing is needed, basically to predict the cost associated with repair, or rehabilitation work. There is limited funding available for maintenance work. The data received from inspection can be utilized in fixing priority of future actions for bridge structures, providing information about which bridges need attention, and rehabilitation, or replacement and thus, helps the authority in logical allocation of the limited funding. Early detection of damage not only reduced the annual maintenance costs, but also

reduced the socio-economic costs which are much higher than the economic costs. It ensures serviceability and safety of bridges (Postema and Van Beek, 2003).

4.2 Related documents

Collapse of Silver Bridge in Point Pleasant over the Ohio River in 1967, killed 46 people. Just after this collapse, the Federal Highway Administration decided to develop guidelines for systematic bridge inspection procedures. According to these guidelines, all bridges on public road must be inspected at least once every two years (AASHTO 1994; NBI 2003). In Canada, a list of documents on bridge inspection was published to guide the inspector (Baxter, Source: http://www.ogra.org/lib/db2file.asp?fileid=20730)

The inspection manuals available for bridge inspection, quoted by Baxter from TSH Engineers Architects and Planners, include

1. Ontario Structure Inspection Manual (OSIM)
2. Municipal Bridge Appraisal Manual
3. Municipal Culvert Appraisal Manual
4. PWGSC Bridge Inspection Manual

Other relevant documents that can also be used in bridge inspection include:

1. Structural Rehabilitation Manual
2. Canadian Highway Bridge Design Code (CSA S6-2006)
3. Structural Manual
4. Low volume Road Guidelines
5. Financial Analysis Manual

4.3 Non-destructive testing (NDT)

The main aim of the bridge inspection is to determine the degree of repair needed to determine whether more detailed testing is required. The 1992 ISTEA (International Surface Transportation Efficiency Act) mandates the use of a quantitative computerized bridge management system by 1996 (Prine, 1995). This needs quantitative bridge inspection methods. Visual inspection can find only surface defect. Therefore, it provides information just after visible defects appear in structural member (Estes, 2003). It cannot find internal flaws or flaws hidden by paint, or coatings. The accuracy of test results are strongly dependent on the inspector's judgment and experience. Destructive test methods require mechanical testing of materials to quantitatively evaluate the specific characteristic of each material. Even though it provides a relatively accurate test result, there are some limitations with this technique that of minor or major damage the structure. The data is applicable only to the tested part of the structure, and it is possible that the rest of the structure may not have the same material properties as the tested part. Most destructive test specimens cannot be reused once the test is completed, and many destructive tests require large, expensive laboratory equipment. These make these tests not ideal in regular inspection. The NDT fulfills these critical requirements.

There is no standard definition of a non-destructive test for concrete structures. Some define NDT as tests that do not alter the concrete. while others define some tests such as drilling of cores as non-destructive, since it does not disturb the functional capability of the structure. The tests that result in less damage to

structure than drilling of cores is also considered in NDT group (Nawy et al. 2008).

Non-destructive testing is more quantitative and identifies the defect that is not visible on surface. It is cost-effective and involves portable equipment. It is based on well-established physical principles, which provide information about the quality of materials, or components. Structure under testing does not get damaged. In addition, it does not disturb the function of the test structure and it is also possible to retest the same test location to evaluate any changes that may occur with time. In this respect, Rens et al. (1997) state that "To keep structures fully functional and structurally safe, inspection must determine the overall condition of the total system. A suitable inspection program should (1) measure the structural characteristics in situ; (2) assess the current operating or serviceability condition accurately; (3) reduce current inspection costs; and (4) require a minimum of specialized training. Non-destructive evaluation methods can help address these problems." This is also supplemented by a case study conducted by Parhizkar et al. (2003). NDT tests were performed to determine different parameters which include concrete uniformity test, compressive strength test, concrete cover thickness, corrosion potential and chloride penetration depth on an existing structure in the Persian Gulf region. This study demonstrated that NDT is an effective method for identifying defects in existing concrete structure.

Non-destructive testing can be applied to both new and old structures. For new structures, it is basically used for quality control and resolution of doubts about quality of materials and workmanship involved in construction e.g. uniformity, compaction, curing, etc.; while in existing structures, it is use to evaluate the

structural integrity and serviceability, by detecting voids, cracks, delamination, and other similar effects. Other applications of NDT include assessment of properties such as density, elastic modulus, strength, surface hardness and surface absorption. It can also be used to determine the location, size and distance of reinforcement from the concrete surface. According to the FHWA Bridge Inspection Training Manual 90, NDE techniques should be used for evaluation of defects found during visual inspection, inspection of items not accessible during visual inspection, inspection of members that have presented problems in the past or in similar structures, sampling of critical elements, inspection of critical members, performance of rapid surveys of a large number of decks, and monitoring of structural performance.

A number of NDT methods have been developed for evaluation of concrete structures. Table 4.1 summarizes some of the non-destructive test methods that are most commonly used in bridge inspection. Each test method has advantages and limitations; none of the method is complete. Therefore, it is necessary to use more than one NDT methods in combination so that limitation of one method can be compensated by the strength of the other. It also gives very useful information when used jointly with destructive testing. This approach can assist with a more accurate determination of the suspected defective zones. Depending upon the result of preliminary NDT test technique, the subsequent detailed testing of the structure can be carried out. This helps in saving time and cost of examining the large mass of the test structure.

The main drawback of the NDT methods is the interpretation of test result. Concrete is heterogeneous material; materials, mix details, workmanship,

environment, etc. influence the test result. Therefore, experienced persons with sufficient knowledge of the test applications are needed to interpret the test results. Implementation of non-destructive testing is limited mainly due to two main reasons. First, NDT is not always readily available and secondly, the lack of availability of experienced inspector having sufficient knowledge of NDT test application. However, according to the 1993 and 1996 surveys by Rens and Transue, the use of NDT is increasing in Bridge Management.

4.4 Fundamental aspects of bridge inspection

Performance of inspection process mainly depends on technical, economical and regulatory factors and is not found uniform. However, for proper inspection of the bridge structure, the basic knowledge of fundamental aspect of bridge inspection is essential. It includes-

A. Bridge inspection personnel qualifications

B. Inspection preparation

C. Inspection types (routine, in-depth)

D. Safety

E. Appropriateness of various NDE techniques

A. Personnel qualifications

Inspector's judgment is very important for proper evaluation of site findings. These problems can be complex and can vary from structure to structure, complicating problem identification. An ideal bridge inspector needs to have sufficient knowledge and experience of the structural behavior and design of bridges, non-destructive testing, changing behavior of materials with age, fatigue,

stress, weathering, and chemical reactions, typical construction practices, maintenance or repair, rehabilitation and load rating. He should be familiar with construction features of bridges and capable of expressing his finding in simple language and also by simple sketches in his report. He should be able to recognize the different causes of deterioration due to corrosion, weathering, fatigue, etc. He should be able to identify the areas where problems commonly occur and able to suggest preventive maintenance programs. He should also have a reasonable knowledge of electrical equipment, machinery, hydrodynamics and soils. It is certainly not possible to have all these qualification in a single person, therefore, it is necessary to have a team of engineer(s) and technician(s) with knowledge and experience in different areas. The National Bridge Inspection Standard (NBIS) requires that the team leader for bridge inspection should be either a professional engineer, or a state-certified bridge inspector or a level III bridge inspector certified by the National Institute for the Certification of Engineering Technologies (NICET). He should have minimum 10 years of experience in the field of bridge construction and inspection. He is responsible for on-site bridge evaluation and with responsibilities for planning, preparing, and performing the bridge inspection. Engineering graduate student from universities with internship programs can be excellent source to assist technicians in bridge inspection program.

B. Inspection preparation

Inspection preparation is an important aspect of bridge inspection. Inspection should always start with proper planning. From the bridge history, it is observed

that proper preparation and planning result in effective and efficient inspection and also save time in the field.

A detail study of bridge history and review of any available plans of a bridge structure provide useful information to an experienced inspector to identify the areas that will need attention. If previous inspection report is available, problems found in the previous report should be tabulated with extra space to note the existing condition for direct comparison.

The bridge records that can be helpful in developing bridge inspection planning include design and construction plans, workshop drawings, as-built drawings; specifications; correspondence; photographs; material certification, material test data, load test data for material information; maintenance and repair history; protective coating history; accident Records; bridge posting actions; permitted load information; flood data; traffic data; inspection history; inspection requirements; structural inventory and appraisal sheets; past inventories and inspection records; and rating records.

any planning of a bridge inspection program should mainly focus on the type of inspection needed, number of personnel needed; ramp closures, detours, time restrictions, flagmen needs, coastguard warnings, permission for efficient traffic control; access equipments with qualified personnel for operation; other tools and equipments, including power needed; estimation of inspection duration; coordination with other relevant agencies; identification of previously defined problem areas; determination of need for underwater inspection; determination of non-destructive testing based on previous visual inspections; identification of

areas/details that may require special inspection like fracture critical members, fatigue-prone details, non-redundant members, unusual or special details.

In some cases, site visit may provide very useful information regarding bridge history. Identification of the member with deficiencies is also important to identify the member for future repair, or further examination. If the drawings, or previous inspection reports exist, it is advisable to use the same identification system to avoid confusion for future inspections.

C. Inspection types

All inspections should be carried out in systematically so that no part or component gets missed. The inspection program should be subdivided into different stages for bridge components. Inspection report must be clear, concise and in standard engineering terms with appropriate photographs and sketches.

A particular type of inspection to be carried out for bridge inspection depends on age, condition, and use of the structure. There are five basic types of bridge inspections.

1. Initial Inspection
2. Routine Inspection
3. In-Depth (Interim) Inspection
4. Damage Inspection
5. Special Inspection

1. Initial inspection

This is the first inspection carried out either after new construction, retrofitting or change of ownership. This inspection is generally carried out at the time of preparing a bridge inventory, along with a detailed description of the bridge. This information is utilized as base information for subsequent inspections for direct

comparison. A detailed structural analysis is conducted to determine the load carrying capacity of the structure, corresponding to the weakest element of the bridge. The problem areas, or suspected problem areas, including fracture critical members (a tension member or component whose failure will produce collapse of a structure) are identified during this inspection and special attention is given to these areas in subsequent inspections.

2. Routine inspection

This is the regular scheduled inspection generally carried out to monitor the condition of structure at every two years. The areas critical to load carrying capacity are closely inspected. Visual inspection and simple NDT methods are used to identify the problem areas for further in-depth or interim inspection. The results of routine inspection with appropriate photographs and clear sketches are documented in a bridge file. The recommendations for further inspection and maintenance are also included in this documentation.

3. In-depth inspection

This involves a detailed inspection of the problem area(s) identified in the routine inspection. It is also carried out in response to the report made by the bridge users. This is generally carried out at 5 to 10 years intervals to estimate the extent of defects identified in routine inspections. It also detects the deficiencies that are not identified during routine inspections. These require use of special lift equipment (Figure 4.1) to closely access the problem area. Appropriate NDT, physical and chemical tests may be needed for a more detailed investigation. Underground inspection is also a part of an in-depth inspection. The findings and procedure

used should be documented in a bridge file. The results of an in-depth inspection may lead to either of the following decisions:

- **No action** is required for bridge with unrestricted vehicular traffic;
- **Long-term monitoring** of the structure if observed defects are not serious enough for immediate action;
- **Load posting** if load carrying capacity is affected; or
- **Assessment of the residual life** of the defective component.

(a) Cherry picker

(b) Bucket snooper

(c) Inspection Plateform

(d) Spider

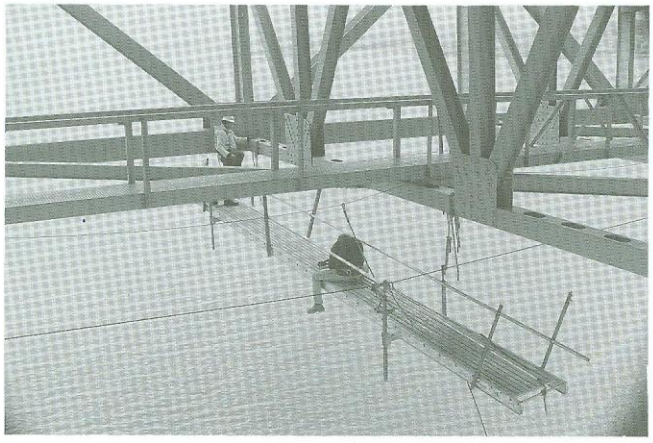

(e) Scaffolding

Figure 4.1 Special lifting equipments (Silano 1993)

4. Damage inspection

This is an unscheduled inspection, normally carried out to assess the damage to the structure resulting from flooding, high winds, deterioration due to aggressive environment, or manmade damage e.g. fire, vehicle collisions, etc.

This inspection may result in load posting or immediate closure of the structure, depending upon the extent of the damage. The engineer makes the decision, regarding the safety of the bridge user. Any defect or deficiencies (misalignment, loss of section or other damages) found during this inspection must be documented appropriately.

5. Special inspection

This inspection is carried out to supplement mainly the in-depth or damage inspection. Special equipment and advanced NDT techniques may be needed. Diving underwater inspection is a type of special inspection (Figure 4.2). According to FHWA, underwater members should be inspected at least once every five years. FHWA has published Bridge Inspector's Training Mannual\90 (FHWA 1991) which provides guidelines for underwater inspection of bridges.

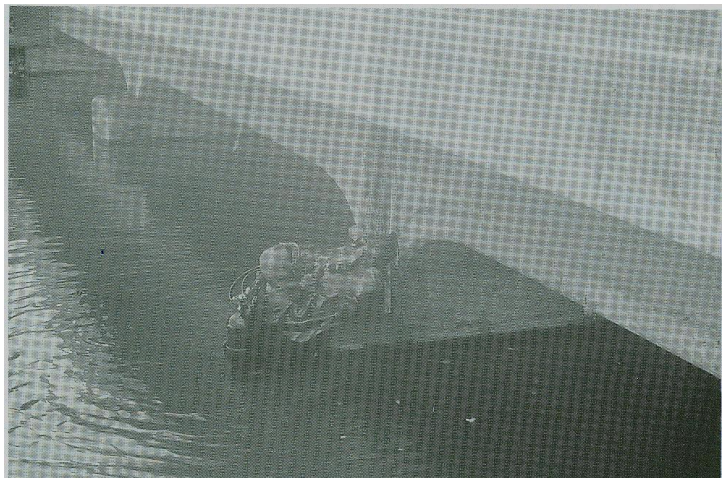

(a)

(b)

Figure 4.2 (a) Scuba diving for under water inspection, (b) Underwater photography (Silano1993)

D. Safety

Bridge inspection is a dangerous task, therefore, it is important to prepare safety programs for both the bridge inspectors as well as for the public using the structure and passing underneath the bridge. Safety program must follow the standard bridge inspection safety procedures and detail site-specific safety requirements. This includes traffic control, personnel contact, emergency telephone numbers, and safe conduct around the specific inspection equipment to be used. Basic rules for traffic control include: inform the drivers in advance; control the speed of the vehicles; provide a clearly marked path to travel through the inspection zone for the driver, etc. Before beginning of each day's work, safety program should be checked. Inspectors should be sent in teams so that if someone gets injury, other can provide help, or call for help. Safety program should be discussed with inspection team prior to the beginning of the inspection. Any questions or confusion regarding safety equipments and working

environment should be cleared before beginning of inspection. Ultimately, each inspector is responsible for his own safety. Attitude, alertness and commonsense are the key parameters in maintaining safety.

E. Appropriateness of NDE techniques

There are many non-destructive testing techniques that can be utilized by a bridge inspection team. Table 4.1 summarizes some of the NDT methods commonly used in bridge inspection. The FHWA nondestructive evaluation validation center (NDEVC) provides the information on available NDT techniques and their performance. Selection of NDT techniques depends on several factors such as structure type and possible deterioration mechanism; safety requirements; weather; overall practicability and feasibility; availability of testing apparatus; access to testing areas on the bridge; expense of the technique; possible subjectivity involved in test results interpretation; and needs of the bridge management system. Therefore, selection of proper test techniques is important. Each NDT technique has limitations and no single testing method may provide complete information. Therefore, it is necessary to use more than one NDT methods in combination so that limitation of one method can be compensated by the strength of the other. The NDT provides useful information when use jointly with destructive testing. Depending upon the result of preliminary NDT test technique, the subsequent detailed testing of the structure can be undertaken, with considerable time savings and costs of examining the large mass of test structure.

4.5 Areas to be inspected

Each and every element of a bridge structure needs to be inspected. However, there are some areas where serious defects are likely to occur and need particular attention during inspection. Some of these areas, suggested by Ghose (1999) include:

1. "Members with high design stresses.
2. Members where water may collect due to inadequate drainage system,
3. Areas which are subjected to alternate wetting and drying.
4. Areas which are not easily accessible to painting,
5. Areas of steel girders where waste water is discharged from passing trains in railway bridges, or areas directly below drainage spouts or weep holes.
6. Areas which are prone to corrosion due to emission of steam blasts or smokes of locomotives.
7. Areas where dew collects, or which are under water during floods.
8. Surfaces of the windward side of a bridge situated near Sea or over creeks which are prone to more corrosion than other areas.
9. Joints of deck system in general, particularly – throats of cleat angles or seating angles, notches in the flange/web at the end of stringers and cross girders for fatigue crack
10. Top and bottom lateral bracings which are liable to be bent or buckled. Also the gussets at the ends and at the middle of bracings
11. Camber of truss
12. Unusual vibration or excessive deflection under passage of heavy load should be noted and the cause investigated.

13. Creep or longitudinal movement of girders.
14. In welded girders fatigue-prone areas should be carefully inspected.
15. In bearings, the common distresses are bent or loose holding down bolts, frozen rollers, cracks in base plates. The bearing should be checked for tilt and also whether all the bearings are at the same level.
16. Special attention should be given to fracture critical members of a structure."

Table 4.1 Summary of nondestructive testing methods for evaluating bridge conditions

Method	Uses/Applications	Advantages	Limitations
Visual inspection	Cracks Geometry Surface roughness	Accessibility Oldest known technique Well established	Subjective Time-consuming Qualitative results
Liquid penetrant dye	Surface flaws Detection of irregularities	Highly Portable Easy to interpret results	Surface preparation is critical Exhausting for inspector Time consuming
Chain drag	Flaw detection inside decks Delaminations	Simple Portable Good for delaminations	Time-consuming Tedious Subjective Not good with overlays May not detect initial delamination.
Half-cell potential	Detect corrosion state in concrete reinforcement Can not indicate the corrosion rate but only indicate zones requiring further investigation	Simple, light weight Portable equipment Inexpensive and quick	Deck needs preparation Time consuming Not good for delaminations Lane closure Not very accurate
Acoustic emission	Cracks Delaminations Corrosion	Real-time response No lane closures Able to detect flaws from a distance Adaptable to continuous monitoring Applicable under normal loading. Can possibly predict failure	Qualitative results only Sensors must contact test surface Multiple sensors required for flaw location Not good with overlays Interpretation Costly; Not reliable Signal interpretation required Requires extensive training for analysis Only detects growing (fatigue-driven) flaws.

Ultrasonic tesing (UT)	Homogeneity of concrete cracks, voids. Strength determination	Portable Easy test procedure at relatively low cost Relatively easy to interpret Thickness information, depth, and type of flaw can be obtained from one side of the component.	Not very reliable for concrete; Material attenuation affects results negatively; Does not provide information about the shape of defect; Usually no permanent record; requires couplant
Ground penetrating radar	Concrete mapping, mining geotechnical, road, and bridge Forensics Detection of voids, honeycombing Delaminations Moisture content	Versatility; Portability Effectiveness; Low cost Good with overlays Minimum traffic control Prediction of repair quantities in roads Access to only one face Applicable in normal traffic Effective even under asphalt cover.	Interpretation Complexity of results Interpretation of results sometimes requires selected destructive testing Considerable equipment and computing power necessary.
Impact echo	Detection of voids, cracks, delaminations, unconsolidated concrete, and debonding Determining thickness	Requires one surface of the tested material to be exposed, Independent of the geometry of the structure Less susceptible to steel reinforcement, High accuracy May detect initial delaminations.	Size of detected flaws is highly dependent on the impact duration Less reliable in the presence of asphalt overlays Interpretation of the results is difficult Greater training required.
Infrared Thermograpy	Detection of thermal differences, delaminations, cracks, voids	Portable; simple, easy interpretation Minimum traffic interference; Possibly able to detect corrosion under coatings Applicable to large areas under normal traffic Provides permanent record	Provides no information about depth of defects; Dependent on environmental conditions More development necessary evaluation requires high skill level.
Eddy current testing (ET)	Steel surface flaws. Virtually all conductive materials can be examined for flaws, metallurgical conditions, thinning, and conductivity.	Quick, versatile, sensitive, can be non-contacting. Able to detect flaws under coatings; easily adaptable to automation and in-situ examinations	Variables must be understood and controlled. Significantly more experience necessary.
Magnetic Particle inspection (MT)	All ferromagnetic materials, for surface and slightly subsurface discontinuities; large and small parts	Relatively easy to use Inexpensive Highly sensitive and fast compared to Penetrant testing (PT) Able to detect flaws under coatings or filled with corrosion	Only surface and a few subsurface discontinuities can be detected. Ferromagnetic materials only. Observation with at least two perpendicular orientations necessary; Requires more training.
Radiographic testing (RT)	Most materials, shapes, and structures. Examples includes welds, castings, composites, etc., as manufactured or in-service	Permanent volumetric record Defines shape and size. High sensitivity. Most widely used and accepted volumetric examination.	Optimized for flaws parallel to beam Requires safety precautions and training Requires access to both faces, Limited thickness based on material density.

Covermeter or Pachometer	Reinforcement location, measure depth of concrete cover	Simple Highly portable	Reduced performance with great depths or close spacing Does not indicate corrosion or fracture.
Magnetic flux leakage Radiography	Reinforcement location Measure diameter of bar and detect reduction of section of rebar	Able to detect even small flaws.	Limited depth.
Magnetostrictive sensor (MsS)	Detect fracture event and locate its position in long length of steel strands and cables	Non-contact sensing Long rang inspection inexpensive, simple to configure, install and operate Use for long term monitoring prestressed concrete structure Inspect physically inaccessible area, inspect larger diameter cables	Monitoring range in concrete is substantially limited (less than 3 meters)
Impulse response (IR)	Detect voids, delamination, honeycombing, cracking in concrete; depth of alkali silica reaction attack; debonding of asphalt and concrete overlays.	Robust (use on rough concrete surface) Fast output Repeatability of test results, economical for testing difficult access	Qualitative test Lack of confidence in accuracy of interpretation
Continuous AE monitoring	Detect and locate corrosion-induced failure in steel wire, strands and cables	Automated, cost-effective Use for inaccessible area Real time, user defined, on-demand generation of report global Establish rate of deterioration (locate future failure)	Cannot use for damage detection of structural rebars Needs continuous measurement Small likelihood of false report Requires permanent data acquisition system with sufficiently high sampling rate Does not provide any information before its implementation

5. Modal Testing

5.1 Introduction

Modal testing is non-destructive testing based on the vibration response of the structure. Its development in the area of health monitoring of civil engineering structures, including bridges, is comparatively recent. It consists of application of vibration to the structure and measurement of corresponding vibration response of the structure. Modal testing is the process of measuring the natural frequencies, damping, and vibration mode shapes of a structure. In the literature, the natural frequency, mode shape and damping value of a mode are referred as the modal parameters of a particular structure. Modal parameters are directly affected by the physical characteristic (mass, stiffness, and damping) of the structure and characterize the behaviour and condition of the structure.

The structure response to applied forces is given by Newton's Second Law, expressed mathematically as:

$$M\,a(t) + C\,v(t) + K\,d(t) = f(t), \qquad (5.1)$$

where M is mass; a(t) is acceleration at time t
C is damping coefficient v(t) is velocity at time t
K is stiffness; d(t) is displacement at time t
t is time; f(t) is applied force at time t

Any damage in the structure reduces the stiffness of the structure and this changes the vibration characteristic. Moreover, changes in the modal parameters may not be the same for each mode since the changes depend on the nature, location and severity of the damage. These characteristics make it possible to detect, locate and

quantify the damage by using data obtained from dynamic testing. Test conducted at different times provide data for monitoring of structural changes with time.

A given structure can vibrate at different natural frequencies, which are function of geometric parameters physical constants such as elastic modulus, density, Poisson's ratio, damping characteristics and support conditions.

Demeter (1973) suggested the relationship for a simply supported beam as shown in Equation 5.2. The various frequencies of vibration of the structure are directly related to the stiffness and the inversely proportional to mass of the structure (Equation 5.2). Consequently, as the structure deteriorates, the stiffness decreases and reduction in stiffness result in reduction in the frequencies of vibration, including the fundamental natural frequency, f_n

$$f_n = \frac{n^2\pi}{2}\sqrt{\frac{EI}{mL^4}} \tag{5.2}$$

where f_n is natural frequency, n is mode number, E is modulus of elasticity, I is second moment of area, m is mass per unit length and L is span length.

Since the frequencies of vibration of the structure are directly related to its stiffness

$$f_n \infty \sqrt{EI} \tag{5.3a}$$

$$f_n^2 \infty (EI) \tag{5.3b}$$

$$f_n^2 = A(EI) \tag{5.3c}$$

Differentiating Equation 5.3(c) gives,

$$2f_n \frac{\delta f_n}{\delta (EI)} = A$$

$$2f_n\delta\, f_n = A\ \delta\ (EI)$$

Substituting value of 'A' from equation (5.3c),

$$2f_n\delta\, f_n = \left(\frac{f_n^2}{EI}\right)\delta\ (EI)$$

Then,

$$2\left(\frac{1}{f_n}\right)\delta\, f_n = \left(\frac{1}{EI}\right)\delta\ (EI) \qquad (5.4)$$

From Equation (5.4), it is apparent that any change in the flexural rigidity (EI) would cause 50% changes in its natural frequency.

The modes of vibration involve the natural frequencies, damping coefficients, and corresponding mode shapes of structure. For each natural frequency, the vibration mode shape corresponds to the deflected shape when structure vibrates at that frequency. The mode shapes could be flexural, torsional, longitudinal, radial, diametrical and/or annular. Each vibration mode is associated with a damping value which is a measure of energy dissipation.

Two methods are used to detect flaws or damage in structures; (1) measurement of natural (resonant) frequency and (2) measurement of the rate of attenuation or damping.

In the natural frequency technique, natural frequencies are measured in the current physical condition of structure and compared to theoretical or earlier measurements recorded in undamaged condition of the structure. As dynamic response is sensitive to flaw present in the structure, any differences between these values indicate the extent of the structural damage. The deviation in

measured global vibration response of the structure must be correlated with the localized damage. This can be achieved by the local response parameter such as the mode shape data. In the measurement of attenuation or damping rate technique, the structure is vibrated in one of its natural frequency modes by a vibration pulse. The pulse is then stopped and the subsequent decay in vibration is measured. The specific damping capacity is determined from the decay curve. The damping coefficient increases with present of flaws in structure.

As mentioned earlier, the chosen modal parameter identified in the undamaged stage is compared with the same modal parameter in the damaged stage. Any change in the modal parameter indicates the nature and extent of damage in the system. Development of modal testing in health monitoring of civil engineering structure is comparatively new. Therefore, bridges built long ago do not have the data available in undamaged condition. In such cases, either modal based integrity assessment method, or the finite element modal updating method can be used (Mendrok et al. 2008). Figure 5.1 demonstrate the procedure of damage detection by vibration monitoring and the different steps involved in the detection procedure.

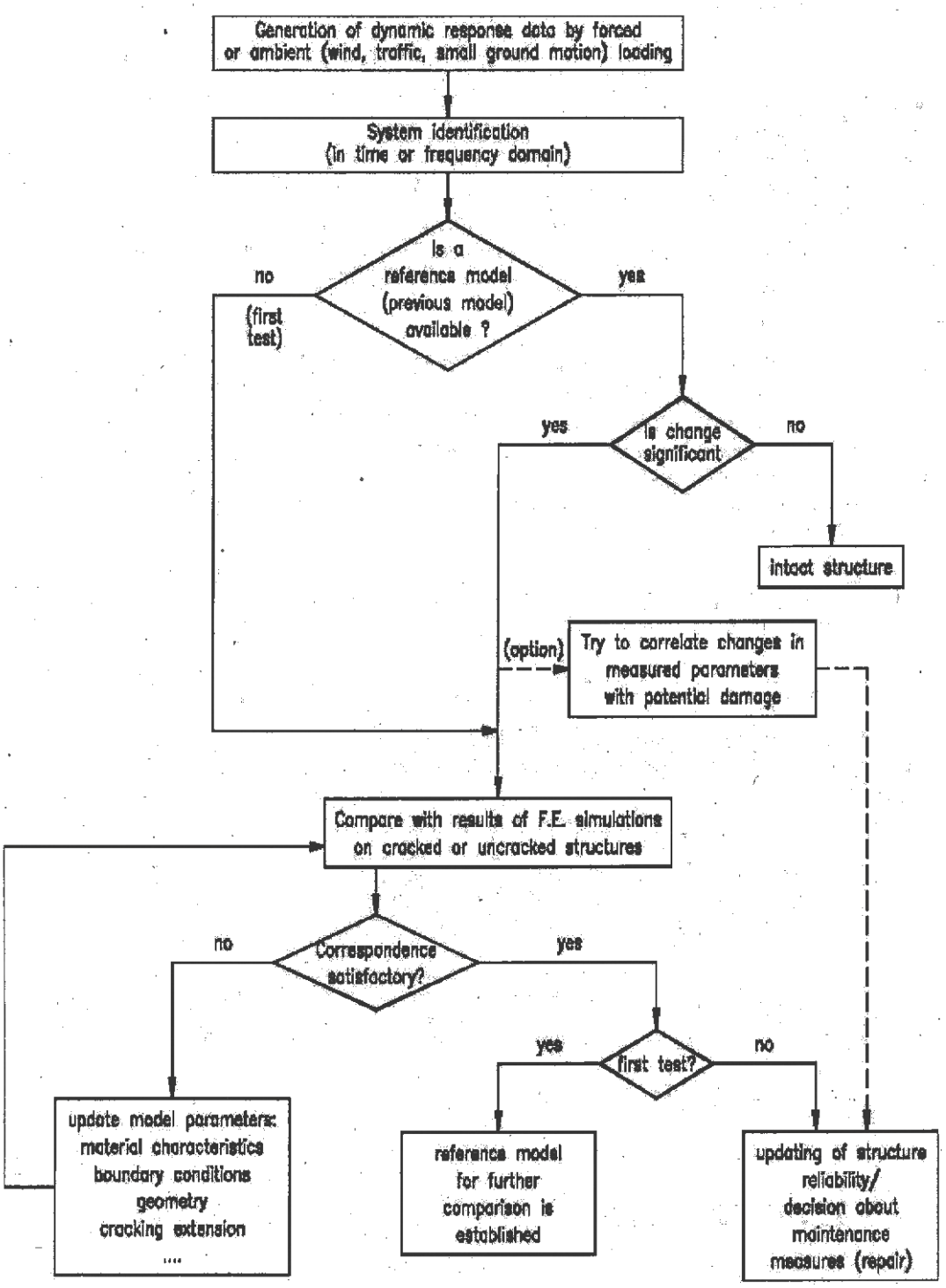

Figure 5.1 Detection procedure (De Roeck et al. 2000)

5.2 Type of modal test

There are two main types of modal tests generally carried out on bridge structure to identify t he modal parameters.

1. Forced vibration testing (FVT)
2. Ambient vibration testing (AVT)

5.2.1 Forced vibration tests (FVT)

FVT is based on the fact that if load on the structure is known and resulting response can be measured, it is possible to determine the structural properties. The structure is artificially excited with physical means, such as an impact hammer, vibrator exciter, eccentric or linear inertial shakers (Halling et al. 2001, Brownjohn et al. 2003), or dropped weights (Abdel Wahab and De Roeck 1998). Some practical methods to generate impact forces have also been found in the literature. The sudden release of a tension cable connected bridge to tug boat was used to generate horizontal impulsive force in the study by Delaunay et al. (1999). In a study by Huang et al. (1999), sudden braking of a truck at a specified location on a bridge was used to generate impact forces in the longitudinal and transverse directions while dropping of the rear wheel from top of the concrete block was used to generate vertical impact forces. Figure 5.2 shows some of the commonly used forced vibration test methods and equipment.

FVT provides more accurate values of the modal parameters than obtained with ambient vibration test, since the source of excitation is always under control, and it is also possible to enhance the response of the vibration mode(s) of interest. Furthermore, it is possible to excite only a local region of the whole structure.

This allows extracting the features sensitive to local structural response rather than the global behaviour of the system. This also facilitates to alleviate the environmental and operation effects.

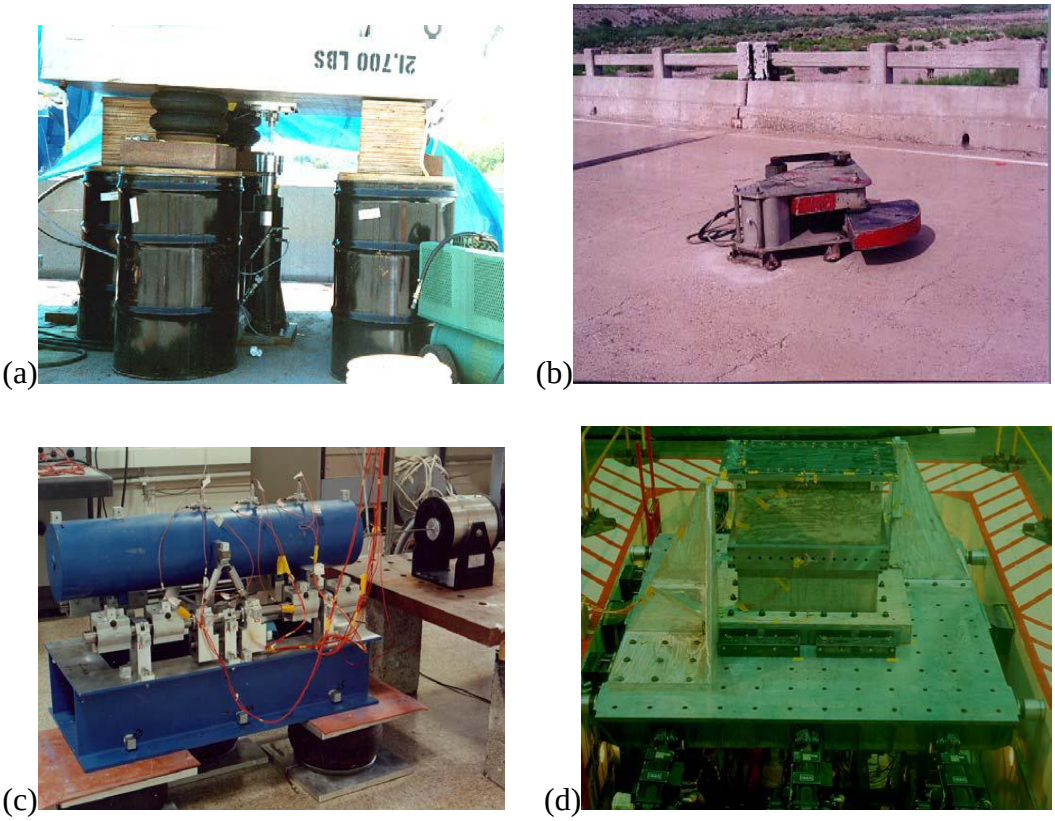

(a) A hydraulic shaker has a higher force capacity than electrodynamic shaker but limited high-frequency capability (b) Mechanical eccentric mass shaker generates sinusoidal excitation, but difficult to apply in vertical direction (c) An electrodynamic shaker, (d) A hydraulic multiaxis shake table

Figure 5.2 Different types of forced excitation methods (Sohn et al. 2003)

The main drawback with this test is that traffic need to be closed during the complete test period. This is a serious problem with heavy traffic bridges. In case of large and flexible bridges, it is difficult and costly to provide controlled excitation at a high level. In addition, the structural response is the result of all sources of excitation, therefore, to avoid many uncertainties in data collection and

processing and to determine the response corresponding to a known force, filtering is used to eliminate local noise. The forced vibration excitation amplitude can be kept higher than the ambient or electronic noise levels to isolate changes in the structure. These operations can be considerably expensive. Some examples of FVT can be found in the literature review in the next chapter.

5.2.2 Ambient vibration test (AVT)

Ambient vibration is the vibration/excitation that the structure experiences under its normal operating conditions. Since bridges experience continuous excitation from natural sources such as traffic, wind, seismic activity, waves, or tidal fluctuations, or ground vibrated by adjacent industries, or their combination; they are used for excitation of the structure and provide a very good alternative to FVT. No external means for excitation are used. Therefore, expensive equipment and procedure for excitation and isolation from local noise are not needed. Since the traffic is not disturbed during the test period, AVT can be used for long term continuous health monitoring of bridges.

Any variation in the external conditions such as ambient temperature, humidity etc may result in wrong diagnosis. The natural frequencies of the bridge decrease with the an increase in ambient temperature. This may cause frequency shift comparable with the one produced by minor or average damage. Therefore, it is necessary to determine the sensitivity of the structure to changes in the external conditions. Environmental filters can be used to eliminate influence of changes in weather conditions for efficient monitoring of the system (Peeters et al., 2000).

Since the input force cannot be measured, it is very difficult to know whether the input force is sufficient to excite the structure with the frequency of interest or the input force is uniform for a particular frequency range. In addition, FRFs (*FRFs is a transfer function and expresses the structural response to applied force as a function of the frequency*) or IRFs calculation is not possible and the test has to depend on output data only. Therefore, it is not possible to obtain an absolute scaling of the identified mode shape (mass normalization) (Peeters 2000). To overcome the problem associated with this unknown input force, an adapted modal identification technique can be used, where vibration accelerations are recorded at selected measuring points and one of these measuring points is used as the base or reference station; the signal of this base station is used as "input". The corresponding FRFs and coherence functions are computed for each response measurement point with respect to the base station. Wenzel and Pichler 2005 described a detailed treatment to ambient vibration monitoring. In fact, the ambient vibration modes are not always accurate since the input cannot be measured (Ren et al. 2004).

Factors, such as variability in amplitude, test duration, uncertain loading direction, frequency content, and difficulty in accurately measuring the excitation make this test less ideal. However, the literature reports more ambient vibration tests conducted on full-scale bridges than FVT's (Salawu et al. 1995). The list includes Tamar suspension bridge (Williams 1983), Spilje Lake bridge, Yugoslavia (Taskov 1988), Foyle Bridge, North Ireland (Sloan et al. 1992), Humber suspension bridge (Brownjohn et al 1987). Conte et al. (2008) also summarised the list of ambient vibration tests (AVT) successfully implemented on bridges

that include “Vincent Thomas suspension bridge (Abdel-Ghaffar and Housner 1978), Golden Gate suspension bridge (Abdel-Ghaffar and Scanlan 1985), Roebling suspension bridge (Ren et al. 2004a), Safti Link Curved cable-stayed bridge (Brown- John et al. 1999), Vasco da Gama cable–stayed bridge (Cunha et al. 2001), twin curved cable-stayed bridges on the north and south sides of Malpensa airport in Milan (Gentile and Martinez y Cabrera 2004), Brent-Spence truss bridge (Harik et al. 1997), and Tennesse River steel arch bride (Ren et al. 2004b)”.

5.3 Effect of structural damage on natural frequency

The natural frequency of vibration of a structure is sensitive to the structural integrity. Presence of damage or deterioration changes the natural frequency of the structure for that mode of vibration. Salawu (1997) summarized the influence of structural damage on frequency changes from the literature review which is reproduced here for completeness.

- The existence of crack at a section reduces the second moment of area at that cross section. This leads to reduction in bending stiffness at that cross section. The reduced bending stiffness decreases the natural frequency in bending. A decreases in natural frequency higher than the expected value indicate significant decrease in stiffness while increased in frequency higher than expected indicates support conditions stiffer than expected (Morgan et al. 1994).
- The natural frequency is directly proportional to the square root of the flexural rigidity (EI). Therefore, a large reduction in bending stiffness is

required for a significant change in natural frequency. Creed (2004) suggested that about 5% of change in the value of natural frequency is necessary for confidently detecting the damage in the structure. However, influences of ambient conditions affect the frequency. Aktan et al. (1994) measured the frequency shift of more than 5% in single day due to ambient conditions.

- Any change in the natural frequency depends on type of structure and the supporting base. If the natural frequency of the support is higher than the frequency of the test structure, any increase in stiffness of connection between them increases the natural frequency.
- At modal node (point of zero modal displacement), the stress is minimum for that particular mode of vibration. Therefore, any minor change in frequency indicates that flaw may be in the vicinity of the modal node.
- There is controversy on sensitivity about the mode of vibration to detect the damage. Moradalizadeh (1990), Slastan et al. (1993) and BrownJohn (1988) suggested that lower modes are more sensitive, or best suited for identification of damage. While Begg et al. (1994) and some other researchers suggest that higher modes are more sensitive to damage detection and provide sufficient information for health monitoring. However, Salawu et al. (1993) suggested that higher modes are not available with full scale structure; therefore, their use in damage detection cannot be fully justified.

- From the test on a concrete portal frame, Moradalizadeh (1990) found that reduction in the natural frequency depends on location of the defect relative to the mode shape for that particular mode of vibration. Reduction of up to 15% was measured with damage in highly stressed areas. Other researchers have also noticed the increased accuracy with damage in highly stressed region. These indicate that detection of damage with natural frequency alone may not give reliable results when damage occurs in low stress region. Thus, change in natural frequency alone may not give sufficient information regarding integrity of structure unless damage occurs in critical load bearing member.
- Alocco et al. (1993) noted that reduction of about 50% of pre-stressing force was not detected by change in the natural frequency. This can be explained by the fact that reduction in pre-stressing force reduces only the load level at which tension opens the crack. Any loading below this load level may not change the frequency. Kato and Shimada (1986) monitored the change in the natural frequency during the failure process of a pre-stressed concrete bridge. They observed very little or no change in the natural frequency due to a crack when the stress in the pre-stressing wire is within elastic limit. When the wire stress exceeds the elastic limit, sudden decreased in natural frequency was observed and it continued to decrease until failure of the bridge.

5.4 Factors affecting the natural frequency for damage detection

Some of the factors to consider when using a natural frequency for damage detection are discussed from literature review.

- Non-controllable variables like **environmental conditions, excitation techniques, data acquisition parameters, data processing methods, and human factors** influence the test result and lead to wrong diagnosis of test result (Ndambi et al., 2002). The natural frequency decreases with increasing temperature. Xu and Wu (2007) also concluded that ambient temperature in an important factor that affect the modal parameter.
- From the analysis of 4 pre-stressed concrete bridge decks, Purkiss et al. (1994) concluded that the deck **soffit temperature** is the most significant variable that affects the vibration response. The natural frequency decreased gradually with increasing soffit temperature and the variation in temperature is not related to time.
- **Added mass due to deck rehabilitation** lower the longitudinal bending frequencies.
- Modal parameters are sensitive to change in **support conditions**. Zhang (1994) noted erroneous results when dynamic response was measured at abutment, pier and other types of support.
- **Consistency and reliability of test procedure** can affect the test result.
- **Operating condition** affect the modal properties. Alampalli (2000) noted significant variation in the modal frequency above and below **freezing temperature**. The damaged modal frequency of the damaged structure

decreased from the undamaged frequency above the freezing temperature, indicating a loss of stiffness. However, below the freezing temperature, damaged modal frequency significantly increased from the frequency in the undamaged condition, indicating an increase in structural stiffness. This could be explained by the fact that freezing of accumulated moisture might have fixed the end of the support. In reality, seasonal changes do not adversely affect the structural integrity but lead to an incorrect diagnosis.

- Ismail et al. (1990) describe that decrease in modal frequency is also affected by the **residual stress**.

5.5 Suggested guidelines

Some of the guidelines for better performance of modal tests are suggested in the literature include the following:

- When planning modal test on bridges in the field, one should consider changing weather conditions, power supply efficiency, sensor placement and their attachment technique, handling of long wires without tangling them, etc.
- There are many variables associated with the environmental factors. This makes it impossible to establish quantitative relationship between modal parameter and environmental factors. Therefore, it is important to develop threshold value of modal parameters beyond which existence of damage can be detected (Salawu 1997).

- Different types of sensors are available for acquiring data. This includes accelerometers, velocity transducers, displacement transducers, strain gauges, tilt meters and weather related sensors to measure and record temperature, humidity, barometric pressure, wind velocity, wind direction, etc. User should select appropriate sensor(s) according to the test conditions.
- Global sensors can detect the change in global structural properties, however, local sensors are required to identify the changes in local properties. For this, substantial analysis and investigation of the structure is required before placing the sensors. Knowledge of type and location of expected damage, analysis and appropriate placing of sensor can be helpful in successful monitoring of the structure, or detecting damage
- Pavic et al. (2002) strongly recommend the use of frequency response function (FRF) measurement, whenever possible, for performing modal testing on large civil engineering structures. This should be followed with an appropriate FRF curve-fitting and evaluation of estimated modal properties.

5.6 Application

Modal testing has been used extensively in testing aerospace and offshore structures. Its application in civil engineering is comparatively new and includes:

1. Monitoring of the overall behaviour of structure by regular inspection.

2. Determination of the integrity of structure after occurrence of overload either due to military manoeuvre, higher environmental loading or natural disaster.
3. Determination of the type of loading, if the nature of loading causing overload is not known (Tsang et al.1988)
4. Validation of the theoretical model of structure
5. Increasing the database of similar structure to predict the response of new structures (Salawu and Williams 1995b).

5.7 Advantages

1. Modal parameters are obtained easily and inexpensively from the measured vibration response.
2. Global in nature and automated.
3. Dynamic characteristic can be measured at one point of the structure and are independent of location of sensor.
4. Location of damage need not to be known in advance as in case of other NDT method.
5. Sensors need not to be located in the vicinity of the damage and a limited number of sensors are often sufficient to detect, locate and quantify the damage.

5.8 Limitations

1. Requires base line (reference) measurement. Dependent on the results from prior analytical model and/or prior test data for comparison. In most cases, as structures built long ago, the modal parameter (natural

frequency) of as-built structure is not available. The lack of availability of such data makes this method impractical.

2. Modal testing may produce variable results on repetition. This is due to influences of ambient conditions such as the environment, electrical disturbance, etc.
3. For large structures, it is required to apply a large imposed load that is costly and in some cases even not practical.
4. As natural frequencies are global properties of structure, it is hard to identify damage of level 2, level 3 and level 4.
5. Natural frequency changes alone may not be sufficient for a unique identification of the location of the structural damage. Cracks associated with similar crack lengths but at two different locations may cause the same amount of frequency change.
6. It is usually difficult to obtain the obvious and accurate mode shape with some stiff civil structures.

5.9 Comparisons with other wave-based NDT methods

This section discusses the comparison of modal test with other wave based non-destructive test methods such as Impact-echo and acoustic emission. **Impact echo method** is based on the transient stress wave generated by an elastic impact, generally used to detect the voids and loss of bond at steel-concrete interface, but it can detect the voids above the upper surface of the steel bars; however, it is difficult to detect the loss of contact on the underside of a bar. By increasing the duration of the impulse, the bars can be made invisible and voids beneath the

reinforcement can be detected. However, the use of long duration impulse limit the detection of void sizes greater than the size of the bar diameter. Furthermore, the effects of lateral boundaries of the structure under investigation produce systematic errors in determination of thickness and flaw depth.

Acoustic Emission (AE) is based on the analysis of sound waves generated by the local stress redistribution. As the material is loaded, the loaded area may be strained beyond its elastic limit, and crushing or micro-cracking of concrete may occur. The kinetic energy released propagates elastic stress waves throughout the specimen. The Kaiser effect (Bungey 1996) is used to detect crack propagation. This means that if a material has been stressed to some level, no emission will be detected on subsequent loading until the previously applied stress level has been exceeded.

With respect to bridge inspections, AE has capability of in-service inspection; the equipment is not affected by extensive rough surfaces since the transducer contact surface is small and requires minimal preparation of the structural component surface. AE can detect active and propagating flaws; however, data interpretation can be difficult for complex geometrical structures. Main difficulties arise from two sources:

(1) Vehicular traffic cannot generate reliably meaningful response from the structure, and

(2) At the level of the significant acoustic response, noise is hard to filter.

Some of the NDT techniques are summarized in Table 4.1. As described above, wave-based NDT methods such as impact-echo and acoustic emission are

localized experimental methods and require that the vicinity of the damage is known in advance, and that the portion of the structure being inspected is readily accessible. They cannot be applied to complex structures. Modal testing seems to be good alternative as it is global in nature, automated and independent of location of the sensor. Modal parameters can be measured easily, and the sensor need not be placed in the vicinity of the damaged region, therefore, the location of damaged region need not be known in advance.

6. Literature Review – Modal Testing

Visual and other localized non-destructive testing techniques require that the location of the damage must be known before testing and part of the structure under testing must be accessible. Dynamic testing is global in nature, and has generated considerable interest among researchers. Application of modal testing in health monitoring and condition assessment of civil engineering structure is relatively new. Salawu (1997) reported that the first application of dynamic testing for assessment of civil engineering structures may be in the field of pile integrity testing. Salawu et al (1995) noted that dynamic testing on bridges have been carried out since late 19^{th} century. Since 1979, many test techniques have been developed for detection, localization and quantification of damage. Humar et al. (2006) describe the various analytical techniques that have been developed for the identification of damage using vibration testing. They are

1. "Methods based on frequency changes.
2. Methods based on mode shape changes.
3. Mode shape curvature method.
4. Methods based on change inflexibility matrix.
5. Methods based on changes in uniform flexibility shape curvature.
6. Damage index method.
7. Method based on modal residual vector.
8. Matrix updates methods.
9. Neural network methods."

Doebling et al. (1996) provide the first comprehensive review of dynamic test methods for damage detection and their application to various structures including bridges. Doebling et al. (1998) also provide a summary review of vibration-based damage identification methods and suggest some critical issues related to them for future research in the field of vibration-based structural identification and health monitoring. Sohn et al. (2003) updated the previous work done by Doebling et al (1996) and added a review of new work published between 1996 and 2001 in this field of structural health monitoring. Rytter (1993), Hemez (1993), and Kaouk (1993) covered literature surveys in their doctoral theses. More recent works have also been published in the proceeding of various conferences and workshops on structural health monitoring. However, a majority of works are on laboratory experiment and development of analytical models. Only a few case studies have been reported in literature on modal testing of full-scale bridges (Huth et al. 2005). The main reasons explained by Pavic et al. (2002) are:

1. Applications of modal testing to full-scale civil engineering structures is a difficult task,
2. It is still a subject of more research rather than design tool for civil engineering structures, and
3. Occasionally, civil engineering community is not confident to apply this test technique.

Salawu et al (1995) pointed out the reasons for conducting full-scale dynamic testing and reviewed full-scale dynamic testing of bridge structures as follows:

1. It increased the database on dynamic behaviour of similar type of structures. This database can be used to determine the behaviour of similar type of new structure. This data can also be used in evaluation and improvement of the current analytical methods.
2. Some assumptions, mainly related to the boundary conditions are made in the mathematical model. More accurate model is required for proper prediction of behaviour of structure. Data from the full-scale structure can be used to validate the theoretical model prepared for that particular structure.
3. It can be used to determine the integrity of structure after occurrence of overloading such as military manoeuvres. It can also be used to determine the type of overloading when nature of loading causing the overload is not known.
4. Structural integrity can be assessed when the structure is subjected to either change of use, or higher environmental loading, or increased in previously allowable loading.
5. Overall structural performance can be monitored by regular measurement of its dynamic response.
6. It can be used to verify the behaviour of the structure as expected in design, just after the completion before open to traffic.

While significant research has been undertaken related to damage detection, localization and quantification using modal testing, a majority of the work is based on laboratory experiments and development of algorithms. Humar et al

(2006) reported that their success is limited and cannot be translated into practice. Therefore, they are not included in this review except those, related to experimental work described in this thesis. An effort has been made to include papers that are based on full-scale dynamic testing of bridge structures. However, some of the useful papers that were not available to the author could not be reviewed here.

Cunha et al. (2006) presented the development of experimental modal testing on large civil engineering structures, such as bridges and dam. Basic theory, equipment and test procedures associated with various modal identification techniques (forced vibration, ambient vibration and free vibration) were described, along with examples of large civil engineering structures.

Humar (2006) reviewed some of the principal methods commonly used for damage identification. He has also presented some practical problems commonly associated with vibration–based condition assessment. The success and loop of these more commonly used algorithms were evaluated through computer simulation studies. He concluded that few methods have performed well in the "idealized case study" and can be applied in the field.

Razak et al (2001) studied the effect of general corrosion on modal parameter; natural frequency and modal damping of reinforced concrete beams. Two beams were deteriorated by inflicting general corrosion to different degree of corrosion. The level of corrosion was determined by visual inspection, measurement of crack

width and spalling. Modal test was performed on both corroded beams and one control beam. Test results obtained from modal testing of corroded test beams were compared with that obtained from the control beam. They also conducted a static load test to determine the load carrying capacity and the results obtained were correlated with the severity of corrosion damage and change in modal parameter. The test results showed significant change in the natural frequency and the damping ratio. The changes were consistent with the level of corrosion damage induced and the load carrying capacity. The author also confirmed that magnitude of change in the natural frequency increases with higher modes as suggested by Proulx et al. (1992). The authors observed change in the damping ratio for the transfer function method and the normal mode method. They found results which were different from those observed by the previous investigators (Kato et al, 1986 and Salawu et al 1995). The author observed consistent trends, for second and third modes, with the severity of the corrosion damage in the test beam. The inconsistency in the damping ratio for the first mode can be explained by the fact that at the early state of corrosion, the bond at the steel-concrete interface increases due to accumulation of rust product compared to uncorroded beam.

Ndambi et al. (2002) studied the damage assessment in reinforced concrete beams using eigenfrequencies, Modal Assurance Criterion (MAC) and Coordinate Modal Assurance Criterion (COMAC) factors, damage indices and change in flexibility matrices. The beams were subjected to progressive cracking by static loading such that damage could be introduced in symmetric and asymmetric

positions. Test result showed that eigenfrequency is sensitive to the accumulation of cracks but the eigenfrequency alone is not adequate to locate the damage. The decrease in eigenfrequency is monotonic with the severity of damage compare to MAC factor; MAC factor is relatively less sensitive to crack damage and is not monotonic in nature. It can identify the symmetrical or asymmetric nature of damage but it cannot localize the damage. A change in flexibility matrix may detect the damage but it is very hard to localize the damage. The test results showed that the COMAC factor and damage indices both could localize the damage but in case of local damage, damage indices technique localized the damage more precisely compared to COMAC factor.

Ndambi et al. (2000) studied the influence of different excitation devices on modal parameters. Impact hammer and two electro-magnetic shaker signals, namely, pseudo-random and swept-sine signals were used to excite reinforced concrete test beams. The results showed that both pseudo-random and swept-sine excitation techniques gave almost the same resonant frequency with a maximum difference of 0.5%. The impact technique resulted in about 2% lower natural frequencies than the other two excitation techniques. This difference may be due to the influence of mass of the shaker that makes the structure comparatively more rigid. The authors also studied the influence of non-linear behaviour of the concrete. They performed modal analysis at different excitation amplitudes using the swept-sine excitation. The test results showed that with increasing excitation amplitude, resonant frequencies decreased and the modal damping ratio increased.

However, it was observed that its influence on resonant frequency and mode shape was negligible compare to modal damping ratio.

Kim et al (2003) presented two methods, namely the frequency-based damage detection (FBDD) and the mode-shape-based damage detection (MBDD) method, to nondestructively locate and estimate the size of damage in beam-type structures for which only a few (two) natural frequencies and/or a few mode shapes are available. They formulated a damage-localization algorithm to locate the damage and a damage-sizing algorithm to estimate the crack-size from changes in the natural frequencies. A damage index algorithm was also formulated to localize and estimate the severity of the damage from monitoring changes in modal strain energy. The author suggested that for FBDD method pre-damage and post-damage natural frequencies, and pre-damage mode shapes are needed. For MBDD method pre-damage and post-damage mode-shapes and natural frequencies are needed. Both FBDD and MBDD methods were evaluated for six damages scenarios in numerically simulated pre-stressed concrete beams, for which only two sets of modal parameters (pre- and post-damage natural frequencies and mode shapes) were available. The test results showed that MBDD method located the damage accurately. The FBDD method could also locate the damage but with a smaller error. Both methods accurately estimated the size of the cracks located at mid-span but the accuracy decrease for cracks located at quarter span.

Kim et al (2003) suggested a temperature correction scheme to adjust the modal data affected by temperature. Other environmental parameters were not

considered. A laboratory experiment was performed on a single-span, stainless steel, plate-girder bridge model (Figure 6.1). A modal test was conducted at various temperatures in undamaged condition. The relationship between temperature and natural frequencies was established. Using the temperature-frequencies correction formula, baseline frequencies in undamaged condition was adjusted for various temperatures. The modal test was also performed in post-damage condition at fixed temperature. A frequency-based damage detection algorithm was applied to locate and estimate the severity of damage. The temperature correction scheme accurately determined the location and severity of the damage at some temperature conditions of pre-damage and post-damage natural frequencies.

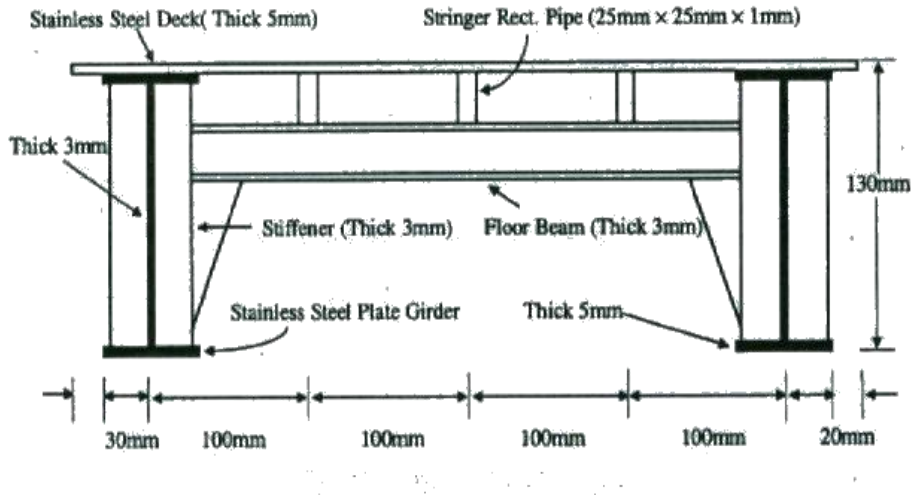

Figure 6.1 Model Plate-Girder Bridge (Kim et al. 2003)

Xu et al. (2007) studied the effect of change in environmental temperature caused due to seasonal weather, i.e., a uniform temperature change, and due to sunshine radiation i.e. asymmetric temperature change on modal parameters through numerical analysis of frequency and mode shape curvature in a cable-

stayed bridge without cracks. They compared the change in natural frequencies and mode shape curvatures due to difference in environmental temperatures with the change due to damage. The test result showed that the change in frequencies and mode shape curvatures due to changes in temperature was more than observed due to small and medium damage. Only in case of heavy damage, change was "comparable" to change due to the temperature change. However, no change in the sequence of mode shape was reported. The changes in frequency occurred in the vertical bending mode, while change in the mode shape curvature was observed at mid-span and one-forth span of central span, and at mid-span of the side span.

Roeck et al. (2000) studied the effect of the environmental conditions, particularly temperature, on modal frequencies of **Z24 Bridge** (Figure 6.2). The test result showed that the changes in temperature influence modal parameters and treatment by proper system identification algorithms can provide accurate values for modal parameters, mainly eigenfrequencies and mode shapes. The various progressive damages tests (PDT) were also conducted on Z24 bridge structure to examine the sensitively of both eigenfrequency and mode shape to relative damage scenarios. Only damage scenarios reducing the stiffness could be identified. The eigenfrequency was more sensitive to the damage than the mode shape. However, mode shapes provided useful information regarding the local changes.

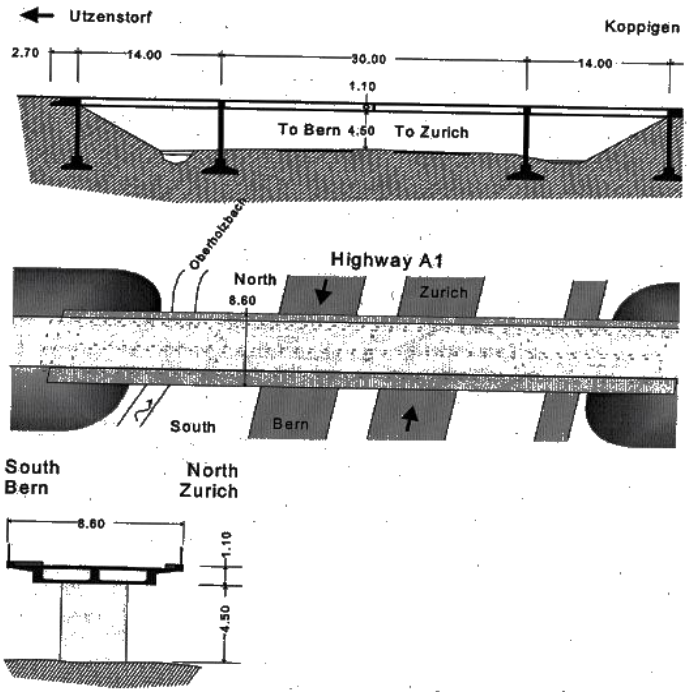

Figure 6.2 Top view, cross-section, elevation of Z24 (Roeck, 2000)

Farrar et al (1997) studied the influence of change in day time temperatures, sources of excitation and service conditions, such as extent of the traffic load on natural frequency and mode shape of the **Alamosa Canoy Bridge** - a two-lane, seven-span, composite slab- on-girder bridge (Figure 6.3). They reported about 5% variation in frequencies during 24 hours time period. Ambient vibration test and impact test were conducted at the same time of day to minimize the temperature effects. Variation in the natural frequencies and the value of the damping ratio were recorded. No difference was noted in the mode shapes. The difference in modal frequency was also observed due to added mass of traffic vehicle. Moreover, without any specific analysis, the authors reported from their own experience that the type of algorithm that was applied for modal parameter identification and the analyst, who was applying it, may influence the data

reduction process but this effect is significantly smaller compared to environmental effects in the case of the forced vibration test.

Figure 6.3 Alamosa Canyon Bridge (Farrar et al.1997)

Kim et al (2003) described the non-destructive crack detection (NCD) algorithm to locate the crack and to estimate the size of the crack directly from the change in the model parameters. The damage-index method and crack-sizing method were used respectively, to locate the damage from mode shapes and to estimate the crack size form the natural frequency. They also demonstrated the feasibility of applying this NCD algorithm to a full scale plate-girder bridge (Figure 6.4) in New Mexico over the Rio Grande River on U.S. Interstate Highway 40. The test results demonstrated that cracks could be localized with small error whereas crack size could be estimated accurately.

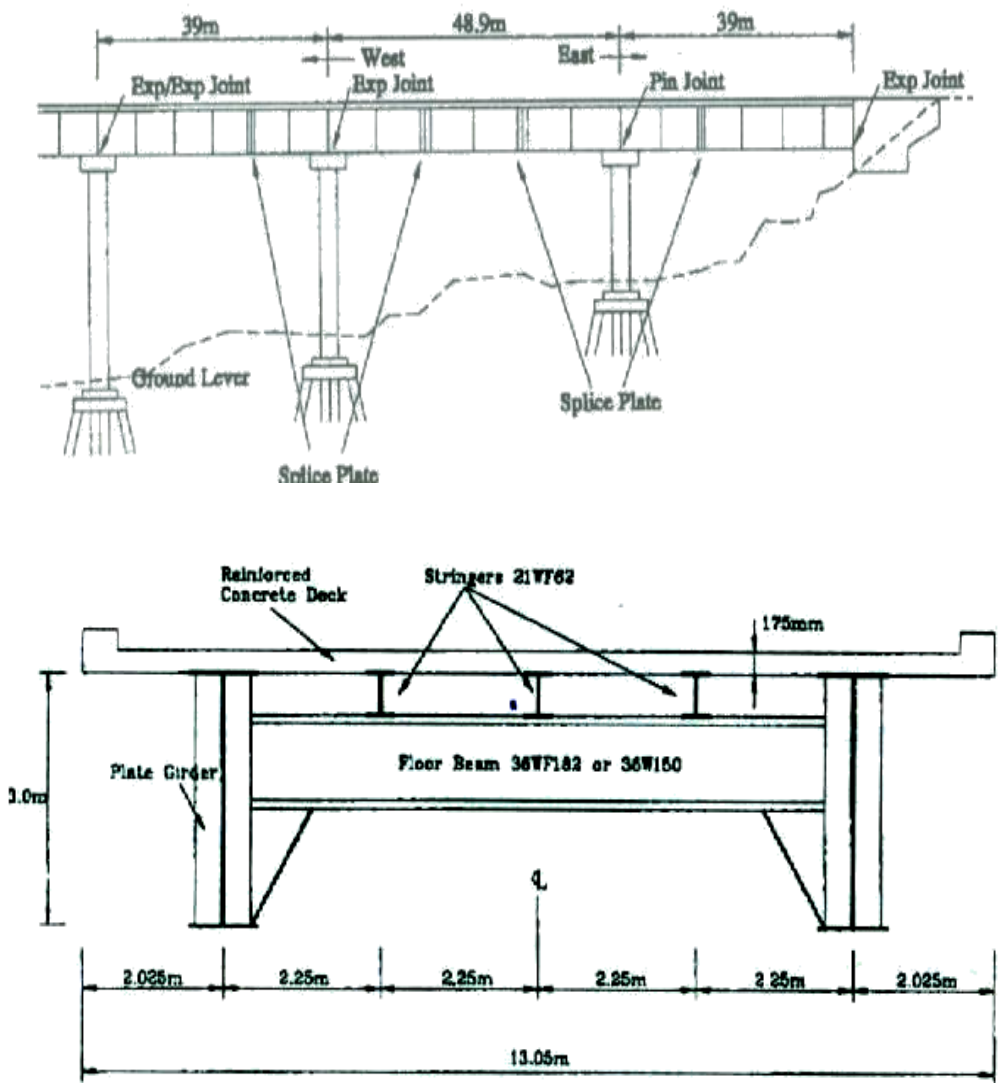

Figure 6.4 Schematic of Plate-girder test bridge (Kim et al 2003)

U.S. Grant Bridge (Figure 6.5) over the Ohio River in Portsmouth was replaced by a cable stayed bridge with steel girders and post-tensioned concrete deck system. This new replacement bridge was designed for a 100 year design life. Vibration testing has been used in design and construction phases, and also for condition assessment throughout service life. **Sexton et al (2005)** described quantifying cable tension by vibration measurement technique - fundamental

frequency using wind, rain and traffic –induced vibration. **Hunt et al (2005)** presented the instrumentation plan and field testing to monitor its performance during construction, for both fabrication and erection phases, and also to study the long term behaviour and any associated changes in its structural condition. The key variables for monitoring include weather conditions, cable acceleration, acceleration of selected deck sections, and longitudinal stress of selected exterior girder and deck section at abutment, pylons and mid-span in response to thermal, wind and traffic load.

(a) 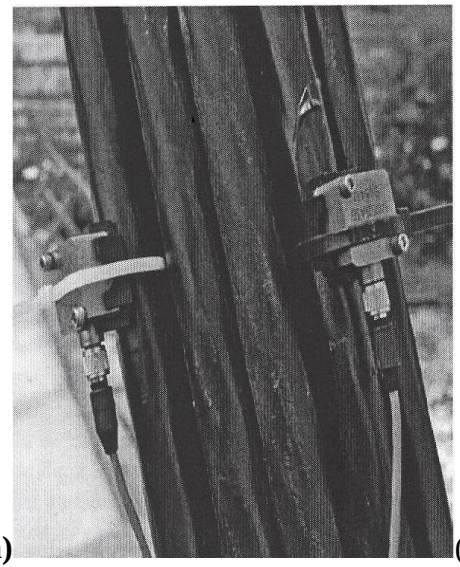 (b) 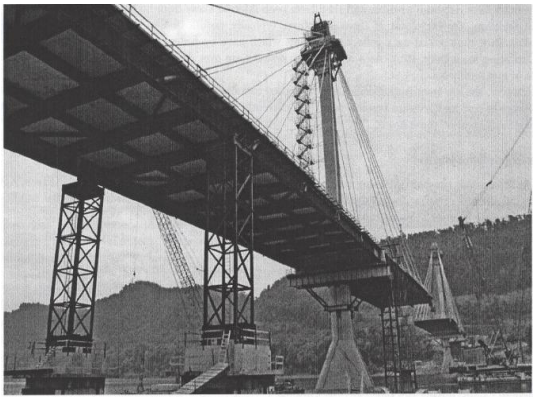

Figure 6.5 (a) Accelerometers mounted on a U.S. Grant Cable Stay; and (b) The partially completed U.S. Grant Bridge (As viewed from the North, August 2005)
(Sexton et al 2005)

Huth et al. (2005) reported a modal test on **Romeo Bridge,** Lucerne, Switzerland - a pre-stressed concrete box girder bridge (Figure 6.6), to study the feasibility of identifying early stage damage (the sensitivity of damage detection, localization and severity on modal parameters) in pre-stressed concrete bridges. The bridge

was artificially damaged by lowering the superstructure at the one of the abutment and by applying loading with hydraulic jacks at middle of the other span. The bridge was monitored to study the temperature effect on modal parameters. The correlation between long-term changes of natural frequencies with that of temperature was established. Several damage identification methods, e.g., natural frequency, mode shape, modal assurance criterion (MAC), change of the mode shape area, changes of the flexibility matrix, sensitivity based model updating methods, and direct stiffness calculation were used to examine their performance as damage detection, localization and quantification. Analysis of the test result showed that none of the applied technique was able to reliably detect, localize or quantify the damage at the early damage stage of a pre-stressed bridge. It was observed that modal parameters were slightly affected even at a significant level of damage. This may be due to recovery of the stiffness loss on closing of the cracks after unloading and also due to the effect of environmental parameters.

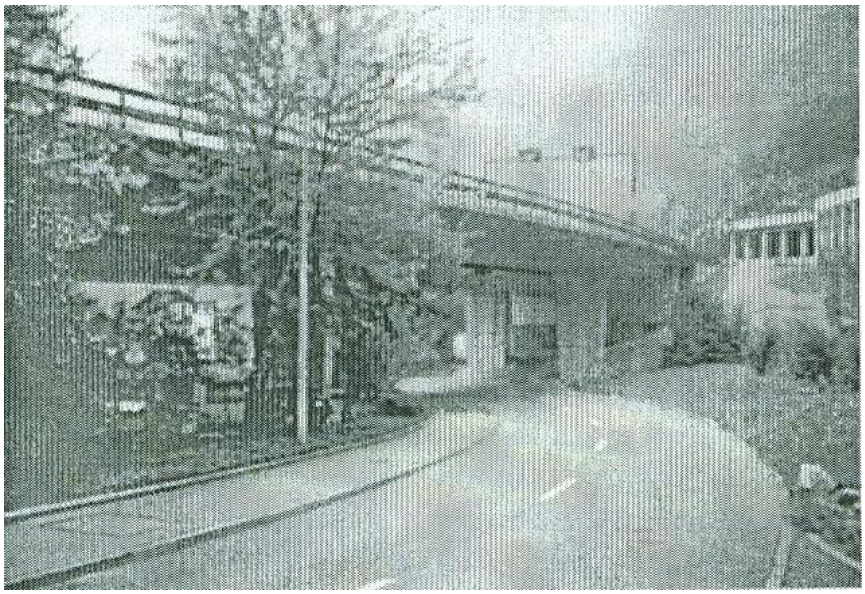

(a)

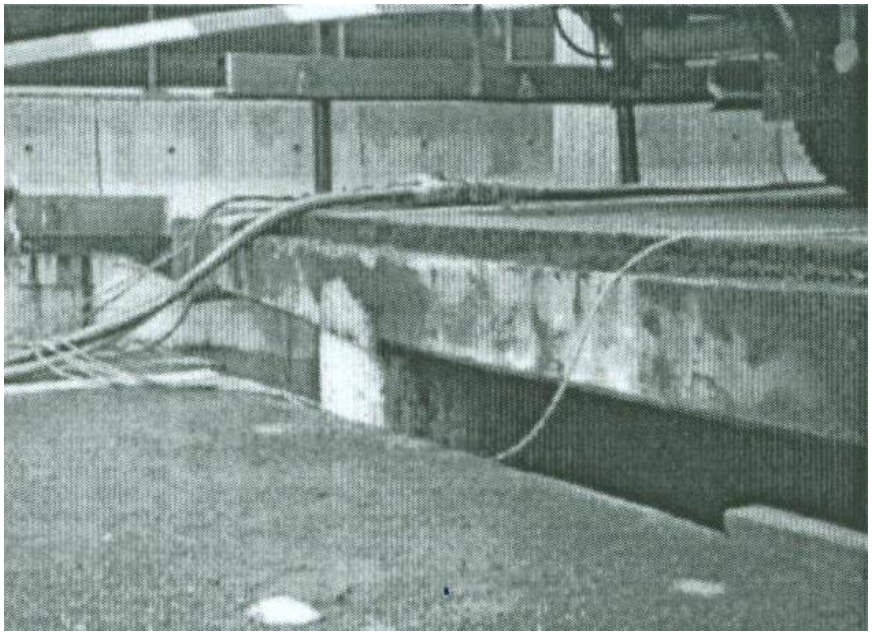

(b)

Figure 6.6 (a) Side view of Romeo Bridge; and (b) Maximum settlement of 59.2 cm at the northern abutment during the first damage scenario (Huth et al. 2005)

Pavic et al (2002) described the problem created with the newly constructed **Millennium Bridge, London**; a shallow suspension foot bridge (Figure 6.7), and the methodology based on modal testing applied as a retrofitting solution of the excessive lateral sway vibration of deck. Measurement of FRF's on the Millennium Bridge, London, was the key part of the retrofitting solution to identify the cause of this excessive lateral sway of the bridge deck and to quantify its dynamic excitation. Modal testing was also used in design and verification of the system that was going to be installed on the bridge to control the vibration to acceptable levels. The test showed that it was possible to measure good quality FRFs around a frequency as low as 0.5 Hz that was the natural frequency of first lateral mode of vibration.

Figure 6.7 Millennium Bridge, London

Hsieh et al. (2006) summarized three basic approaches – forced vibration, ambient vibration and free vibration – normally used in vibration testing. They also suggested guidelines for selection of sensor. Three case studies on structural heath monitoring are presented. Long term instrumentation was installed on **I-80 Flyover Bride** (Figure 6.8), 21st South Interchange of I-15 in Salt Lake City; to monitor changes in the dynamic behavior of the bridge on a daily basis. Both forced vibration and ambient vibration techniques were applied to obtain the frequency data. The data recorded in June 2001, for both test techniques showed an average difference of 0.9%, with largest difference of 3.12% for mode 2. The average difference of 4.4% between the lowest mean value and the largest mean value for first 10 modes was recorded with a maximum difference of 8.3% for mode 1 between June 2001 and April 2004.

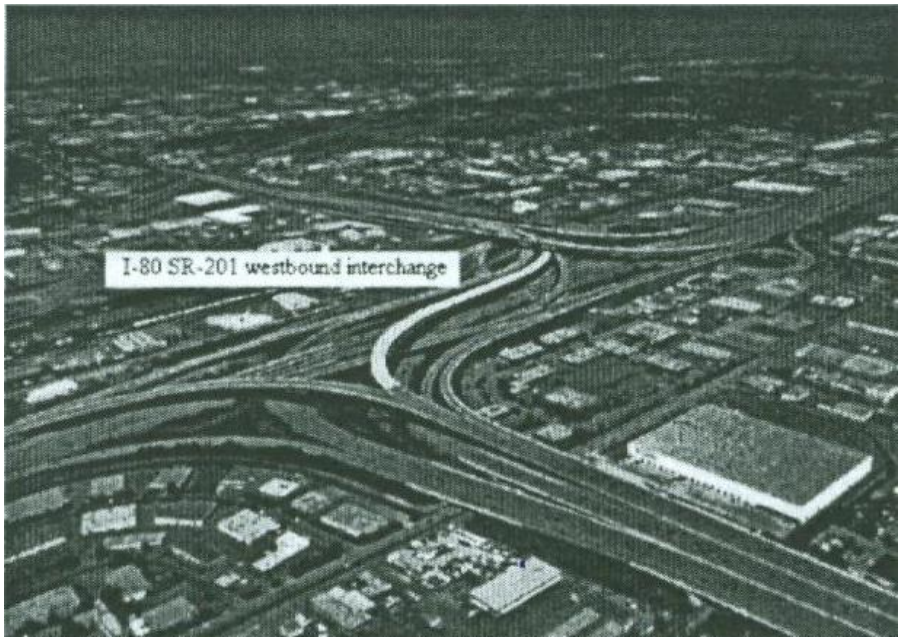

Figure 6.8 Aerial View of I–80 Flyover Bridge (Hsieh et al. 2006)

Forced vibration test was carried out on **South Temple Bridge,** South Temple Street, Salt Lake City; to assess the structural integrity of bridges. The test was performed for seven different conditions that were obtained either by damaging or repairing of the bridge. An eccentric mass shaker was used for excitation. The test results showed that natural frequency increases or decreases, with degree of retrofit or damage, respectively.

Forced vibration and live-load testing was performed on **I-215 bridge,** south Lack City; a continuous three span, welded curved steel plate girder bridge (Figure 6.9) to determine the feasibility of both testing techniques for condition assessment. The test was performed under two different boundary conditions. Firstly, the concrete bridge deck and parapets were completely separated from the bridge abutments and the integral approach aprons; and secondly, "restraints" at the girder support locations were reduced. An eccentric mass shaker was used for

dynamic excitation. For live load testing, loaded trucks were slowly driven along pre-determined routes. The test result showed that the frequency for each mode shape reduced with reduction in restraint of the bridge. The result also indicated that forced vibration test was much more sensitive to changes in boundary conditions of the curved girder steel bridge in comparison to the live-load test.

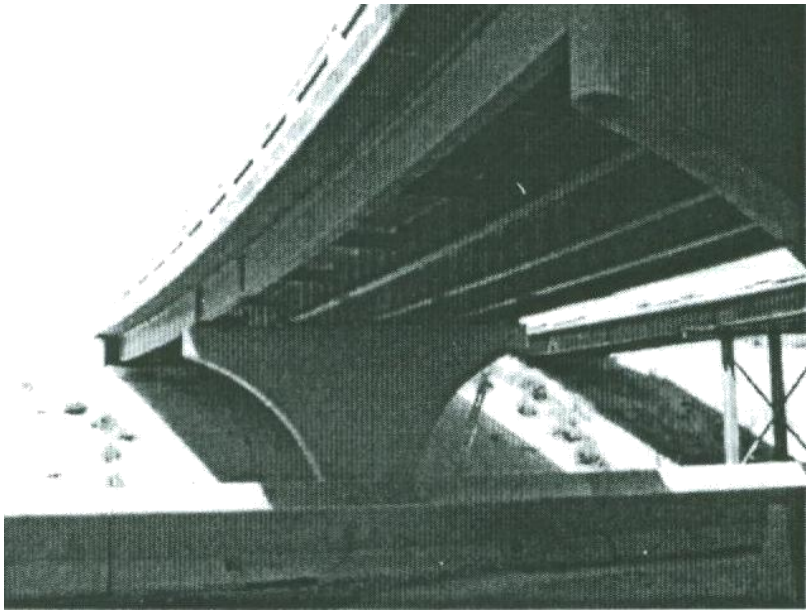

Figure 6.9 I-215 Curved Girder Bridge (Hsieh et al. 2006)

Salawu (1997) study the effect of repairs on the 4-span reinforced concrete **Holway Road Bridge**, Taunton, Somerset, United Kingdom (Figure 6.10). He is the first investigator to use dynamic testing before and after installation of a new bearing. The natural frequency, mode shape and damping ratio were measured before and after installation of new bearing and compared. The frequency response function (FRF) gave some indication of changes in the structure. The natural frequency did not change significantly by replacement of the bearing. The maximum natural frequency changed by about 4%. The change in the damping

ratio was reported at about 21%. The test result showed a lower vertical stiffness of the new bearing than the one originally designed.

Figure 6.10 Holway Road Bridge (Salawu 1997)

Robinson et al (2000) performed forced vibration tests on full scale, six-span reinforced concrete bridge for its condition assessment (Figure 6.11). An eccentric mass shaker was used to excite the test bridge. The bridge was intentionally damaged for three different conditions. About one-fourth of the cross-section of one of the column and about one-third of the cross-section of one more column was removed respectively, as the first and second damaged state and one of the piles was removed from the pile cap as the third damage state. Modal testing, especially natural frequency and mode shape testing was carried out prior to and after each damaged state. The test results showed a decrease in the natural frequencies and also changes in the mode shapes of the structure with an increasing level of damage. However, they were not able to correlate the change

in modal parameters to localize the damage. The changes in the mode shapes were global changes, and not local changes.

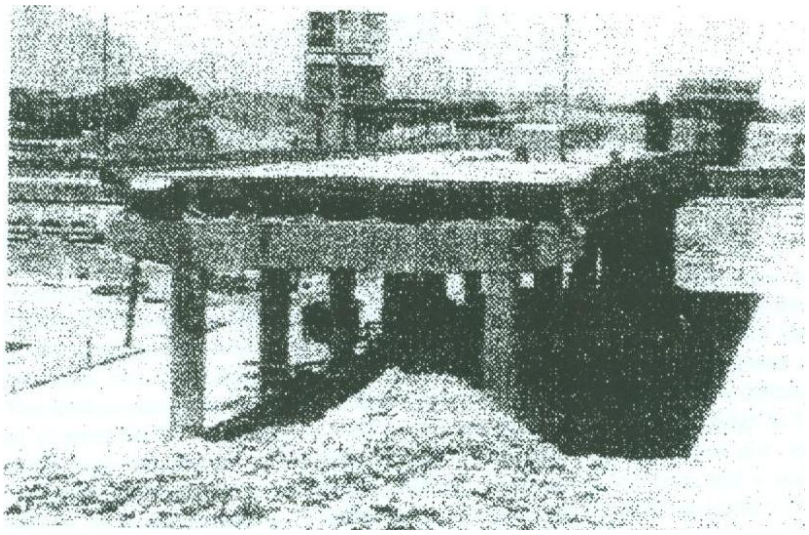

Figure 6.11 5th South Viaduct, Salt Lake City (Robinson et al 2000)

Ren et al (2004) present the methodology for evaluation of load carrying capacity of the historical **Roebling Suspension Bridge** (Figure 6.12) over the Ohio River between Covington, Kentucky, and Cincinnati, Ohio, relative to current safety standards. Dynamic properties were determined using ambient vibration testing and used to modify the three dimensional finite element model by adjusting the FE model stiffness parameters to correlate the FE model frequencies with ambient test frequencies to represent current bridge properties; material properties, cross sectional properties and additional extreme live loading. The cable area was also reduced by 10 to 40% to estimate the safety margin against future deterioration and corrosion of the cables. The test results demonstrated that even though cross-sectional area of cable was reduced by 40%, safety of main cables and forces in the truss member remained within the range of maximum load carrying capacity.

Figure 6.12 Roebling Suspension Bridge (Ren et al 2004)

Conte et al. (2008) described in detail the set of dynamic field tests conducted on the **Alfred Zampa Memorial Bridge** (Figure 6.13)**,** The Carquinez Strait, 32 km northeast of San Francisco; the first suspension bridge in the U.S. with an orthotropic steel deck, reinforced concrete towers and large diameter drilled shaft foundation. Both ambient vibration tests and forced vibration tests were conducted just before the opening of this new suspension bridge to traffic in 2003. Ambient vibration tests were mainly wind induced, whereas forced vibration tests were based on controlled traffic loads and vehicle-induced impact loads. Since the bridge was not affected by previous traffic loads, or seismic excitation, the test result data available are in an "as –built condition". This test data can be used to validate and/or update the finite element model used in bridge design and also to use as reference for future condition assessment, or health monitoring of this bridge. The test result showed that ambient vibration test provide more practical information than the forced vibration tests; as forced vibration can excite only vibration mode with natural frequencies above 1 Hz (higher modes of vibration),

whereas the ambient vibration test can excite vibration mode with lower natural frequencies (< 1 Hz) as well as some higher mode with natural frequency (>1 Hz).

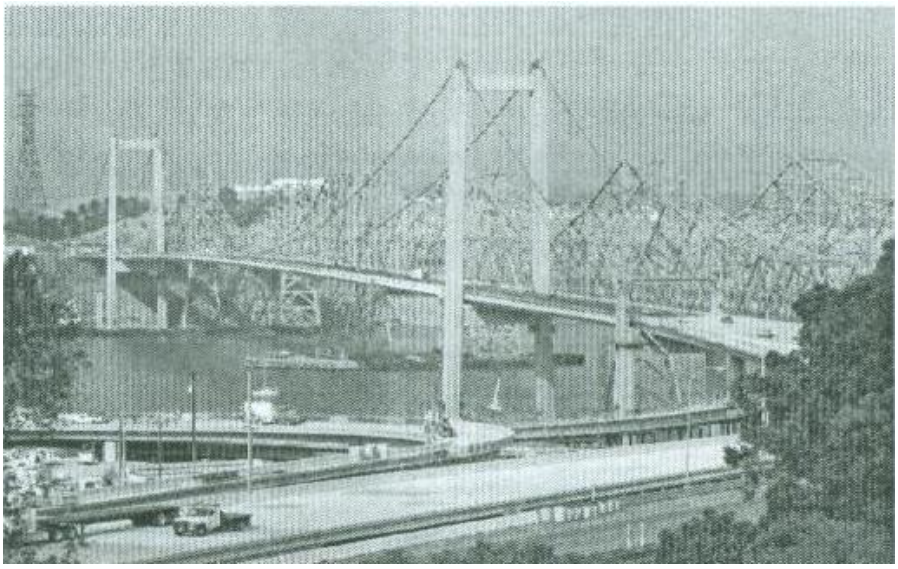

Figure 6.13 Alfred Zampa Memorial Bridge (Conte et al. 2008)

Lauzon et al (2006) reported on the dynamic response of destructive tests conducted on full-scale steel-girder highway bridge, southwestern Conneticut; using full-size small truck for excitation. A vertical crack was introduced near the middle of the exterior girder in five stages until the crack extended to two-third of the girder depth. The natural frequencies, their corresponding amplitudes, mode shapes using signature assurance criteria (SAC) and cross signature assurance criteria (CSAC), and the various combinations of these modal parameters were reviewed to determine major structural changes that led to collapse of multi-girder highway bridge. The test result showed that the amplitudes of natural frequencies and the frequency response spectrum (FRS) using the CSAC identify the cracks developed in bridge girder.

Mendrok et al. (2008) presented the practical problems associated with modal testing of large civil engineering structures like bridges and via-ducts. Two different case studies were presented. The first case study dealt with an environmental filter. The test result showed that an environmental filter is not needed in bridge monitoring in the regular frequency range. The second case study described the structural integrity assessment of a via-duct based on modal analysis. The results showed that in-operational modal analysis can be applied for both monitoring of new bridges as well as damage assessment of existing bridges.

In summary, it appears that since 1979, considerable research has been undertaken to detect, localize and quantify the structural damage of large civil engineering structures through various techniques based on changes in modal properties of the structure. From the previous reviews and current review, it is clear that modal testing is a powerful test technique for monitoring long-term behaviour of a new structure as well as for assessment of existing structures. There is sufficient evidence in the literature that promotes the use of this vibration-based technique. Measurement of the natural frequency can accurately identify the damage in the bridge structure. However, the natural frequency alone is not sufficient to know the location of damage. The mode shape is more sensitive to the local damage. Changes in damping are not reliable to detect the damage in bridge structures, and, it is still an area needing more research. However, presently, there is limited application of these techniques on full-scale bridge structures.

7. Experimental Work

7.1 Introduction

An experimental investigation was conducted to study the effect of the extent of cracking, caused by incremental static loading on the natural frequency of vibration of the beam. The test specimens were prepared and tested in the Jamieson Structures Laboratory of the Department of Civil Engineering and Applied Mechanics of McGill University. The levels of damage were determined through measurement of crack length and width and spalling. Visual inspection, changes in load carrying capacity (strain in tension bar) and deflection were also utilized to assess the state of damage. The forced vibration test was conducted to determine the natural frequency of vibration of the beam at different levels of damage. The measured vibration frequencies were compared with the reference values for the undamaged beam.

7.2 Description of test beams

Five identical reinforced concrete beams, 2 m long x 200 mm wide x 300 mm high were designed and constructed, satisfying the requirements of CSA A 23.3-2006 (Appendix A) to meet the following criteria:

1. A rectangular cross-section to avoid coupling effects between horizontal and vertical bending modes.
2. Adequate transverse reinforcement to avoid shear failure and to ensure the failure occur in bending

3. Considerable difference between the cracking load and the ultimate load of the beam by selection appropriate steel reinforcement ratio (Appendix B).

The beams were reinforced with 2-15M steel bars as tension reinforcement and 2-10M steel bars as compression reinforcement, corresponding to a tension reinforcement ratio of 0.7% to keep the test specimen under-reinforced. The transverse reinforcement consisted of 10M stirrups placed at 160mm on centres within 1/3 of beam length from each end. A uniform cover of 20 mm was used along the length of beam. Figure 7.1 shows the details of the reinforcing bars, the beam geometry and cross-section of test beam. The beam design calculations are presented in Appendix B. The total mass of the each test beam was about 300 kg corresponding to a density of reinforced concrete ρ = 2500 kg/m^3. The natural frequency of vibration is proportional to h/L^2. A beam of 300 mm height and 2.0 m length (1.9 m span) would normally have a fundamental frequency of about 125 Hz. The detailed calculations for fundamental frequency of vibration are presented in Appendix C.

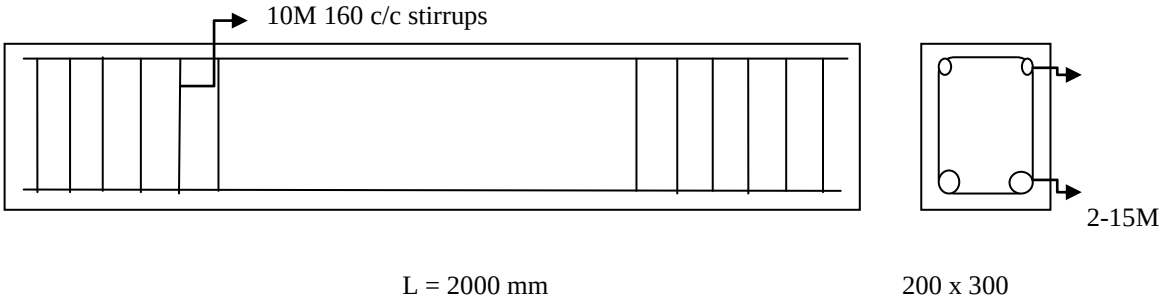

Figure 7.1 Geometry and cross-section of test beam

7.3 Test set-up and instrumentation

The purpose of this experimental test was to evaluate the relationship between the progressive cracking in reinforced concrete beams and the resulting changes in stiffness. Two types of experiments, the static load test and the forced vibration tests, were conducted on each beam. A series of "step loaded static tests" were applied to produce the successive and propagating cracks in the beams. After each static load step, forced vibration was performed by striking the centre of the bottom face of each beam with a hammer. This test was conducted on all test beams in the undamaged condition, prior to application of load for the reference frequency for the test beam. The extent and severity of the damage of the damaged (cracked) beams is illustrated in Appendix D.

7.3.1 Load test

For static load test, the beam was simply supported at both ends with a cantilever end of 50mm. A concentrated load was applied across the beam at mid span using a load actuator controlled by a servo hydraulic pump. Figure 7.2 shows the symmetric static load configuration for the simply supported beams. The three-point and four-point bending test configurations were adopted in the tests. The beam was loaded symmetrically at a distance of 670mm from each end in case of four- point bending while in case of three-point bending beam; it was loaded at the centre of the beam. An increasing static loading was applied in steps to induce successive damage in the test specimen. The loading rate was controlled and maintained at a constant rate until the beam failed. A displacement transducer was positioned at the beam soffit at mid-span and a load cell placed directly above the

load actuator to measure the deflection corresponding to the applied load. The measurements were acquired using the Strain Book 616 high speed, multichannel data acquisition system.

This enables measurement of the applied loading, the corresponding deflection and the strain gauge readings during testing.

It was ensured that no crack was developed before application of load, either due to self weight of beam, or due to any other loading, or during handling of the test specimen. At the end of each static load step, prior to dynamic testing, the beam surface was visually inspected to locate and quantify the cracks. The damage level, crack width and crack patterns were recorded for each loading cycle. Appendix E shows the observed crack patterns and damages for each static load step.

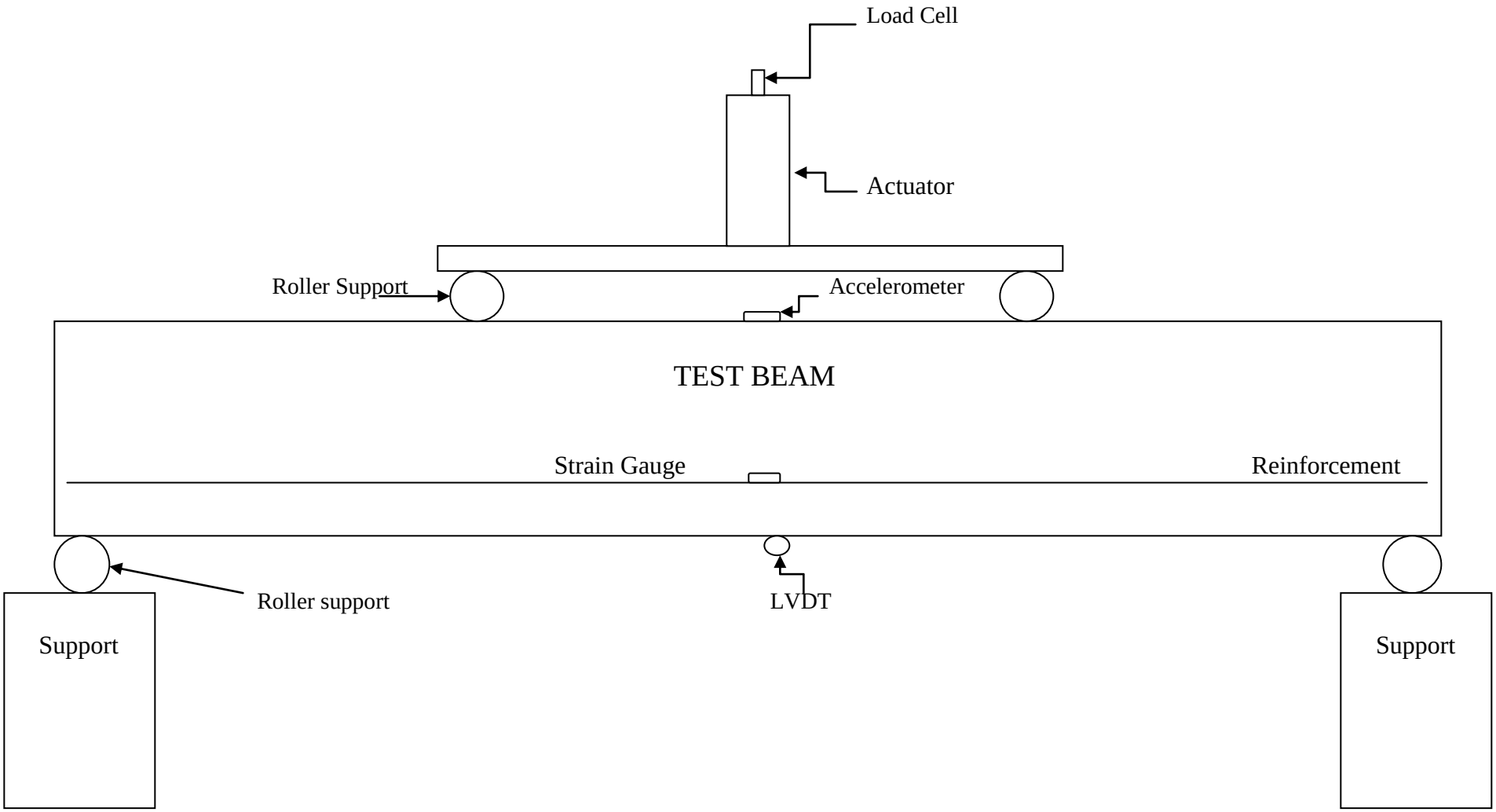

Figure 7.2 Schematic diagram for the test set-up

7.3.2 Frequency measurement

The frequency measurements were conducted to determine the dynamic characteristics of the beams; it consisted of determining the dynamic response of the beam using forced vibration. The excitation force was applied in the vertical direction using impact from a hammer to excite only the vertical bending mode. The frequency was first measured under undamaged condition of the beams prior to application of the loading. These test readings were utilized as reference reading for later comparison of dynamic characteristics at different damage stages. After each static load cycle, frequency measurements were obtained for the cracked beam, under two loading conditions – one with the load set-up on the beam and another without it (with just the self-weight of the beam). For each stage, three hammer impact tests were carried out to ensure repeatability and reliability of the measurements and to obtain an average value.

7.4 Instrumentation

This section describes the instrumentation used to perform the dynamic response tests.

Excitation: A hammer was used to generate the excitation force in the test specimen. The hammer impacts were applied at the middle of the centre line on the bottom face of the beam in the vertical direction (perpendicular to the longitudinal axis).

Dynamic response: The vibration responses (vertical accelerations) were measured by using an accelerometer; PCB (3801D2FB20G/AY) SN 410 accelerometer with sensitivity ±100 mv/g was used. The StrainBook 616 data

acquisition system was utilized to record the frequency, displacement and two strain gauge measurements. The data acquisition system was fixed to measure frequency at the rate of 60 kHz. Figure 7.3 shows the schematic diagram for the instrumentation.

Strain gauges: Strain gauges with gauge resistance (120 ± 0.3) ohms (Ω) and gauge factor 2.11 ± 1% were fixed on each tension reinforcing bar to measure the strain in the steel bar and to determine if the bar had yielded.

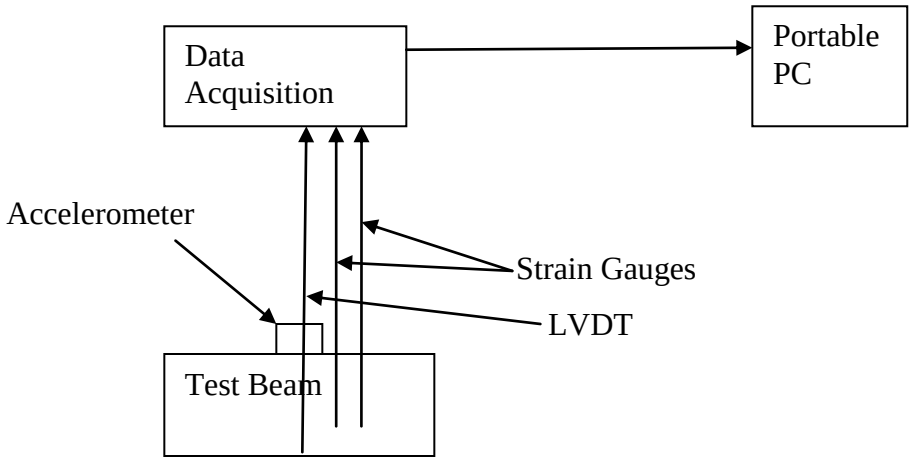

Figure 7.3 Schematic diagram for instrumentation

7.5 Problem faced and modification made during the experiment

1. The most challenging problem faced during the experiment was arranging the test set-up; this was so sensitive that any eccentricity resulted in a torsional mode. This made it difficult to identify the flexural mode. As a solution, capping compound was used to level the support to eliminate all other modes, except bending.

2. Protection of accelerometer from getting damaged was another issue. The load cell and the accelerometer were needed at the centre of beam to eliminate any eccentricity. The accelerometer was installed on upper face of the beam at the center to measure the frequency, as the load set-up and cracking could interfere with the accelerometer. The accelerometer was installed at the centre of the beam top and was protected by a channel section spanning over it. However, crushing of the concrete under the tips of the channel flanges led to the adoption of a two bearing plates on each side of the accelerometer with another plate spanning over the two plates and welded to it.
3. After testing of first test beam, arrangements were made to measure the crack widths with the help of crack width template and a LVDT was fixed at the bottom face of the beam. The LVDT was also connected to the data acquisition system to display deflection corresponding to apply loading.
4. The strain gauges were installed on the tension reinforcement to measure steel strains. During the test, it was found that strain gauges in one of the test beam was damaged and not working. All strain gauges were checked before casting of beams; a very few gauges were damaged during casting. Instead of getting all five beams in the same manner, it was decided to test one beam whose strain gauges had been damaged by inverting it so that 10M bar acted as tension reinforcement and 15M bar as compression reinforcement, which gave a lower tension steel ratio.

7.6 Test results and discussion

The test results obtained for all five beams are presented and discussed individually, and comparisons drawn among the beams with different loading conditions. Test beam 1and 2 were tested under three-point bending, while test beams 3, 4 and 5 were tested under four-point bending. Beam 4 was tested in inverted position, with 10M bars as the tension reinforcement. During the test, the changes in the natural frequency and in steel strains were recorded for each loading cycle. Three sets of frequencies were measured for each load step and the average frequency was obtained. The first frequency was measured in undamaged condition of the beam prior to application of the loading, to form the reference, or control frequency. The frequency was also recorded at the cracking load (Detailed calculation is presented in Appendix B) even though no visible cracks were detected. The frequencies were measured at first observed visible crack and at different loadings to establish relationship between the damaged condition and the corresponding changes in the natural frequency. The extent of damage was determined by the crack length and width; the crack patterns were recorded which are presented in Appendix D.

As mentioned previously, beams 1 and 2 were tested under three-point bending, while four-point bending test was used for the remaining three beams. Deflections were recorded under static loading conditions, while dynamic test was conducted after releasing the applied loading, and therefore, the beams were under uniformly distributed loading only (self weight of beam).

Test beam 1

Table 7.1 shows the tests result for test beam 1. Figure 7.4 illustrates the load-frequency relationship while Figure 7.5 demonstrates the load-steel strain curves.

Table 7.1 Test results for beam 1

Loading kN	**Steel strains (x 10^{-6})**		**Frequency Hz**	**Remarks**
Channel-5	Strain Gauge-1 Channel-1	Strain Gauge-2 Channel-2	Channel - 8	
0	0	0	122.5	LS-0
26.34	343	352	119.6	LS-1 Cracking load
29.86	721	743	112.7	LS-2 First visible crack
35.5	999	1049	110.7	LS-3
40.26	1134	1206	109.8	LS-4
46.7	1371	1475	108.8	LS-5
57.16	1672	1782	107.8	LS-6
66.18	1912	2014	106.86	LS-7
72.36	2121	2156	94.1	The concrete under the channel tips crushed. Replaced by a steel bearing plate
80.1	2450	2445	106.8	
88.1	2681	2672	105.88	LS-10
97.4	4452	2975	105.88	LS-11
103.75	8831	7312	94.95	LS-12 Ultimate load

Table 7.2 Percentage decrease in natural frequency and stiffness at each loading stage for beam 1

Load P	Frequency (experimental)	Stiffness K	% Decrease in natural frequency	% Decrease in stiffness
kN	Hz	(kN/mm)		
0	122.5	168.67	0.00	0.00
26.34	119.6	160.78	2.37	4.68
29.86	112.7	160.78	7.95	15.27
35.5	110.7	137.74	9.63	18.34
40.26	109.8	135.51	10.37	19.66
46.7	108.8	133.05	11.18	21.12
57.16	107.8	130.62	12.00	22.56
66.18	106.8	130.62	12.77	23.90
80.1	106.8	128.21	12.82	23.99
88.1	105.88	126.01	13.57	25.29
97.4	105.88	126.01	13.57	25.29
103.75	94.95	103.74	22.49	39.92

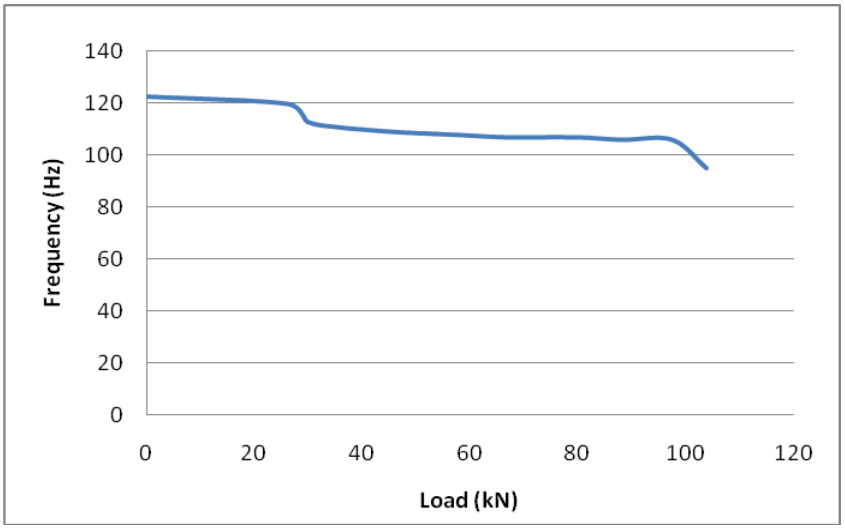

Figure 7.4 Load – frequency relationship for beam 1

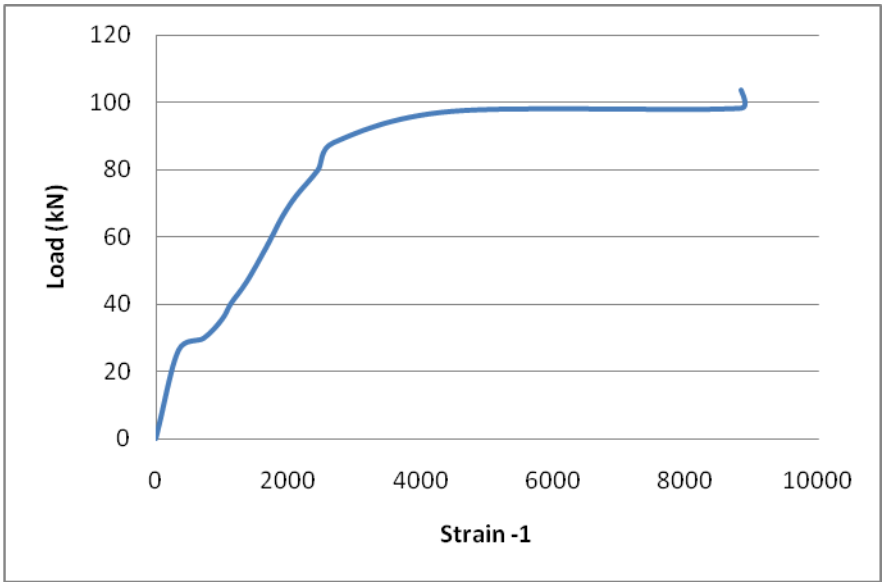

(a) Load-steel strain-1 curve for reinforcing bar 1(#15 bar)

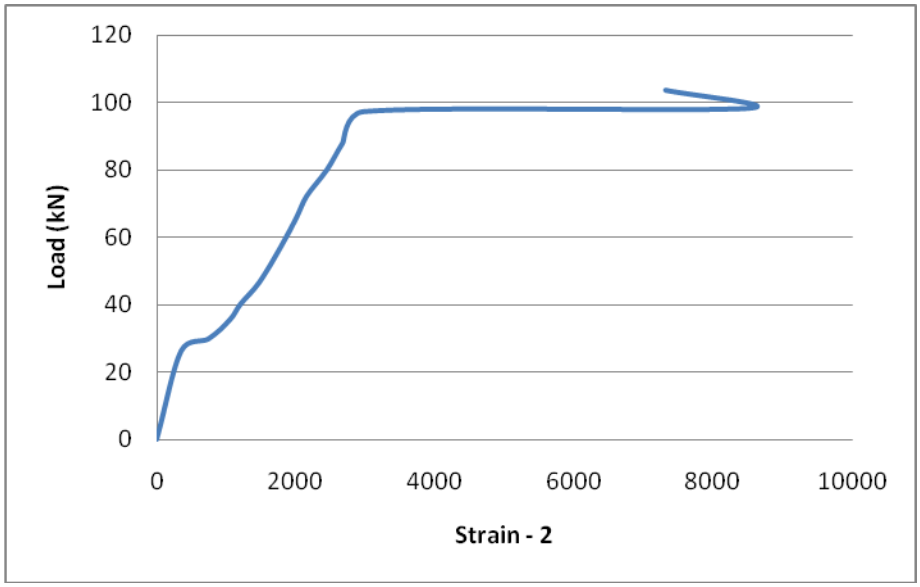

(b) Load-steel strain curve for reinforcing bar 2(#15 bar)

Figure 7.5 Load – steel strain curves for beam 1

The following observations can be drawn from the experimental results:

- The frequency in the undamaged condition prior to loading was 122.5 Hz which is about 2.4% lower than the calculated natural frequency of 125.55 Hz (Appendix C).
- A frequency decrease of 2.4% (122.5 Hz to 119.6 Hz) was recorded from undamaged condition to cracking load (26.34 kN), even though no visible cracks were noted. This can be due to development of internal cracking.
- The frequency decreased by about 8% (122.5 Hz to 112.7 Hz) at first visible crack (load = 29.86 kN) from undamaged condition.
- The frequencies decreased gradually with the increasing damage due to cracking as the applied load was increased. At an applied load of 72.36 kN, the beam top got partially crushed under the tips of the flanges of the channel placed over the accelerometer on top of the beam to protect it from damage. The beam had not failed as it had not reached its ultimate load (Figure 7.5). The channel was replaced by two bearing plate on each side of the accelerometer and another plate welded on top of these plates, and the test was continued with further load increments.
- The beam failed at an ultimate load of 103.75 kN which is about 60% higher than the calculated value of 65 kN (Appendix B). The measured steel strain values at the ultimate load (or beam failure) were 8831 x 10^{-6} and 7312 x 10^{-6}, showing considerable strain hardening of the No 15 reinforcing steel bars, resulting in stresses considerably higher than the steel yield strength. This large increase in the steel strength near the

ultimate load causes a considerable increase (60% in this case) in the beam moment resistance.

- The natural frequency decreased by 22.5% (122.5 Hz to 94.95 Hz) from undamaged state to the ultimate load or failure stage; 8.9% of the frequency decrease (105.88 Hz to 94.95 Hz) was recorded between last two loading stages before failure.
- Load-frequency curve also illustrates the changes in the beam natural frequency with an increase in damage due to cracking at higher load levels. As a consequence, the related stiffness at each load stage also decreases along a similar pattern as for the load-frequency relationship (Figure 7.4).
- The changes in stiffness for each loading stage and the percentage decreases in stiffness and frequency are presented in Table 7.2. The percentage decreases in frequency is approximately half the percentage decrease in stiffness. According to Equation 5.4; this ratio should be exactly 0.5, therefore, the experimental results are satisfactory.

Test beam 2

Test beam 2 was subjected to three-point bending; the frequencies were measured with the beam under loading condition with the applied load maintained as well as just after releasing the applied loading (without the applied load). Table 7.2 presents the test results for the test beam 2. Figure 7.6 show the load-mid-span deflection relationship. Figures 7.7 and 7.8 show the load-steel strain and load-frequency behaviour of the test specimen, respectively.

Table 7.3 Test result for beam 2

Loading kN	**Mid-span deflection (mm)**	**Steel strains ($x10^{-6}$)**		**Frequency Hz** (Channel – 8)		**Remarks**
Channel-5	Channel -7	Strain Gauge-1 Channel-1	Strain Gauge-2 Channel-2	With applied load removed (under beam self-weight only)	With applied load maintained	
0.0	0.04	0	0	110.78	-	LS-0
25.96	0.467	137	150	110.78	138.23	LS-1
28.2	0.699	545	603	109.77	138.2/123.5	LS-2 (First visible crack)
34.7	1.01	870	965	108.8	122.54	LS-3
42	1.46	1164	1259	106.86	120.6	LS-4
50.2	2.01	1412	1516	105.88	118.6	LS-5
57.3	2.47	1676	1744	104.9	118.62	LS-6
65.4	2.95	1954	2021	104.9	110.78	LS-7
72.99	3.4	2214	2266	103.9	109.8	LS-8
80.4	3.9	2468	2533	103.9	109.8	LS-9
87.7	4.4	2721	2721	103.9	109.8	LS-10
95.4	5.1	4854	2794	96.1/102.9	108.8	LS-11
103.2	9.37	9282	10352	87.25	106.86	LS-12 (Ultimate load)

Table 7.4 Percentage decrease in natural frequency and stiffness at each loading stage for beam 2

Load	Mid-span deflection	Frequency (experimental)	Stiffness based on measured frequency	% Decrease in natural frequency	% Decrease in stiffness
P	Δ		K		
kN	mm	Hz	(kN/mm)		
0.0	0.03	110.78	137.94	0	0.00
25.96	0.29	110.78	137.94	0	0.00
28.2	0.44	109.77	135.44	0.91	1.82
34.7	0.63	108.8	133.05	1.79	3.54
42	0.91	106.86	128.35	3.54	6.95
50.2	1.26	105.88	126.01	4.42	8.65
57.3	1.54	104.9	123.68	5.31	10.33
65.4	1.84	104.9	123.68	5.31	10.33
72.99	2.13	103.9	121.34	6.21	12.04
80.4	2.44	103.9	121.34	6.21	12.04
87.7	2.75	103.9	121.34	6.21	12.04
95.4	3.19	102.9	119.01	7.11	13.72
95.4	3.19	96.1	103.80	13.25	24.75
103.2	5.86	87.25	85.56	21.24	37.97

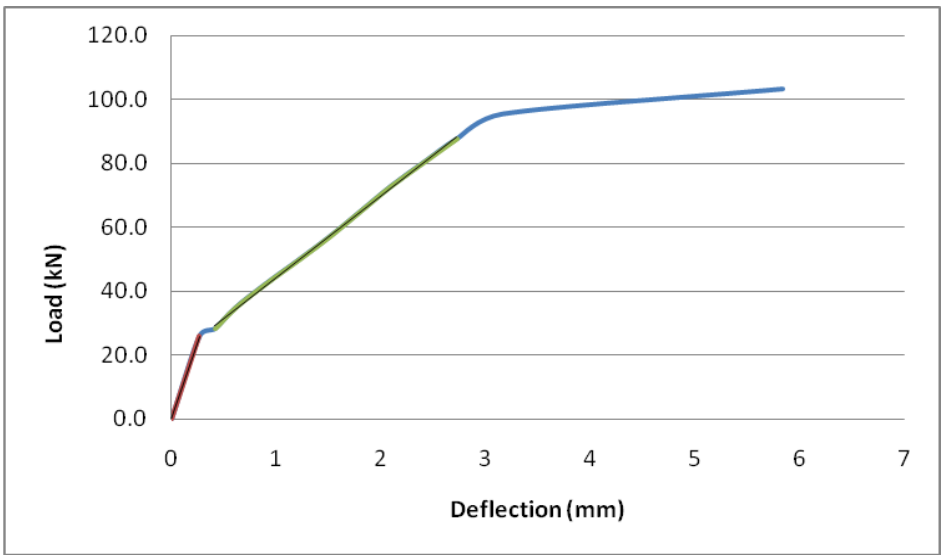

Figrue 7.6 Load – mid-span deflection curve for beam 2

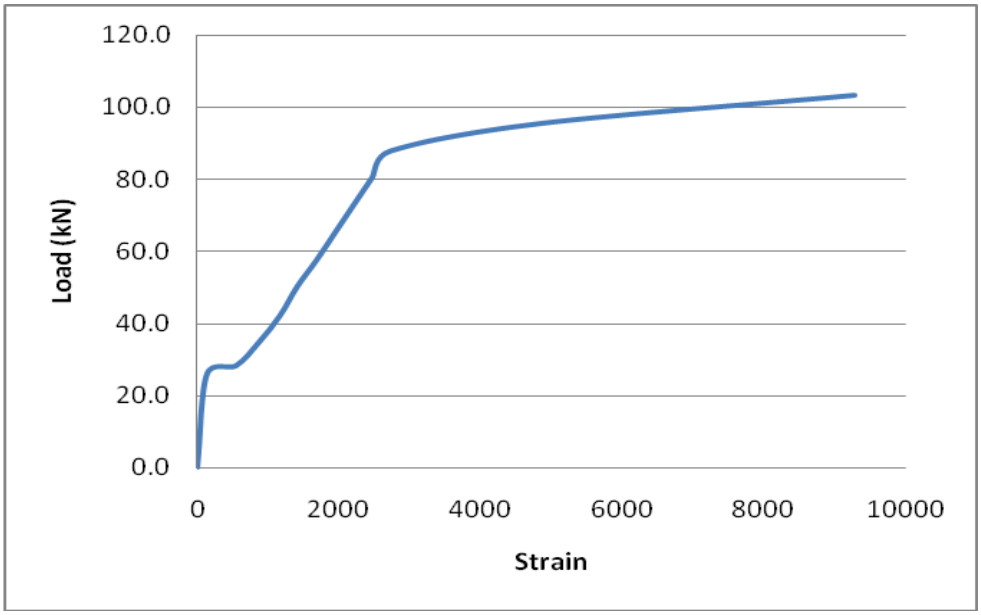

(a) Load-steel strain curve for reinfocing bar 1(#15 bar)

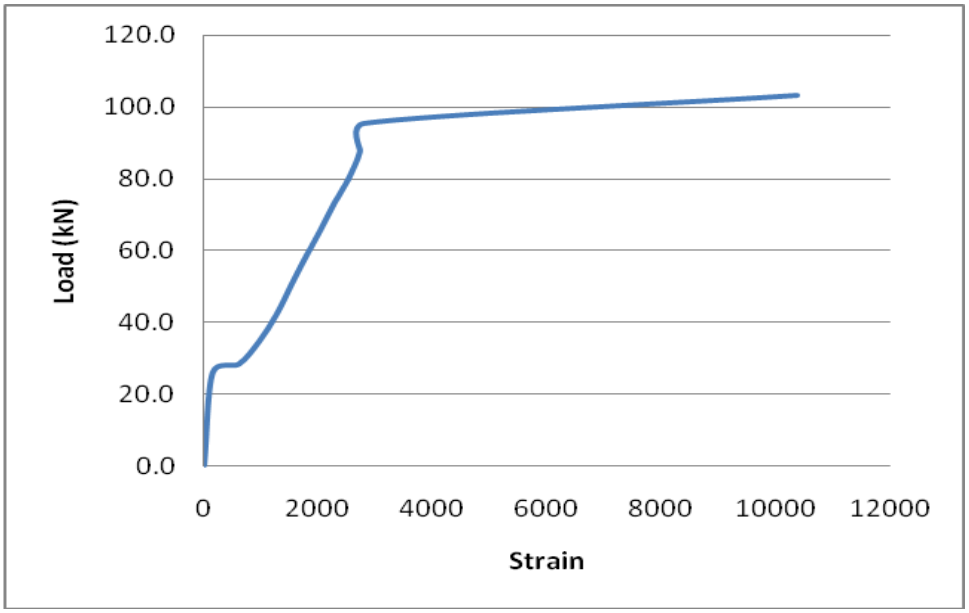

(b) Load-steel strain curve for reinfocing bar 2 (#15 bar)

Figure 7.7 Load – steel strain curves for beam - 2

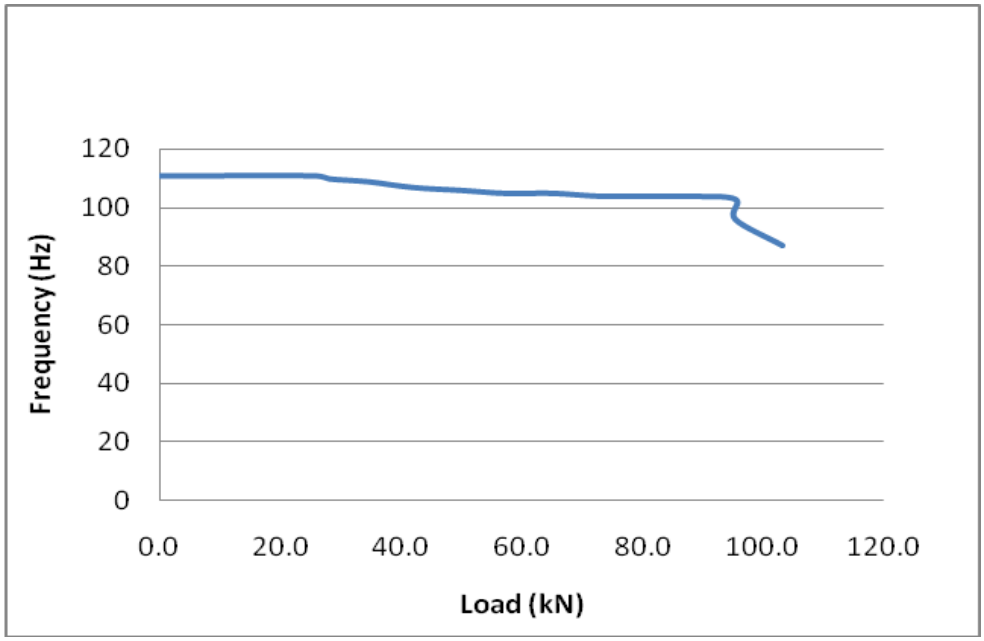

(a) With applied load removed, under beam self-weight only

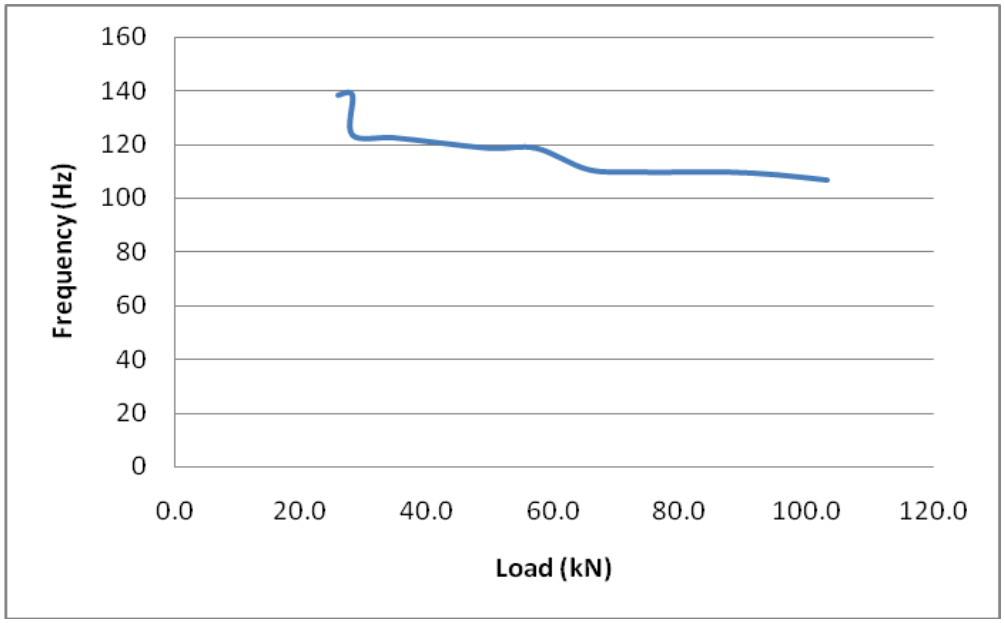

(b) With applied load maintained on the beam

Figure 7.8 Load – frequency relationships for beam 2

The following observations can be drawn from the experimental results:

- The natural frequency in the initial (undamaged) stage was 110.78 Hz which is about 12% lower than the calculated natural frequency (Appendix C).
- With the applied load left on the beam, the frequency at cracking load was higher (138.23 Hz) than calculated natural frequency of 125.55 Hz which was without the loading set-up on the beam (Appendix C).
- The frequency decreased by 0.9% (110.78 Hz to 109.77 Hz) at the first visible cracking, by 13.25% (110.78 Hz to 96.1 Hz) at steel yielding, and about 21.24% (110.78 Hz to 87.25 Hz) at the ultimate load, or the failure stage.
- With the applied loading left on the beam, the natural frequency decreased by 21.3% (138.23 Hz to 108.8 Hz) at yielding and 22.7% (138.23 Hz to 106.86 Hz) at failure from cracking load.
- Figure 7.6 shows the load-mid-span deflection curve. The beam stiffness from static test for a concentrated load at mid-span was 60.8 kN/mm before cracking occurred and decreased to 15.5kN/mm after cracking.
- The changes in stiffness for each loading stage and the percentage decreases in stiffness and frequency are presented in Table 7.4. The beam stiffness from dynamic test based on experimental natural frequency in the undamaged condition was 137.94 kN/mm compared to experimental value of 60.8 kN/mm drawn from static load-deflection test.

- The load-frequency and load-stiffness both curves have the same pattern. The natural frequencies of vibration changed with changes in stiffness (Equation 5.2).
- The beam failed at an ultimate load of 103.2 kN which is about 60% higher than calculated value (Appendix B). The measured strain values at ultimate load (or beam failure) were 9,282 x 10^{-6} and 10,352 x 10^{-6}, showing considerable strain hardening of the No 15 reinforcing steel bars, resulting in stresses considerably higher than the steel yield strength. This large increase in the steel strength near the ultimate load causes a considerable increase (60% in this case) in the beam moment resistance.
- The changes in stiffness for each loading stage and the percentage decreases in stiffness and frequency are presented in Table 7.4. The percentage decreases in frequency is almost half the percentage decrease in stiffness (Equation 5.4).

Test beam 3

Four-point bending was used to crack the test beam 3. The frequencies were measured under two conditions as for the test beam 2 – one without the concentrated loads and just the beam weight and the second with the applied load left on the beam. Table 7.5 presents the test results for beam 3. Table 7.6 shows the stiffnesses calculated from measured frequencies, and percentage decreases in frequencies and stiffness relative to the corresponding reference value for each loading cycle. Figure 7.10 show the load-frequency relationship. Figure 7.9 and

7.11 show the load-steel strain and load-mid-span deflection response respectively.

Table 7.5 Test result for beam 3

Loading kN	**Mid-span deflection (mm)**	**Steel strains ($x10^{-6}$)**		**Frequency Hz** (Channel – 8)		**Remarks**
Channel-5	Channel -7	Strain Gauge-1 Channel-1	Strain Gauge-2 Channel-2	With load removed (under beam self-weight only)	With applied load maintained	
0	0	0	0	120.88		LS-0
23.09	0.26	98.4	84.3	117.65	122.55/ 130.4	LS-1
33.7	0.495	380.5	226.3	109.8	120.59	LS-2 (First visible crack)
45.6	1.068	1005	726	112.75	120.59	LS-4
52.1	1.39	1195	885	111.76	118.63	LS-5
59.02	1.72	1350	1022	110.78	116.67	LS-6
68.08	2.11	1569	1207	108.82	116.67	LS-7
75.4	2.49	1737	1347	108.82	116.67	LS-8
81.5	2.68	1878	1468	107.84	115.68	LS-9
88.996	3.05	2042	1624	107.84	115.68	LS-10
95.35	3.3	2176	1725	107.83	111.6	LS-11
99.78	3.62	2299	1822	107.84	110.78	LS-12
111.6	3.97	2515	2005	106.86	108.82	LS-13
122.32	4.5	2742	2201	104.9	104.9/ 98.04	LS-14 Large noise was heard due to breaking of one of the tension reinforcement
131.95	4.99	2929	2350	99.02	98.04	LS-15
139.4	5.45	6110	2527	98.04	95.098	LS-16

Table 7.6 Percentage decrease in natural frequency and stiffness at each loading stage for beam 3

Load	Mid-span deflection	Frequency (experimental)	Stiffness based on measured frequency	% Decrease in natural frequency	% Decrease in stiffness
P	Δ		K		
kN	mm	Hz	(kN/mm)		
0.0	0.01	120.88	164.24	0	0.00
23.09	0.19	117.65	155.58	2.67	5.27
33.7	0.36	109.8	135.51	9.17	17.49
45.6	0.78	112.75	142.89	6.73	13.00
52.1	1.02	111.76	140.39	7.54	14.52
59.02	1.26	110.78	137.94	8.36	16.01
68.08	1.55	108.82	133.10	9.98	18.96
75.4	1.83	108.82	133.10	9.98	18.96
81.5	1.97	107.84	130.71	10.79	20.41
88.996	2.24	107.84	130.71	10.79	20.41
95.35	2.42	107.83	130.69	10.80	20.43
99.78	2.58	107.84	130.71	10.79	20.41
111.6	2.91	106.86	128.35	11.60	21.85
122.32	3.30	104.9	123.68	13.22	24.69
131.95	3.66	99.02	108.04	18.08	32.90
139.4	4.00	98.04	108.04	18.89	34.22

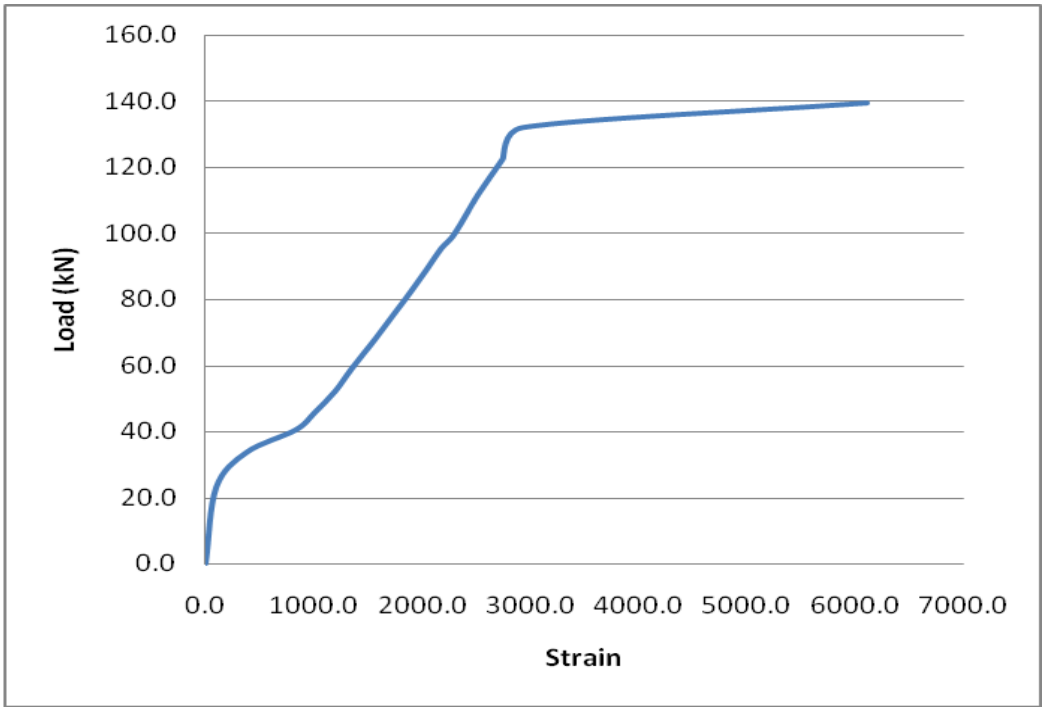

(a) Load-steel strain curve for reinfocing bar 1 (#15 bar)

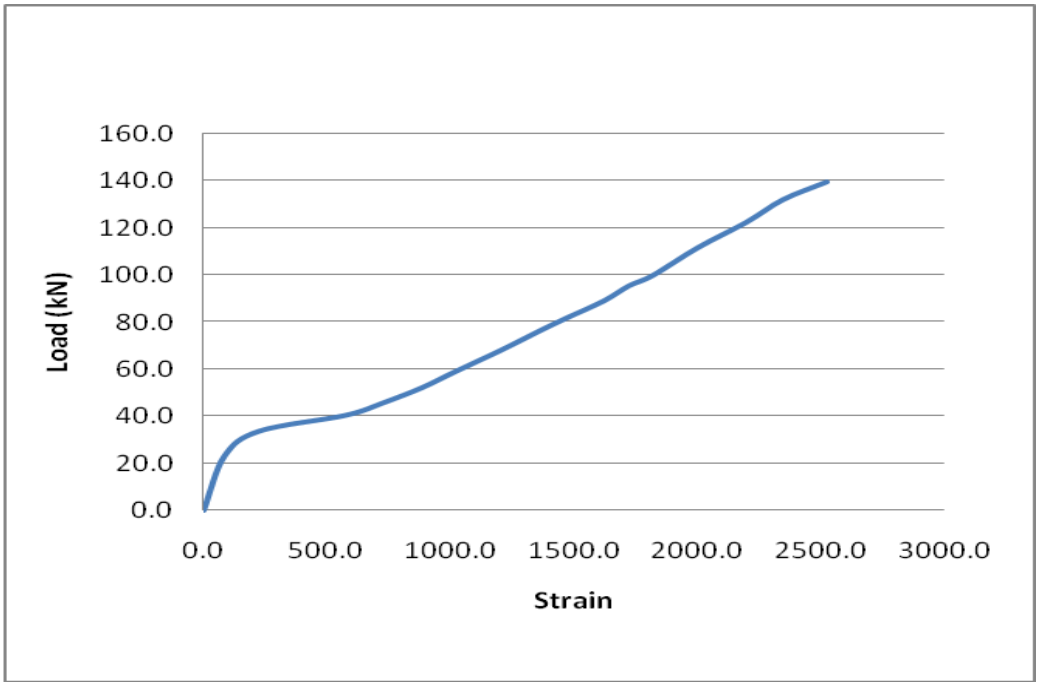

(b) Load-steel strain curve for reinfoced bar 2 (#15 bar)

Figure 7.9 Load – steel strain curves for beam 3

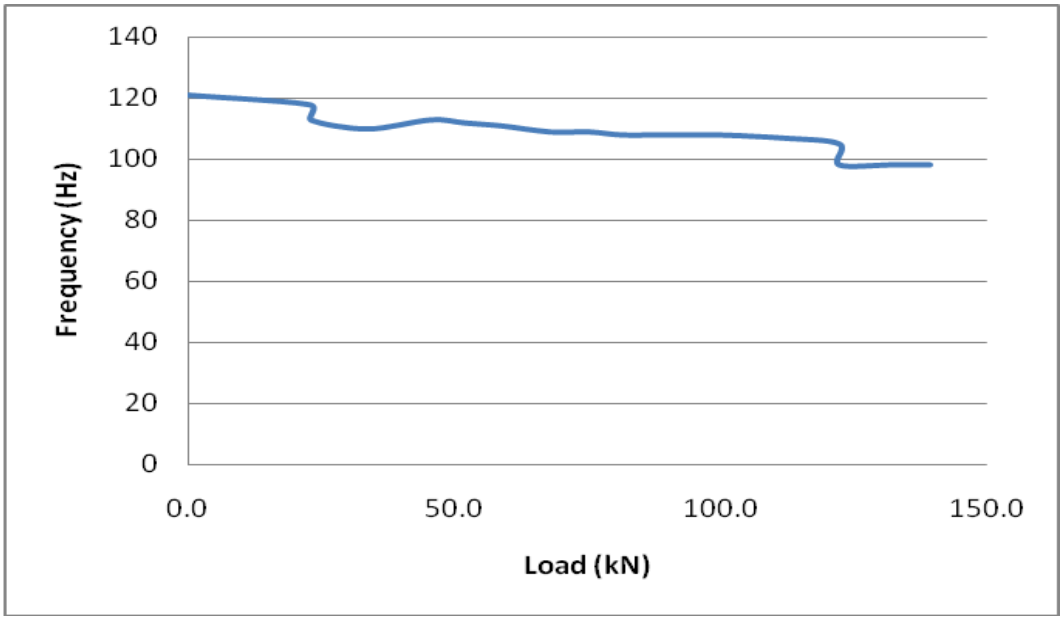

(a) With applied load removed, under the uniformly distributed beam self-weight only

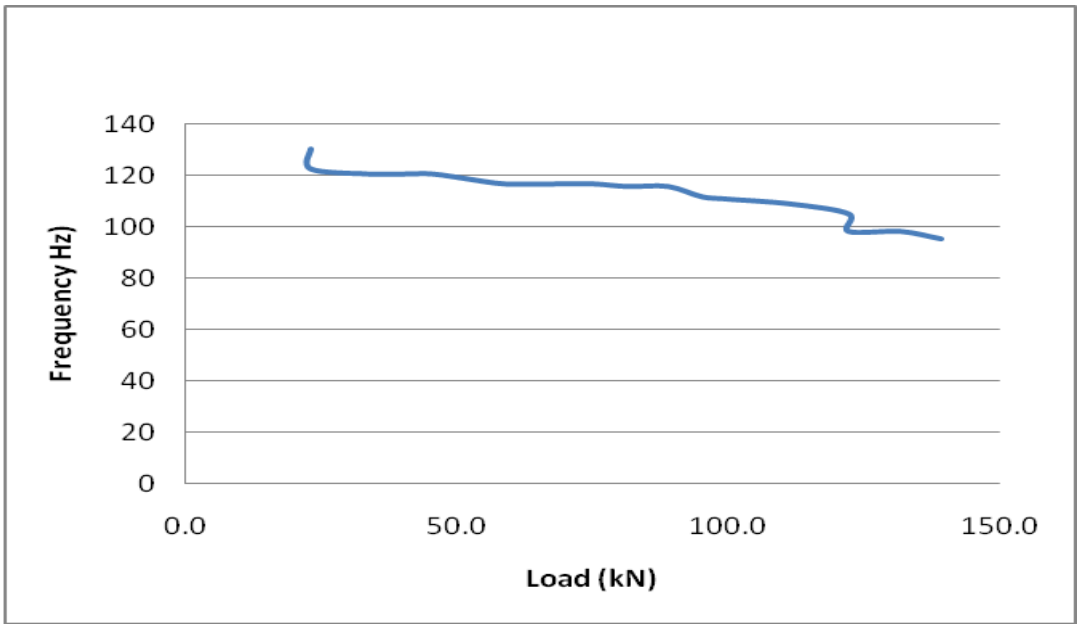

(b) With applied load maintained on the beam

Figure 7.10 Load – frequency relationships for beam 3

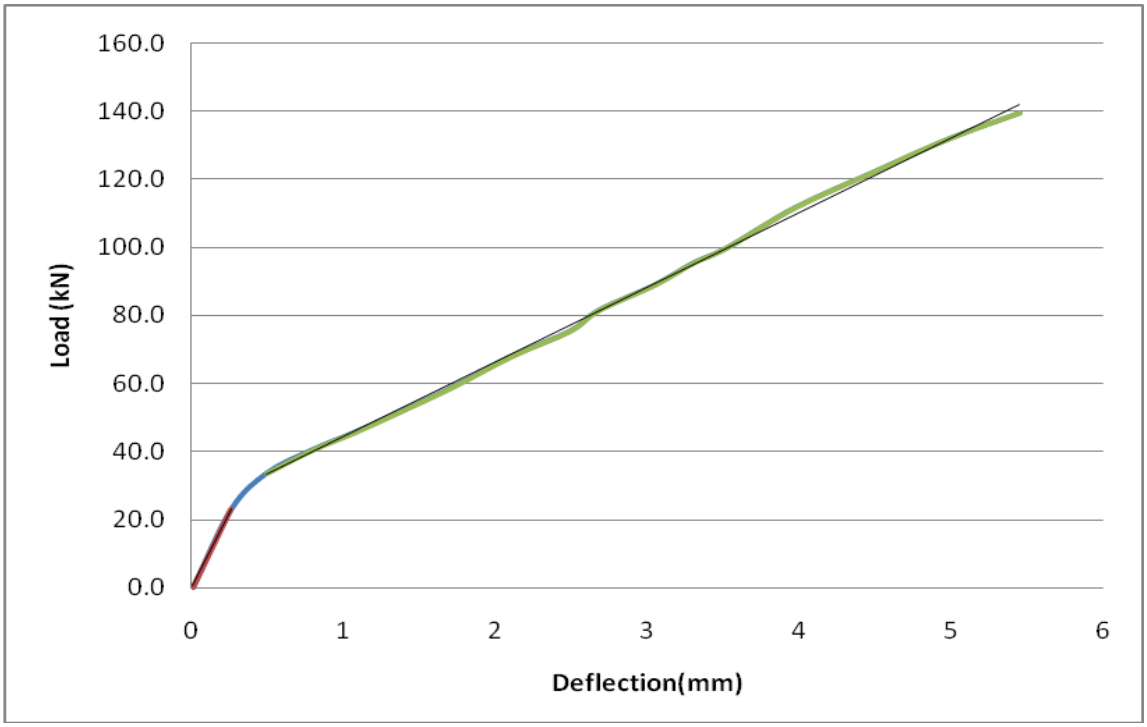

Figure 7.11 Load – deflection curve for beam 3

The following observations can be made from the test data for beam 3:

- The frequency of vibration of the uncracked beam was 120.88 Hz which is 3.7% lower than the calculated natural frequency of 125.55 Hz (Appendix C).
- A large noise was heard at a load of 122.32 kN. An examination of the load-strain (Figure 7.9a) curve shows very large strain (6110 x 10^{-6}) in reinforcing bar No 1(#15 bar) near failure and it could have fractured; the noise was associated with the energy release. To maintain safety, the test was discontinued at this stage.

- The natural frequency decreased by 2.7% (120.88 Hz to 117.65 Hz) from the undamaged condition to the 23.09 kN loading stage, even though no visible cracks were noted. This is due to development of internal cracking.
- The natural frequency of vibration decreased by 6.7% (from 120.88 to 112.75) at first visible cracking and 18.89% (from 120.88 to 98.04) at yielding of steel and remained the same at failure stage.
- With the applied load left on the beam, the frequency decreased by 24.82% (from 130.4 Hz to 98.04 Hz) at yielding and 27.07% (from 130.4 Hz to 95.098Hz) at failure from cracking load stage.
- Figure 7.11 shows the load-mid-span deflection response of the beam. The experimental beam stiffness from static test for two third point loads was 88.72 kN/mm before cracking occurred and decreased to 21.9 kN/mm after cracking.
- Changes in stiffness for each loading cycle and percentage decreases in stiffness and frequency are presented in Table 7.6. The beam stiffness based on the dynamic test results in the undamaged condition was 164.24 kN/mm compared to 88.72 kN/mm stiffness drawn from static load-mid-span deflection curve.
- Load-frequency and load-stiffness curves display a similar pattern. The natural frequencies of vibration change with changes in stiffness (Equation 5.2).
- The beam failed at an ultimate load of 139.4 kN which is about 40% higher than calculated value (Appendix B). The measured strain values at

ultimate load (or beam failure) were 6110 x 10^{-6} and 2527 x 10^{-6}, showing considerable strain hardening of the No 15 reinforcing steel bars, resulting in stresses considerably higher than the steel yield strength. This large increase in the steel strength near the ultimate load causes a considerable increase (40% in this case) in the beam moment resistance.

- The changes in stiffness for each loading cycle and percentage decreases in stiffness and frequency are presented in Table 7.6. The percentage decreases in frequency is approximately half the percentage decrease in stiffness (Equation 5.4).

Test beam 4

This beam was tested in an inverted position, using 10M bars as tension reinforcement. Four-point bending was adopted to crack the beam. Frequencies were measured just after releasing the load as well as for the case of the applied load being left on beam for each loading stage. Table7.7 presents the test results for beam 4. Table 7.8 shows the stiffness drawn from measured frequency, and percentage decrease in frequencies and stiffness relative to corresponding reference value for each loading cycle. Figure 7.13 shows the load-frequency relationship and Figure 7.12 shows the load-deflection behaviour. It was not originally planned to test the beam in inverted position, strain gauge were not installed on the 10 M bars. Therefore, no load-strain relationship is available.

Table 7.7 Test result for beam 4

Loading kN	**Mid-span deflection (mm)**	**Frequency Hz** (Channel – 8)		**Remarks**
Channel-5	Channel -7	With applied load removed (under beam self-weight only)	With applied load maintained on the beam	
0.0	0.002	116.67	115.69	LS-0
25.23	0.55	109.8	117.65	LS-1 (First visible crack)
30.2	1.09	104.9	107.84	LS-2
35.19	1.3	102.94	106.86	LS-3
39.66	2.2	93.14	102.94	LS-4
45.4	2.76	92.16	101.96	LS-5
49.51	3.35	92.16	92.16	LS-6
56.02	3.87	92.16	92.16	LS-7
60.9	4.33	91.18	91.18	LS-8
66.57	4.79	91.18	91.17	LS-9
70.24	7.87	81.37	89.2	LS-10 (Ultimate loading)

Table 7.8 Percentage decrease in natural frequency and stiffness at each loading stage for beam 4

Load	Mid-span deflection	Frequency (experimental)	Stiffness based on measured frequency	% Decrease in natural frequency	% Decrease in stiffness
P	Δ		K		
kN	mm	Hz	(kN/mm)		
0.0	0.00	116.67	153.00	0	0.00
25.23	0.40	109.8	135.51	5.89	11.43
30.2	0.80	104.9	123.68	10.09	19.16
35.19	0.95	102.94	119.11	11.77	22.15
39.66	1.61	93.14	97.51	20.17	36.27
45.4	2.02	92.16	95.47	21.01	37.60
49.51	2.46	92.16	95.47	21.01	37.60
56.02	2.84	92.16	95.47	21.01	37.60
60.9	3.18	91.18	93.45	21.85	38.92
66.57	3.51	91.18	93.45	21.85	38.92
70.24	5.77	81.37	74.42	30.26	51.36

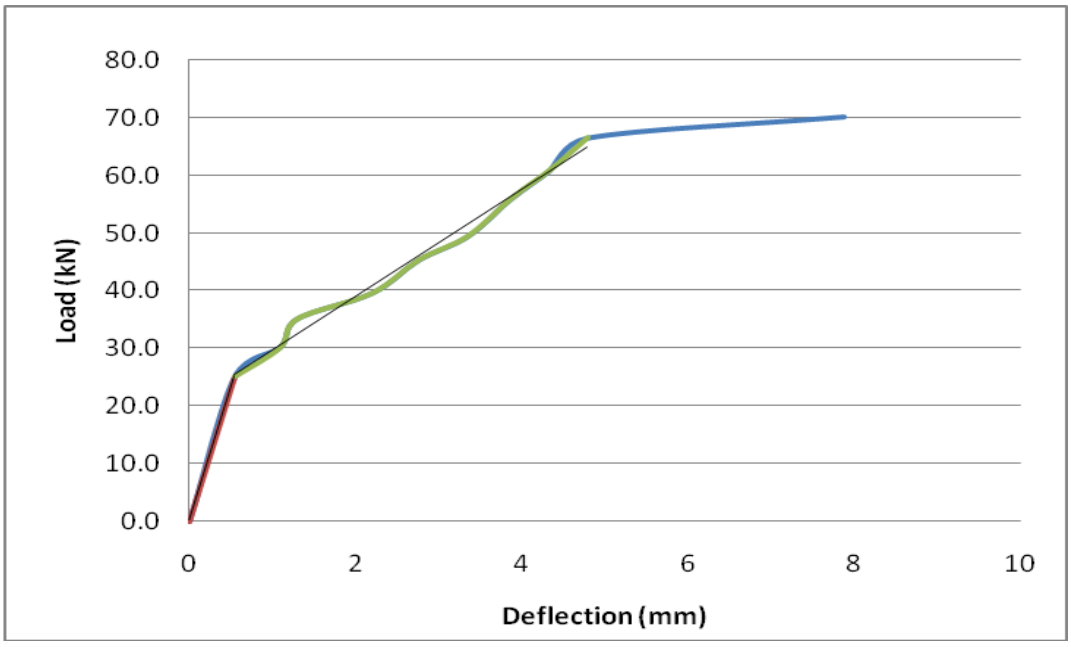

Figure 7.12 Load – mid-span deflection curve for beam - 4

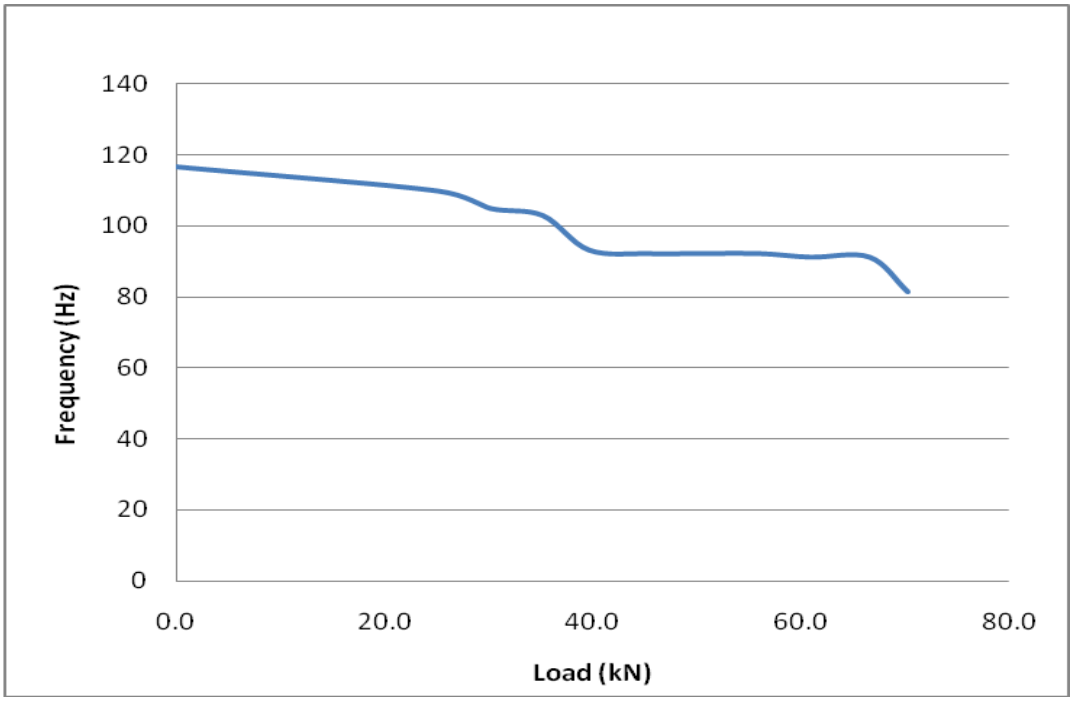

(a) With applied load removed, under the beam self-weight only

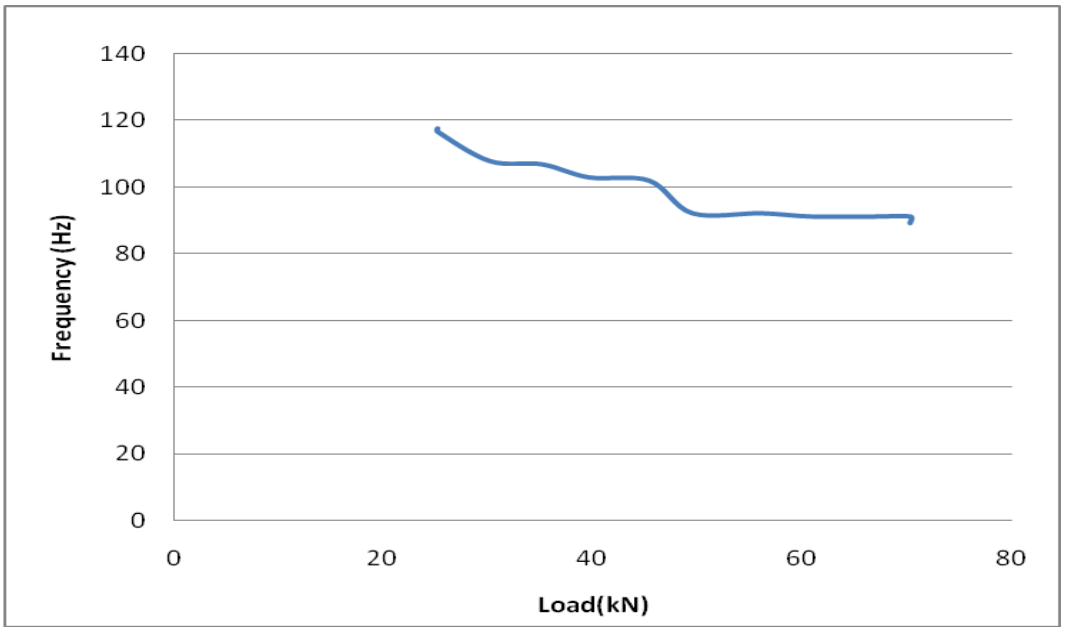

(b) With applied load maintained on the beam

Figure 7.13 Load-frequency relationships for beam - 4

The following observations can be drawn from the experimental data for beam 4:

- The frequency in the undamaged condition prior to loading was 116.67 Hz, which is about 7% lower than the calculated natural frequency of 125.55 Hz (see Appendix C).
- A frequency decreased of 5.9% (116.67 Hz to 109.8Hz) from undamaged condition to first visible crack, 21.8% (from 116.67 Hz to 91.18 Hz) at yielding of steel and 30.2% (from 116.67 Hz to 81.37 Hz) at failure stage.
- With the applied load left on the beam, the natural frequency decreased by 22.5% (from 117.65 Hz to 91.18 Hz) at yielding of steel, and 24.2% (from 117.65 Hz to 89.2 Hz) at failure from the first visible cracking stage.
- Figure 7.12 shows the load-mid-span deflection curve. The beam stiffness for two symmetric concentrated loads at one-third span of the beam was 45.9 kN/mm before cracking and decreased to 9.3kN/mm after cracking.
- The beam failed at an ultimate load of 70.24 kN which is about 30% higher than calculated value (Appendix B).
- The changes in stiffness for each loading stage and the percentage decreases in stiffness and frequency are presented in Table 7.8. The beam stiffness based on the dynamic test results in the undamaged condition was 153 kN/mm compared to 45.9 kN/mm stiffness drawn from load-mid-span deflection curve.
- Figure 7.16 also demonstrate the changes in the beam natural frequency with an increase in damage due to cracking at higher load levels. As a

consequence, the related stiffness at each load stage also decreased along a similar pattern as the load-frequency relationship.

- The changes in stiffness for each loading stage and percentage decreases in stiffness and frequency are presented in Table 7.8. The percentage decreases in frequency is approximate half the percentage decrease in stiffness (Equation 5.4).

Test beam 5

Four-point bending was used to crack the test beam 5. Table 7.9 presents the test results for the test beam 5.Table 7.10 presents the stiffnesses corresponding to the damage induced by each loading cycle. Figure 7.14, 7.15 and 7.16 show the load-deflection, load-steel strain and load-frequency relationship, respectively.

Table 7.9 Test result for test beam – 5

Loading kN	**Mid-span deflection (mm)**	**Steel strains ($x10^{-6}$)**		**Frequency Hz** (Channel – 8)		**Remarks**
Channel-5	Channel -7	Strain Gauge-1 Channel-1	Strain Gauge-2 Channel-2	With applied load removed (under beam self-weight only)	With the applied load maintained on the beam	
0.0	0	0	0	106.86		LS-0
20.45	0.22	58.69	78.5	106.86	119.61	LS-1
34.89	0.67	131.5	213.5	105.88	119.61	LS-2 (First visible crack)
44.42	1.29	368.3	542.5	103.92	109.8	LS-3
55.06	1.92	620.7	876.1	102.94	106.86	LS-4
64.63	2.4	823.3	1107.5	94.12	104.9	LS-5
74.4	2.84	1027.12	1338.8	93.13	103.92	LS-6
85.36	3.43	1242.3	1584.1	93.13	103.92/ 102.94	LS-7
95.03	3.97	1449.4	1816.4	93.13	102.94	LS-8
104.48	4.49	1662.2	2042.2	93.13	102.94	LS-9
114.67	5.13	1898.8	2304.0	93.13	93.13	LS-10
124.86	5.72	2090.3	2513.0	93.13	93.13	LS-11
135.19	6.45	2449.83	2692.6	92.15	92.15	LS-12
138.49	9.87	2565.34	2718.16	86.27	90.19	LS-13 (Ultimate loading)

Table 7.10 Percentage decrease in natural frequency and stiffness at each loading stage for beam 5

Load	Mid-span deflection	Frequency (experimental)	Stiffness based on frequency	% Decrease in natural frequency	% Decrease in stiffness
P	Δ		K		
kN	mm	Hz	(kN/mm)		
0.00	0.00	106.86	128.35	0	0.00
20.45	0.16	106.86	128.35	0	0.00
34.89	0.49	105.88	126.01	0.92	1.83
44.42	0.95	103.92	121.38	2.75	5.43
55.06	1.41	102.94	119.11	3.67	7.20
64.63	1.76	94.12	99.57	11.92	22.42
74.4	2.08	93.13	97.49	12.85	24.05
85.36	2.52	93.13	97.49	12.85	24.05
95.03	2.91	93.13	97.49	12.85	24.05
104.48	3.29	93.13	97.49	12.85	24.05
114.67	3.76	93.13	97.49	12.85	24.05
124.86	4.20	93.13	97.49	12.85	24.05
135.19	4.73	92.15	95.45	13.77	25.64
138.49	7.24	86.27	83.65	19.27	34.82

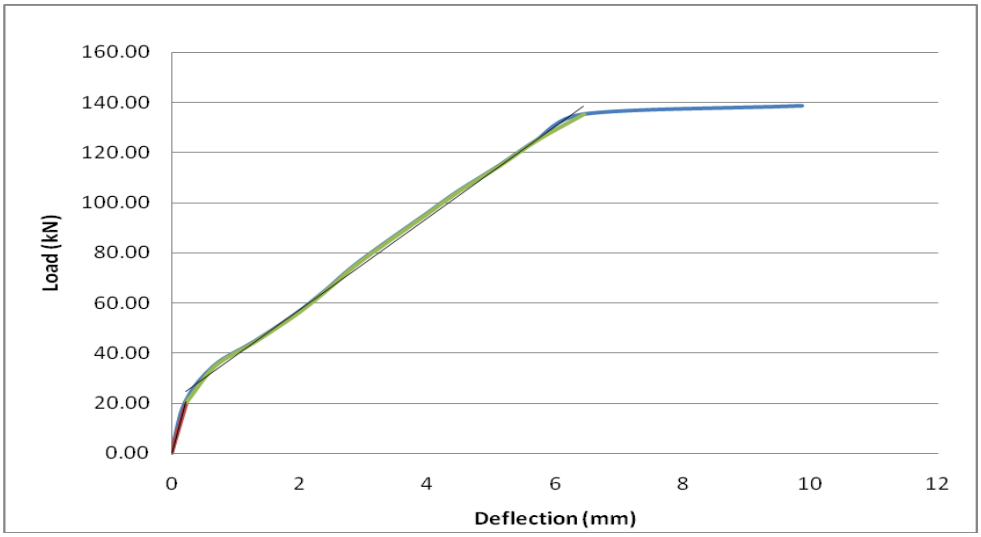

Figure 7.14 Load – mid-span deflection curve for beam 5

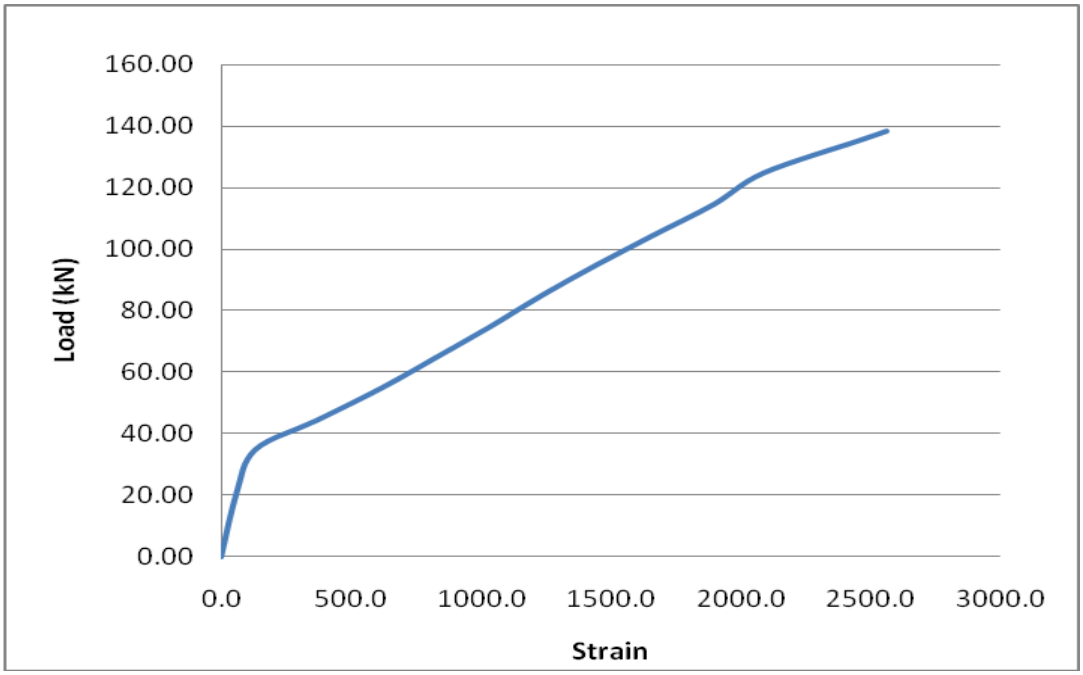

(a) Load-steel strain curve for reinforcing bar 1 (#15 bar)

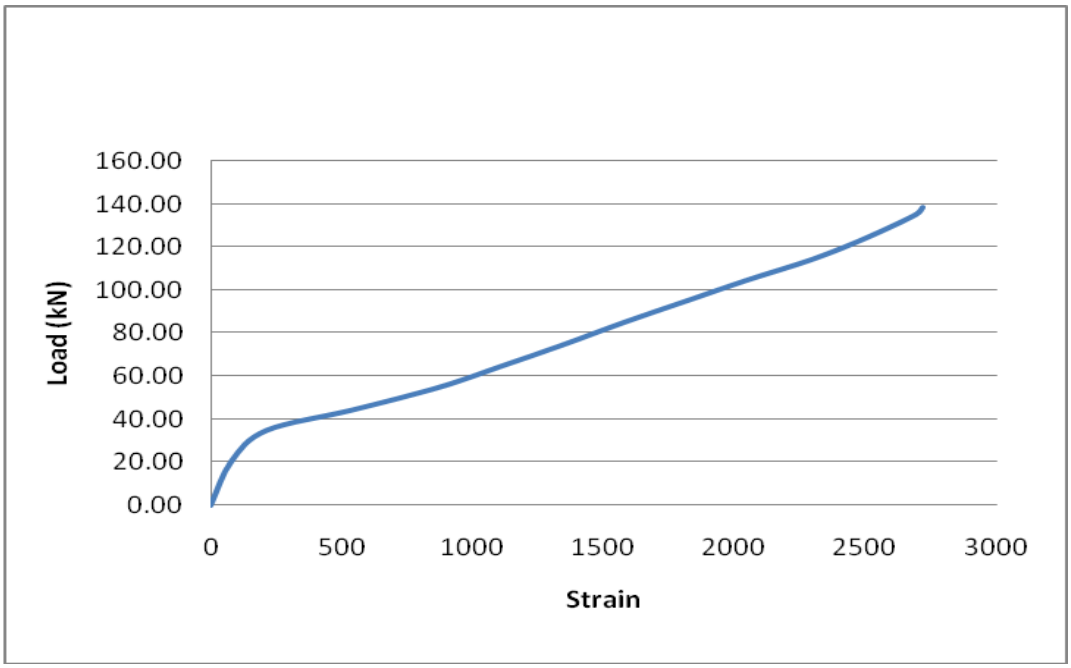

(b)Load-steel strain curve for reinforcing bar 2 (#15 bar)

Figure 7.15 Load - steel strain curves for beam 5

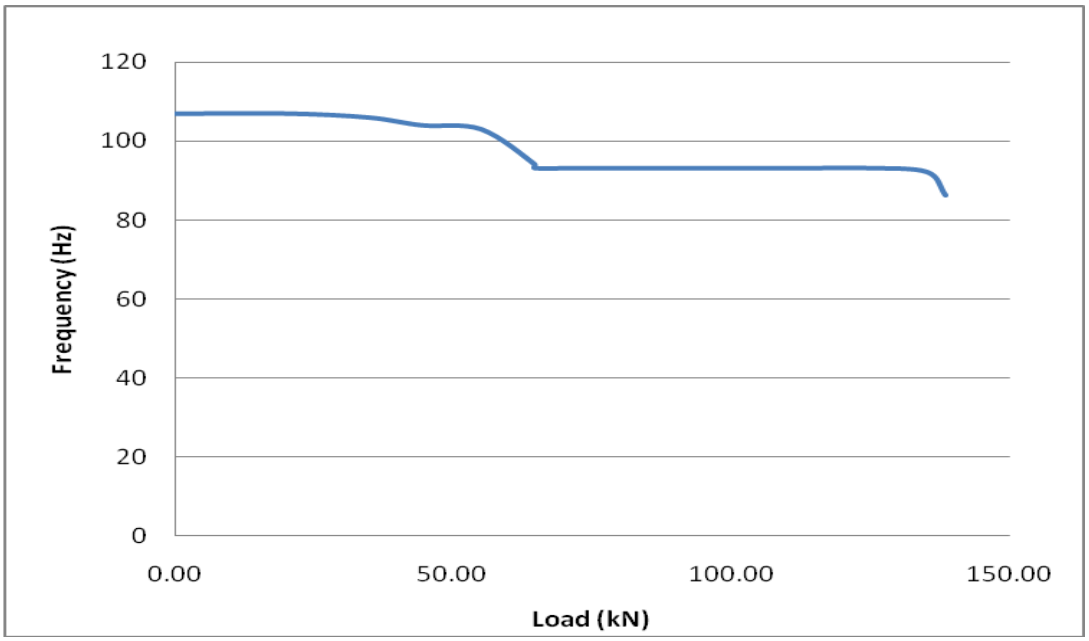

(a) With applied load removed, under the beam self-weight only

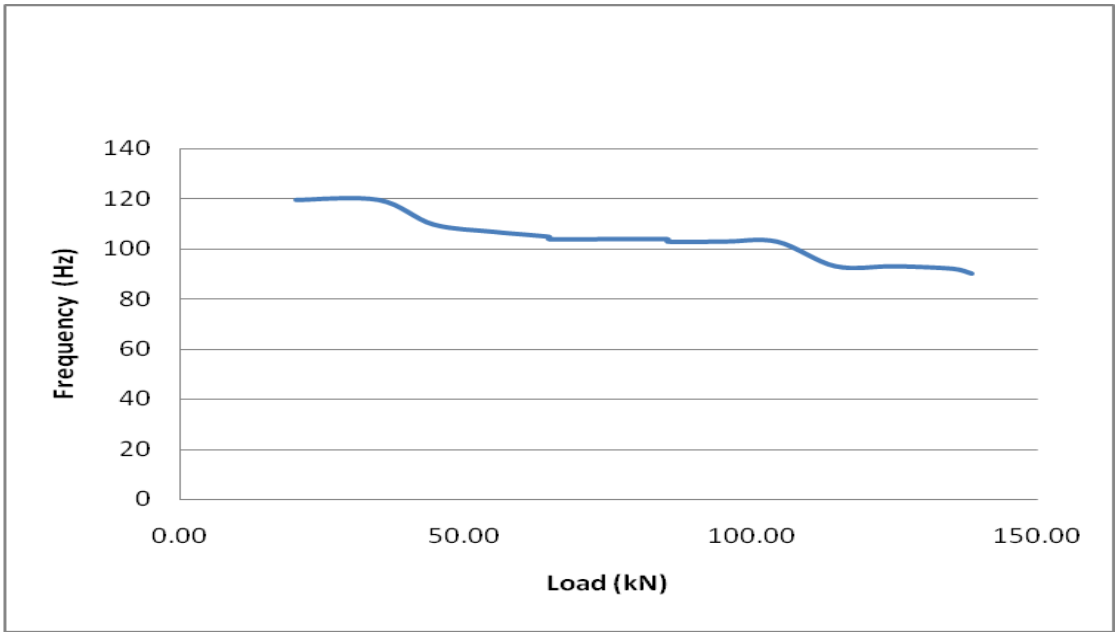

(b) With applied load maintained on the beam

Figure 7.16 Load-frequency relationships for beam 5

The following observations can be drawn from the test results for beam 5:

- The natural frequency in the undamaged stage was 106.86 Hz which is about 15% less than the calculated natural frequency of 125.55 Hz (see Appendix C).
- A frequency decreased of 0.92% (106.86 Hz to 105.88 Hz) from undamaged condition to first visible cracking, and 13.76% (106.86 Hz to 92.15 Hz) and 19.27% (106.86 Hz to 86.27 Hz) at steel yielding and at failure stage, respectively.
- With the applied load left on the beam, the natural frequency decreased by 23% (from 119.61 Hz to 92.15 Hz) at yielding and 24.6% (from 119.61 Hz to 90.19 Hz) at failure from the values at the cracking load.
- Figure 7.12 shows the load-deflection curve at mid-span. The experimental beam stiffness for third point loads was 92.95 kN/mm before cracking occurred and decreased to18.28 kN/mm after cracking.
- The changes in stiffness for each loading stage and the percentage decreases in stiffness and frequency are presented in Table 7.10. The beam stiffness based on the dynamic test results in the undamaged condition was 128.35 kN/mm which is about 32% higher than experimental value of 92.9 kN/mm drawn from static load-mid-span deflection curve.
- Figure 7.16 also demonstrates the changes in the beam natural frequency with increase in damage due to cracking at higher load levels. As a consequence, the related stiffness at each load stage also decreases along a similar pattern as the load-frequency relationship.

- The beam failed at an ultimate load of 138.5 kN which is about 40% higher than calculated value (Appendix B). The measured strain values at ultimate load (or beam failure) were 2565 x 10^{-6} and 2718 x 10^{-6}, showing strain hardening of the No 15 reinforcing steel bars, resulting in stresses higher than the steel yield strength. This large increase in the steel strength near the ultimate load causes a considerable increase (40% in this case) in the beam moment resistance.
- The changes in stiffness for each loading cycle and percentage decreases in stiffness and frequency are presented in Table 7.10. The percentage decreases in frequency is approximately half the percentage decrease in stiffness.

7.7 Summary and discussion of results

- With the applied load left on the beam, the initial natural frequency is higher than calculated natural frequency and the natural frequency with the applied load removed (vibration under beam self-weight only).
- Beams failed at an ultimate load higher than calculated value mainly due to strain hardening of reinforcing steel bar, resulting in stresses considerably higher than the steel yield strength.
- The load-frequency curves illustrate the changes in the beam natural frequency with increase in damage due to cracking at higher load levels. This suggests that changes in structural integrity can be identified with this modal test.

- The percentage decreases in stiffness and percentage decrease in frequency approximately match the relationship given in Equation 5.4 (Chapter 5); percentage decreases in frequency is nearly half the percentage decrease in stiffness.
- Changes in frequency are recorded at cracking, yielding and failure of beams. Table 7.11 describes the frequency changes in all five test beams after releasing the applied load at three different stages of damage; at first cracking, steel yielding and at failure of beam.

Table 7.11 Summary of decreases in frequency with increase in damage in five beams

Beam	Reduction in frequency (with applied load removed; under self weight of beam only)		
	% Decrease in frequency at first visible crack	% Decrease in frequency at yielding	% Decrease in frequency at failure of beam
1	8.0	13.56	22.49
2	0.91	13.25	21.24
3	9.2	18.89	18.89
4	5.89	21.85	30.25
5	0.92	13.76	19.27

- Table 7.12 presents the decrease in the stiffnesses evaluated from theoretical and experimental tests for all five test specimens. Theoretical static stiffness for 3-point bending loading at mid-span and 4-point bending with two equal concentrated loads, symmetrically placed, are calculated using standard structural analysis equations (7.2) and (7.3), respectively, while the experimental values are evaluated from the static

load-deflection curves. Dynamic stiffnesses are calculated using equation 7.1 from the calculated theoretical and measured experimental frequency values for K(Dynamic), respectively.

A comparison of the stiffness values for the uncracked and cracked beams shows that the percentage changes for the calculated static and dynamic stiffness from the uncracked beam to cracked beam are quite close.

The beam stiffness decreased to about 75% to 80% from uncracked beam to cracked beam in case of static load test.

There is a difference in the stiffnesses obtained from static load-deflection test and dynamic test. This can be explained by the fact that the modulus of elasticity of concrete depends on the rate of loading. There are reports in the literature of values of dynamic modulus of elasticity obtained from dynamic test being up to 50 percent higher than that value obtained from static tests (Williams, 2000).

Table 7.12 Summary evaluation of stiffness for beams with applied load removed; under self weight of beam only

	Type of loading	**K (Static) (Experimental stiffness based on P/Δ curve)**		**K (Static) Theoretical stiffness**		**K (Dynamic) based on experimental natural frequency (*f*)**		**K (Dynamic) based on theoretical natural frequency (*f*)**	
		kN/mm		kN/mm		kN/mm		kN/mm	
		Before cracking	After cracking	Before cracking	After cracking	Before cracking	After cracking	Before cracking	After cracking
Beam 1	3 point Bending	-	-	93.5	24.3	168.7	-	189.4	50.3
Beam 2	3 point Bending	60.8	15.5	93.5	24.3	137.9	135.4 –103.8	189.4	50.3
Beam 3	4 point Bending	88.7	21.9	106	28.1	164.2	155.6 –108.0	189.4	50.3
Beam 4	4 point Bending	45.9	9.3	102.8	16.9	153.0	135.5 – 93.5	183.6	30.1
Beam 5	4 point Bending	92.9	18.3	106	28.1	128.4	126.0 – 95.5	189.4	50.3

$$K(dynamic) = (2\pi f)^2 m_t \tag{7.1}$$

$$K(static) = \frac{48\,EI}{L^3}$$ (For 3-point bending loading at mid-span) (7.2)

$$K(static) = \frac{48\,EI}{a(3L^2 - 4a^2)}$$ (For 4-point bending with two equally concentrated loads symmetrically placed) (7.3)

8. Summary and Conclusions

This thesis focuses mainly on evaluation of vibration frequency using non-destructive test technique (modal testing) for condition assessment of beam-type structures. A literature review based on previous research works related to modal testing, focusing mainly on full scale structures is summarized. The state of Canada's bridges, focusing mainly on aging and useful life of bridges, role of all levels of governments, investment trends, and importance of timely maintenance and current deficiency are discussed. A brief state-of-the-art report on deterioration of concrete bridges and their causes is presented along with the time-dependent analytical relationship to predict the chloride-induced deterioration over the entire service life. The fundamental aspects of bridge inspection and the importance of non-destructive testing techniques have also been briefly reviewed to provide practical guidance for bridge inspection.

The experimental program was carried out to study the effect of deterioration (cracking) on natural frequency and check its practicability to implement this advanced test method in the field on large-scale beam type civil engineering structures. A method of assessing the structural condition of reinforced concrete beams using natural frequency of vibration is presented. Five reinforced concrete beams were tested in this preliminary research program within the framework of the development of health monitoring system as a part of any bridge management system. The tests consisted of subjecting the reinforced concrete beams to

progressive cracking at increasing load levels and measuring the changes observed in their natural frequencies of vibration. The damage or deterioration caused noticeable changes in the modal parameter, namely the natural frequency. A decrease in the natural frequency indicates that the system has undergone damage or some deterioration. The test results show that the natural frequencies were affected by the level of cracking developed in the beams, resulting in decreases in the measured natural frequencies with higher levels of cracking damage. The changes in the natural frequencies are related to the changes in the structural stiffness of the beam that indicates the severity of the damage induced from the static load increments. The magnitude of this change is an indicator of the severity or state of the changes experienced; however, it does not locate the location of damage but detects only the damage in the structure. The results from the tests indicate that vibration testing is a useful tool for obtaining information on the condition of the structural system. Although the test was performed on reinforced concrete beams, it can be extended to bridges for obtaining information related to structural integrity of the bridge. This method can be used to detect the "actual" condition of the structure and support bridge management office to optimize decisions related to bridge maintenance/repair programs. It can be applied for monitoring of new bridges as well as for damage assessment of older structures.

In conclusion, the use of modal testing to detect damage in beam type structure is shown to be viable. There is also sufficient evidence in the literature that promotes the use of this vibration-based technique. Measurement of natural frequency can accurately identify the damage in the bridge structure. However,

natural frequency alone is not sufficient to know the location of damage (level 2 or higher level damages). Mode shapes are more sensitive to localized damage. Changes in damping are not reliable to detect the damage in bridge structures. More research is needed in this area. Majority of tests have been performed on small-scale models in the laboratories. Limited applications of modal testing are available on full-scale bridge structure. More co-operations is needed among the researchers, industry and government organizations for future research to promote the use of modal test for monitoring of new and rehabilitated bridges and assessment of existing bridges which have suffered damage due to inadequate maintenance.

Recommendation for future research

This section describes the issues in relation to this primary test that must be addressed to make the detection of damage using modal testing practical in field. This preliminary experimental program is concerned with the reduction in stiffness of cracked beams caused by application of increasing static loading to study the effect of deterioration in the beam using natural frequency of vibration. Other modal parameters, mode shapes and damping ratio have not considered. More work is needed for detection of level 2, level 3 and level 4 damages as defined by Rytter, 1993 using different modal parameters individually, or in combination.

The natural frequency (flexural mode) is the focused of this study. As the natural frequencies of the higher modes are more indicative of the damage in large civil engineering structures, higher mode of natural frequencies should be taken into

account in testing of actual bridge structures in the field. More research is needed in this area.

One of the primary issues with this test is the general level of sensitivity to small flaws in a structure. The test results show minor changes in frequency between undamaged state and when the first crack develops. This information can be useful in developing repair/rehabilitation programs.

In summary, the deterioration (cracking) in this preliminary study was induced by application of static loading. Further work is required to study other higher modes of deterioration. More research is needed on full-scale bridge structure, in the prevailing environments, coupled with laboratory tests on rmodels of representative structure in the laboratory for more detailed studies.

References

1. AASHTO (1994) “Manual for condition evaluation of bridges”, Second Edition, Washington, D.C.
2. Abdel-Ghafffar, A. M., and Housner, G. W. (1978) “Ambient vibration tests of suspension bridge,” Journal of the Engineering Mechanics Division, 104(5), 983-999
3. Abdel Wahab, M. M., and De Roeck, G. (1998), “Dynamic testing of prestressed concrete bridges and numerical verification.” Journal of Bridge Engineering, 3(4), 159 – 169
4. Ahlskog, J. J. (1990), “Bridge management, the answer to the challenge,” Proceedings of the NATO Advanced Workshop on Bridge Evaluation, Repair and Rehabilitation, Baltimore, Marybond, May, 1990
5. Aktan, A. E., Lee, K. L., Chuntavan, C. And Aksel, T. (1994) “Modal testing for structural identification and condition assessment of constructed facilities” Proceeding of 12th International Modal Analysis Conference, Proc. SPIE Vol. 2251, pp. 462-468, 1994
6. Alampalli, S. (2000). "Effects of testing, analysis, damage, and environment on modal parameters." Mechanical Systems and Signal Processing, 14(1): 63-74.
7. Alocco, V., F. Buccino, et al. (1993). "Evaluation of structural safety margins for existing post-tensioned concrete bridges via dynamic tests." Proceedings, 5th International Conference on Structural Faults and Repair, 1: 263-271.

8. Andrade C. (1994), “Quantification of durability of reinforcing steel”, Concrete Technology: New Trends, Industrial Applications, (Aguado A., Gettu R. and shah S. P., Editors). E & FN SPON, London etc., pp.157-175
9. AOL India News, August 03, 2007 “More than 70,000 bridges rated deficient” http://www.aol.in/news/story/200708030152000177343 5
10. Armer, G.S.T. (1988) “Structural Safety: some problems of achievement and control”, in Beedle, L. S. (Ed.), The Second Century of the Skyscraper, New York: Van Nostrand Reinhold, pp. 741-57
11. Bamforth, P. B., Chapman-Andrews, (1994), “Long term performance of RC elements under UK coastal exposure conditions” Proceedings, International Conference On Corrosion and Corrosion Protection of Steel in Concrete, R. N. Swamy (Ed.), Sheffield Academic Press, 24-29 July 1994, 139-156
12. Baxter, D., Bridge Department, TSH Engineers, Architects, Planners “Bridge Inspection” http://www.ogra.org/lib/db2file.asp?fileid=20730
13. Beddoe, R. E. and M. J. Setzer (1988). "A low-temperature DSC investigation of hardened cement paste subjected to chloride action" Cement and Concrete Research 18(2): 249-256.
14. Beddoe, R. E. and M. J. Setzer (1990). "Phase transformations of water in hardened cement paste a low-temperature DSC investigation." Cement and Concrete Research 20(2): 236-242.
15. Begg, R. D., A. C. Mackenzie, et al. (1976). "Structural integrity monitoring using digital processing of vibration signals." Proceedings of the Annual Offshore Technology Conference: v 2 pap otc 2549 p 305-311.

16. Bisby L.A and Briglio M.B., “ISIS Canada educational module No.5: an introduction to structural health monitoring”, Prepared by ISIS Canada, Page 3, 2004.
17. Brownjohn, J. M. W., J. Lee, et al. (1999). "Dynamic performance of a curved cable-stayed bridge." Engineering Structures, 21(11): 1015-1027.
18. Brownjohn, J. M. W., Dumangolu, A. A., Severn, R. T. and Taylor, C. A. (1987) “Ambient vibration measurements of the Humber suspension bridge and comparison with calculated characteristics” Proceedings, Institute of Civil Engineers, Part 2, 1987, 83, 561-600
19. Brownjohn, J. M. W. (1988) “Assessment of structural integrity by dynamic measurements” Ph.D Thesis, Department of Civil Engineering, University of Bristol, Bristol, 1988
20. Brownjohn, J. M. W., Moyo, P., Omenzetter, P., and Lu, Y. (2003) “Assessment of highway bridge upgrading by dynamic testing and finite-element model updating.” Journal of Bridge Engineering, 8(3), 162-172.
21. Canadian Standards Association (2006), CSA Standard S6 – 2006, Design of Highway Bridges, Rexdale, Ontario
22. Carpenter S. T., “Structural Mechanics”, John Wiley & Sons, Inc., 1960
23. CEB (1992), “Design guide for durable concrete structures”, Second Edition, Thomas Telford Publishers
24. Conte, J. P., X. He, et al. (2008). "Dynamic testing of Alfred Zampa Memorial Bridge." Journal of Structural Engineering, 134(6): 1006-1015.
25. Creed, S. G. (2004). "Assessment of large engineering structures using data collected during in-service loading." Structural Assessment: 55-62.

26. Cunha, A., E. Caetano, et al. (2001). "Dynamic tests on large cable-stayed bridge." Journal of Bridge Engineering, 6(1): 54-62.
27. Cunha, A. and E. Caetano (2006). "Experimental modal analysis of civil engineering structures." Sound and Vibration 40(6): 12-20.
28. Delaunay, D., Grillaud, G., Bietry, J., and Sacre, C. (1999). "Wind response of long span bridges: In situ measurements and modal analysis." Proceedings of the 17th International Modal Analysis Conference, 719-725.
29. Demeter GF., "Free vibration of two-degree spring-mass systems", Dynamic and Vibration of Structures, Wiley-Interscience, 1973, pp. 31-35
30. Dennis Baxter "Bridge Inspection" http://www.ogra.org/lib/db2file.asp?fileid=20730
31. Doebling, S. W., C. R. Farrar, et al. (1998). "A summary review of vibration-based damage identification methods." Shock and Vibration Digest, 30(2): 91-105.
32. Doebling, S. W., C. R. Farrar, et al. (1996). "Damage identification and health monitoring of structural and mechanical systems from changes in their vibration characteristics: A literature review." Los Alamos National Laboratory Report LA 13070-MS.
33. EN 206 – 1:2000, "Concrete – Part 1: Specification, Performance, Production and Conformity", European Committee for Standardization.
34. Elsener, B. (2004). "Corrosion of steel in concrete: prevention, diagnosis, repair". Weinheim; Cambridge:, Wiley-VCH.

35. Estes, A. C. and D. M. Frangopol (2003). "Updating bridge reliability based on bridge management systems visual inspection results." Journal of Bridge Engineering 8(6): 374-382.
36. Farrar, C. R., S. W. Doebling, et al. (1997). “Variability of modal parameters measured on the Alamosa Canyon Bridge”. Proceedings of the International Modal Analysis Conference - IMAC.
37. Gaal, G. C. M. and J. C. Walraven (2005). “Prediction model for deterioration of concrete bridge stocks”. Transportation Research Board - 6th International Bridge Engineering Conference: Reliability, Security, and Sustainability in Bridge Engineering.
38. Gaal GCM, Veen. CVD, Djorai MH. In: Casa JR, Frangopol DM, Nowak AS, Editors. “Prediction of deterioration of concrete bridges in the Netherlands”. CIMNE; 2002. CD-ROM Proceedings.
39. Gaudreault, V. and P. Lemire, “The Age of Public Infrastructure in Canada”, Statistic Canada, 2006.
40. Gentile, C. and F. Martinez y Cabrera (2004). "Dynamic performance of twin curved cable-stayed bridges." Earthquake Engineering and Structural Dynamics, 33(1): 15-34.
41. Ghosh, U. K. (2000). “Repair and rehabilitation of steel bridges”. Rotterdam, Netherlands; Brookfield, VT :, Balkema.
42. Glass, G. K. and Buenfeld N. R. (2000). "The inhibitive effects of electrochemical treatment applied to steel in concrete." Corrosion Science, 42(6): 923-927.

43. Glass, G. K. and Buenfeld N. R. (2000b). “Chloride-induced corrosion of steel in concrete”, Prog. Struct. Engng Mater.; 2:448-458
44. Goltermann P, Andersen ME, Jensen FM. “Smart structures: possibilities, experiences and benefits from permanent monitoring” International Conference on Bridge Maintenance, Safety and Reliability, Editors: Casas JR, Frangopol DM, Nowak AS, IABMAS. CIMNE; 2002. CD-ROM Proceedings.
45. Halling, M. W., Muhammad, I., and Womack, K. C. (2001). “Dynamic field testing for condition assessment of bridge bents.” Journal of Structural Engineering,127(2), pp 161-167
46. Hammad A., Yan J. and Mostofi B., “Recent development of bridge management systems in Canada”, Annual Conference of the Transportation Association of Canada, Saskatoon, Saskatchewan, 2007.
47. Harik, I. E., D. L. Allen, et al. (1997). "Free and ambient vibration of Brent-Spence bridge." Journal of Structural Engineering 123(9), pp 1262-1268.
48. Hassanain, M. A. and R. E. Loov (2003). "Cost optimization of concrete bridge infrastructure." Canadian Journal of Civil Engineering 30(5), pp 841-849.
49. Hemez, F. M., (1993) “Theoretical and experimental correlation between finite element models and modal tests in the context of large flexible space structures”, Ph. D. Dissertation, Department of Aerospace Engineering Sciences, University of Colorado, Boulder, CO.

50. Hsieh, K. H., M. W. Halling, et al. (2006). "Overview of vibrational structural health monitoring with representative case studies" Journal of Bridge Engineering 11(6), pp 707-715.
51. Huang, C. S., Yang, Y.B., Lu, L. Y., and Chen, C. H. (1999). “Dynamic testing and system identification of a multi-span highway bridge” Earthquake Engineering and Structural Dynamics, 28(8), pp 857-878
52. Humar, J., A. Bagchi, et al. (2006). "Performance of vibration-based techniques for the identification of structural damage." Structural Health Monitoring, 5(3): 215-241.
53. Huth, O., G. Feltrin, et al. (2005). "Damage identification using modal data: Experiences on a prestressed concrete bridge." Journal of Structural Engineering 131(12): 1898-1910.
54. Hunt V., Helmicki, A., Swanson J. (2005), “Instrumentation and monitoring of the U.S. Grant Bridge” ASNT Conference, October 2005
55. Ismail, F., A. Ibrahim, et al. (1990). "Identification of fatigue cracks from vibration testing." Journal of Sound and Vibration, 140(2): 305-317.
56. Kaouk, M., (1993) “Finite element model adjustment and damage detection using measured test data”, Ph. D. Dissertation, Department of Aerospace Engineering Mechanics and Engineering Science, University of Florida, Gainesville, FL
57. Kato, M. and S. Shimada (1986). "Vibration of pc bridge during failure process." Journal of Structural Engineering New York, N.Y. 112(7): 1692-1703.

58. Kim, J.-T., C.-B. Yun, et al. (2003a). "Temperature effects on frequency-based damage detection in plate-girder bridges." KSCE Journal of Civil Engineering, 7(6): 725-733.
59. Kim, J. T., Y. S. Ryu, et al. (2003b). "Damage identification in beam-type structures: Frequency-based method vs mode-shape-based method." Engineering Structures, 25(1): 57-67.
60. Kim, J. T. and N. Stubbs (2003c). "Nondestructive crack detection algorithm for full-scale bridges." Journal of Structural Engineering, 129(10): 1358-1366.
61. Liu, Y. (1996), "Modeling the time-to-corrosion cracking of the cover concrete in chloride contaminated reinforced concrete structures" Ph.D. Thesis, Faculty of the Virginia Tech, Blacksburg, Virginia.
62. Lounis, Z. (2005). "Uncertainty Modeling of Chloride Contamination and Corrosion of Concrete Bridges". Applied Research in Uncertainty Modeling and Analysis: 491-511.
63. Lounis, Z. (2007). "Aging highway bridges." Canadian Consulting Engineer, 48(1).
64. Lounis, Z and Daigle, L. (2008), "Reliability-based decision support tool for life cycle design and management of highway bridge decks", Annual Conference of the Transportation Association of Canada (TAC), Toronto, Ontario, September 21-24, 2008, pp. 1-19
65. Lounis Z. (2007)"Aging highway bridges," Canadian Consulting Engineer, 48(1), pp. 30-34, January, 2007

66. Lounis Z.(1999), “A stochastic and multiobjective decision model for bridge maintenance management”, Infra99 International Convention, Montreal, pp 1-12, 1999.
67. Lounis et al. (1999), “Towards standardization of service life prediction of membranes”, ASTM STP 1349, American Society for Testing and Materials, pp 3-18, 1999.
68. Lauzon, R. G. and J. T. DeWolf (2006). "Ambient vibration monitoring of a highway bridge undergoing a destructive test." Journal of Bridge Engineering 11(5): 602-610.
69. Mehta, P. K. (1991). “Concrete in the marine environment”. London; New York:, Elsevier Applied Science.
70. Mendrok, K. and T. Uhl (2008). “Modal analysis of bridges for the SHM purposes” Applied Mechanics and Materials, 9 pp 143-155.
71. Miller, G. (2004) “The quest for sustainability keeps rolling along” Ontario Planning Journal, 19 (5) pg. 15
72. Mirza, M. S. And Siddiqui, S. (1996), “FCM-McGill Survey of Canada’s Municipal Infrastructure” Department of Civil Engineering, McGill University, Montreal and Federation of Canadian Municipalities, Ottawa, January 1996
73. Mirza, M. S. (2007), “Danger Ahead: The Coming Collapse of Canada’s Municipal Infrastructure”. A Report for the Federation of Canadian Municipalities, FCM, Ottawa, November 2007
74. Mirza, M. S. (2007), The Gazette, Montreal, Saturday, June 16, 2007

75. Mirza M. S. (2004), "Urgency of addressing Canada's infrastructure needs", Special presentation, Canadian P3: Under the Microscope, The 12th Annual Conference on Public-Private Partnership, Toronto, Canada, 1-6
76. Moradalizadeh, M. (1990) "Evaluation of crack defects in frames structures using resonant frequency techniques", M. Phil Thesis Civil Engineering Department , University of Newcastle Upon Tyne, Newcastle, 1990.
77. Morgan, B. J. and R. G. Oesterle (1985). "On-site modal analysis - a new, powerful inspection technique", pp 108-114
78. Murphy J. F., "Transverse vibration of a simply supported beam with symmetric overhang of arbitrary length", Journal of Testing and Evaluation, JTEVA, 25(5), pp 522-524, 1997
79. Mychele Gagnon, Valerie Gaudreault and Donald Overton,(2008) "Age of public infrastructure: A provincial perspective", Statistic Canada, 2008.
80. National Bridge Inventory (NBI) (2003), United States NBI Rep. 2003, www.nationalbridgeinventory.com/nbireport200322.html
81. National Bridge Inventory (NBI) (2006). http://fhwa.dot.gov/bridge/nbi.htm (Nov. 2006)
82. National Bridge Inspection Standards (NBIS), Federal Regulations 69 FR74436. Federal Highway Administration, U.S.A. December 14, 2004
83. Nawy, E. G. (2008). "Concrete construction engineering handbook". Boca Raton :, CRC Press.

84. Ndambi, J. M., B. Peeters, et al. (2000). "Comparison of techniques for modal analysis of concrete structures." Engineering Structures, 22(9): 1159-1166.

85. Ndambi, J. M., J. Vantomme, et al. (2002). "Damage assessment in reinforced concrete beams using eigenfrequencies and mode shape derivatives." Engineering Structures, 24(4): 501-515.

86. Neville, A. M. and Brooks J. J. (1987), "Concrete Technology", Longman Scientific and Technical

87. Parhizkar, T., Ramezanianpour, A. A., Hillemerier B., and Mozafari, N., (2003) "The role of non-destructive tests for evaluation of a concrete structure in the Persian Gulf Region – Case study". International Symposium (NDT-CE 2003), September 16-19, Berlin, Germany.

88. Pavic, A., T. Armitage, et al. (2002). "Methodology for modal testing of the Millennium Bridge, London." Proceedings of the Institution of Civil Engineers: Structures and Buildings 152(2): 111-121.

89. Peeters B., Maeck J., De Roeck, G., "Dynamic monitoring of the Z24-bridge: separating temperature effects from damage", Proceedings of the European COST P3 Conference on System Identification and Structural Health Monitoring, pp. 377-386, Madrid, Spain, Lipiec 2000

90. Peeters, B. (2000), "System identification and damage detection in civil engineering." Ph.D thesis, K. U. Leuven, Belgium.

91. Phares, B., (2001) "Highlights of study of reliability of visual inspection," Proceedings of the Annual Meeting of TRB Subcommittee A2C05 (1):

Non-destructive Evaluation of Structures, FHWA Report Nos FHWA-RD-01-020 and FHWA-RD-01-021.

92. Postema, F. and A. Van Beek (2003). "NDT used in the Netherlands from a principal point of view." Proceedings of the International Symposium on Nondestructive Testing in Civil Engineering.
93. Polder, R. B. and Larbi, A. (1995), "Investigation of concrete exposed to North Seawater submersion for 16 years" Heron (Delft), 40(1), pp. 31-56.
94. Prine, D. W. (1995). "Problems associated with nondestructive evaluation of bridges". Proceedings of SPIE - The International Society for Optical Engineering, 2456, pp 46-52.
95. Proulx J, Hebert D, Paultre P. "Evaluation of the dynamic properties of a steel arch bridge". In: Proceedings of the Tenth International Modal Analysis Conference, Society for Experimental Mechanics, Vethel, CN, 1992:160-5
96. Purkiss, J. A., Bailey, M., Friswell, M. I., Penny, J. E. T. and Wood, M. G. (1994) "The dynamic response of prestressed concrete bridge decks" Institution of structural engineers Library, London.
97. Radomski, W. (2002). "Bridge rehabilitation". London, Imperial College Press.
98. Razak, H. A. and F. C. Choi (2001). "The effect of corrosion on the natural frequency and modal damping of reinforced concrete beams." Engineering Structures, 23(9): pp 1126-1133.

99. Ren, W. X., I. E. Harik, et al. (2004). "Roebling suspension bridge. II: Ambient testing and live-load response." Journal of Bridge Engineering 9(2): pp 119-126.

100. Ren, W. X., T. Zhao, et al. (2004). "Experimental and analytical modal analysis of steel arch bridge." Journal of Structural Engineering, 130(7): pp 1022-1031.

101. Rens, K. L. and D. J. Transue (1998). "Recent trends in nondestructive inspections in state highway agencies." Journal of Performance of Constructed Facilities 12(2): pp 94-96.

102. Rens K., Wipf T. And Klaiber F. (1997), "Review of non-destructive evaluation techniques of civil infrastructure", Journal of Performance of Constructed Facilities, 11(4) pp 152-160

103. Ren Wei-Xin; Harik, Issam E., M. ASCE; Blandford George E., M. ASCE; Lenett, M., M.ASCE; and Baseheart, T. M., M.ASCE (2004) "Roebling Suspension Bridge.II: Ambient Testing and Live-load Response" Journal of Bridge Engineering, 9(2), pp 119-126.

104. Robinson, M. J., M. W. Hailing, et al. (2000). "Condition assessment of a six span full-scale bridge using forced vibration". Proceedings of SPIE - The International Society for Optical Engineering, 3995, pp 404-413.

105. Roeck G. De, Peeters B. and Maeck J., 2000 "Dynamic monitoring of civil engineering structures", Computational methods for shell and spatial structures, IASS-IACM 2000

106. Roeck De G., Peeters B. and J. Maeck, (2000) “Dynamic monitoring of civil engineering structures”, Computational methods for shell and spatial structures IASS-IACM 2000

107. Rytter, A. (1993) “Vibration based inspection of civil engineering structures”, Ph.D. Dissertation, Department of Building Technology and Structural Engineering, Aalborg University, Denmark

108. Rytter, A. (1993). “Vibration based inspection of civil engineering.” Ph.D Dissertation, University of Aalborg, Denmark.

109. Salawu O. S. and Williams C. (1995), “Review of full-scale dynamic testing of bridge structures”, Engineering Structure, 17(2).

110. Salawu, O. S. (1997). "Assessment of bridges: Use of dynamic testing." Canadian Journal of Civil Engineering 24(2): pp 218-228.

111. Salawu, O. S. and C. Williams (1993). “Structural damage detection using experimental modal analysis - A comparison of some methods” Proceedings of SPIE- The International Society for Optical Engineering, 1923, pp 254-260.

112. Salawu, O. S. and C. Williams (1995). "Review of full-scale dynamic testing of bridge structures." Engineering Structures, 17(2): pp 113-121.

113. Sexton R., Koganti S., Helmicki A. Hunt V. Swanson J. (2005), “Aspect of Health Monitoring for Cable Stay Bridges” Final Draft: September 1, 2005

114. Silano, L. G. and B. Parsons (1993). “Bridge inspection and rehabilitation: a practical guide”. John Wiley and Sons, New York, U.S.A.

115. Slastan, J. and S. Pietrzko (1993). “Changes of RC-beam modal parameters due to cracks”. Proceedings of SPIE - The International Society for Optical Engineering, 1923, pp 70-76.

116. Sloan, T. D., Kirkpatrick, J., Boyd, J. W. And Thompson, A. (1992) “Monitoring the in-service behaviour of the Foyle bridge”, Structural Engineer, 70(7), pp 130-134

117. Sohn, H., Farrar, C., Hemez, F., Shunk, D., Stinemates, D., and Nadler, B. (2003). “A review of structural health monitoring literature: 1996 – 2001.” Report No. LA-13976-MS, Los Alamos National Laboratory, Los Alamos, N.M.

118. Sohn, H., C. R. Farrar, et al. (2003). "A review of structural health monitoring literature: 1996-2001." Los Alamos National Laboratory Report LA-13976-MS.

119. Structural Rehabilitation Manual (1996). Manual SO-88-7, Ontario Ministry of Transportation, Canada

120. Taskov, L. A. (1988) “Dynamic testing of bridge structures applying forced and ambient vibration methods”, Proceedings, Conference on Civil Engineering Dynamics, Society for Earthquakes and Civil Engineering Dynamics, London, UK, 1988, Paper 6

121. The Daily, “Study: the age of Canada’s public infrastructure”, Monday, January 30, 2006.

122. Transportation Research Board (TRB), National Cooperative Highway Research Program Report No. 312, “Condition surveys of

concrete bridge components - User's Manual," National Research Council, National Academy of Sciences, Washington, D. C., December, 1988

123. Tsang, W. F. And Rider, E. (1988) "Modelling of structures using experimental forced vibration data with a particular application in force prediction" RNEC Research Report RNEC-RP-88023. Royal Naval Engineering College, Plymouth, UK, 1988

124. Wallbank RJ. (1989) "The performance of concrete in bridge: a survey of 200 highway bridges". London: Department of Transport, Her Majesty's Stationery Office.

125. Wenzel, H. and D. Pichler (2005). "Ambient vibration monitoring" Chichester, England; Hoboken, NJ:, John Wiley and Sons, New York, U.S.A.

126. Williams, C. (1983) "Vibration monitoring of some civil engineering structures", B.S.S.M./Mech. E. Joint Conf. Measurement in the Vibration Environment, British Society for Strain Measurement, Durham, UK

127. Xu, Z. D. and W. Zhishen (2007). "Simulation of the effect of temperature variation on damage detection in a long-span cable-stayed bridge." Structural Health Monitoring, 6(3): pp 177-189.

128. Zhan, Z.(1994). "Error study of bridge tests for the purpose of structural identification" in Proceedings, 12th International Modal Analysis Conference, Honolulu, Hawaii, 1, pp 433-441.

Appendix A

Design of Beam

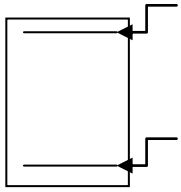

f'c = 30 MPa

fy = 400 MPa

Cover = 20 mm

200 x 300 mm

L = 2.0 m

The effective depth,

$$d = 300 - 20 - 11.3 - \frac{16}{2} = 260 \text{ mm}$$

The minimum steel cross-sectional area,

$$As_{min.} = \frac{0.2\sqrt{f'c}}{fy} b\ h$$

$$= 0.2 \frac{\sqrt{30}}{400} * 200 * 300$$

$$= 165 \text{ mm}^2$$

Steel area provided,

$$As_{provided} = 2 * 200 = 400 \text{ mm}^2 > As_{min.} \text{ (o.k.)}$$

Steel ratio,

$$\rho = \frac{As}{bd} = \frac{2*200}{200*260} = 0.00769 = 0.77\ \%$$

For ρ = 0.77%, kr = 2.4 (CSA A 23.3 Table 2.1)

$$Mr = kr\ bd^2 * 10^{-6}$$

$$= 2.4 * 200 * (260)^2 * 10^{-6}$$

$$= 32.45 \text{ kN.m}$$

For a concentrated load at mid span, the maximum moment,

$M_r = \frac{PL}{4}$

$32.45 = \frac{P * 1.9}{4}$

P = 65 kN

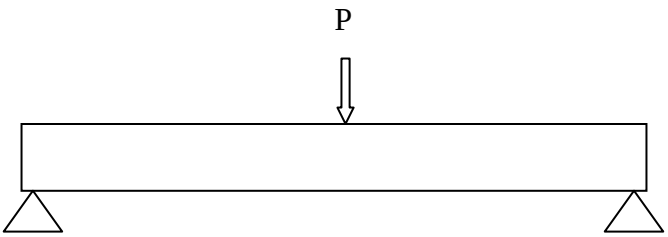

For two concentrated loads at one-third span, as shown:

$Mr = \frac{P}{2}\frac{L}{3} = \frac{PL}{6}$

$32.45 = \frac{P * 1.9}{6}$

P = 99 kN

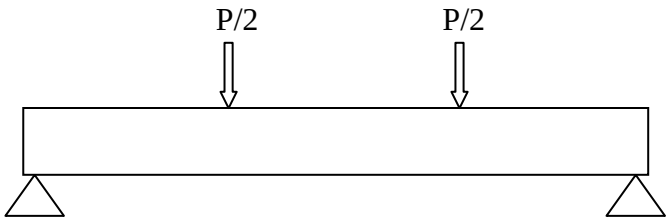

Check for spacing between bars

$$s \geq \begin{cases} 1.4\ db = 1.4 * 16 = 23 \\ 1.4\ amax = 1.4 * 20 = 28 \\ 30\ mm \end{cases}$$

s = [200 – 2(20) – 2(11.3) – 2(16)]/1

= 105.4 mm > 30 mm (O.K.)

Design for shear

Effective shear depth,

d_v = 0.9 d = 0.9 * 260 = **234 mm** (Governs)

or

d_v = 0.72 h = 0.72 * 300 = 210 mm whichever is greater

$V_c = \Phi_c\ \lambda\ \beta\ \sqrt{f'c}\ b_w\ d_v$

= 0.65* 1.0* 0.18 * $\sqrt{30}$ * 200 * 234* 10^{-3}

= 30 kN

$V_{r\,max} = 0.25\ \Phi_c\ f'_c\ b_w\ d_v + V_p$

$= 0.25 * 0.65 * 30 * 200 * 234 + 0$

$= 228$ kN

$V_r = 0.18\ \Phi_c\ \lambda\ \sqrt{f'c}\ b_w\ d_v + 1.43\ \Phi_s\ \frac{Av}{s}\ fy\ d_v$

$V_r \geq V_f = 65$ kN or **99 kN**

$0.18\ \Phi_c\ \lambda\ \sqrt{f'c}\ b_w\ d_v + 1.43\ \Phi_s\ \frac{Av}{s}\ fy\ dv \geq 99 * 10^3$

$0.18 * 0.65 * 1.0 * \sqrt{30} * 200 * 234 + 1.43 * 0.85\ \frac{Av}{s}\ 400 * 234 \geq 99 * 10^3$

$\frac{Av}{s} \geq$ 0.6065 mm^2 / mm

For 10M stirrups,

$A_v = 2 * 100 = 200$ mm2

$s \leq \frac{200}{0.6065} = 329$ mm

The maximum stirrup spacing (CSA 23.3 Clause 11.3.8.1)

$\frac{V_f}{b_w d_v} = \frac{99*10^3}{200*234} = 2.115$ MPa

$0.125\ \lambda\ \Phi_c\ f'_c = 0.125 * 1.0 * 0.65 * 30 = 2.4375$ MPa

$\frac{V_f}{b_w d_v} < 0.125\ \lambda\ \Phi_c\ f'_c$

$s_{max} = 600$ mm or

$0.7\ d_v = 0.7 * 234 =$ **163.8 mm** whichever is less

(b) $A_{v\,min} = \frac{0.06\sqrt{f'c}}{fy}\ b_w\ s$ (CSA 23.3 Clause 11.2.8.2)

$s_{max} = \frac{Av\ fy}{0.06\ bw\ \sqrt{f'c}} = \frac{(2*200)(400)}{0.06*200\ \sqrt{30}} = 2434$ mm

Stirrup spacing of 160 mm on centres is provided.

Check V_r for s = 160 mm

$V_r = V_c + V_s$

$$= \emptyset_c \lambda \beta \sqrt{f'_c}\, b_w d_v + \frac{\emptyset_S A_v f_y d_v \cot\theta}{s}$$

$$= 065 * 1.0 * 0.18 * \sqrt{30} * 200 * 234 + \frac{0.85*(2*100)*400*234*\cot\theta}{160}$$

= 172 kN > V_f = 65 and 99 kN (O.K.)

α_1 =0.85 – 0.15 f'c

= 0.85 – 0.0015 (30)

= 0.805 > 0.67 O.K.

β_1 = 0.97 – 0.0025 f'c

= 0.97 – 0.0025 (30)

= 0.895 > 0.67 O.K.

From equilibrium,

the steel tensile force = compressive force resultant in the concrete (ignoring the compression reinforcement)

$$\emptyset_s A_s f_y = \alpha_1 \emptyset_c f'_c \beta_1 c\, b$$

$$c = \frac{\emptyset_s A_s f_y}{\alpha_1 \emptyset_c f'_c \beta_1 b} = \frac{0.85*400*400}{0.805*065*30*0895*200} = 84.40 \text{ mm}$$

$$c_b = \left(\frac{700}{700+fy}\right)d = \left(\frac{700}{700+400}\right)260 = 246 \text{ mm}$$

$c < c_b$

Therefore, the beam is under reinforced.

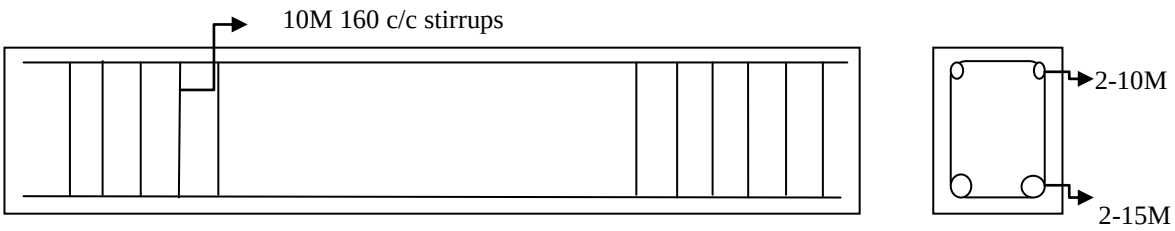

Beam details

Appendix B

Cracking and Ultimate Load

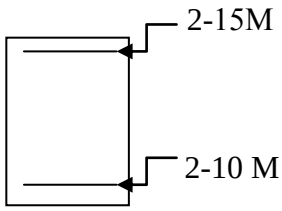

f'c = 34.5 MPa

fy = 400 MPa

Cover = 20 mm

200 x 300 mm

Ultimate load calculation

$$d = 300 - 20 - 11.3 - \frac{11.3}{2} = 263 \text{ mm}$$

$$A_{s\ min.} = \frac{0.2\sqrt{f'c}}{fy} b\ h$$

$$= 0.2\ \frac{\sqrt{34.5}}{400} * 200 * 300$$

$$= 177\ mm^2$$

$$A_{s\ provided} = 2 * 100 = 200\ mm^2 > A_{s\ min.}\ \text{(o.k.)}$$

$$\rho = \frac{As}{bd} = \frac{2*100}{200*263} = 0.0038 = 0.38\ \%$$

For ρ = 0.38%, k_r = 1.23 (CSA A 23.3 Table 2.1)

$$M_r = k_r\ bd^2 * 10^{-6}$$

$$= 1.233 * 200 * (263)^2 * 10^{-6}$$

$$= 17.06\ \text{kN.m}$$

For a concentrated load at mid-span, the maximum moment,

$$M_r = \frac{PL}{4}$$

$$17.057 = \frac{P*1.9}{4}$$

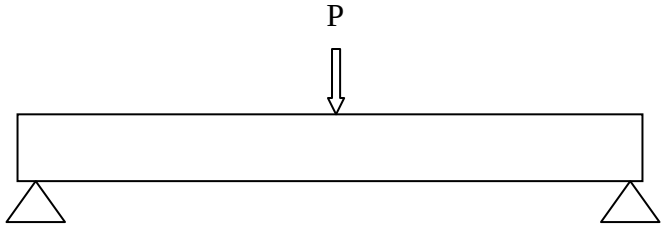

Therefore, the ultimate load, P_u, is

P_u = 36 kN

For two symmetric third-point concentrated loads, as shown:

$M_r = \frac{P}{2}\frac{L}{3} = \frac{PL}{6}$

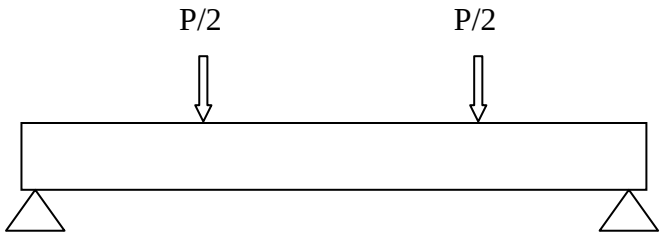

$17.057 = \frac{P*1.9}{6}$

Therefore, the ultimate load,

P_u = 53.86 kN

Cracking load calculation

Theoretical cracking load calculation

Modulus of rupture, $f_r = 0.6\ \lambda \sqrt{f'c}$ CSA A 23.3 (8.6.4)

$= 0.6 * 1* \sqrt{34.5} = 3.52$ N/mm^2

Cracking moment, $M_{cr} = f_r * Z_t$

$= 3.52 * (\frac{1}{6} * 200 * (300)^2 * 10^{-6})$ kN-m

= 10.56 kN.m

For a concentrated load at mid-span, the maximum moment is,

$M_r = \frac{PL}{4}$

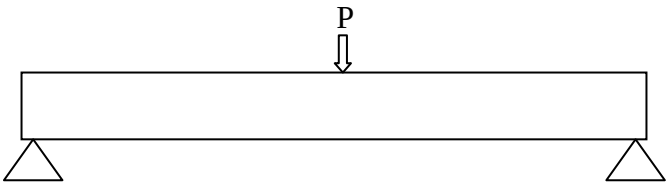

$10.56 = \frac{P*1.9}{4}$

Therefore, the cracking load, P_{cr}, is

P_{cr} = 22.23 kN

For two symmetric third-point concentrated loads, as shown:

$M_r = \frac{P}{2}\frac{L}{3} = \frac{PL}{6}$

$10.56 = \frac{P*1.9}{6}$

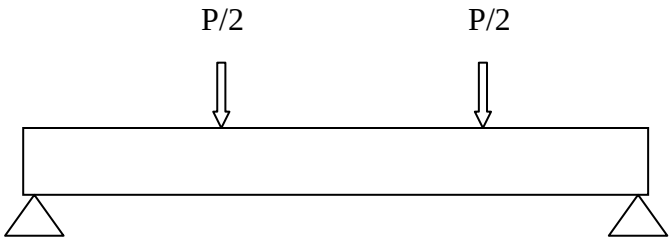

Therefore, the cracking load, P_{cr}, is

P_{cr} = 33.35 kN

Experimental cracking load calculation

Modulus of rupture, f_{cr} = 4.0 N/mm^2

Cracking moment, $M_{cr} = f_{cr} * Z_t$

$= 4.0 * (\frac{1}{6} * 200 * (300)^2 * 10^{-6})$ kN.m

= 12 kN.m

For a concentrated load at mid-span, the maximum moment is:

$M_r = \frac{PL}{4}$

$12 = \frac{P*1.9}{4}$

Therefore, the cracking load, P_{cr}, is

P_{cr} = 25.26 kN

For two symmetric third-point concentrated loads, as shown:

$M_r = \frac{P}{2}\frac{L}{3} = \frac{PL}{6}$

$12 = \frac{P*1.9}{6}$

Therefore, the cracking load, P_{cr}, is

P_{cr} = 36 kN

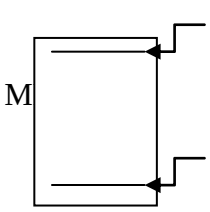

Concrete compressive strength f'c = 34.5

Steel yield strength f_y = 400 MPa

Concrete cover thickness = 20 mm

200 x 300 mm

Therefore, effective depth, d, is

$$d = 300 - 20 - 11.3 - \frac{16}{2} = 260 \text{ mm}$$

Ultimate load calculation

$$A_{s\ min.} = \frac{0.2\sqrt{f'c}}{fy} b\ h$$

$$= 0.2\ \frac{\sqrt{34.5}}{400} * 200 * 300$$

$$= 177\ mm^2$$

$A_{s\ provided} = 2 * 200 = 400\ mm^2 > A_{s\ min.}$ Therefore, O.K.

$$\rho = \frac{As}{bd} = \frac{2*200}{200*260} = 0.00769 = 0.77\ \%$$

For ρ = 0.77%, k_r = 2.4 (CSA A 23.3 Table 2.1)

$$M_r = k_r\ bd^2 * 10^{-6}$$

$$= 2.4 * 200 * (260)^2 * 10^{-6}$$

$$= 32.45\ kN.\ m$$

For a concentrated load at mid-span, the maximum bending moment is,

$$M_r = \frac{PL}{4}$$

$$32.45 = \frac{P*1.9}{4}$$

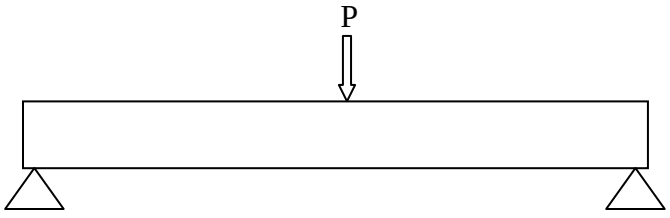

Therefore, the ultimate load, P_u, is

$P_u = 65$ kN

For two symmetric third-point concentrated loads, as shown,

$M_r = \frac{P}{2}\frac{L}{3} = \frac{PL}{6}$

$32.45 = \frac{P*1.9}{6}$

Therefore, the ultimate load, P_u, is

$P_u = 99$ kN

<u>Cracking load calculation</u>

The theoretical cracking load,

Modulus of rupture, $f_{cr} = 0.6\sqrt{fck}$

$= 0.6\sqrt{34.5} = 3.52$ N/mm^2

Cracking moment, $M_{cr} = f_{cr} * Z_t$

$= 3.52 * (\frac{1}{6} * 200 * (300)^2 * 10^{-6})$ kN.m

$= 10.56$ kN.m

For a concentrated load at mid-span, the maximum moment is:

$M_r = \frac{PL}{4}$

$10.56 = \frac{P*1.9}{4}$

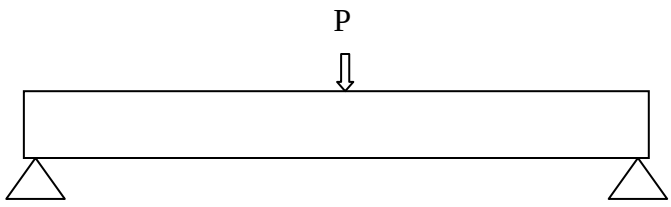

Therefore, the cracking load, P_{cr}, is

$P_{cr} = 22.23$ kN

For two symmetric third-point concentrated loads, as shown:

$M_r = \frac{P}{2}\frac{L}{3} = \frac{PL}{6}$

$10.56 = \frac{P*1.9}{6}$

Therefore, the cracking load, P_{cr}, is

$$P_{cr} = 33.35 \text{ KN}$$

Experimental cracking load

Modulus of rupture, $f_{cr} = 4.0 \text{ N/mm}^2$

Cracking moment, $M_{cr} = f_{cr} * Z_t$

$$= 4.0 * \left(\frac{1}{6} * 200 * (300)^2 * 10^{-6}\right) \text{ kN.m}$$

$$=12 \text{ kN.m}$$

For a concentrated load at mid-span, the maximum moment is:

$$M_r = \frac{PL}{4}$$

$$12 = \frac{P*1.9}{4}$$

Therefore, the cracking load is

$$P_{cr} = 25.26 \text{ kN}$$

For two symmetrical third point concentrated loads, as shown:

$$M_r = \frac{P}{2}\frac{L}{3} = \frac{PL}{6}$$

$$12 = \frac{P*1.9}{6}$$

Therefore, the cracking load, P_{cr}, is

$$P_{cr} = 37.89 \text{ kN}$$

Appendix C

Frequency Calculations

The unit weight of concrete, γ_c = 2500 kg/m^3

= 24.53 kN/m^3

Characteristic strength of concrete, f'$_c$ = 34.5 MPa (Based on compression cylinder test results)

The modulus of elasticity of concrete,

$$E_c = \left(3000\sqrt{f'_c} + 6900\right)\left(\frac{\gamma_c}{2300}\right)^{1.5}$$

= 27782 MPa

The second moment of area of the beam cross-section, ignoring steel:

$$I = \frac{1}{12} b\, d^3$$

$$= \frac{1}{12} * 0.200 * (0.300)^3$$

$$= 4.5 * 10^{-4}\ m^4$$

The mass per unit length of the beam is:

m = 2500 * 0.200 * 0.300

= 150 kg/m

According to Carpenter (1960), the angular frequency is,

$$\omega = \sqrt{\frac{EI}{m}}\ \frac{n^2\pi^2}{L^2}$$

$$\omega = \sqrt{\frac{(27782 * 10^6)N/m^2\ (4.5 * 10^{-4})m^4}{150\ kg/m}}\ \frac{1^2 * \pi^2}{1.9^2}$$

= 788.5 cycle/second

The natural period of vibration, T, is,

$$T = \frac{2\pi}{\omega}$$

The natural frequency of vibration, *f*, is

$$f = \frac{1}{T} = \frac{\omega}{2\pi}$$

$$= \frac{788.5}{2\pi}$$

= **125.6 Hz**

Alternatively,

An approximate solution to the frequency equation for simply supported beams (Murphy 1997) with symmetric overhang is

$f^2 = 2.467 \frac{EI\ gL}{S^4 W}$ (where L= length of the beam; S = span of beam, 'm';

W = total wt. of beam)

$f^2 = 2.467 \frac{EI}{S^4 m}$ (where W/gL = mass per meter length of beam, 'm')

$$f^2 = 2.467 \frac{(27782 * 10^6)(4.5 * 10^{-4})}{1.9^4 * 150}$$

= 15777.55

f **= 125.6 Hz**

Appendix D

Photographs – Cracking Pattern

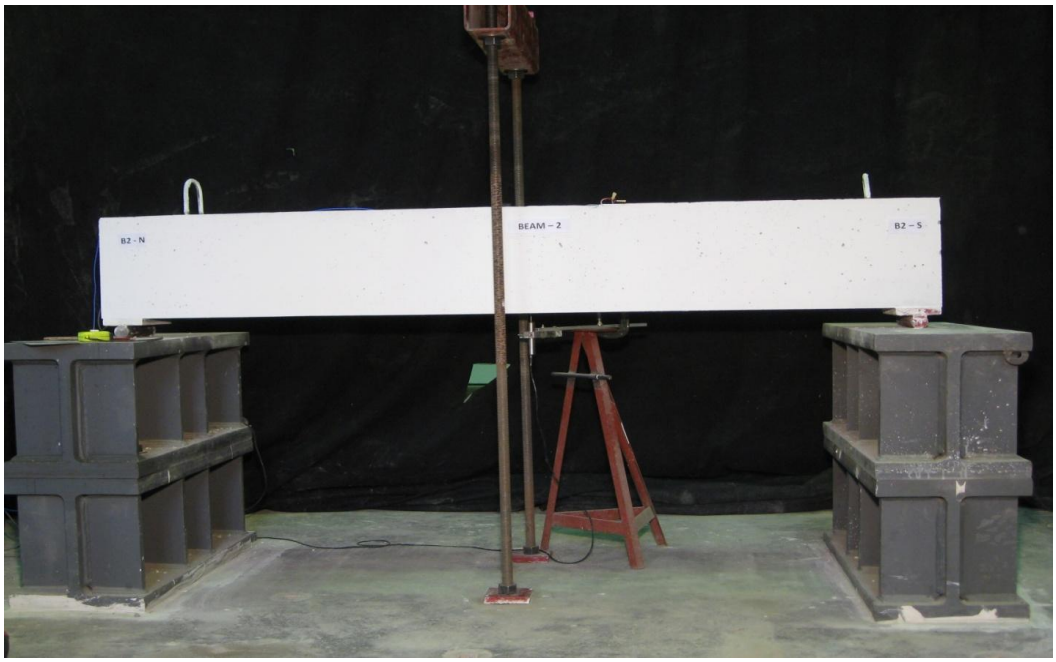

Figure D.1 – Cracking pattern for beam 2 at a load of 25.96 kN (B2-LS1)

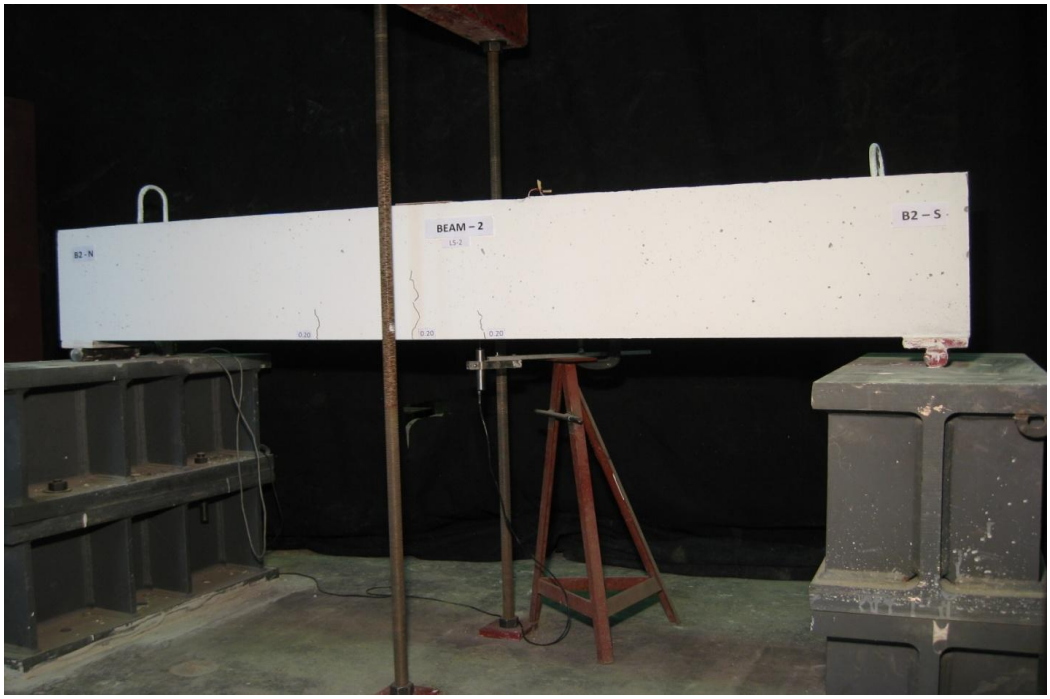

Figure D.2 – Cracking pattern for beam 2 at a load of 28.2kN (B2-LS2)

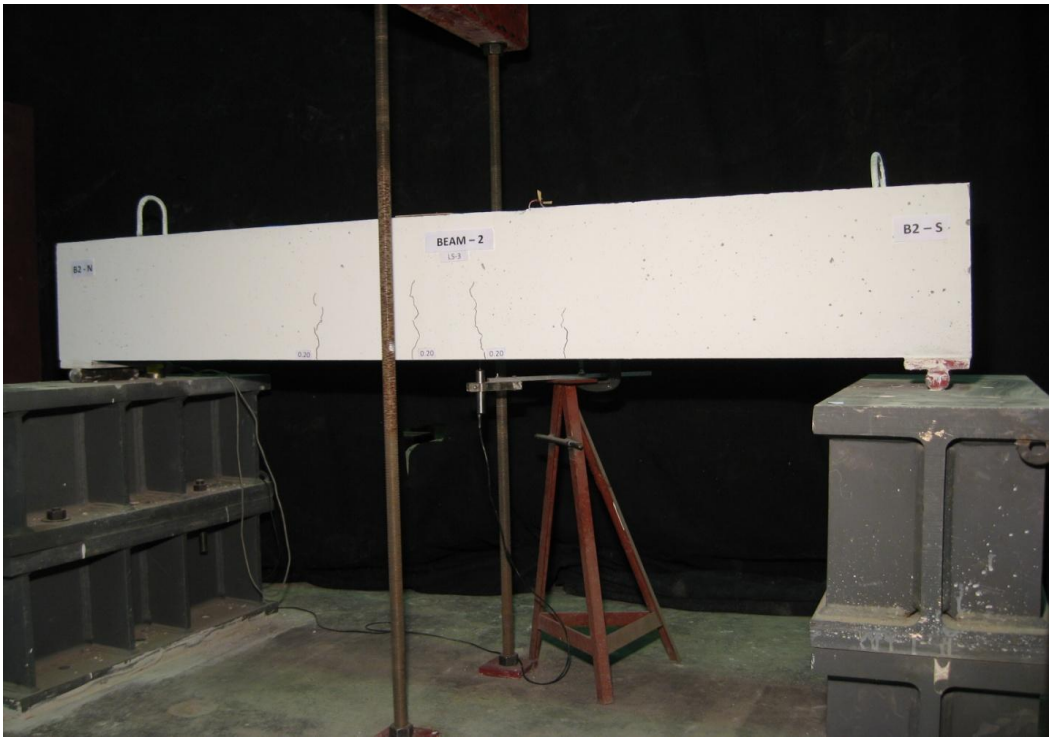

Figure D.3 – Cracking pattern for beam 2 at a load of 34.7kN (B2-LS3)

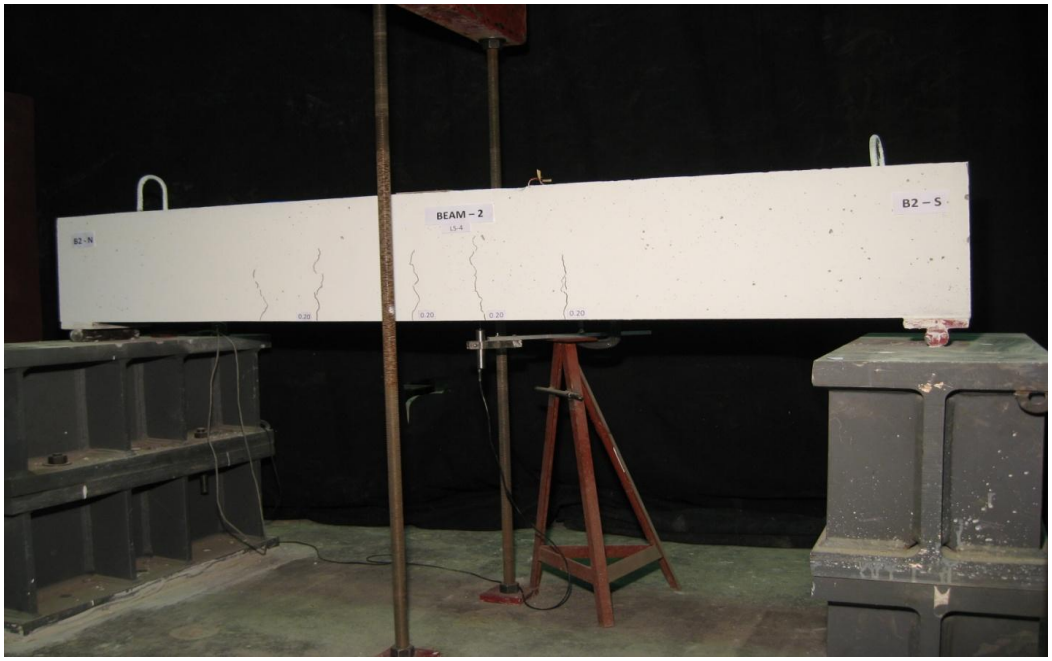

Figure D.4 – Cracking pattern for beam 2 at a load of 42 kN (B2-LS4)

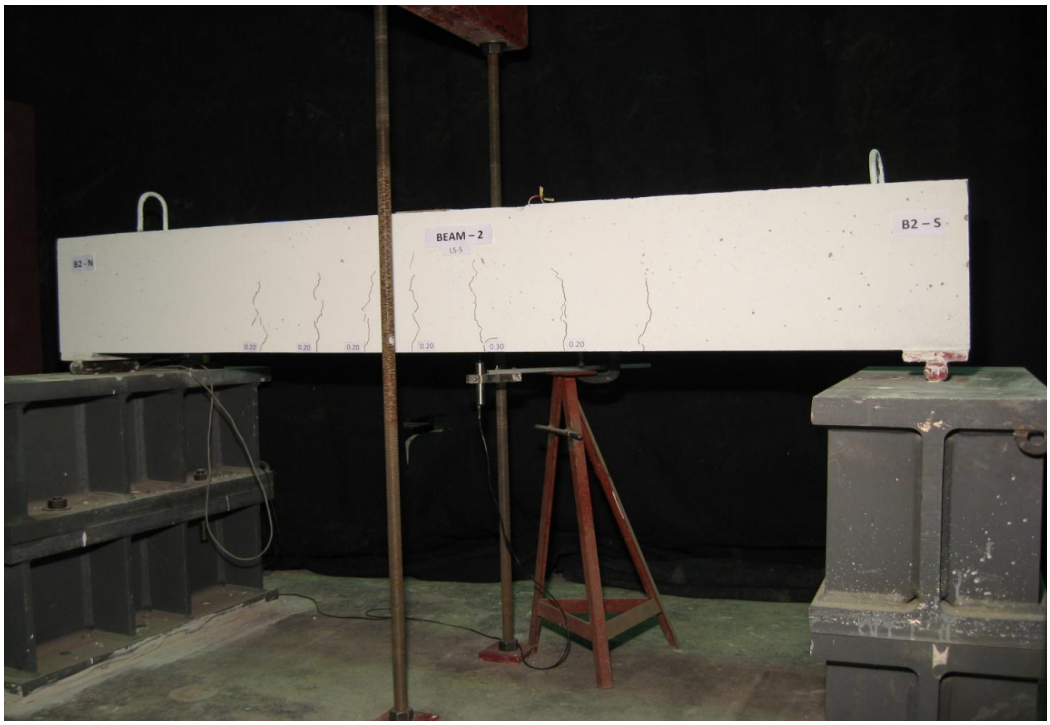

Figure D.5– Cracking pattern for beam 2 at a load of 50.2 kN (B2-LS5)

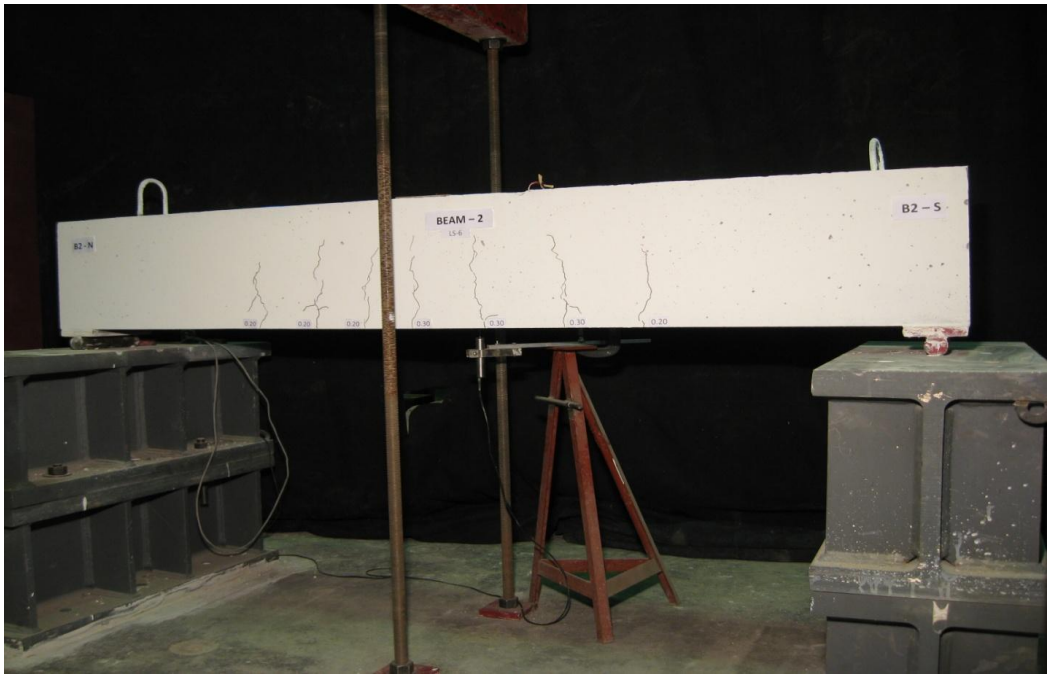

Figure D.6– Cracking pattern for beam 2 at a load of 57.3 kN (B2-LS6)

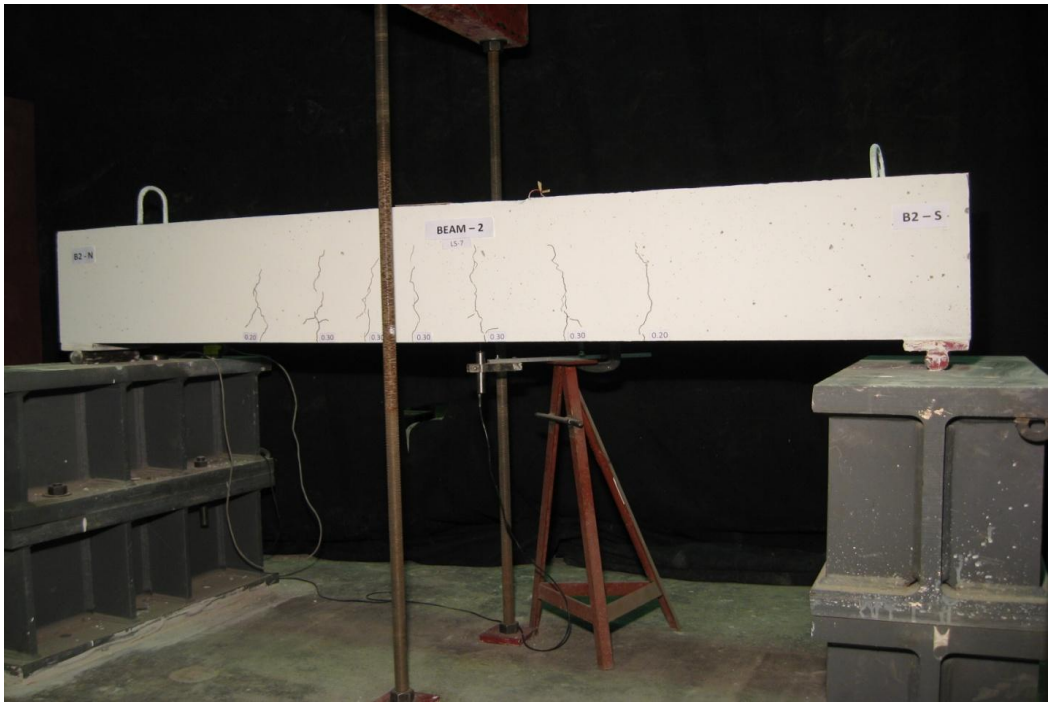

Figure D.7– Cracking pattern for beam 2 at a load of 65.4kN (B2-LS7)

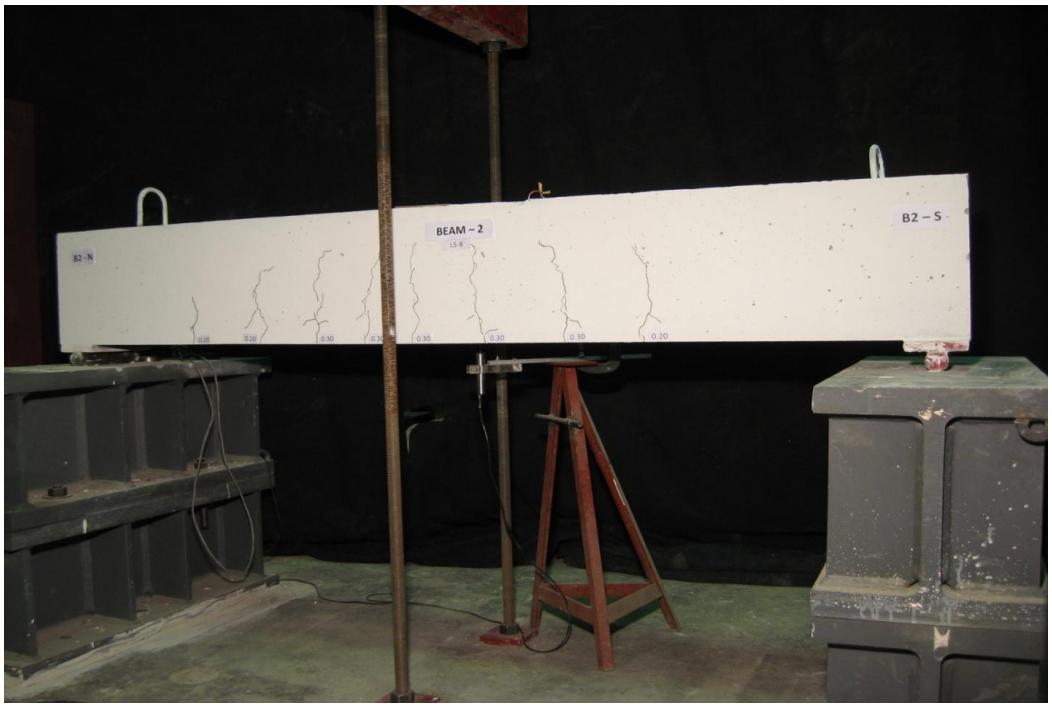

Figure D.8 – Cracking pattern for beam 2 at a load of 72.99 kN (B2-LS8)

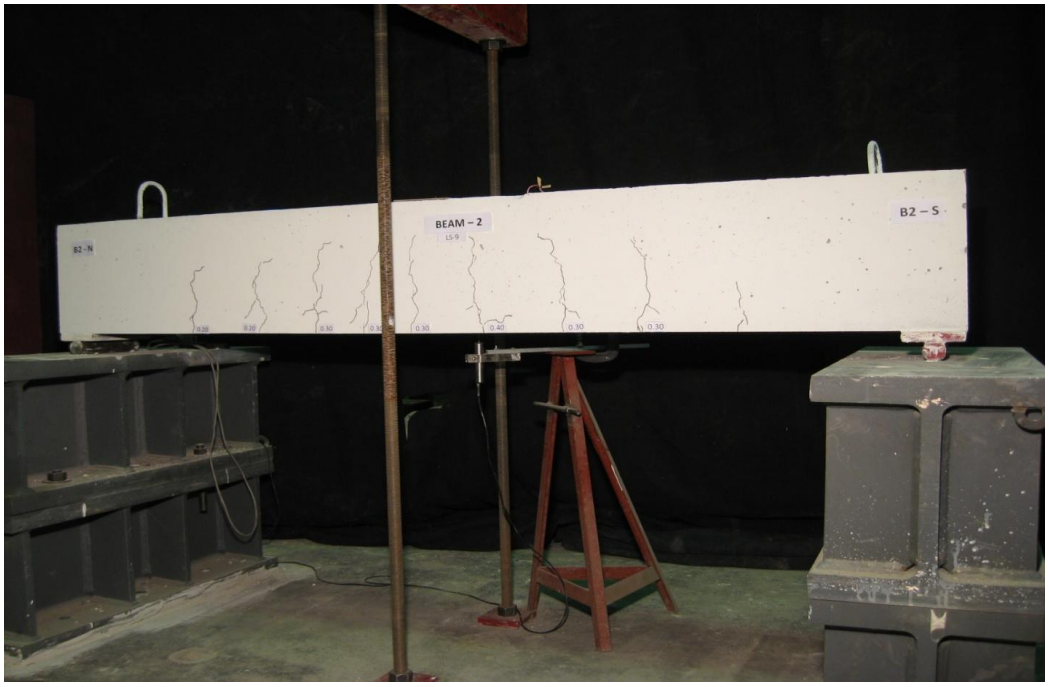

Figure D.9– Cracking pattern for beam 2 at a load of 80.4 kN (B2-LS9)

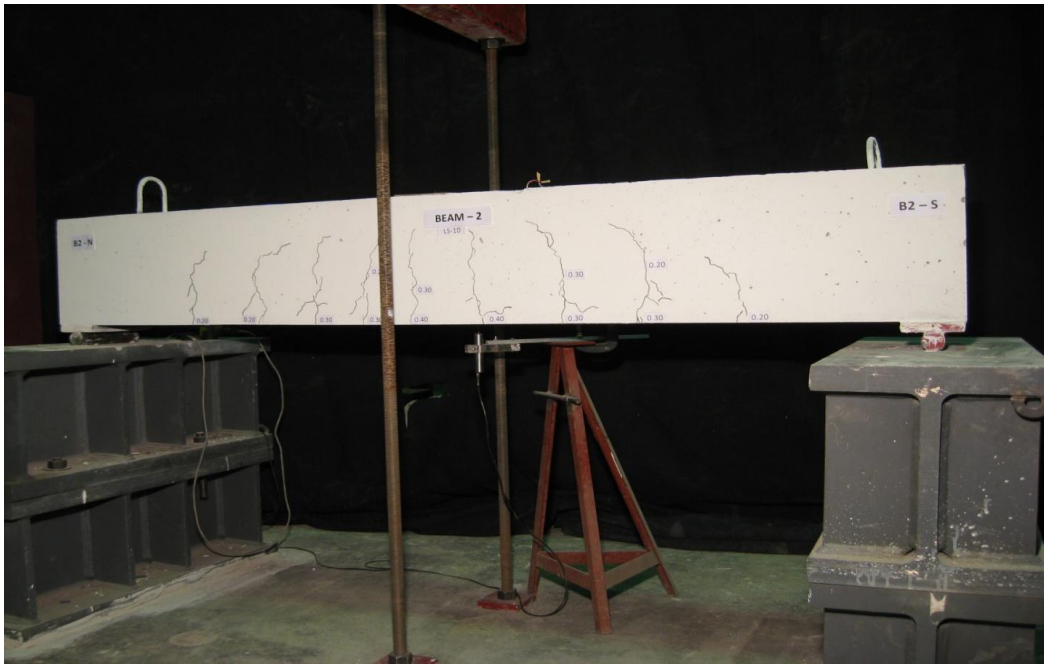

Figure D.10 – Cracking pattern for beam 2 at a load of 87.7 kN (B2-LS10)

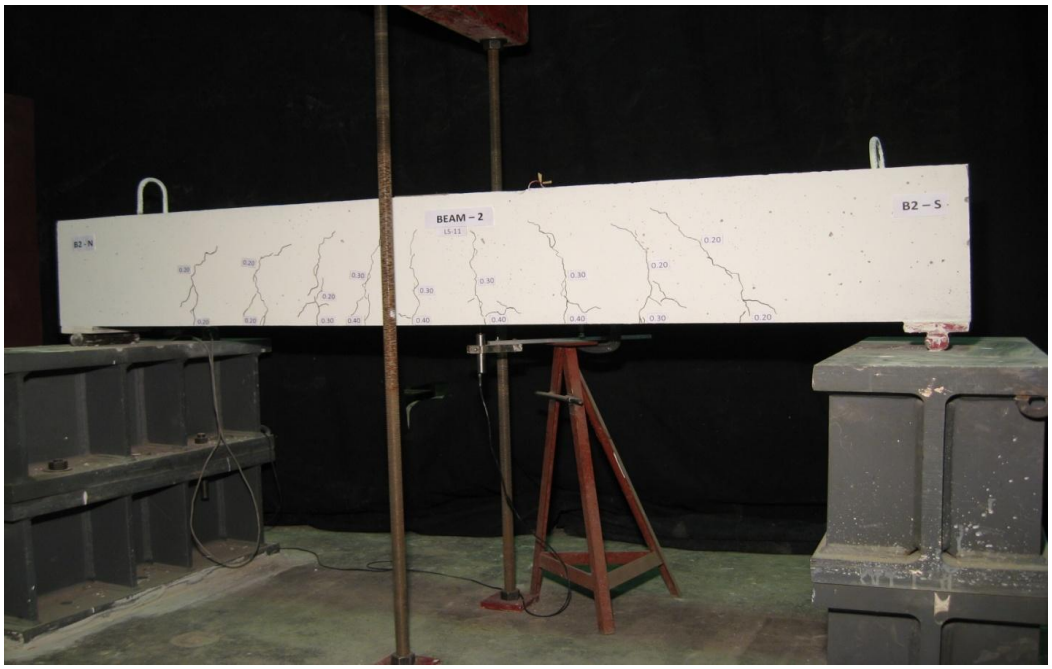

Figure D.11 – Cracking pattern for beam 2 at a load of 95.4 kN (B2-LS11)

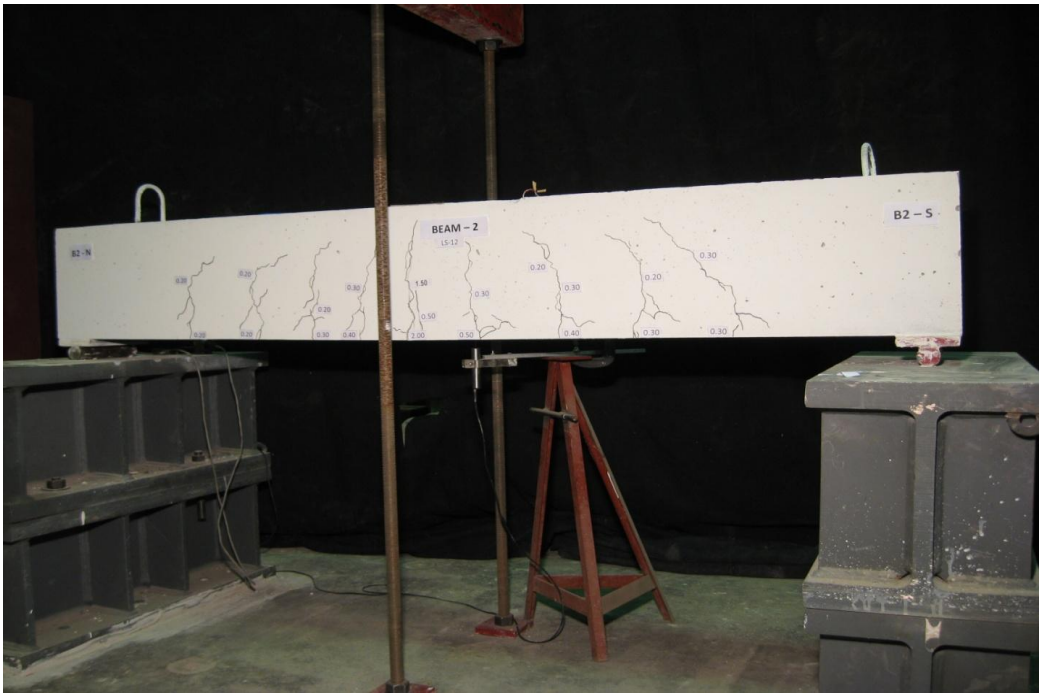

Figure D.12– Cracking pattern for beam 2 at a load of 103.2 kN
B2-LS12 (Ultimate loading)

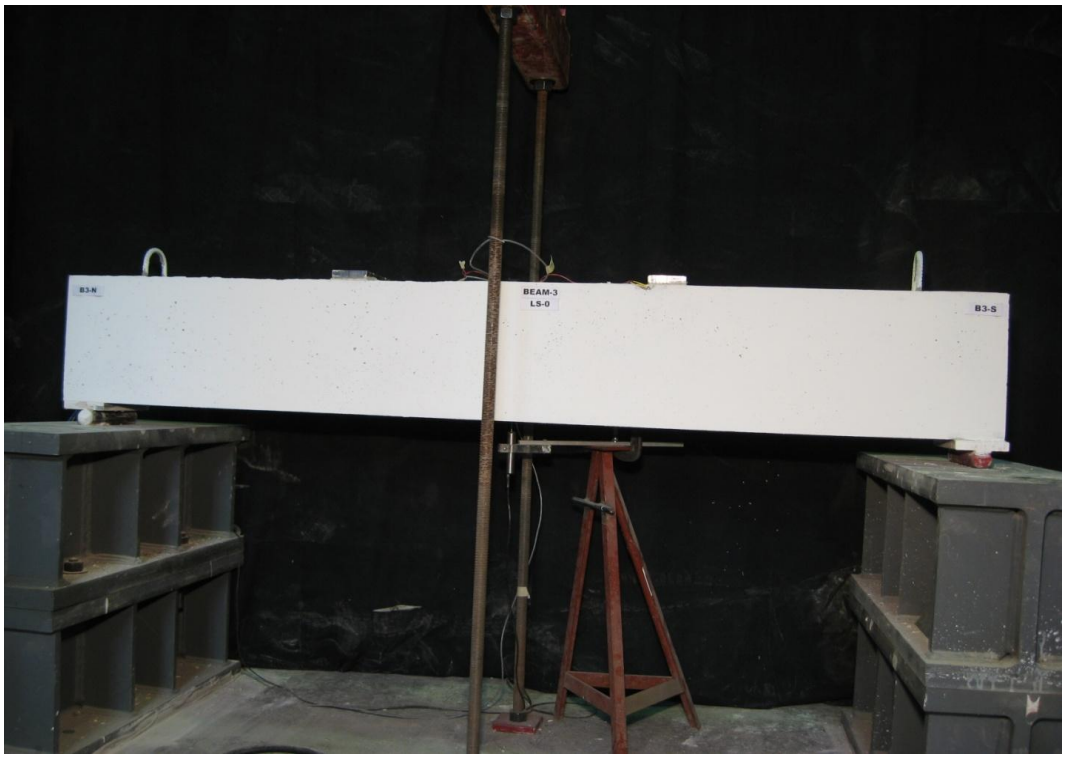

Figure D.13– Cracking pattern for beam 3 at zero load (B3-LS0)

Figure D.14– Cracking pattern for beam 3 at a load of 23.09 kN (B3-LS1)

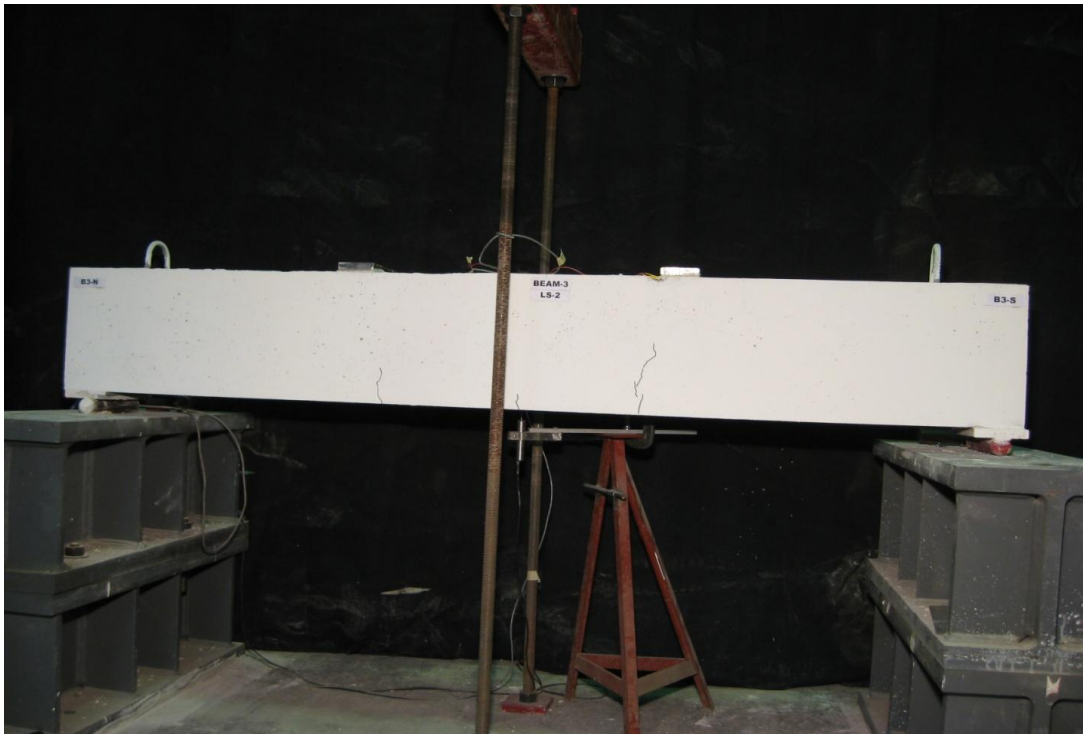

Figure D.15– Cracking pattern for beam 3 at a load of 33.7 kN (B3-LS2)

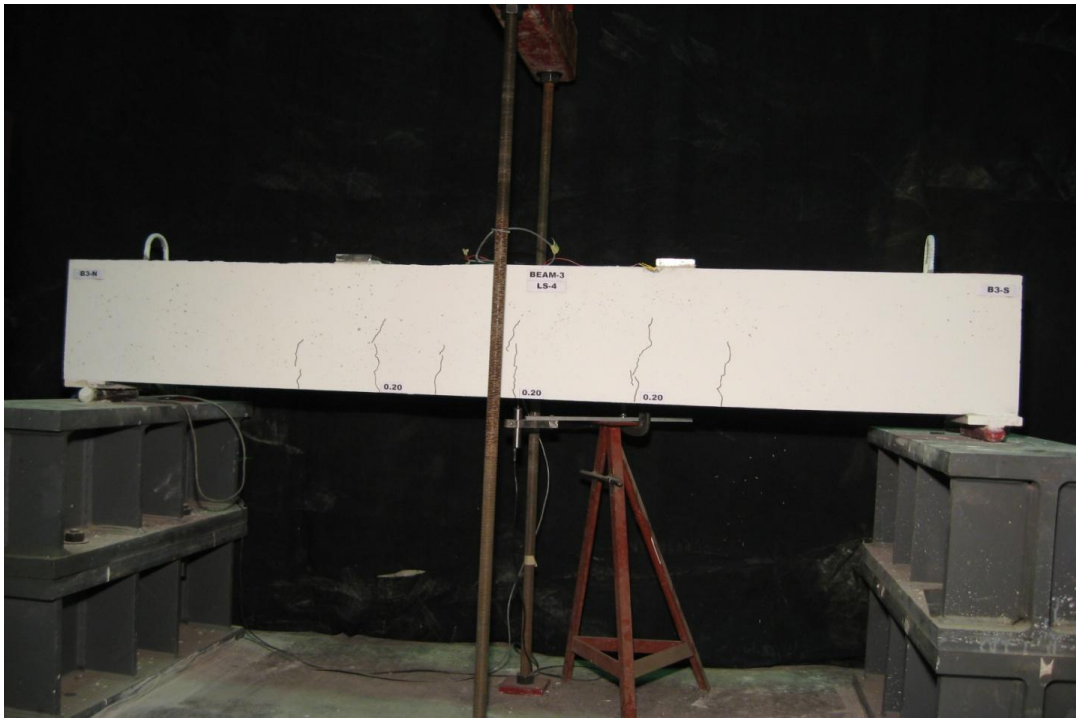

Figure D.16– Cracking pattern for beam 3 at a load of 45.6 kN (B3-LS4)

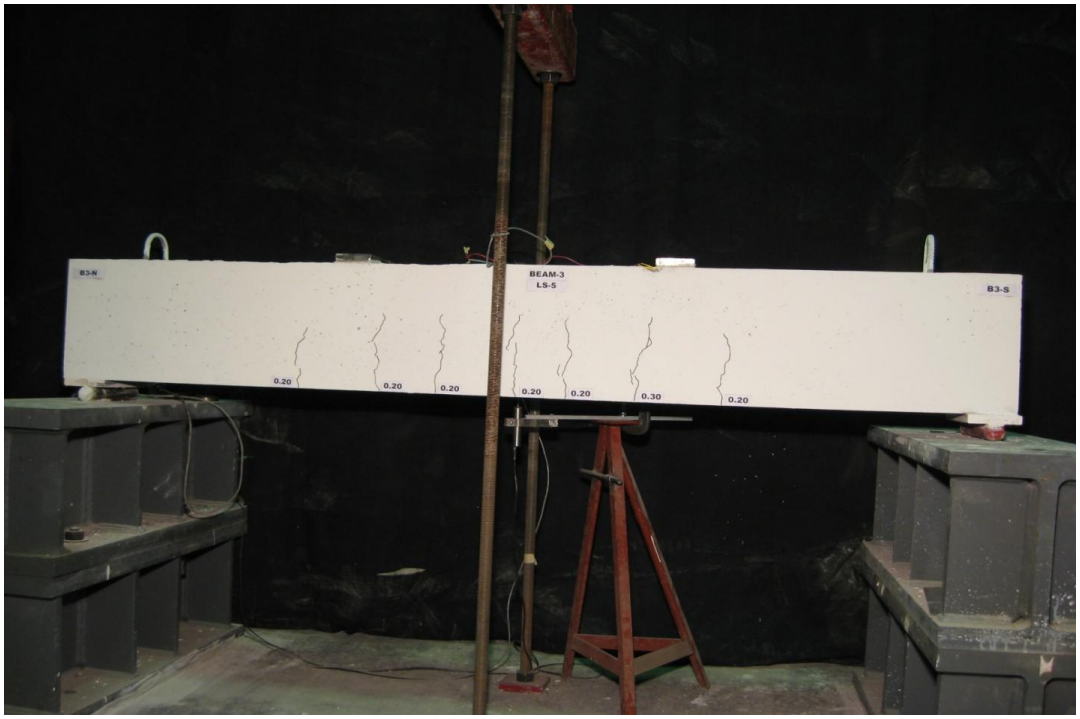

Figure D.17– Cracking pattern for beam 3 at a load of 52.1 kN (B3-LS5)

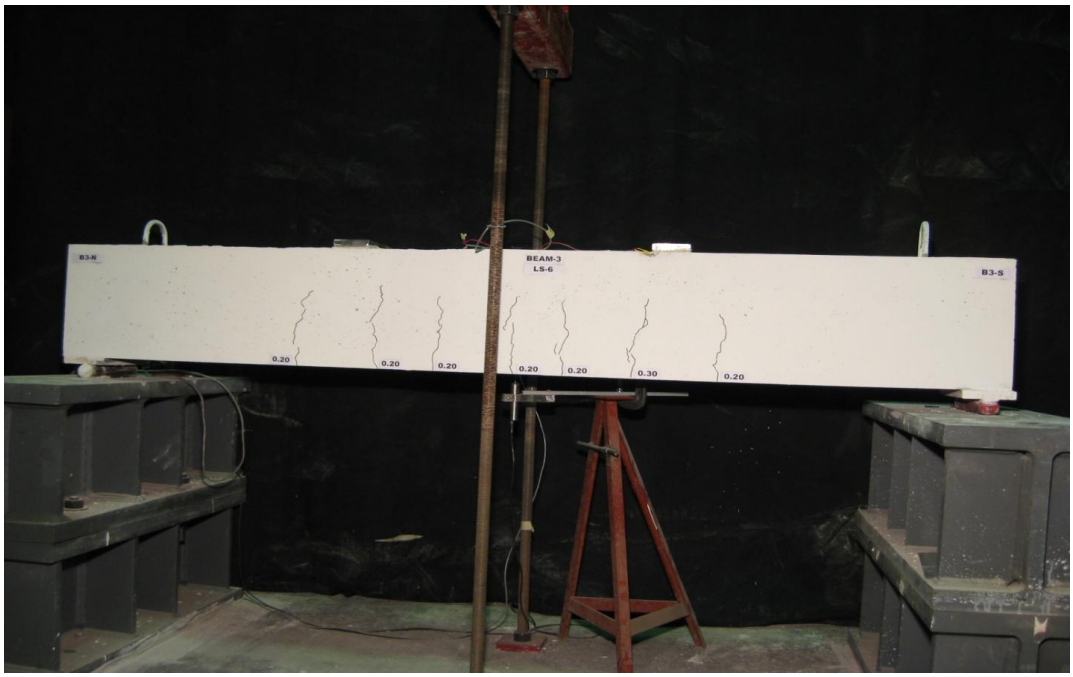

Figure D.18 – Cracking pattern for beam 3 at a load of 59.02 kN (B3- LS6)

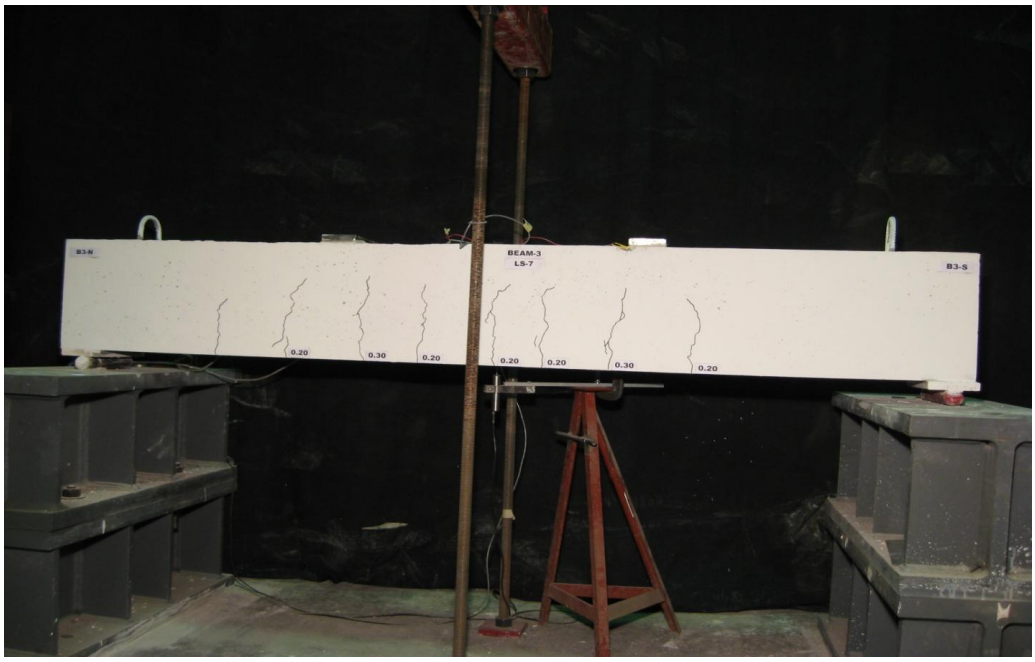

Figure D.19– Cracking pattern for beam 3 at a load of 68.08 kN (B3-LS7)

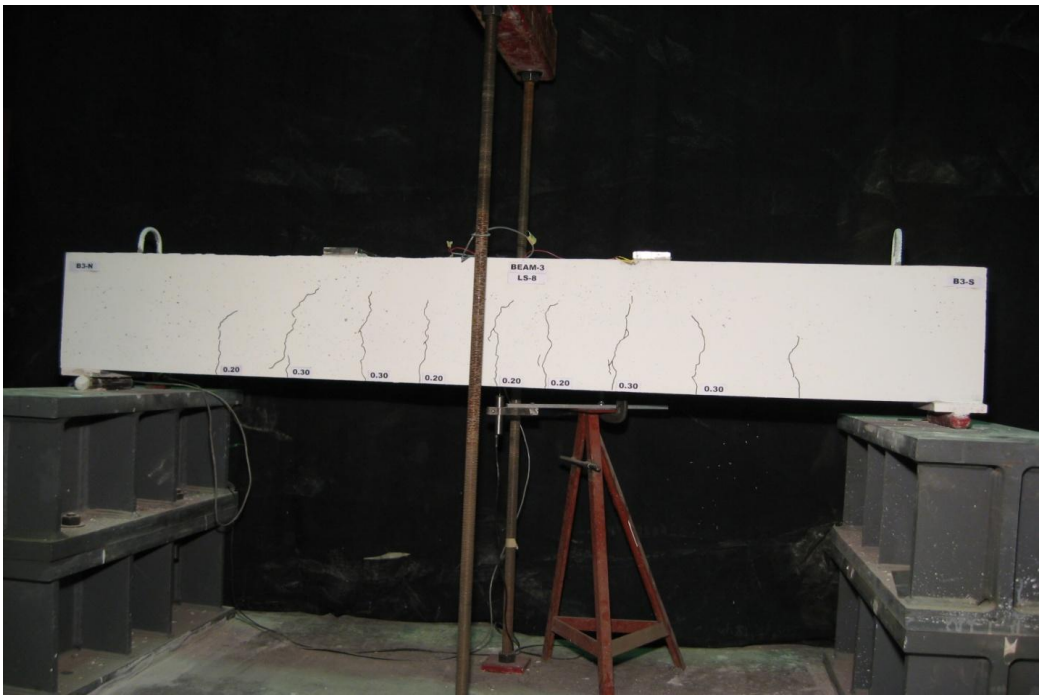

Figure D.20 – Cracking pattern for beam 3 at a load of 75.4 kN (B3-LS8)

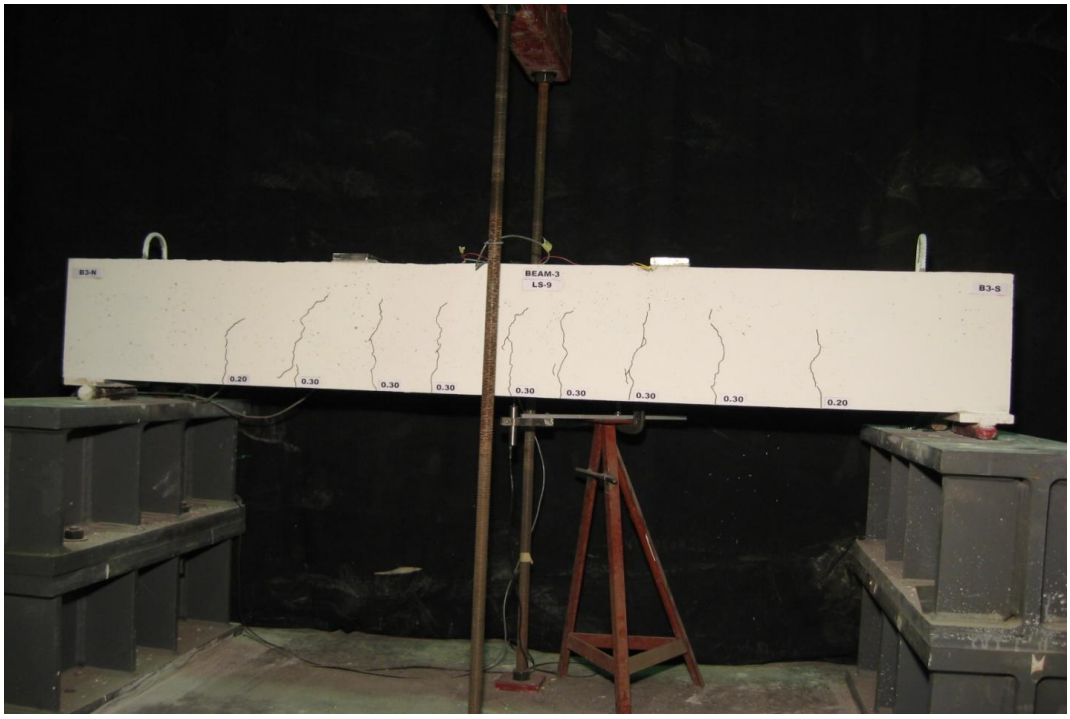

Figure D.21 – Cracking pattern for beam 3 at a load of 81.5 (kN B3-LS9)

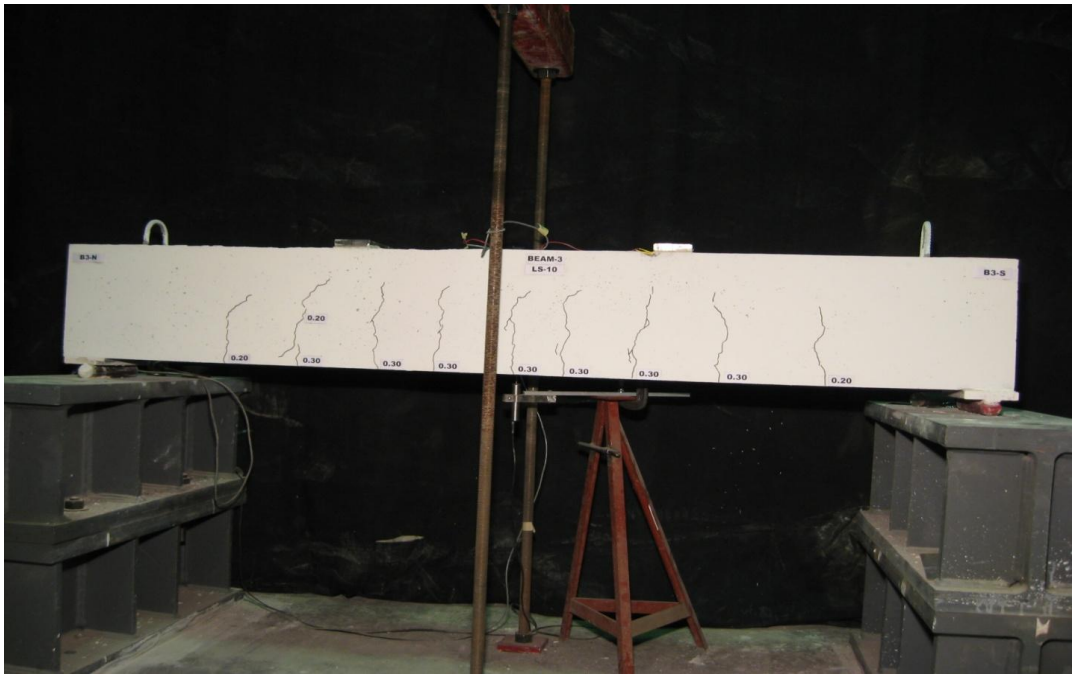

Figure D.22– Cracking pattern for beam 3 at a load of 88.996 kN (B3- LS10)

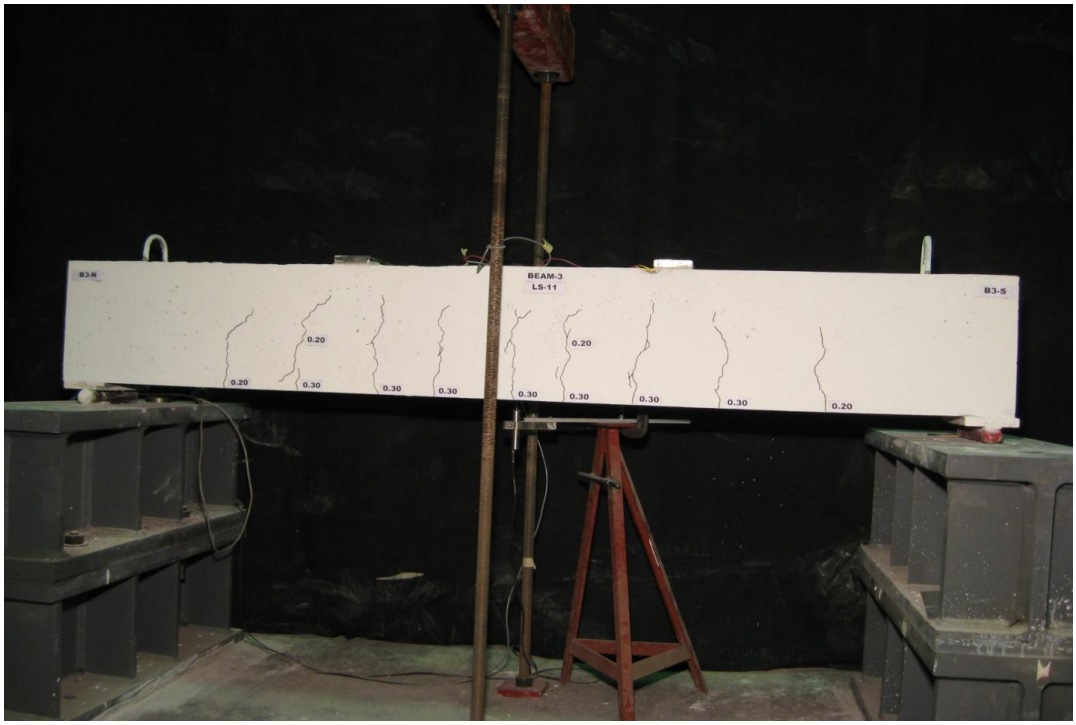

Figure D.23– Cracking pattern for beam 3 at a load of 95.35 kN (B3-LS11)

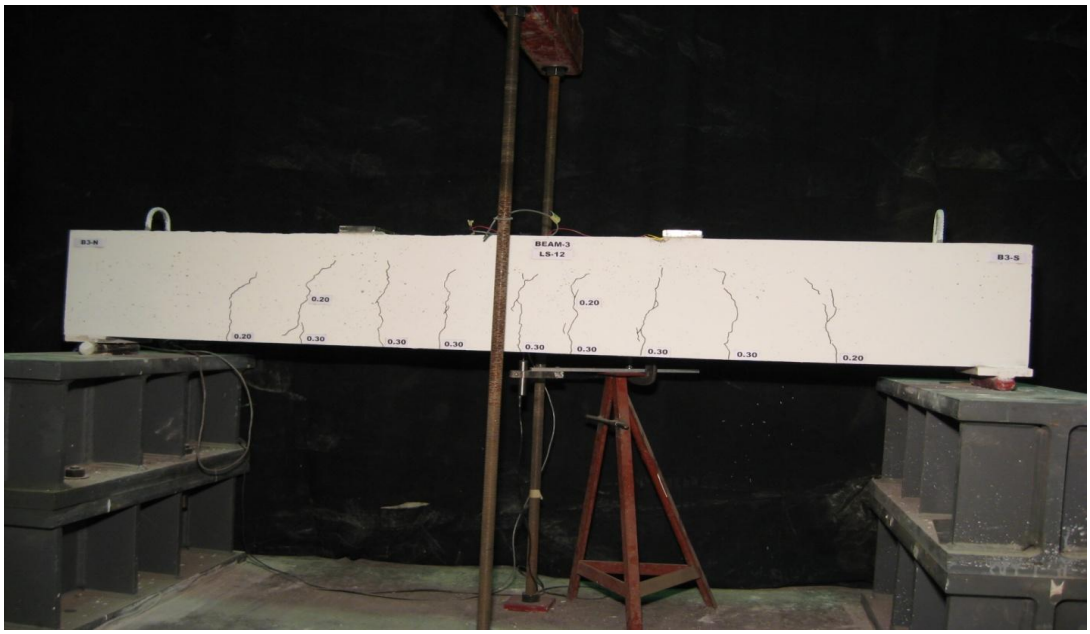

Figure D.24– Cracking pattern for beam 3 at a load of 99.78 kN (B3-LS12)

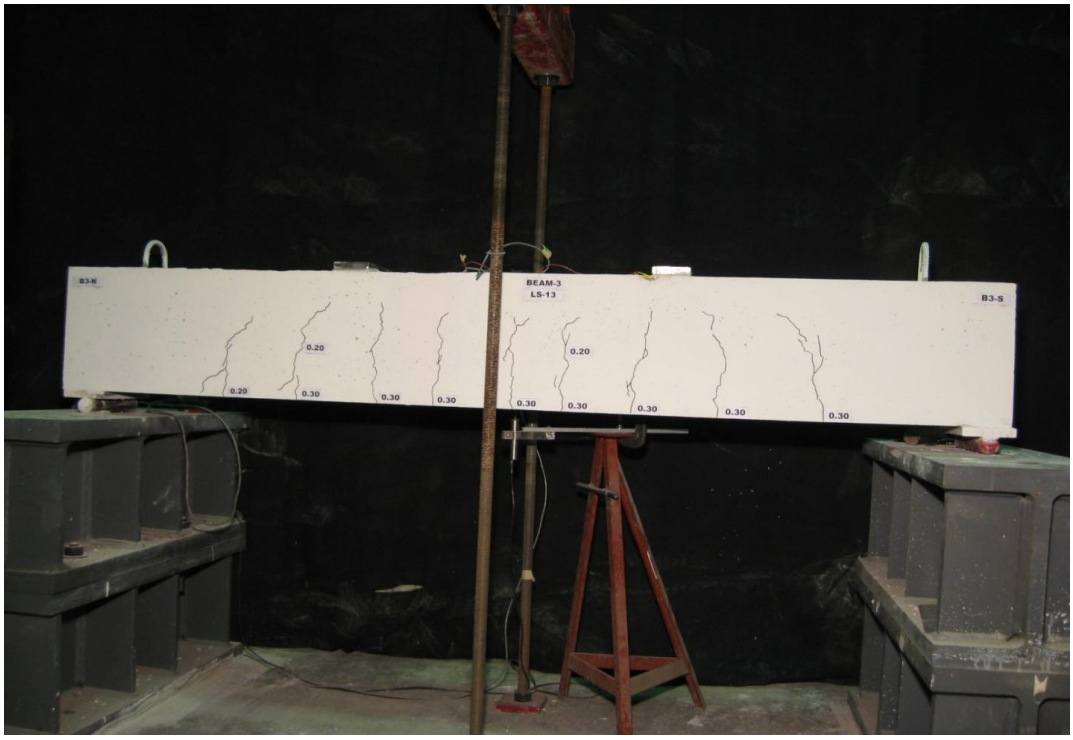

Figure D.25– Cracking pattern for beam 3 at a load of 111.6 kN (B3-LS13)

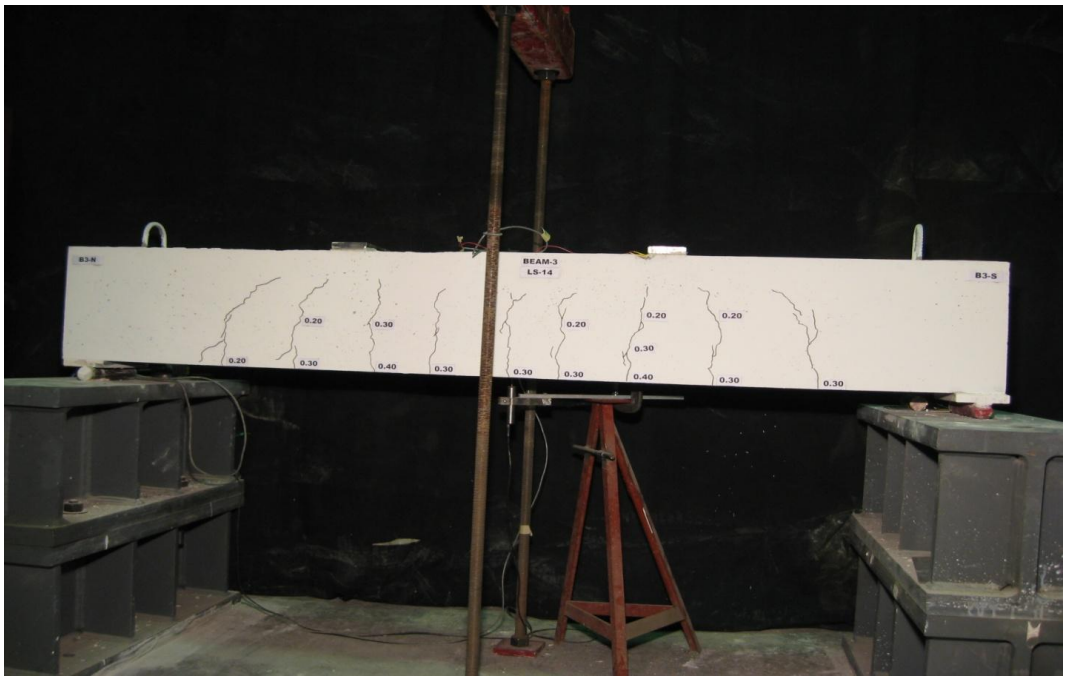

Figure D.26 – Cracking pattern for beam 3 at a load of 122.32 kN (B3-LS14)

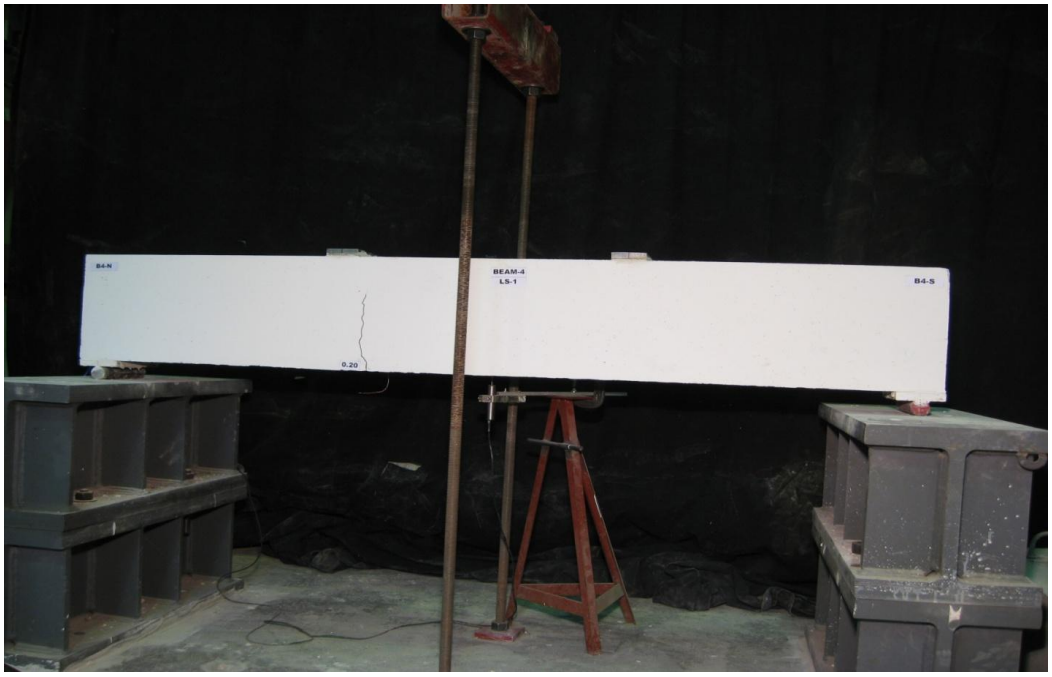

Figure D.27– Cracking pattern for beam 4 at a load of 25.23 kN (B4-LS1)

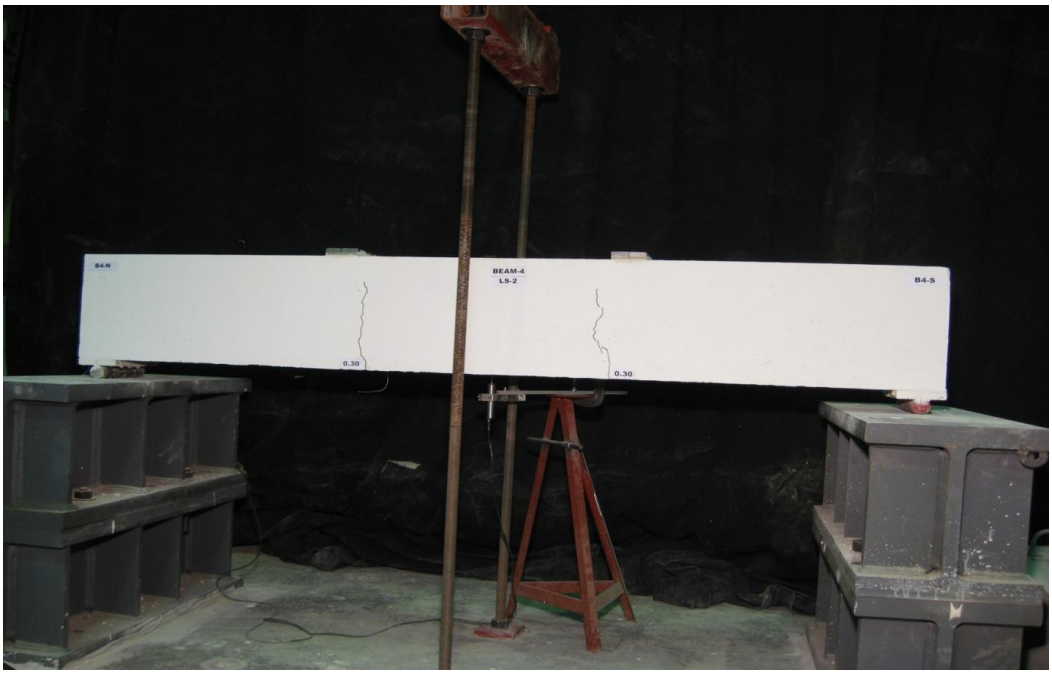

Figure D.28– Cracking pattern for beam 4 at a load of 30.2 kN (B4-LS2)

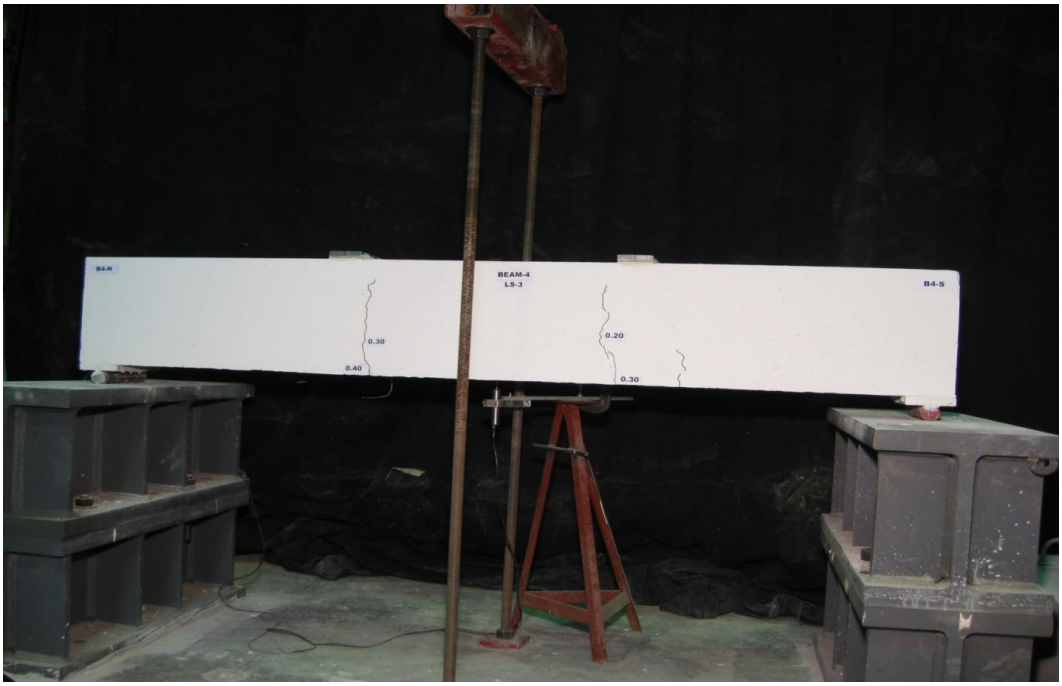

Figure D.29– Cracking pattern for beam 4 at a load of 35.19 kN (B4-LS3)

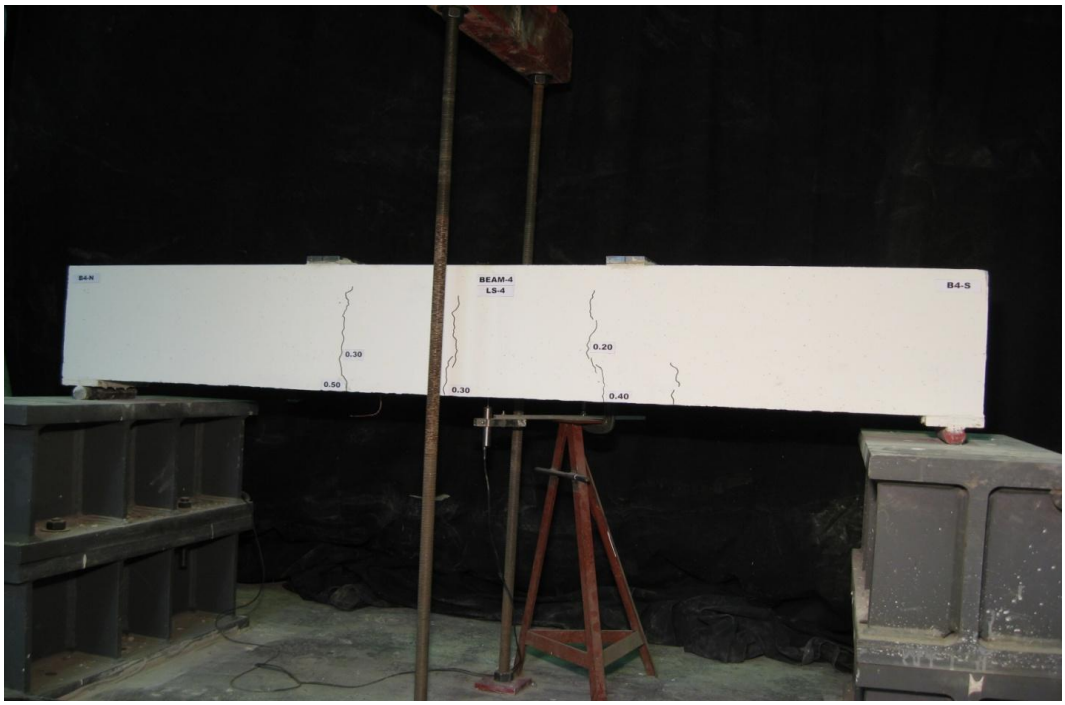

Figure D.30– Cracking pattern for beam 4 at a load of 39.66 kN (B4-LS4)

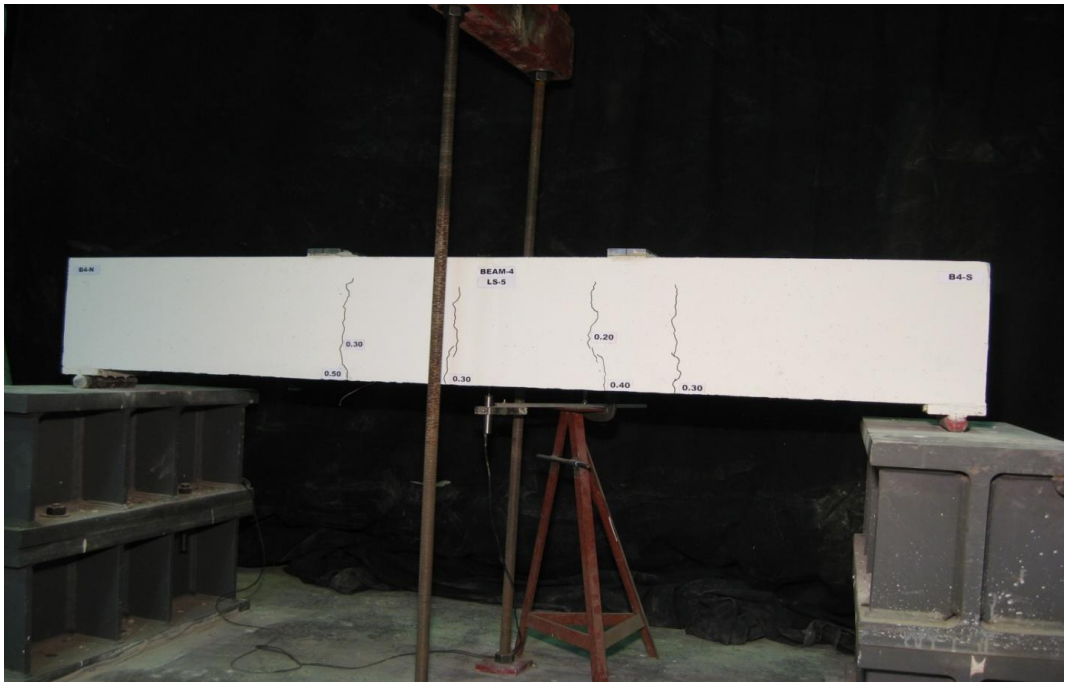

Figure D.31 – Cracking pattern for beam 4 at a load of 45.4 kN (B4-LS5)

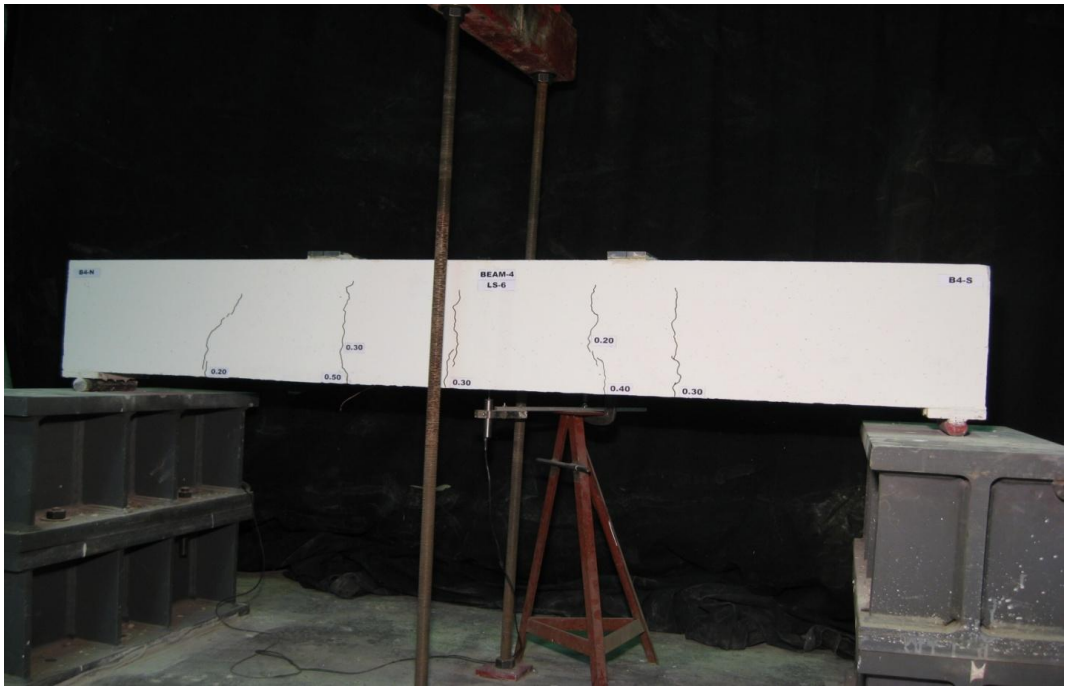

Figure D.32– Cracking pattern for beam 4 at a load of 49.51 kN (B4-LS6)

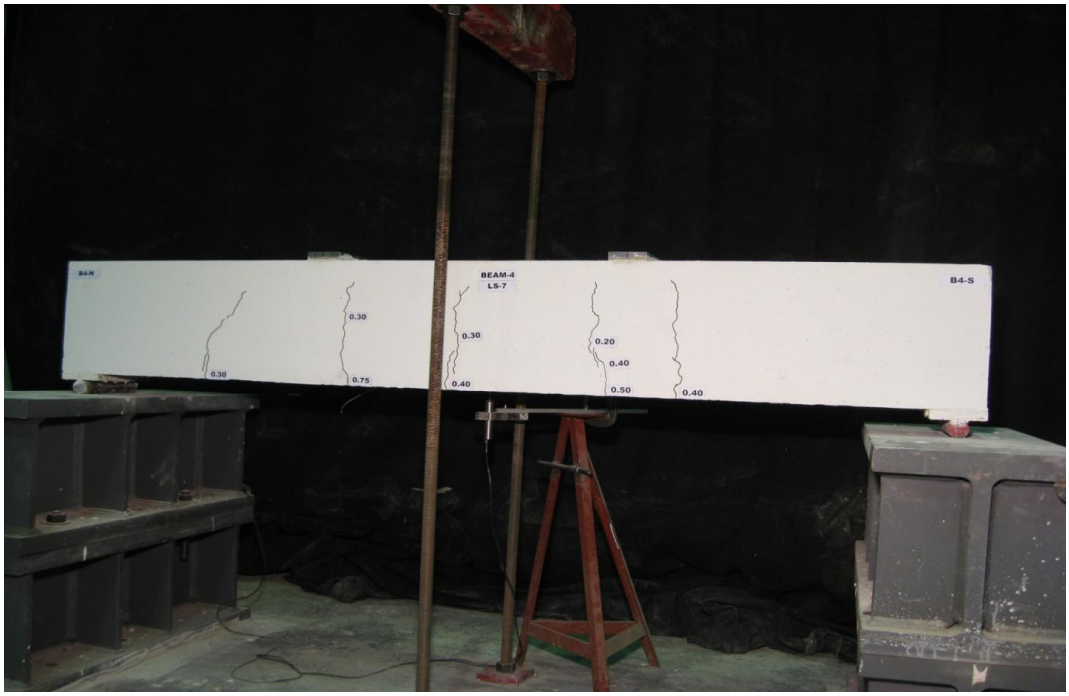

Figure D.33– Cracking pattern for beam 4 at a load of 56.02 kN (B4-LS7)

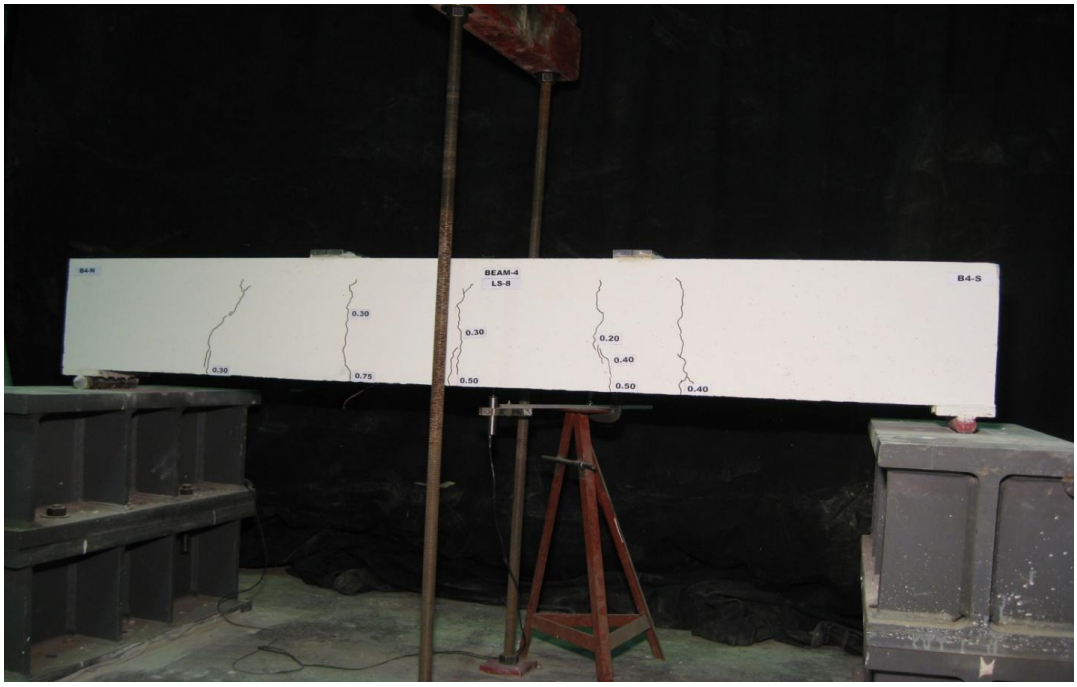

Figure D.34– Cracking pattern for beam 4 at a load of 60.9 kN (B4-LS8)

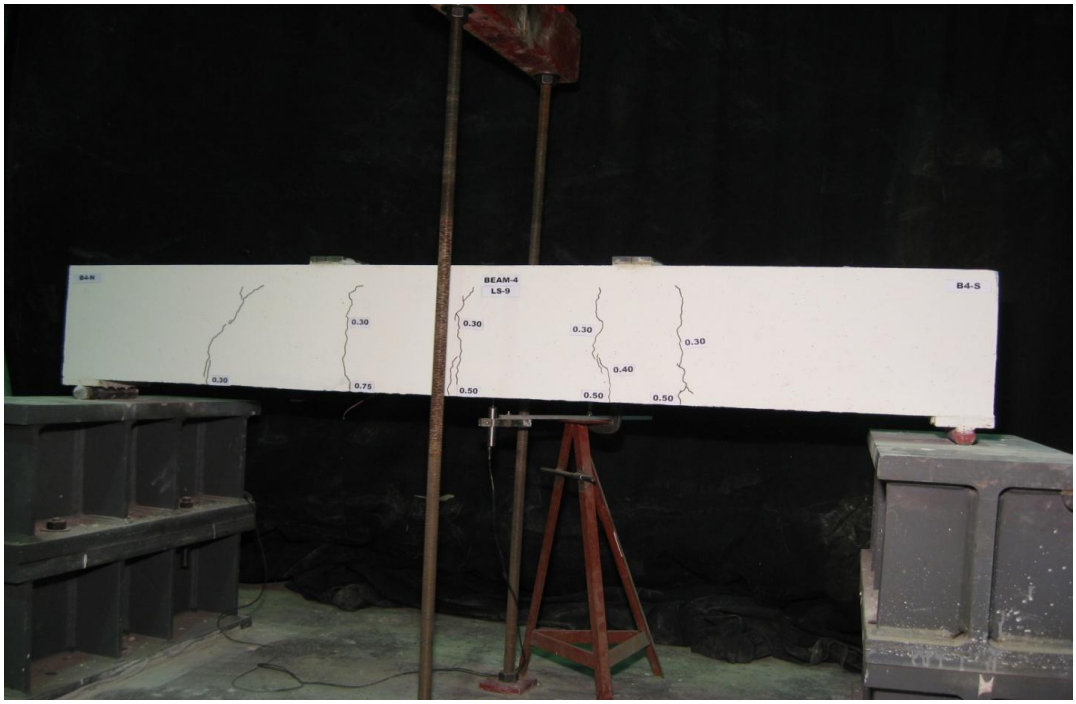

Figure D.35– Cracking pattern for beam 4 at a load of 66.57 kN (B4-LS9)

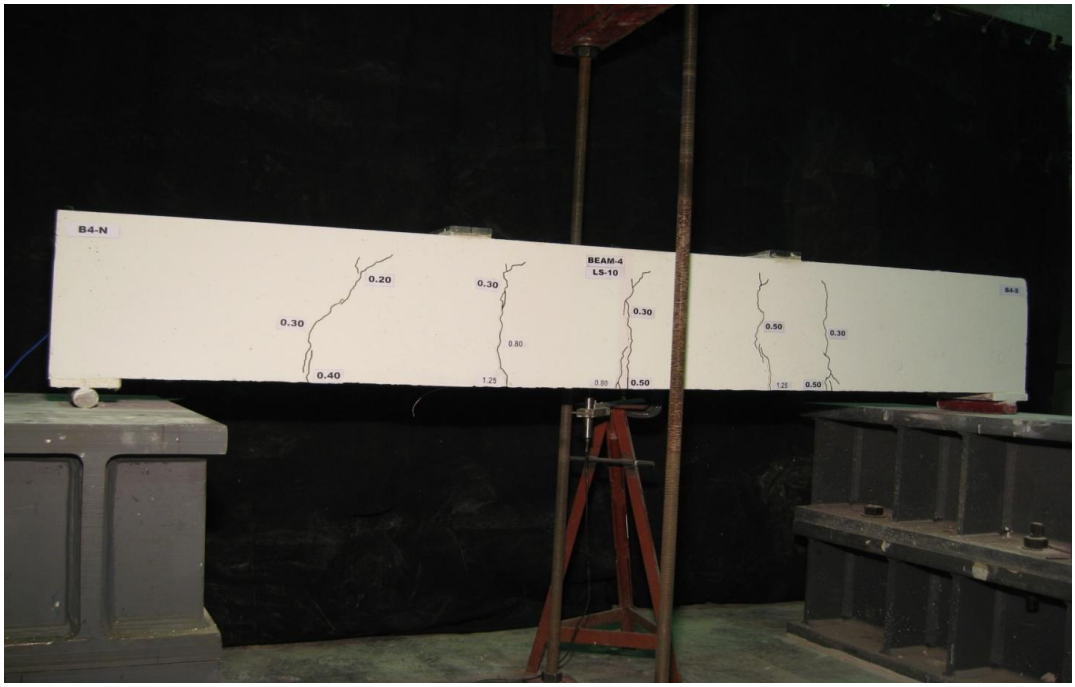

Figure D.36– Cracking pattern for beam 4 at a load of 70.24 kN (B4-LS10)

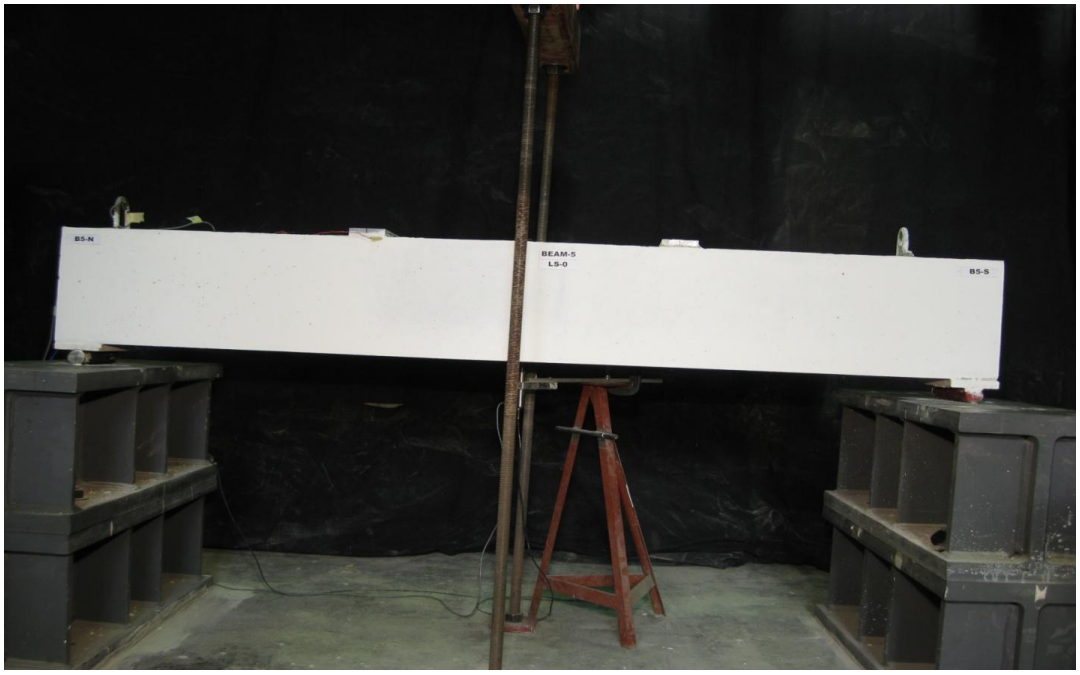

Figure D.37– Cracking pattern for beam 5 at zero load (B5-LS0)

Figure D.38– Cracking pattern for beam 5 at a load of 20.45 kN (B5-LS1)

Figure D.39 – Cracking pattern for beam 5 at a load of 34.89 kN (B5-LS2)

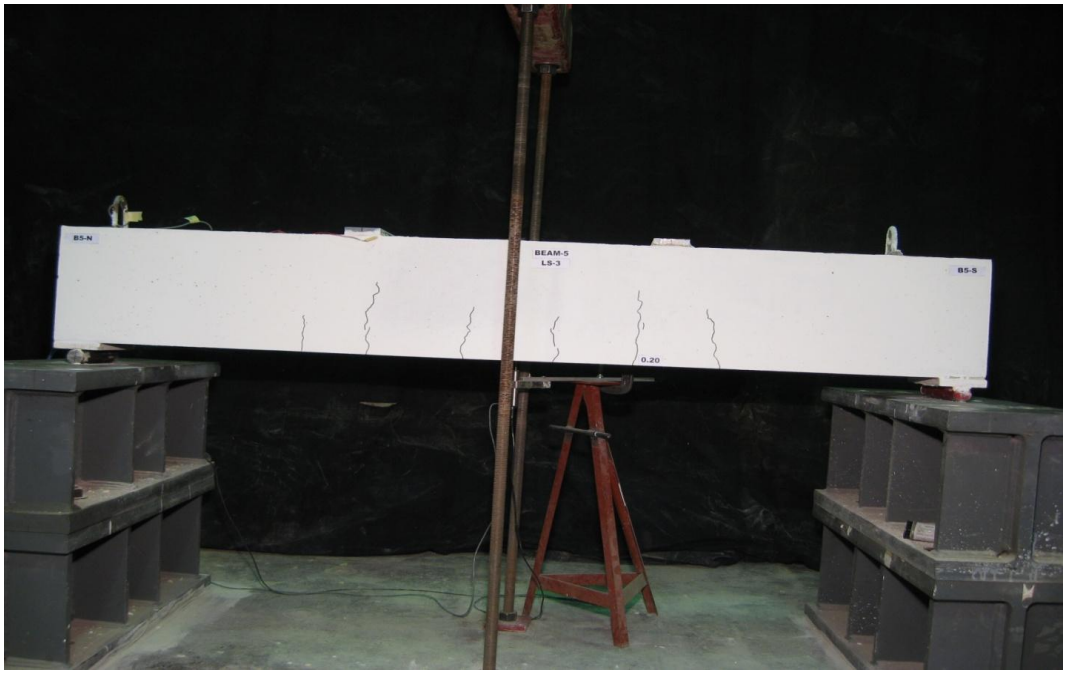

Figure D.40– Cracking pattern for beam 5 at a load of 44.42 kN (B5-LS3)

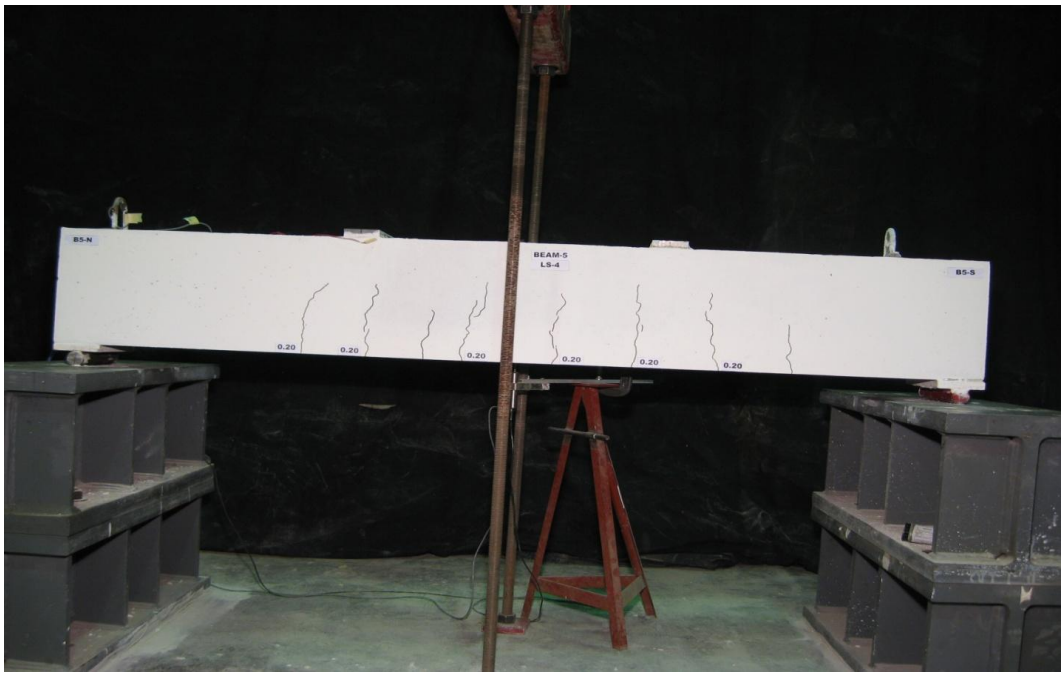

Figure D.41– Cracking pattern for beam 5 at a load of 55.06 kN (B5-LS4)

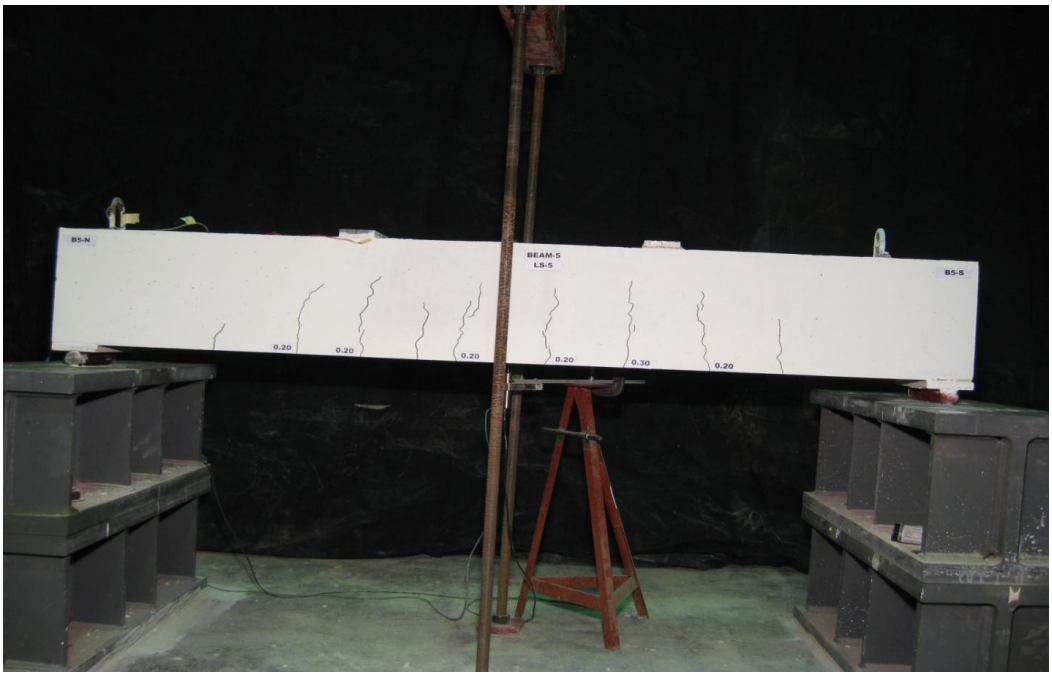

Figure D.42– Cracking pattern for beam 5 at a load of 64.63 kN (B5-LS5)

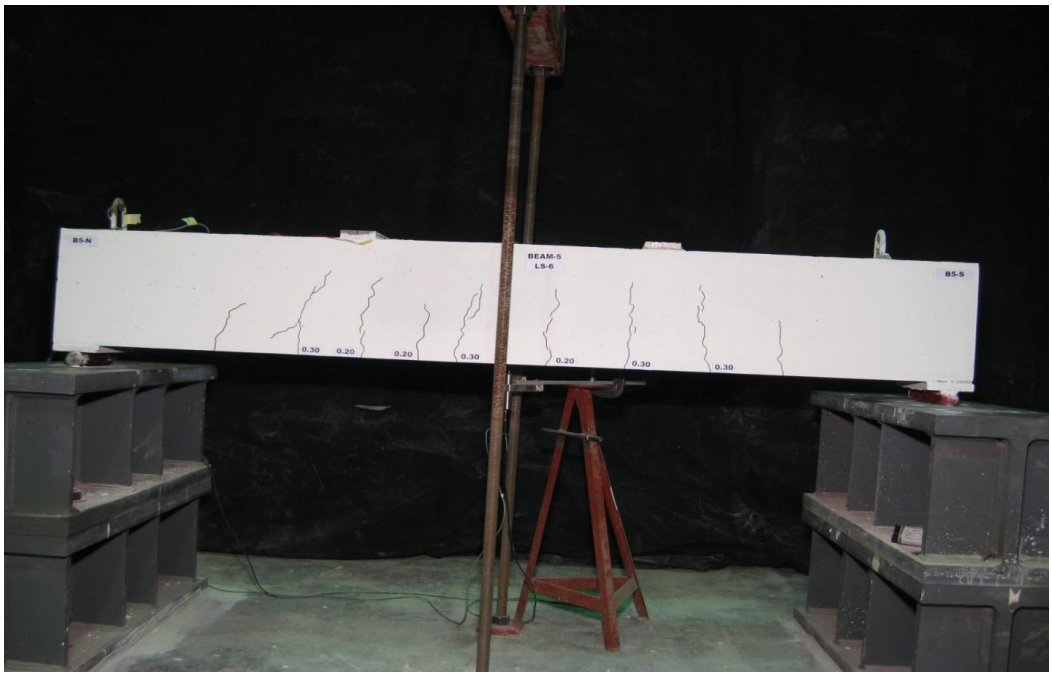

Figure D.43– Cracking pattern for beam 5 at a load of 74.4 kN (B5-LS6)

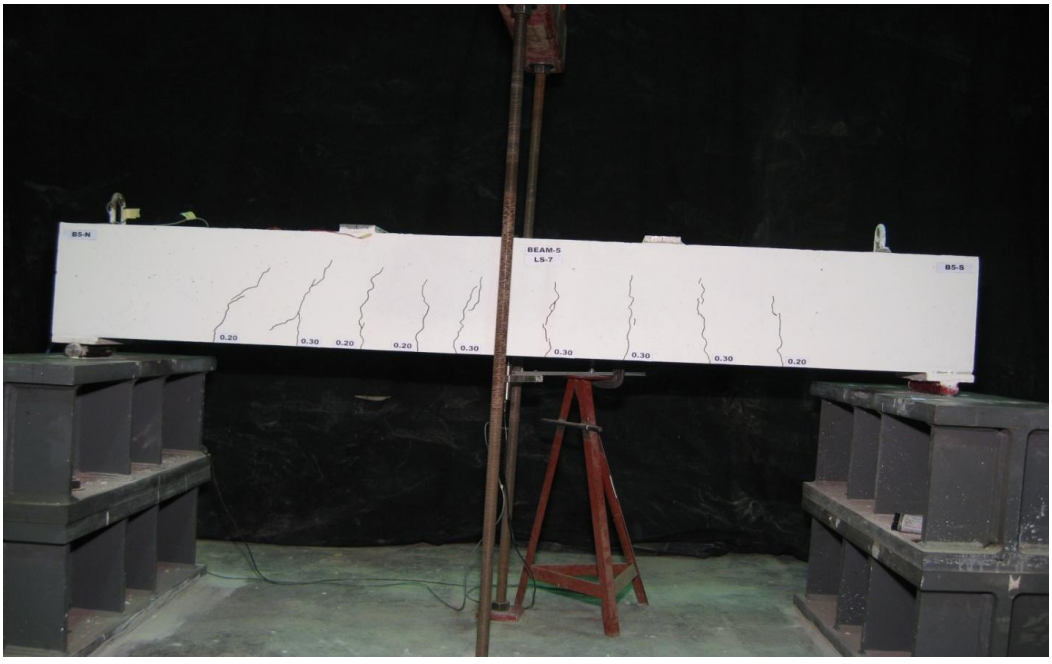

Figure D.44 – Cracking pattern for beam 5 at a load of 85.36 kN (B5-LS7)

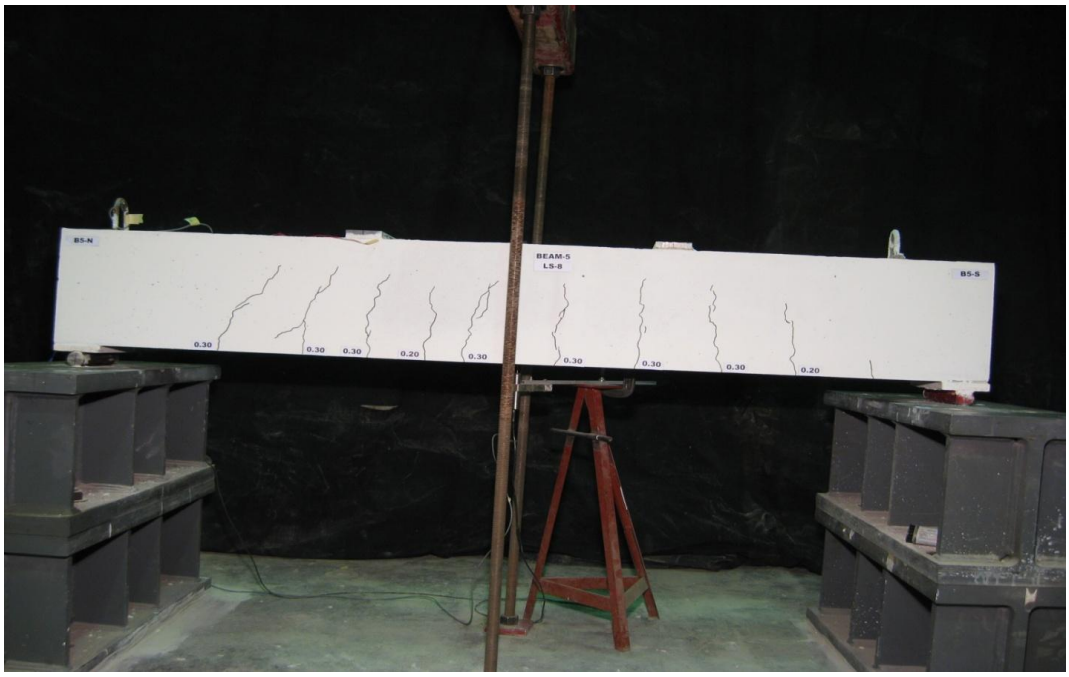

Figure D.45 – Cracking pattern for beam 5 at a load of 95.03 kN (B5-LS8)

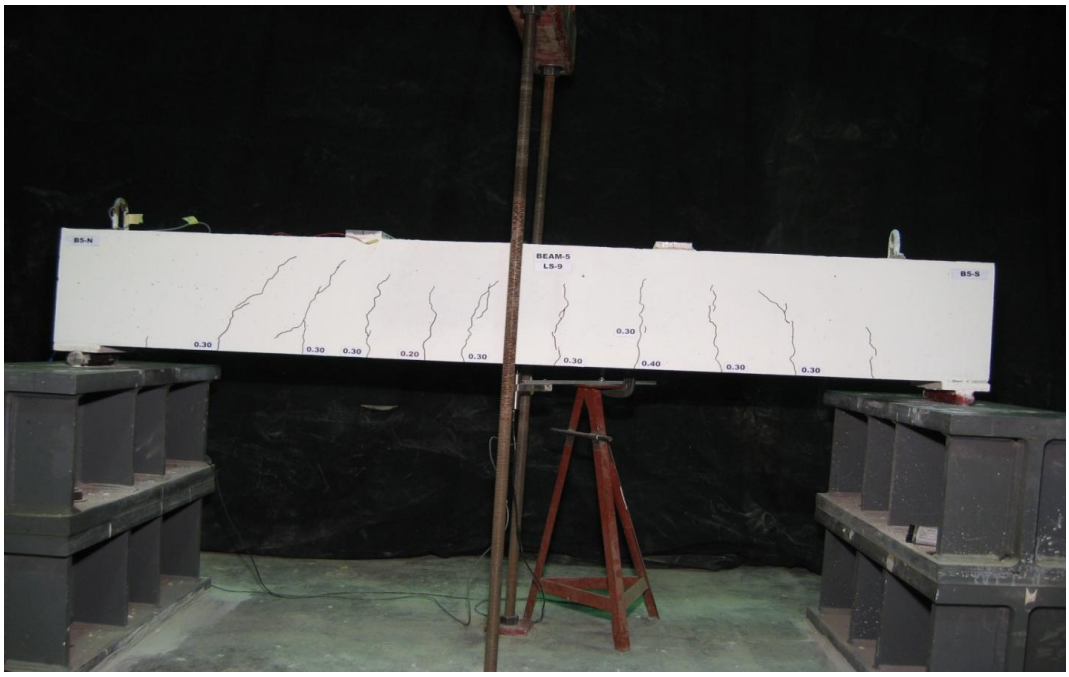

Figure D.46 – Cracking pattern for beam 5 at a load of 104.48 kN (B5-LS9)

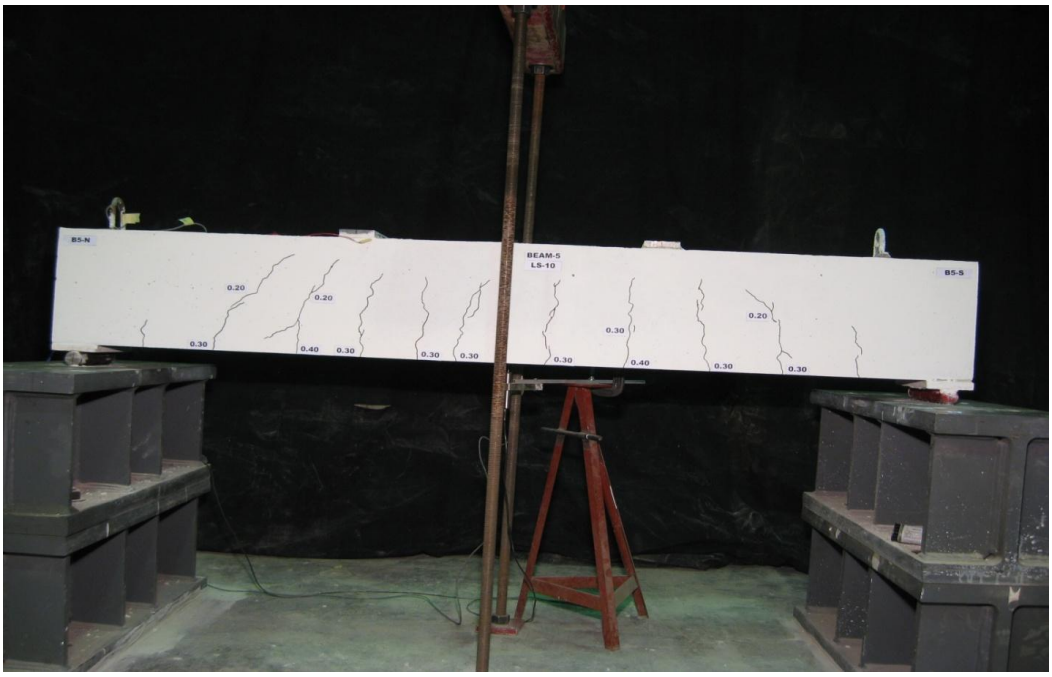

Figure D.47 – Cracking pattern for beam 5 at a load of 114.67 kN (B5-LS10)

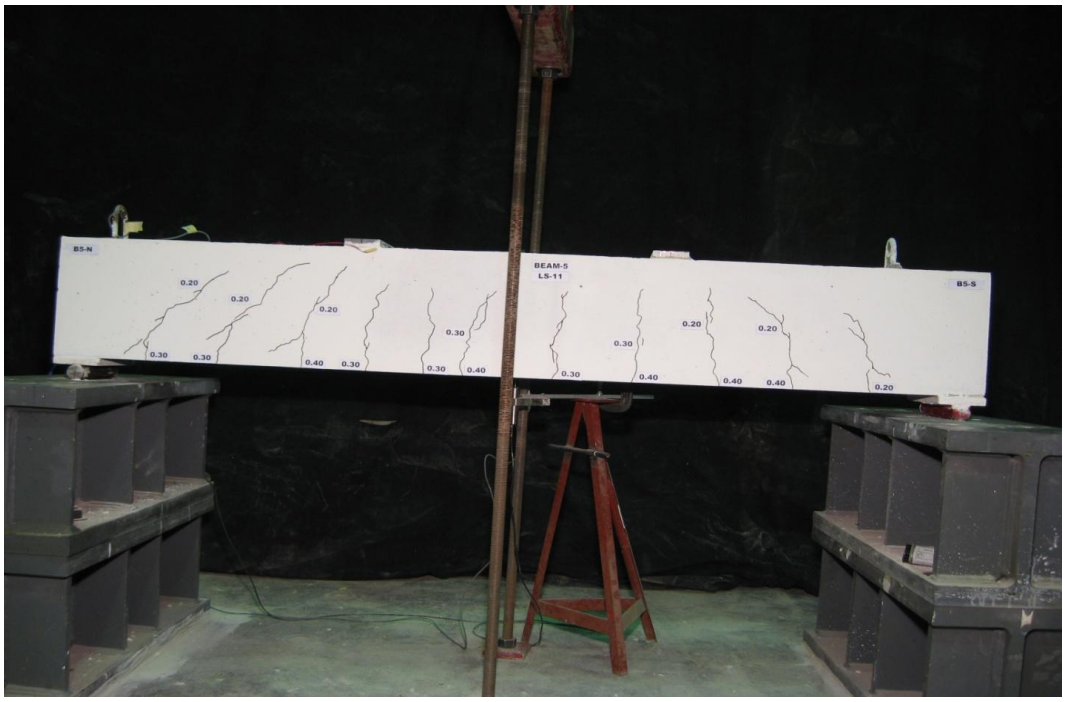

Figure D.48 – Cracking pattern for beam 5 at a load of 124.86 kN (B5-LS11)

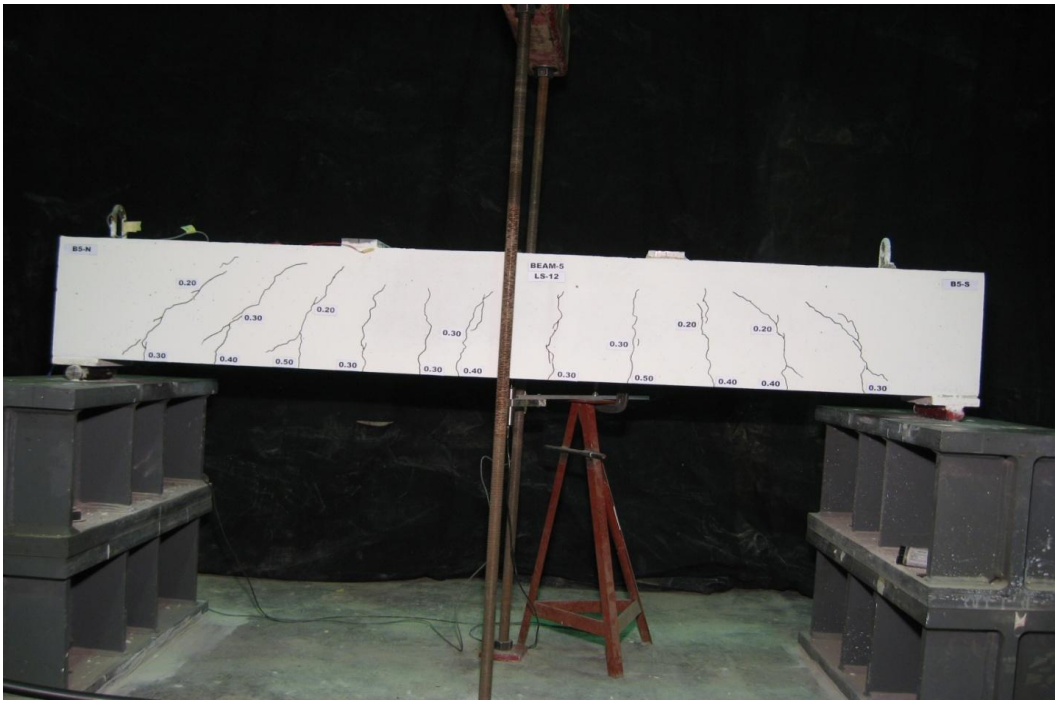

Figure D.49 – Cracking pattern for beam 5 at a load of 135.19 kN (B5-LS12)

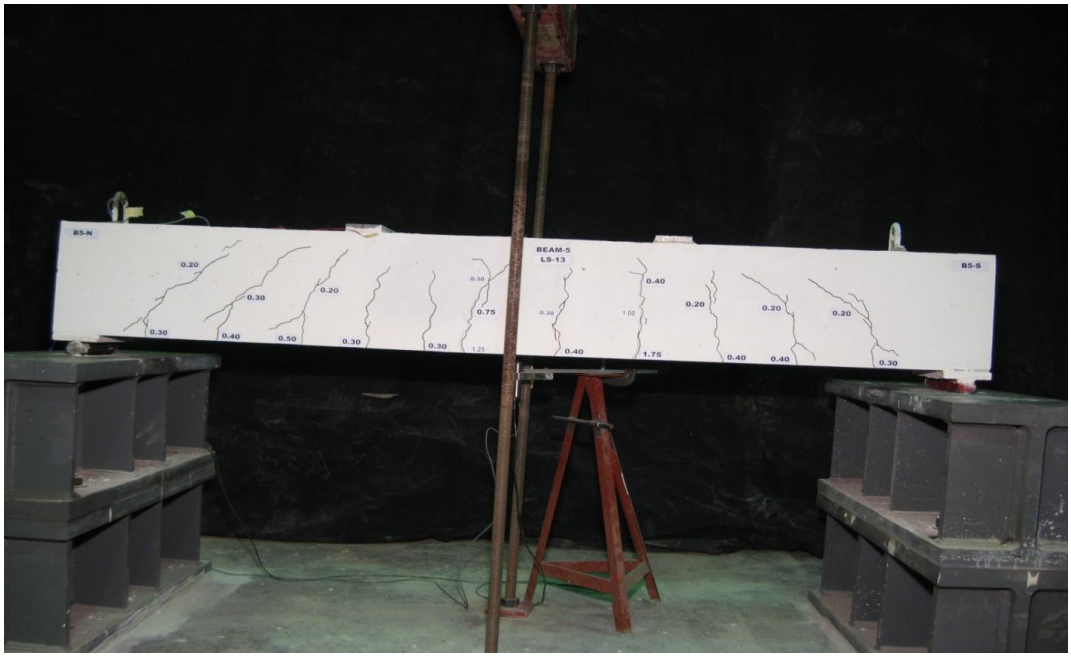

Figure D.50 – Cracking pattern for beam 5 at a load of 138.49 kN (B5-LS13)

Appendix E

Experimental Frequencies

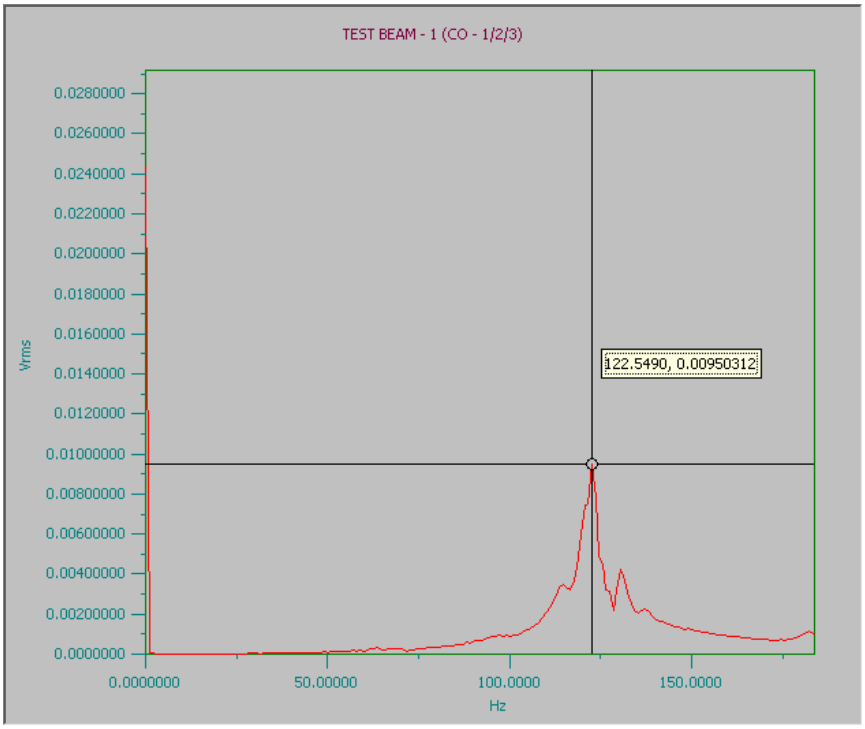

Figure E.1 Frequency for beam 1 at zero load

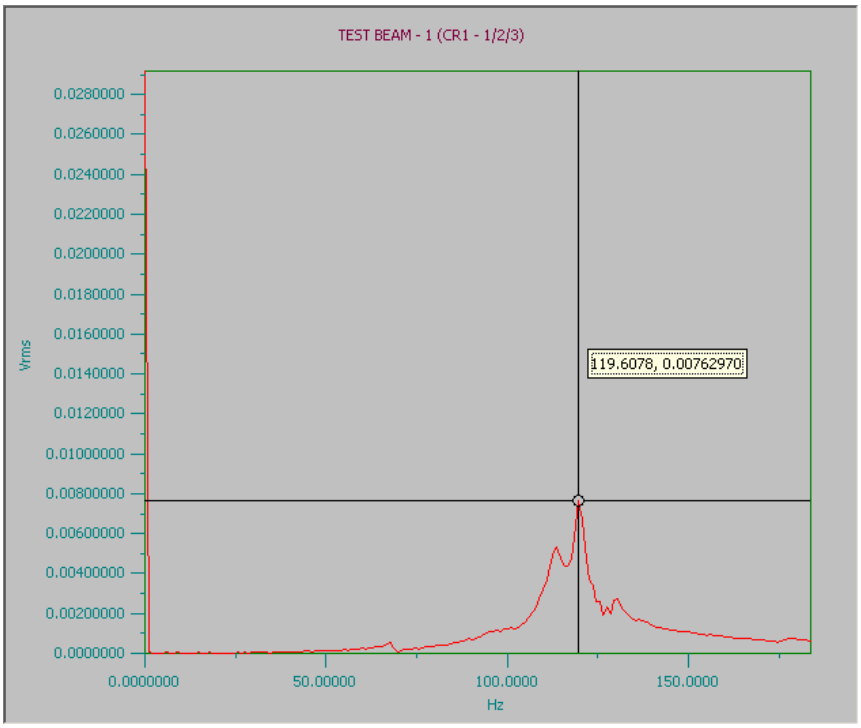

Figure E.2 Frequency for beam 1at a load of 26.34 kN

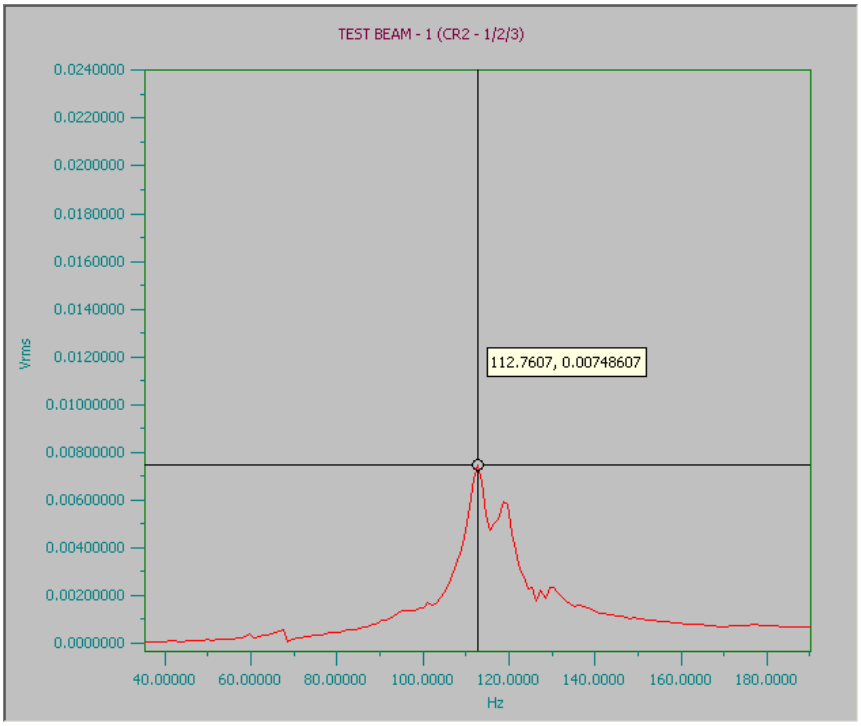

Figure E.3 Frequency for beam 1at a load of 29.86 kN

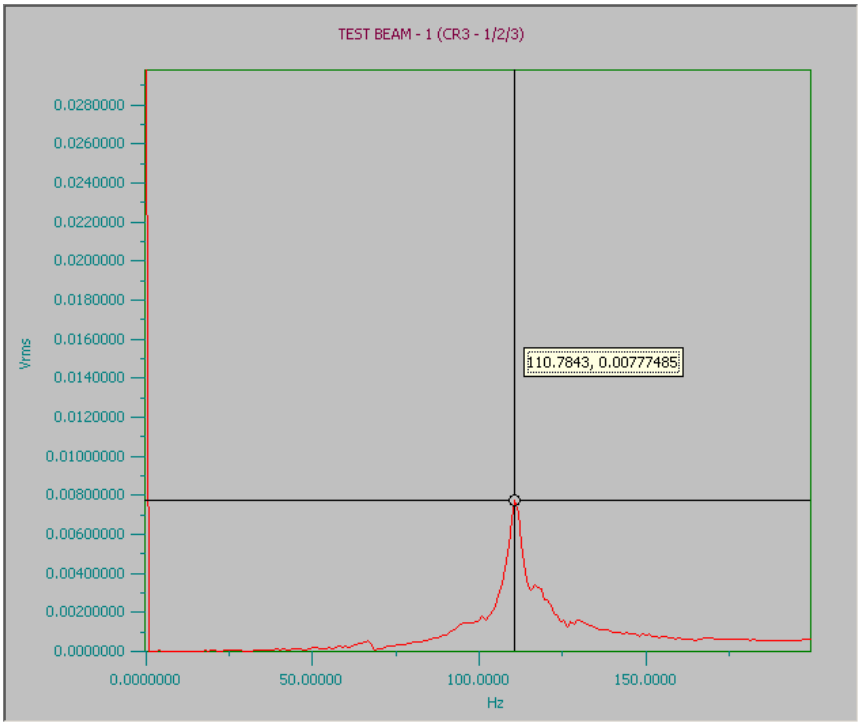

Figure E.4 Frequency for beam 1at a load of 35.5 kN

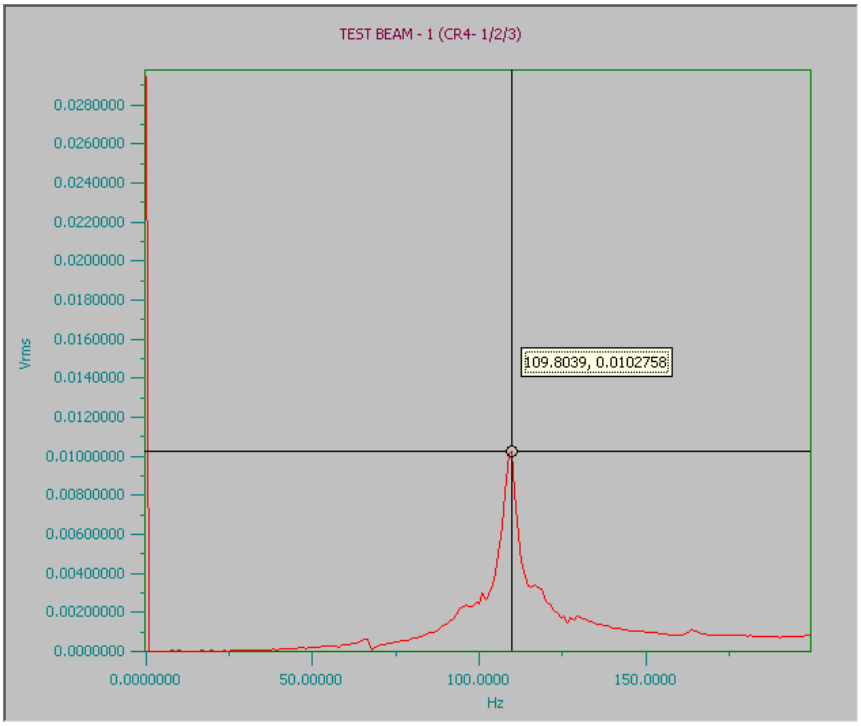

Figure E.5 Frequency for beam 1at a load of 40.26 kN

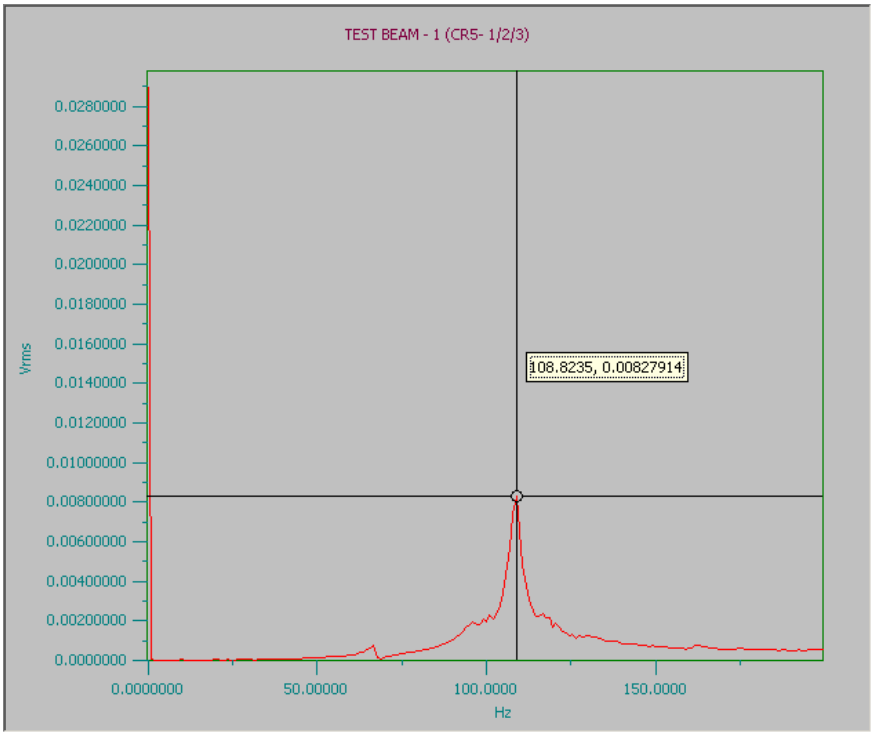

Figure E.6 Frequency for beam 1at a load of 46.7 kN

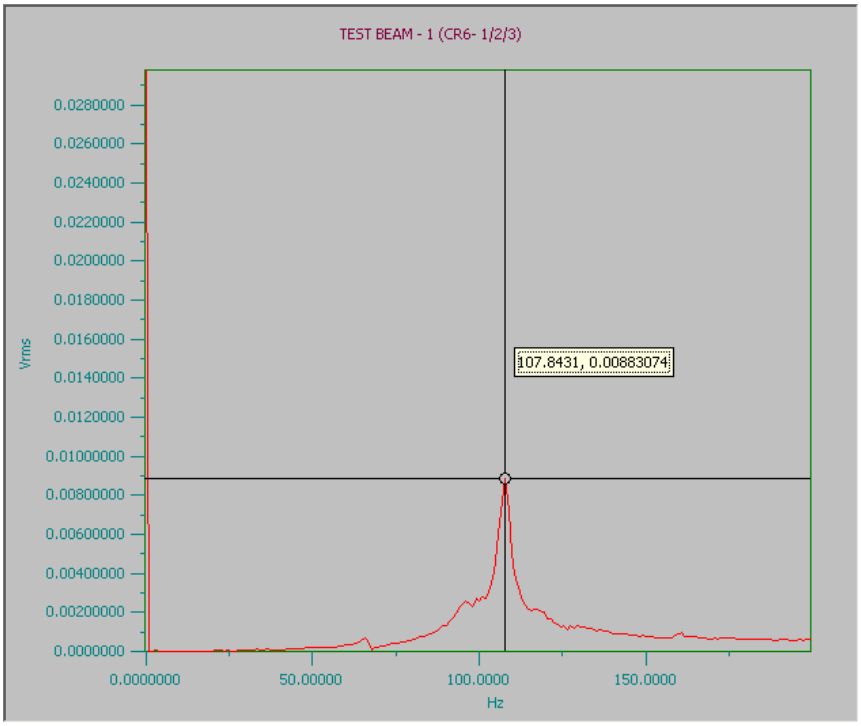

Figure E.7 Frequency for beam 1at a load of 57.16 kN

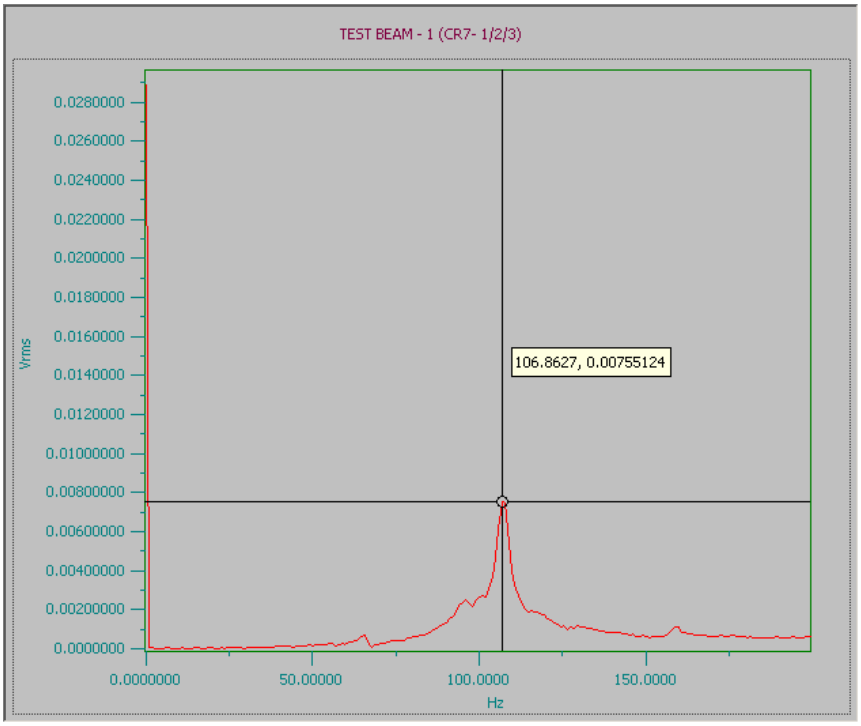

Figure E.8 Frequency for beam 1at a load of 66.18kN

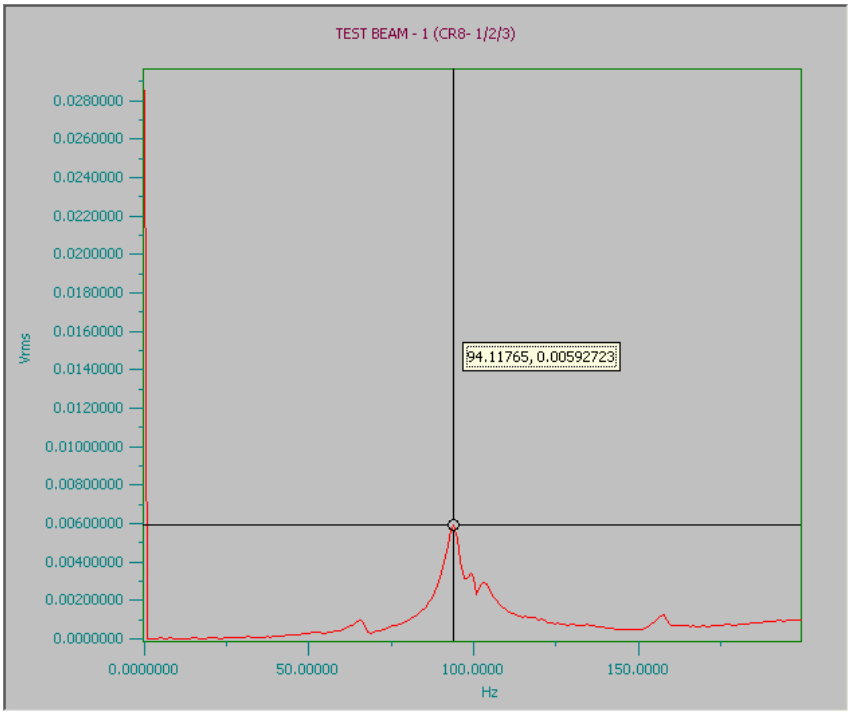

Figure E.9 Frequency for beam 1at a load of 72.36 kN

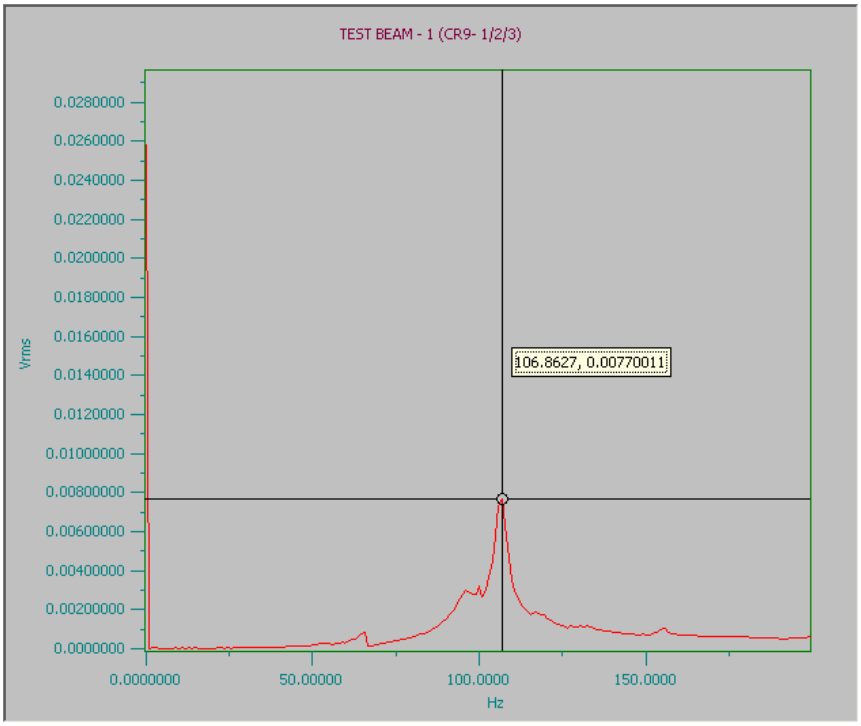

Figure E.10 Frequency for beam 1at a load of 80.1kN

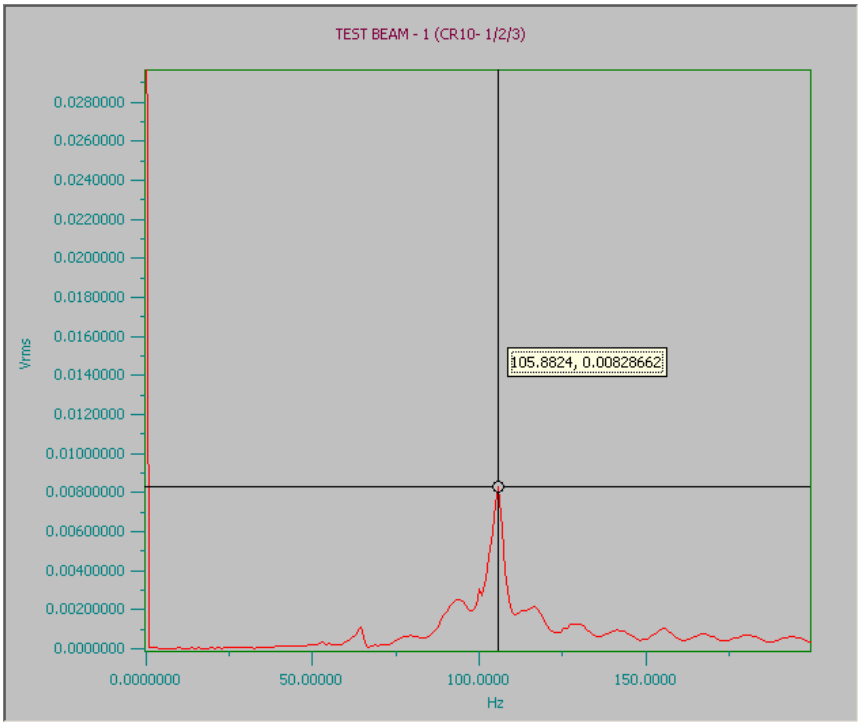

Figure E.11 Frequency for beam 1at a load of 88.1 kN

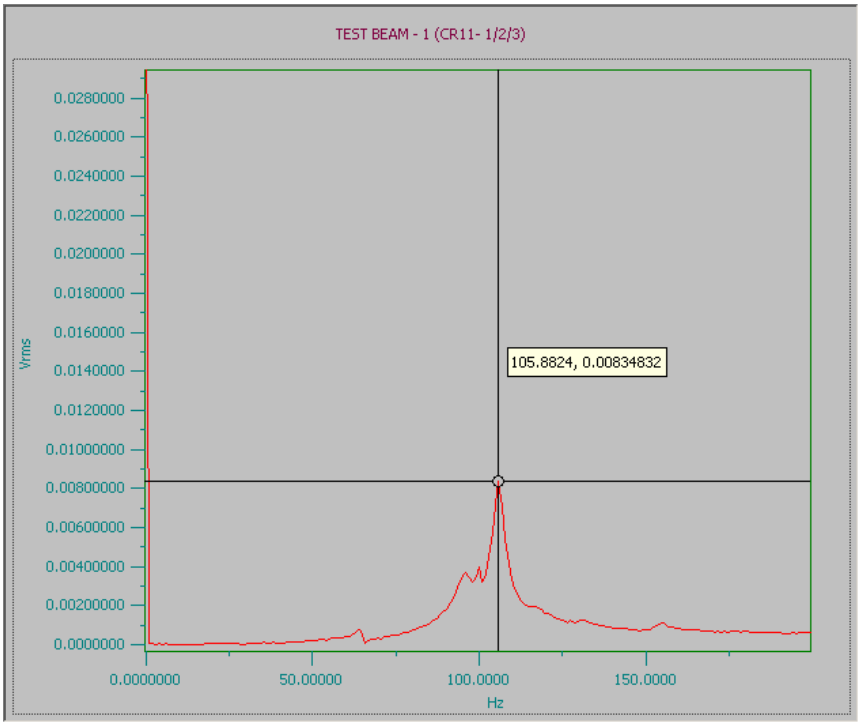

Figure E.12 Frequency for beam 1at a load of 97.4 kN

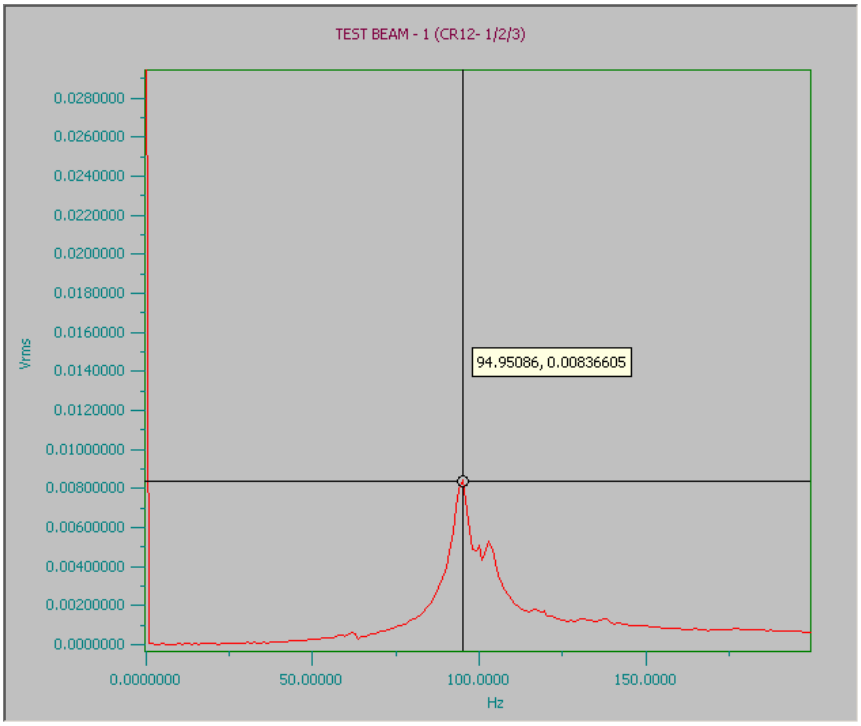

Figure E.13 Frequency for beam 1at a load of 103.75 kN

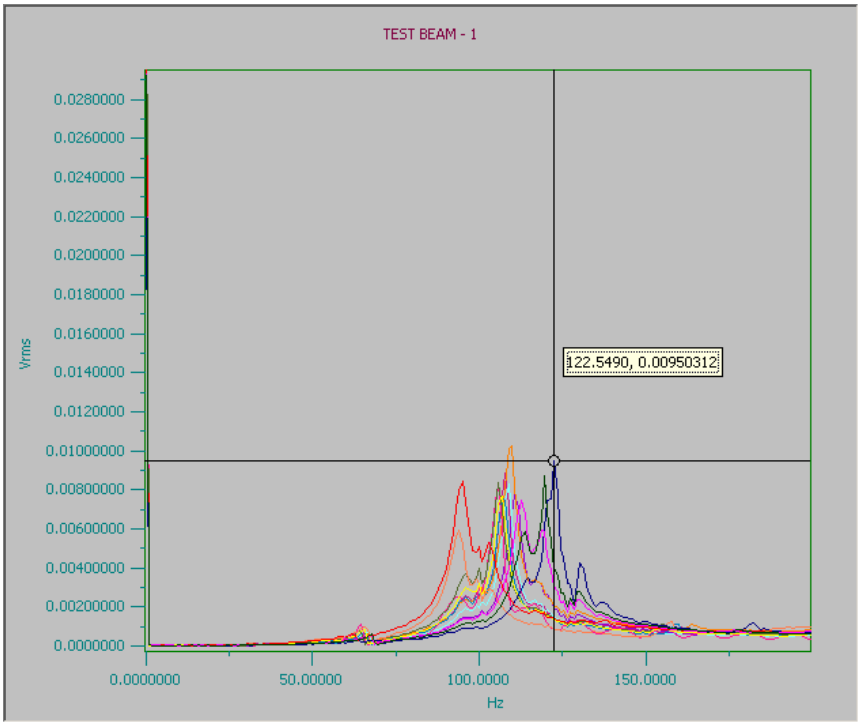

Figure E.14 Frequency for beam 1for all load stages

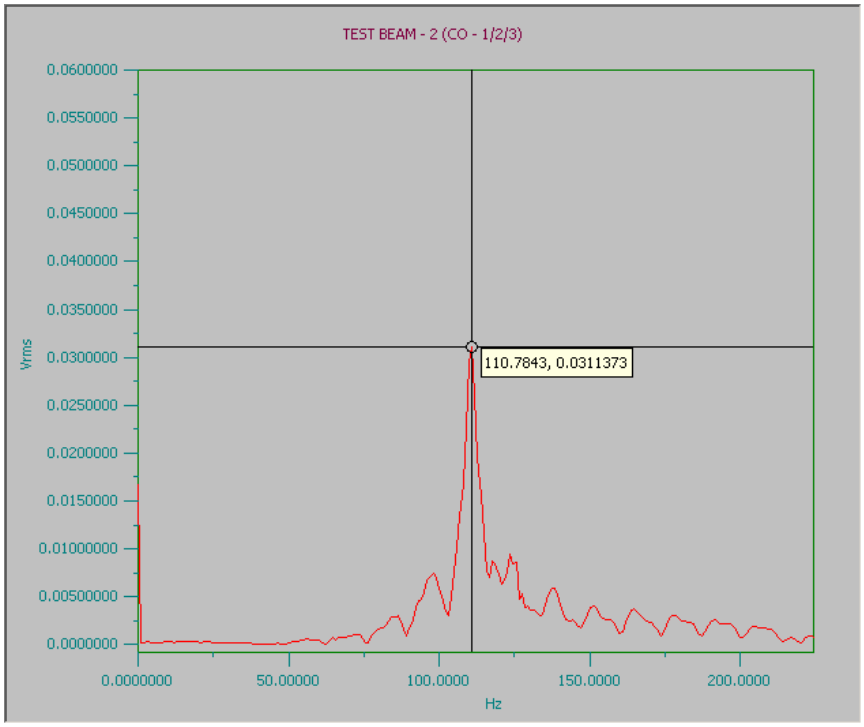

Figure E.15- Frequency for beam 2 at zero load

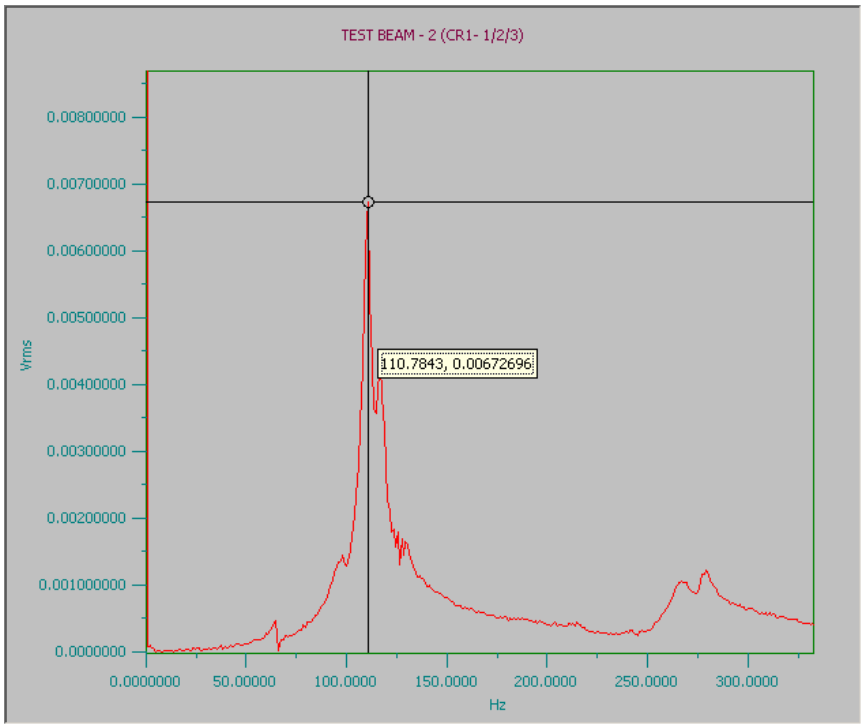

Figure E.16- Frequency for beam 2 at a load of 25.96 kN

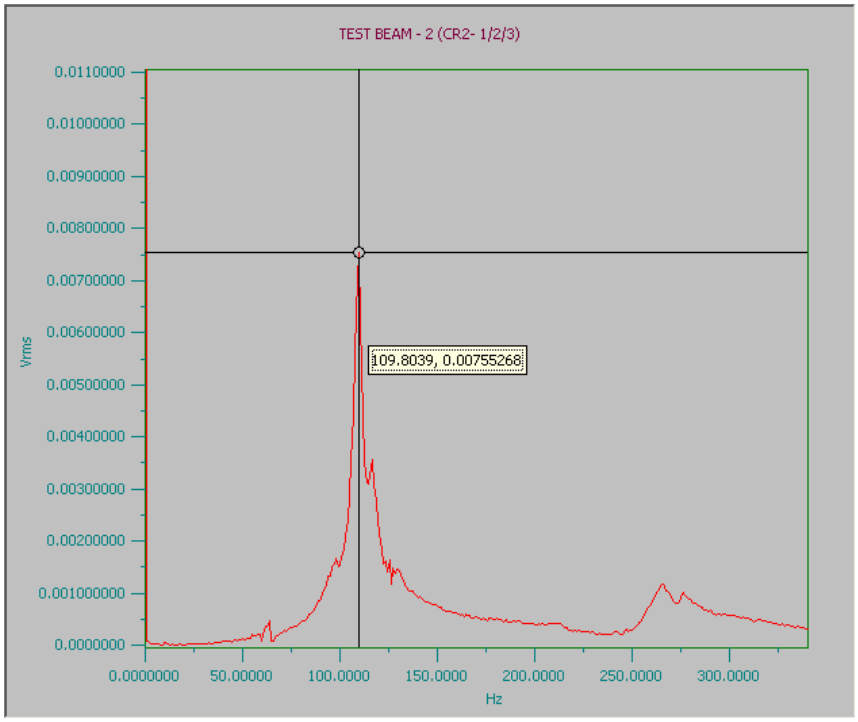

Figure E.17- Frequency for beam 2 at a load of 28.2 kN

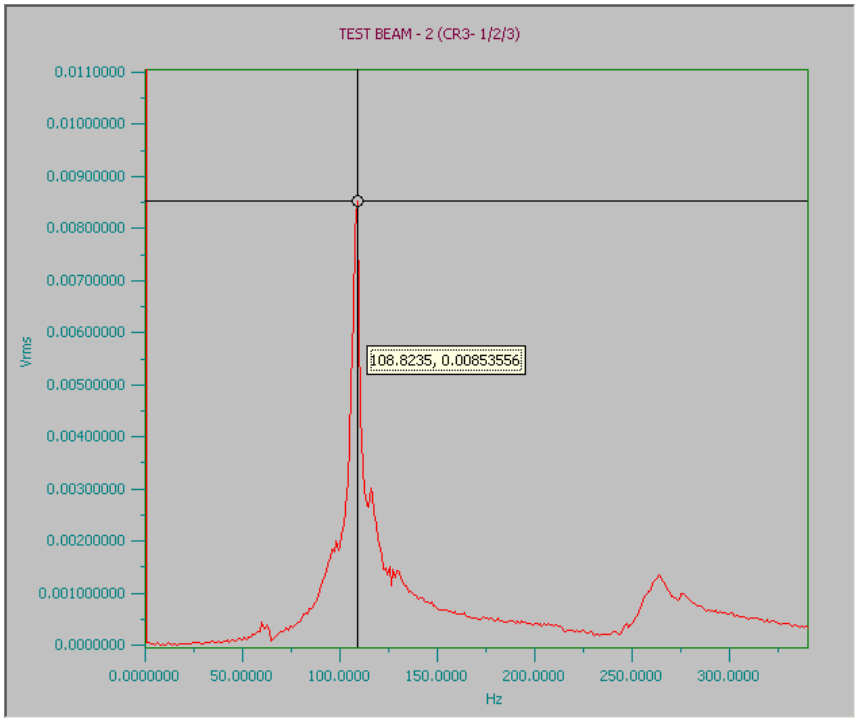

Figure E.18- Frequency for beam 2 at a load of 34.7 kN

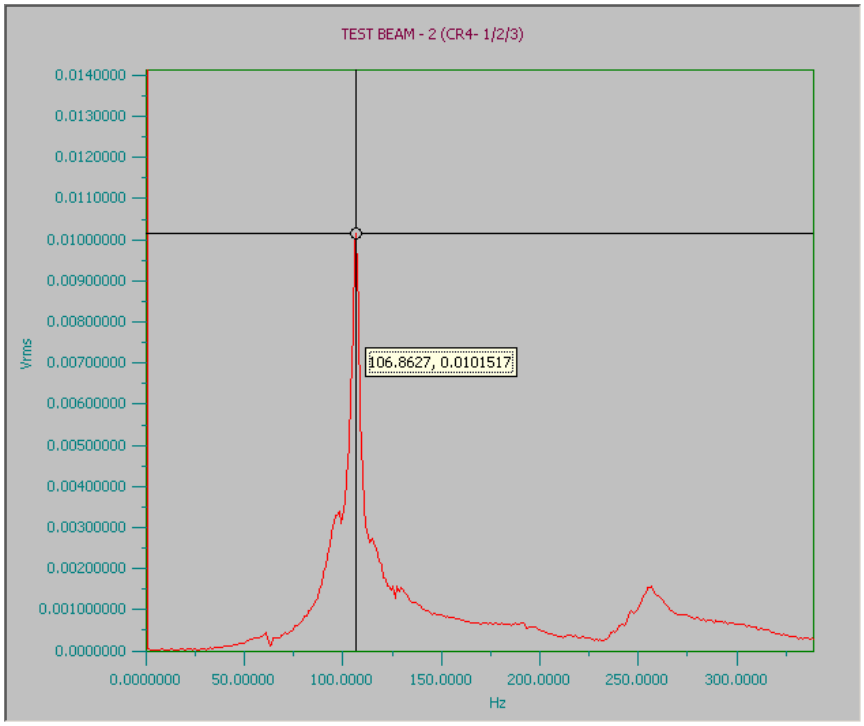

Figure E.19- Frequency for beam 2 at a load of 42.0 kN

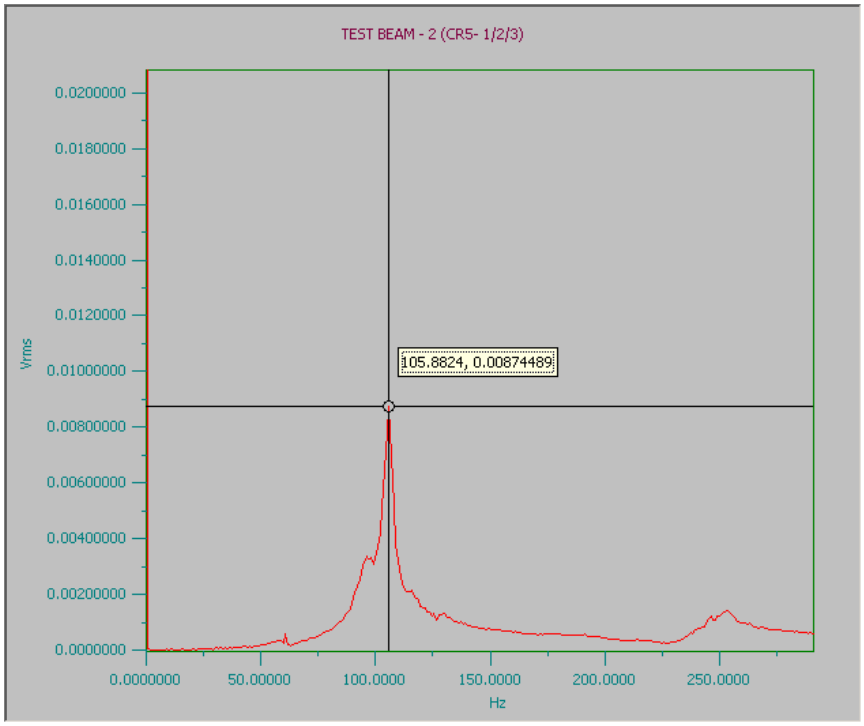

Figure E.20- Frequency for beam 2 at a load of 50.2 kN

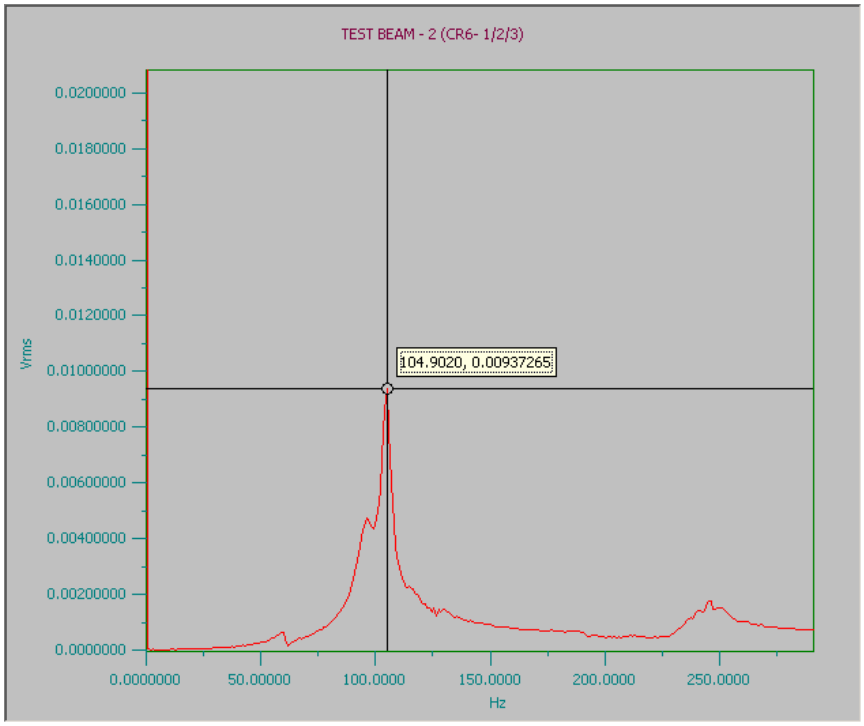

Figure E.21- Frequency for beam 2 at a load of 57.3 kN

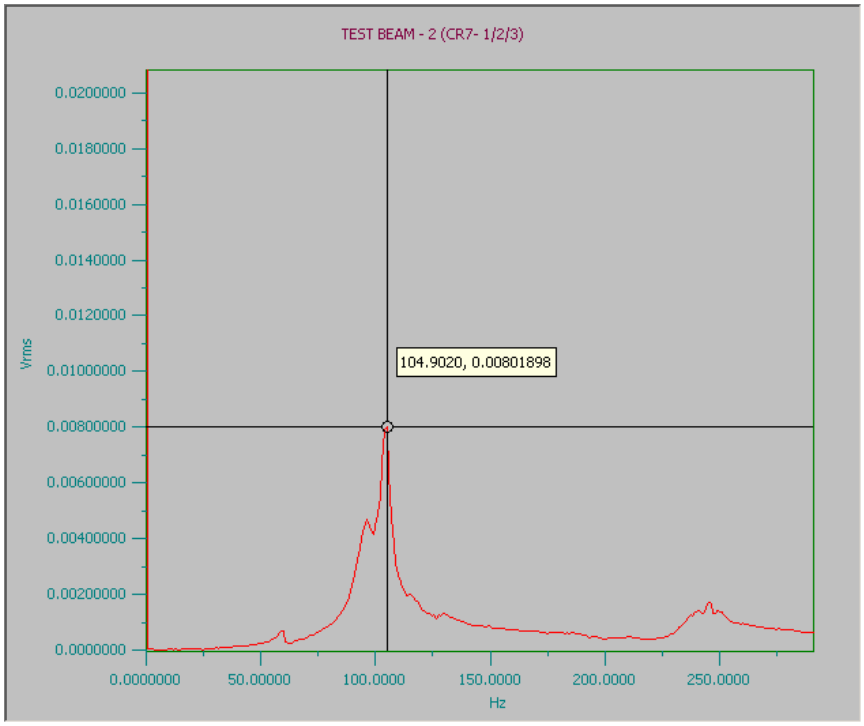

Figure E.22- Frequency for beam 2 at a load of 65.4 kN

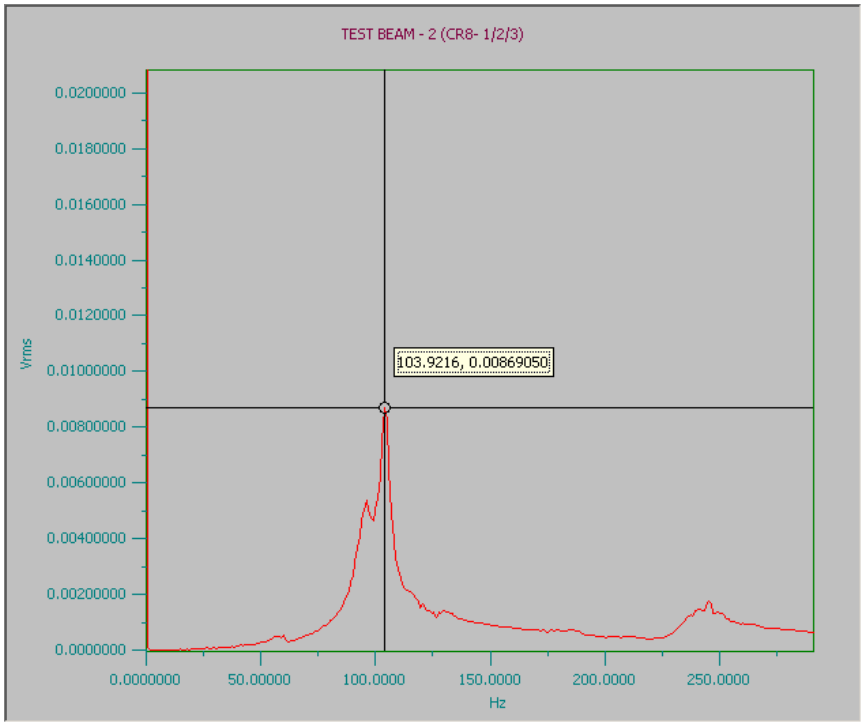

Figure E.23- Frequency for beam 2 at a load of 72.99 kN

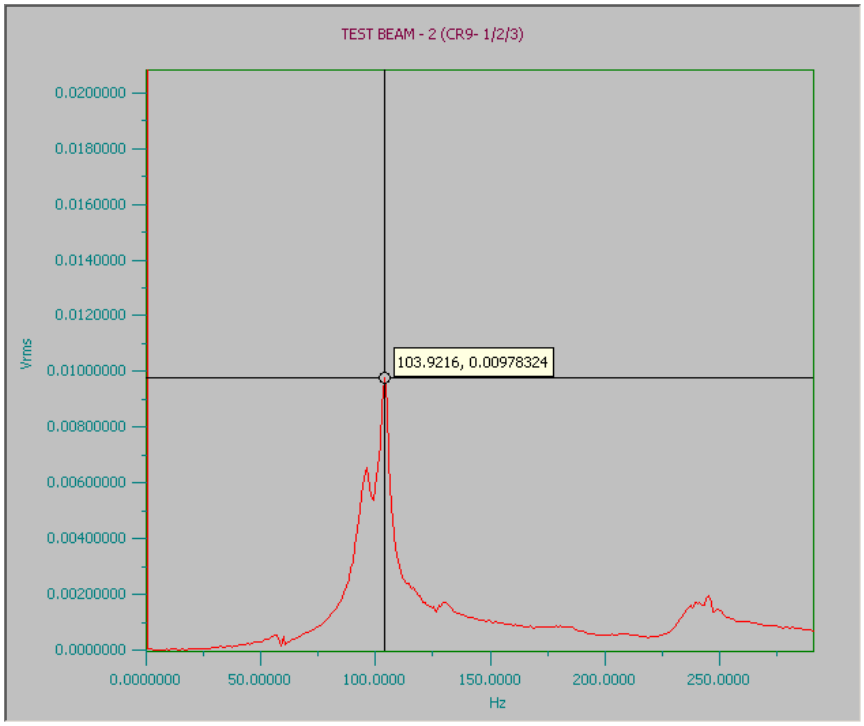

Figure E.24- Frequency for beam 2 at a load of 80.4 kN

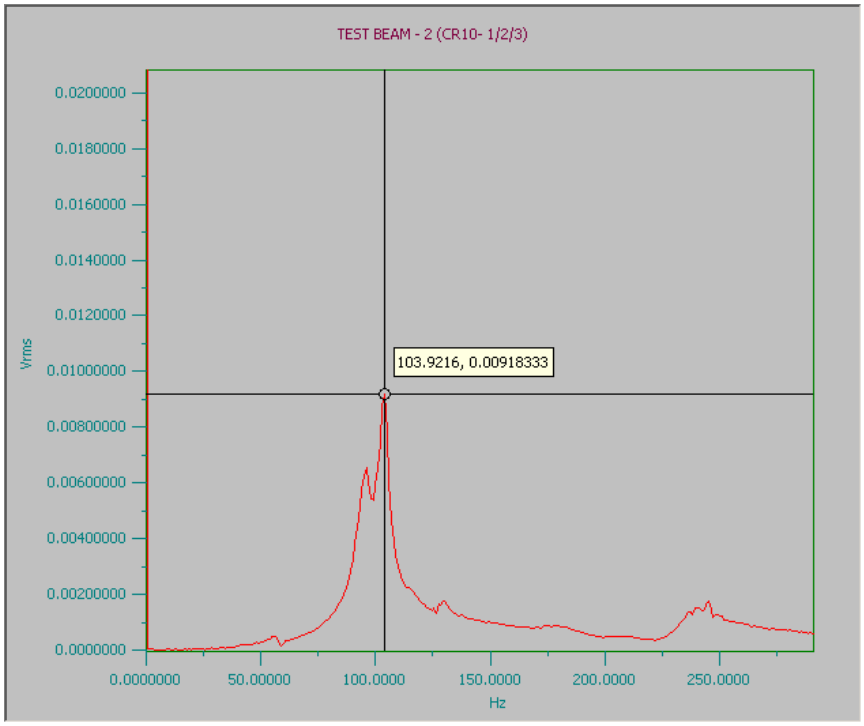

Figure E.25- Frequency for beam 2 at a load of 87.7 kN

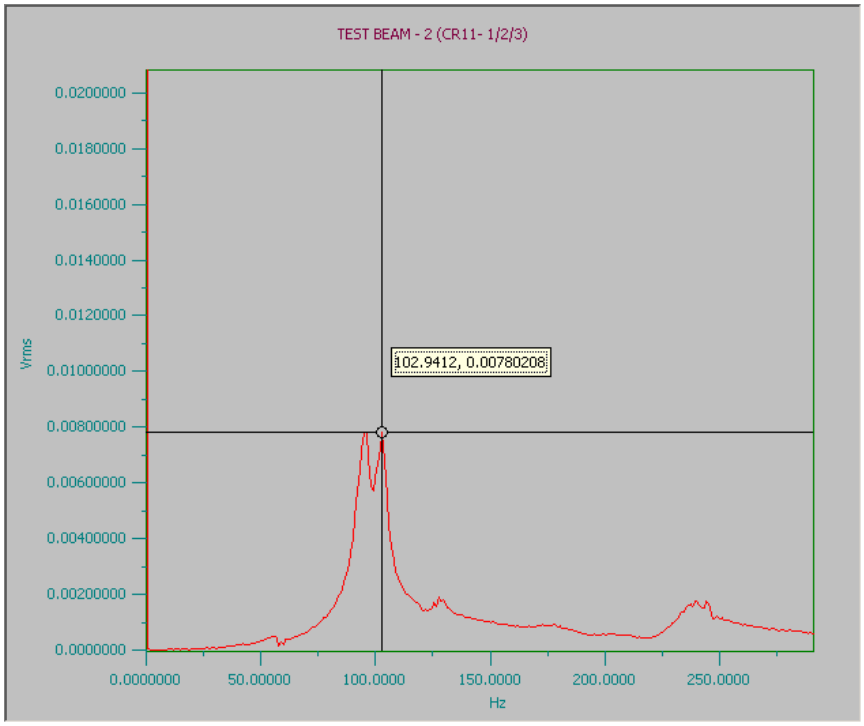

Figure E.26- Frequency for beam 2 at a load of 95.4 kN

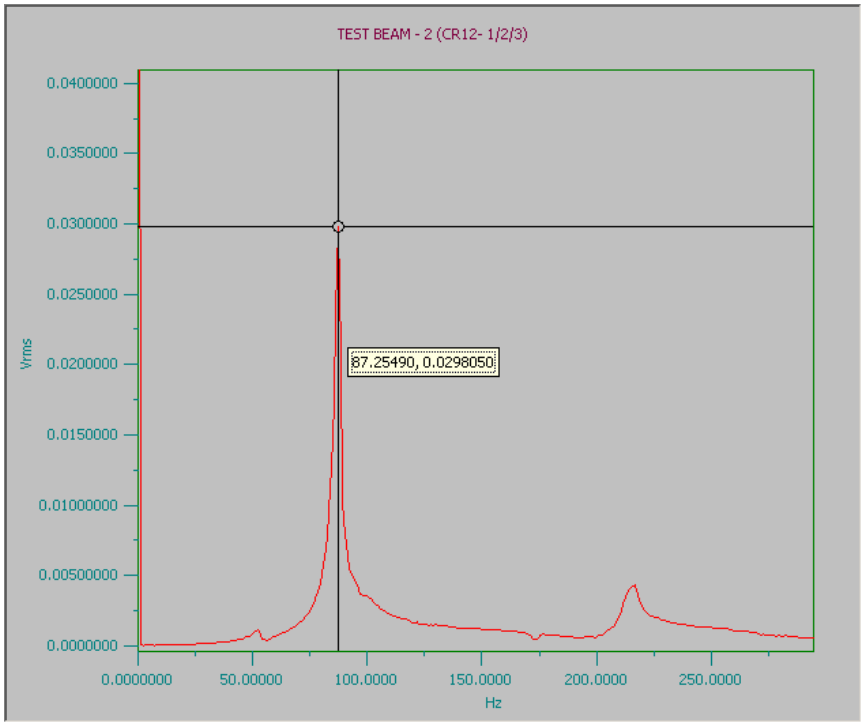

Figure E.27 Frequency for beam 2 at a load of 103.2 kN

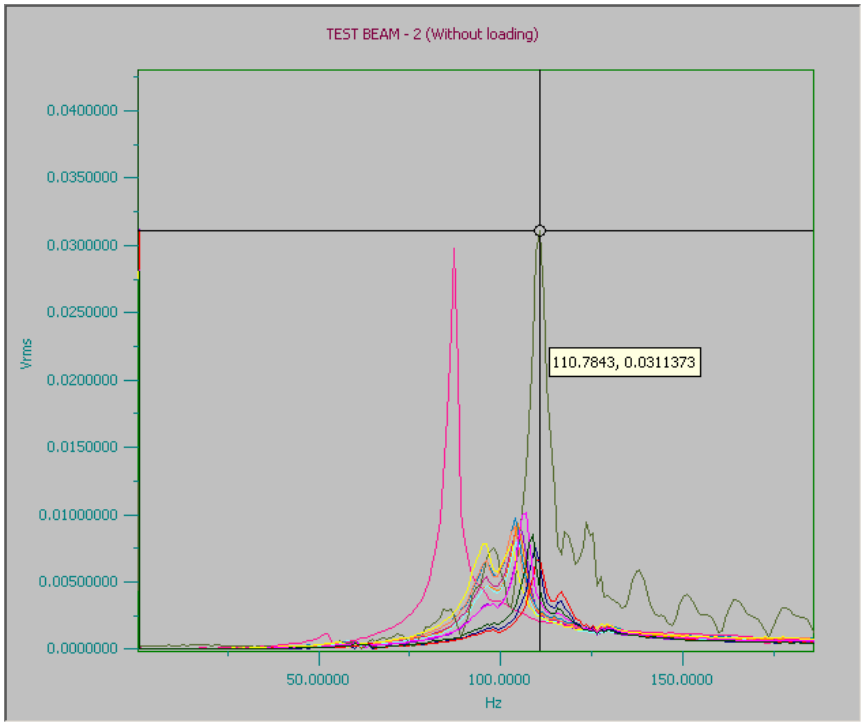

Figure E.28- Frequency for beam 2 for all load stages

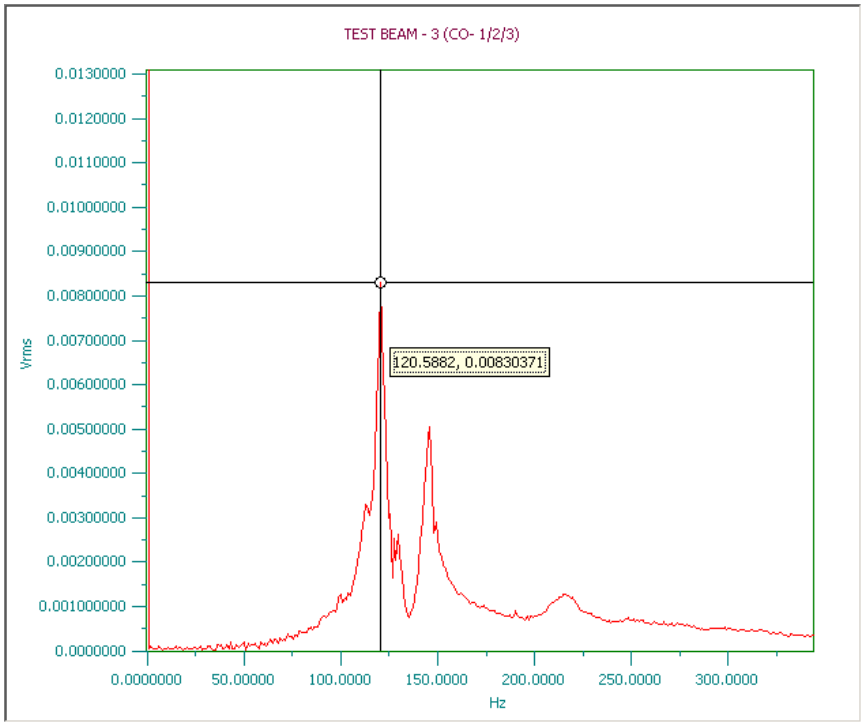

Figure E.29 Frequency for beam 3 at zero load

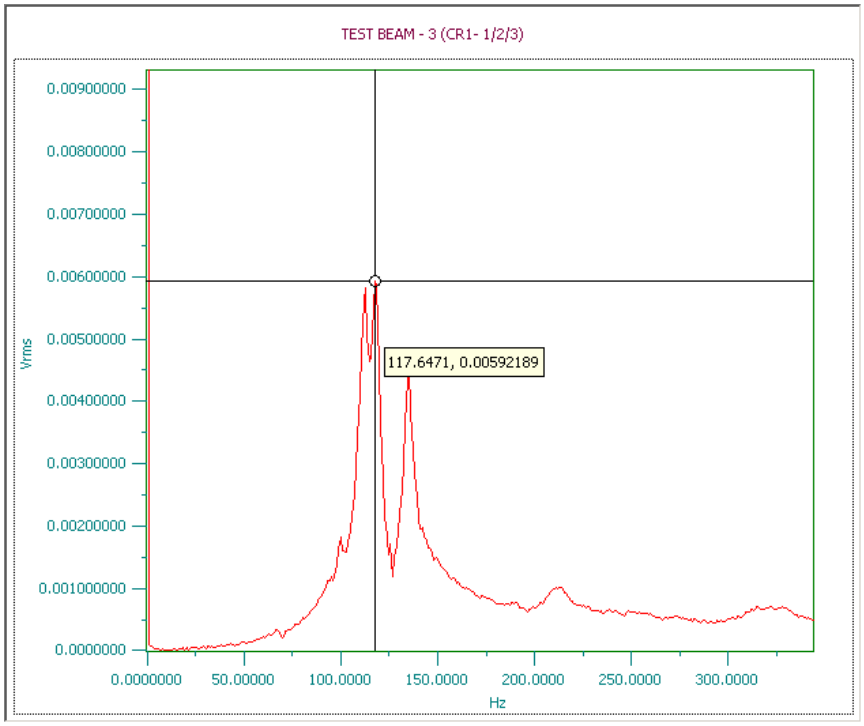

Figure E.30 Frequency for beam 3 at a load of 23.09 kN

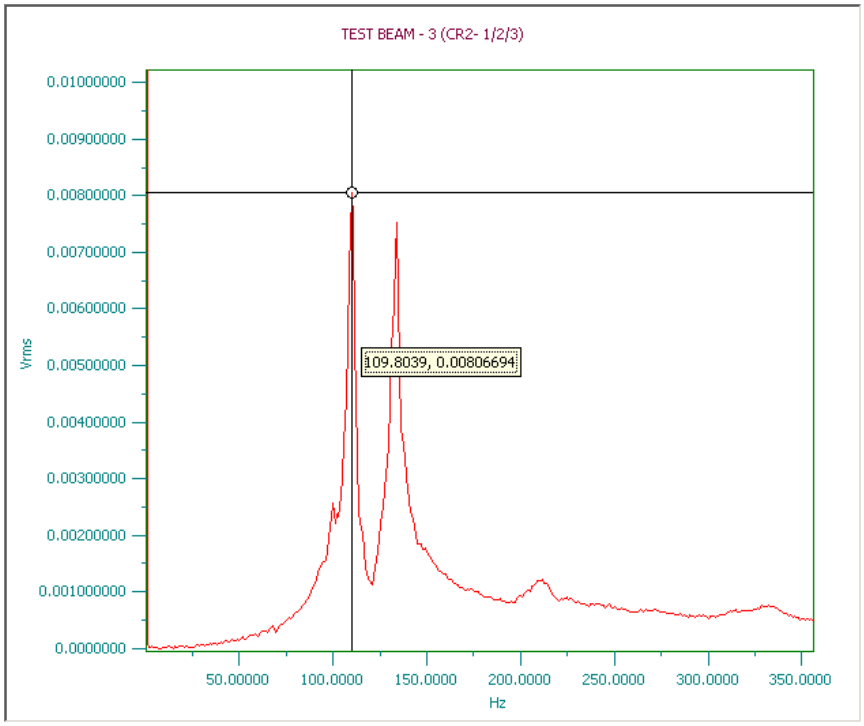

Figure E.31 Frequency for beam 3 at a load of 33.9 kN

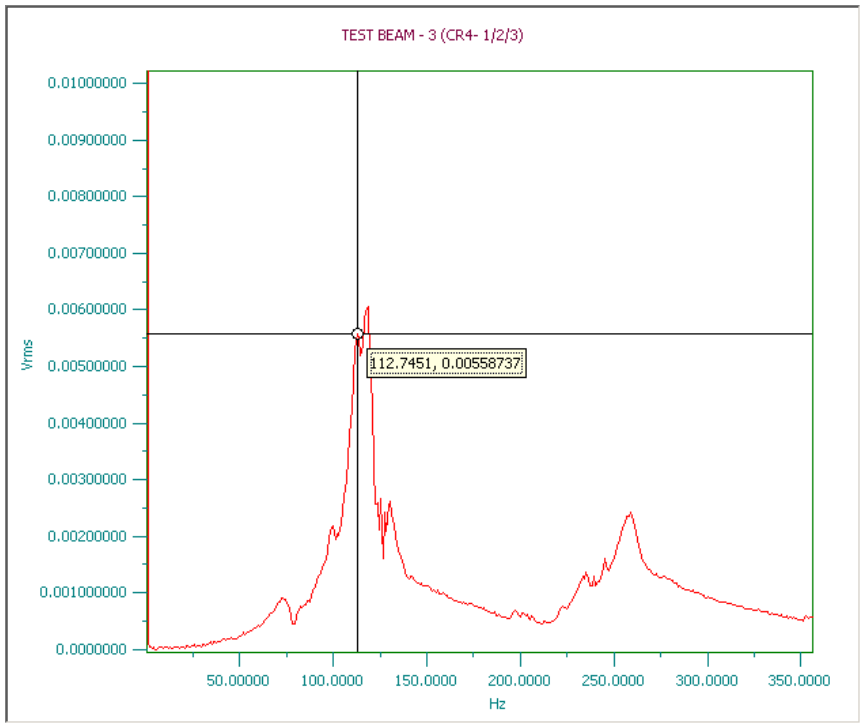

Figure E.32 Frequency for beam 3 at a load of 45.6 kN

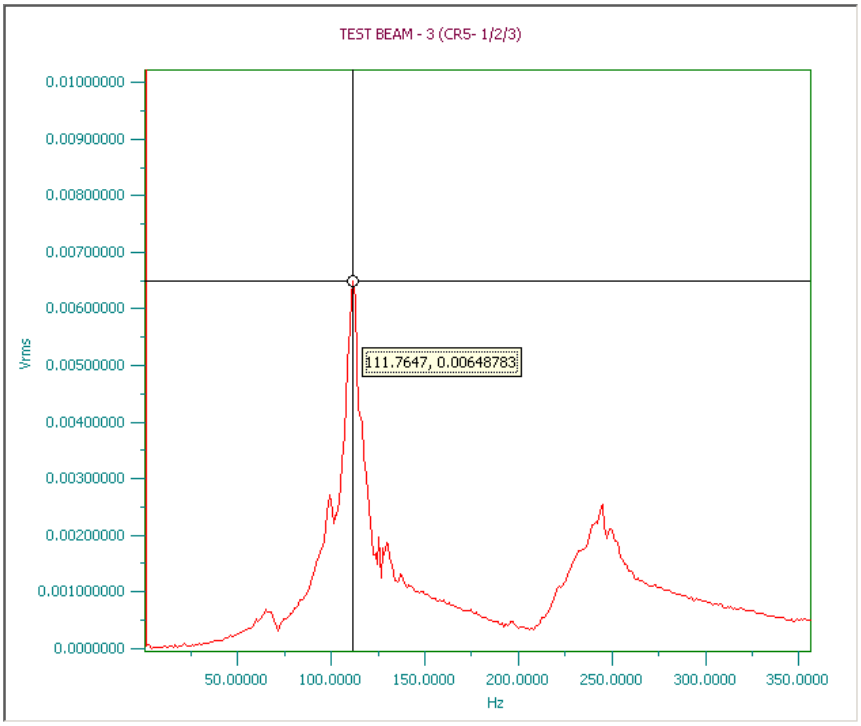

Figure E.33 Frequency for beam 3 at a load of 52.1 kN

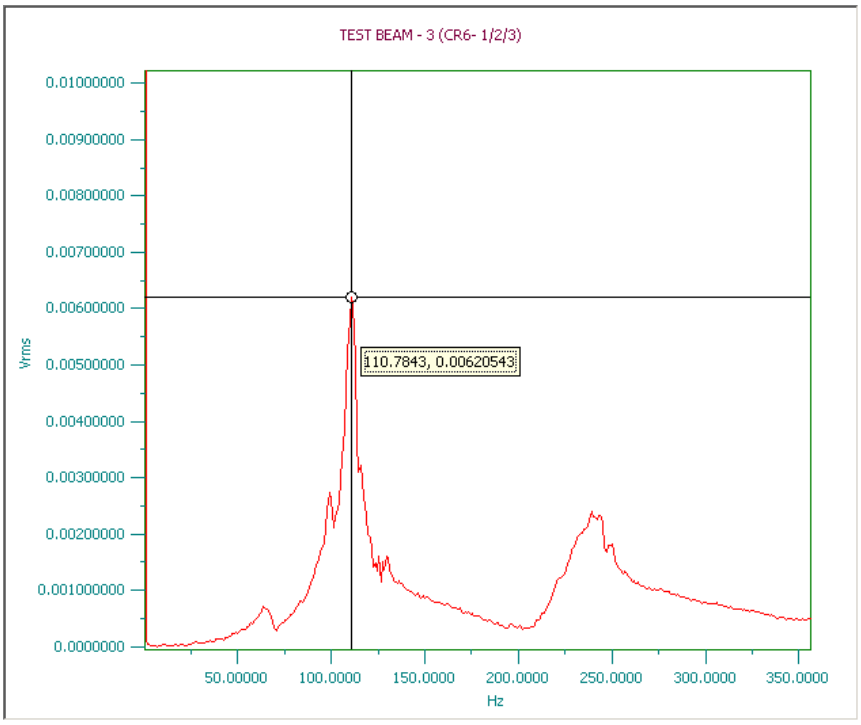

Figure E.34 Frequency for beam 3 at a load of 59.02 kN

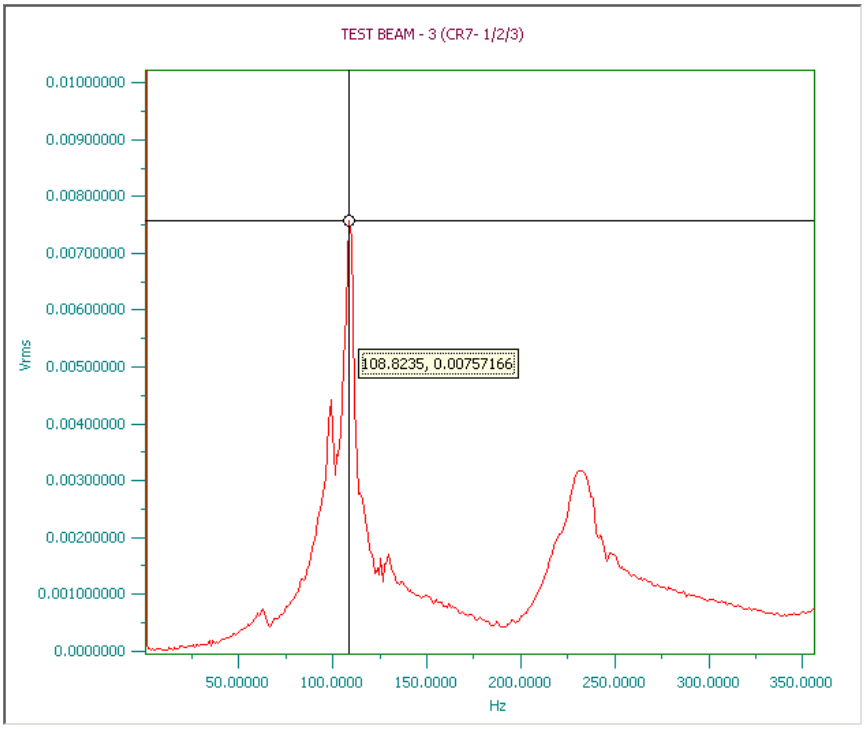

Figure E.35 Frequency for beam 3 at a load of 68.08 kN

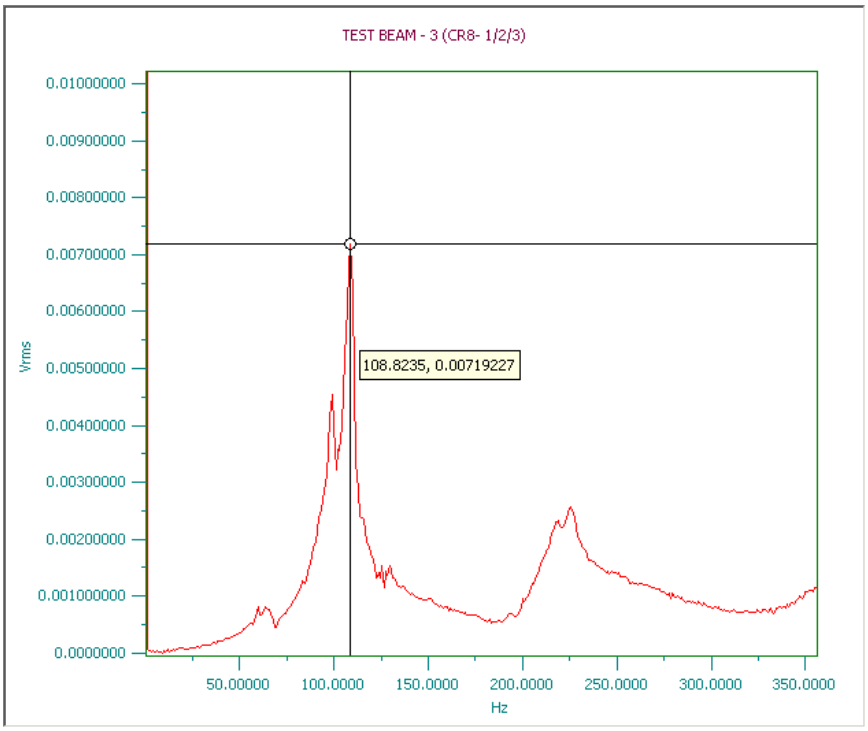

Figure E.36 Frequency for beam 3 at a load of 75.4 kN

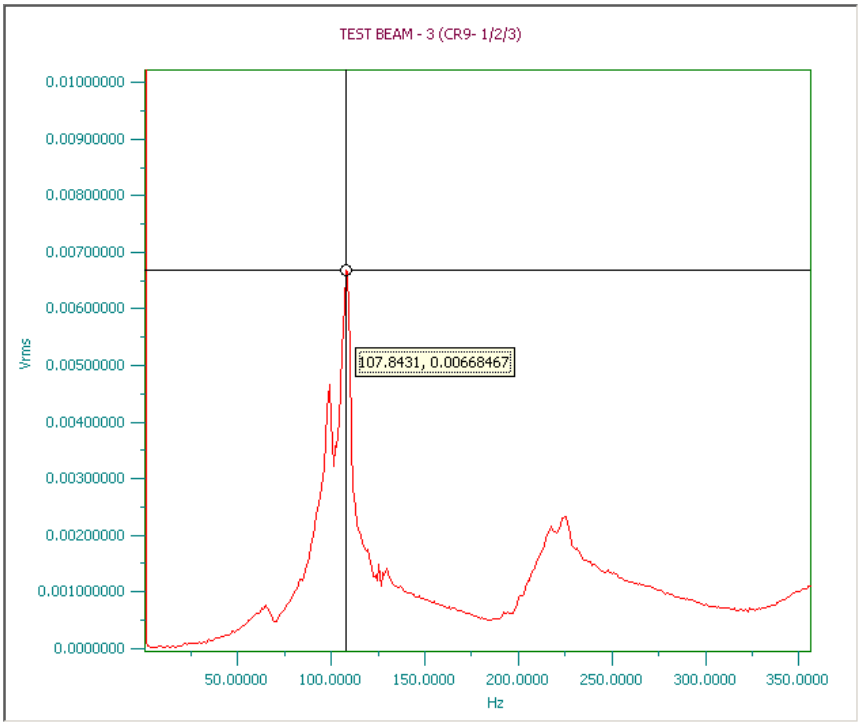

Figure E.37 Frequency for beam 3 at a load of 81.5 kN

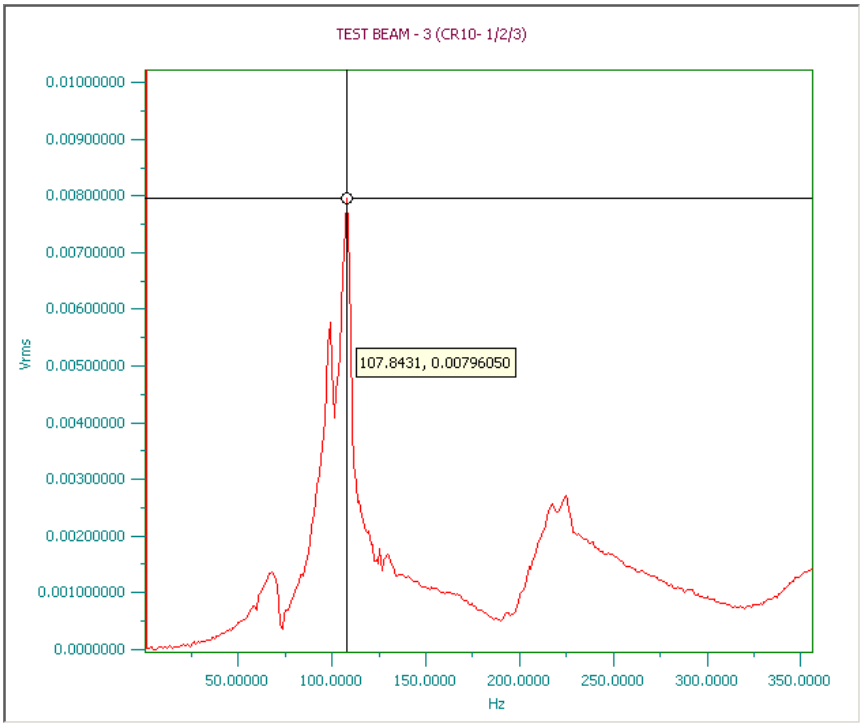

Figure E.38 Frequency for beam 3 at a load of 88.996 kN

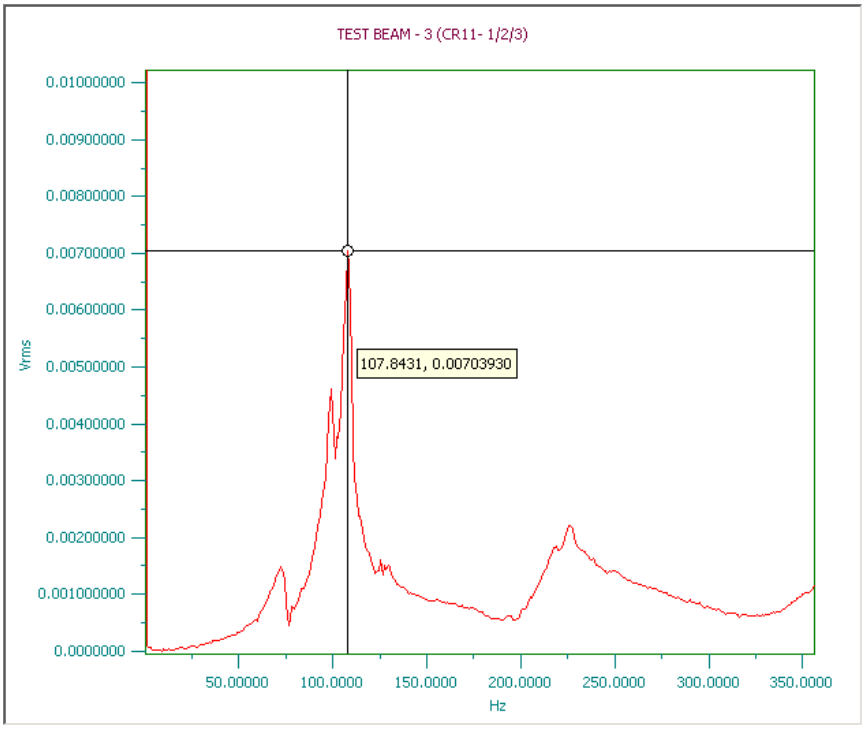

Figure E.39 Frequency for beam 3 at a load of 95.35 kN

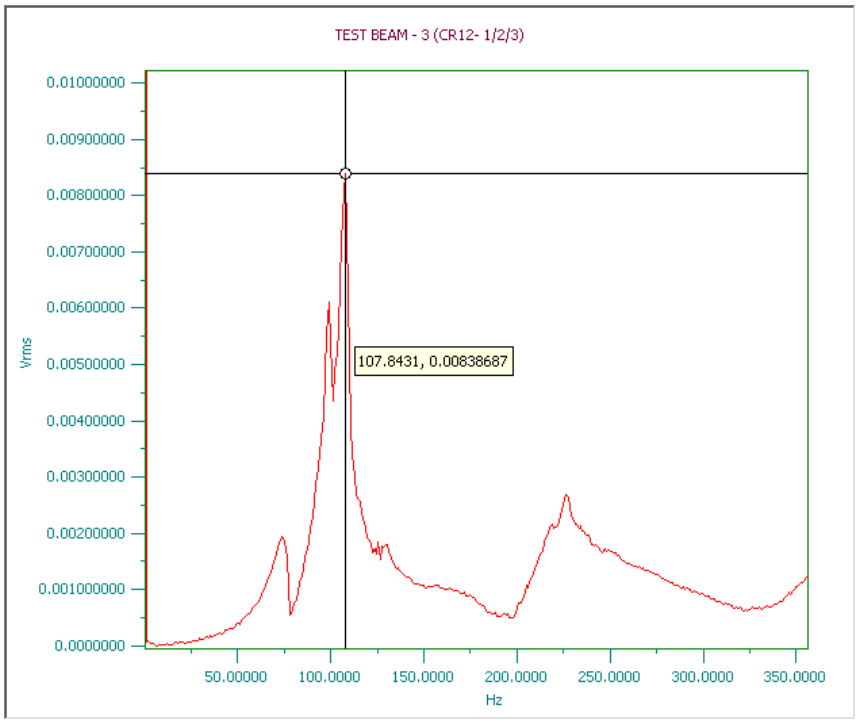

Figure E.40 Frequency for beam 3 at a load of 99.78 kN

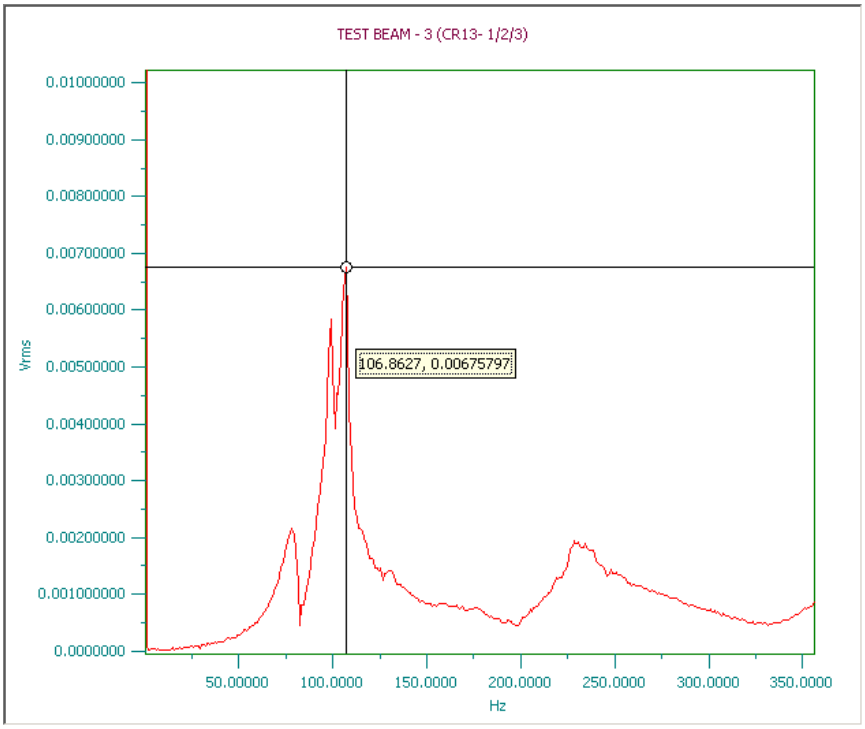

Figure E.41 Frequency for beam 3 at a load of 111.6 kN

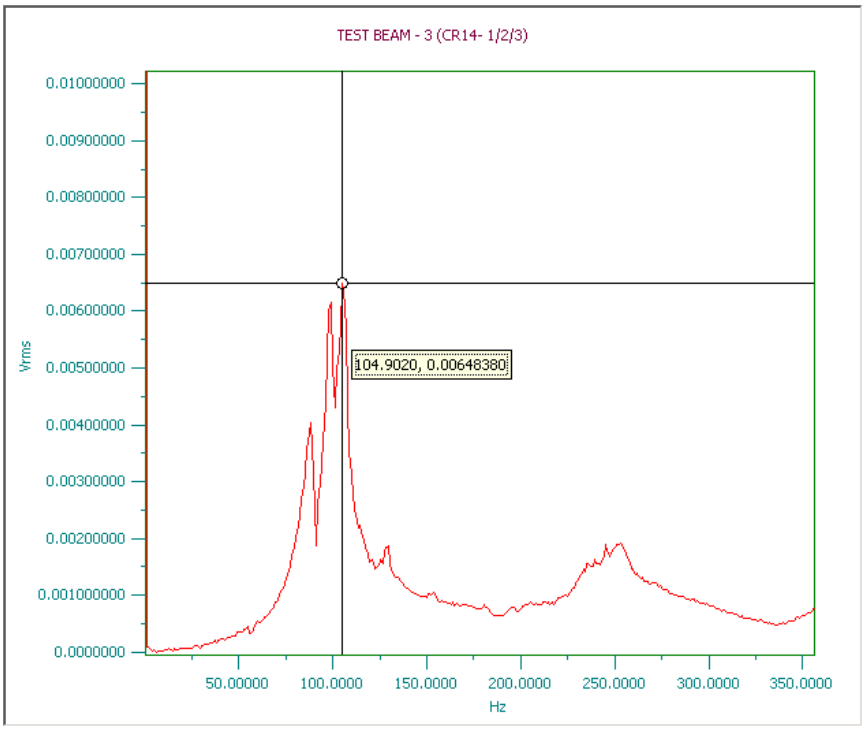

Figure E.42 Frequency for beam 3 at a load of 122.32 kN

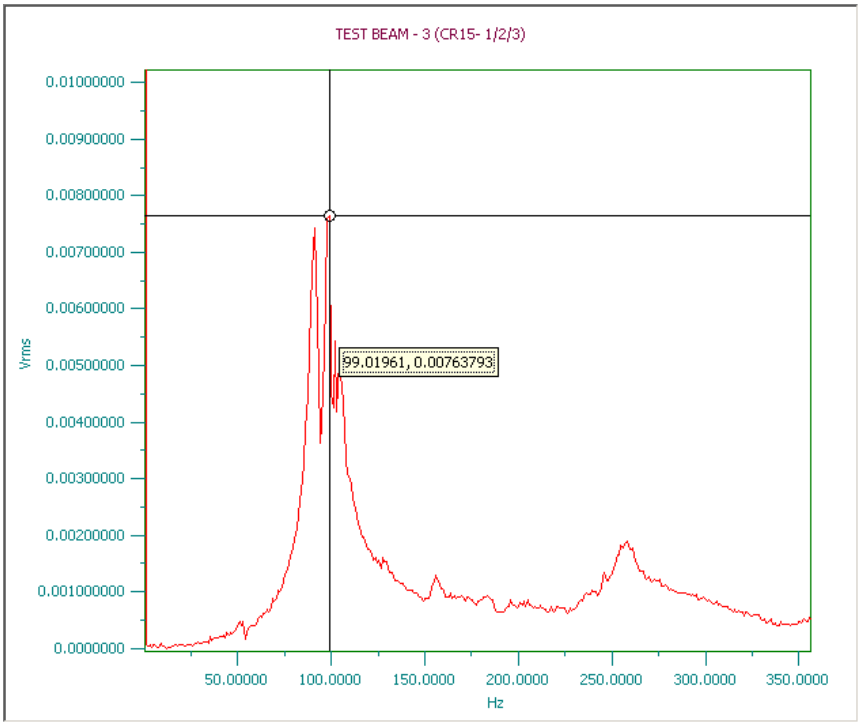

Figure E.43 Frequency for beam 3 at a load of 131.95 kN

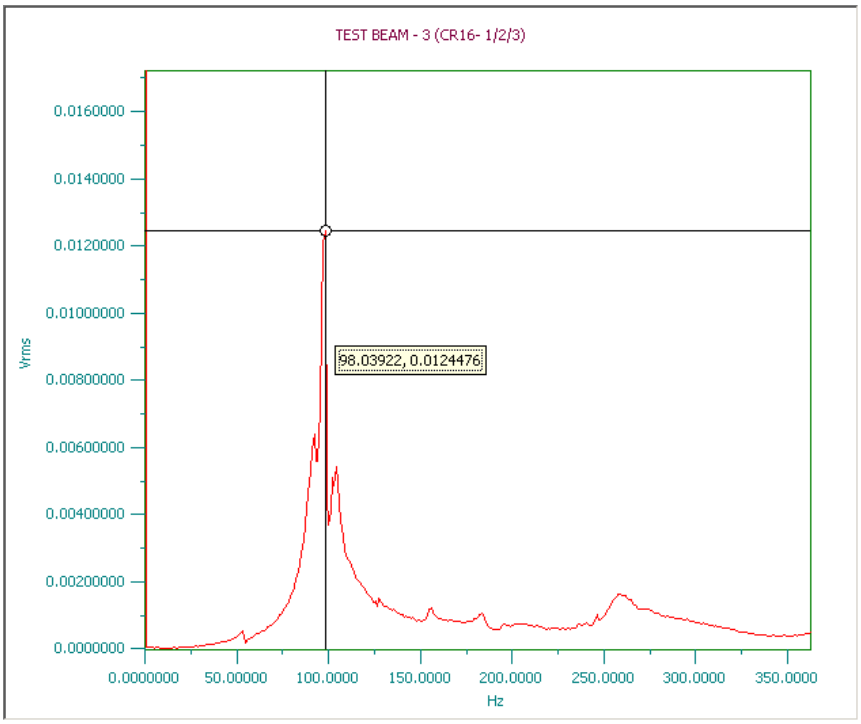

Figure E.44 Frequency for beam 3 at a load of 139.4 kN

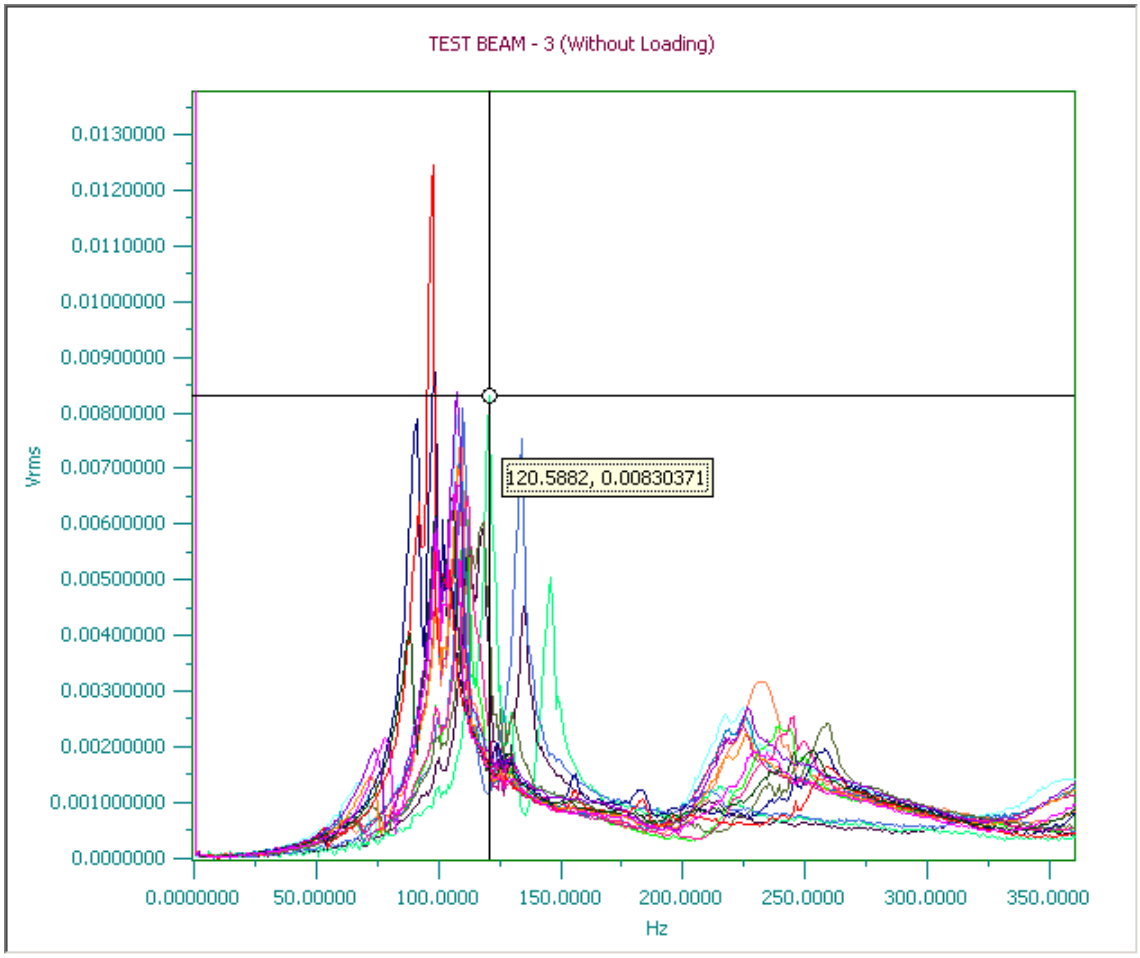

Figure E.45 Frequency for beam 3 for all load stages

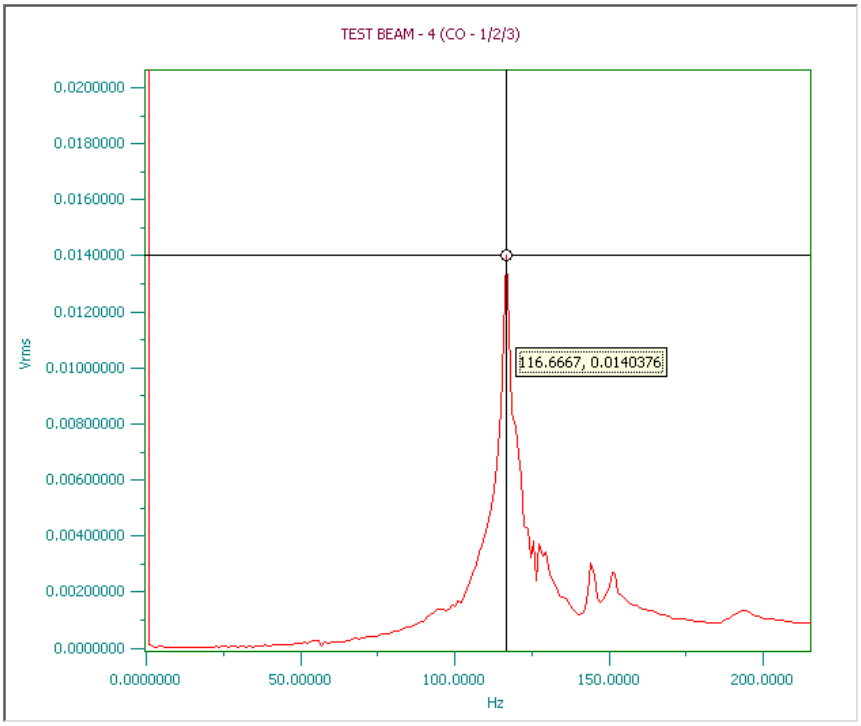

Figure E.46 Frequency for beam 4 at zero load

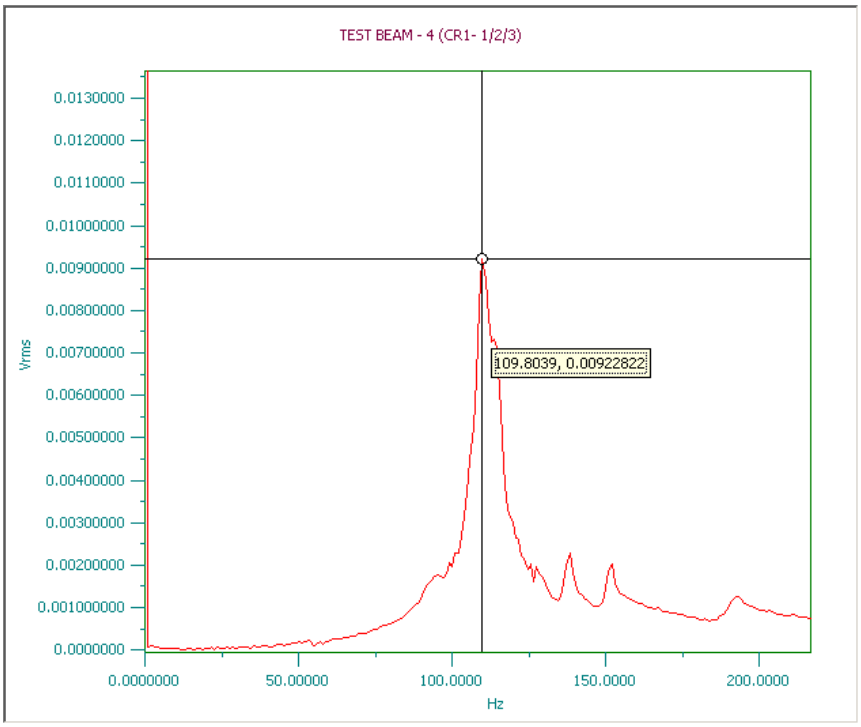

Figure E.47 Frequency for beam 4 at a load of 25.23 kN

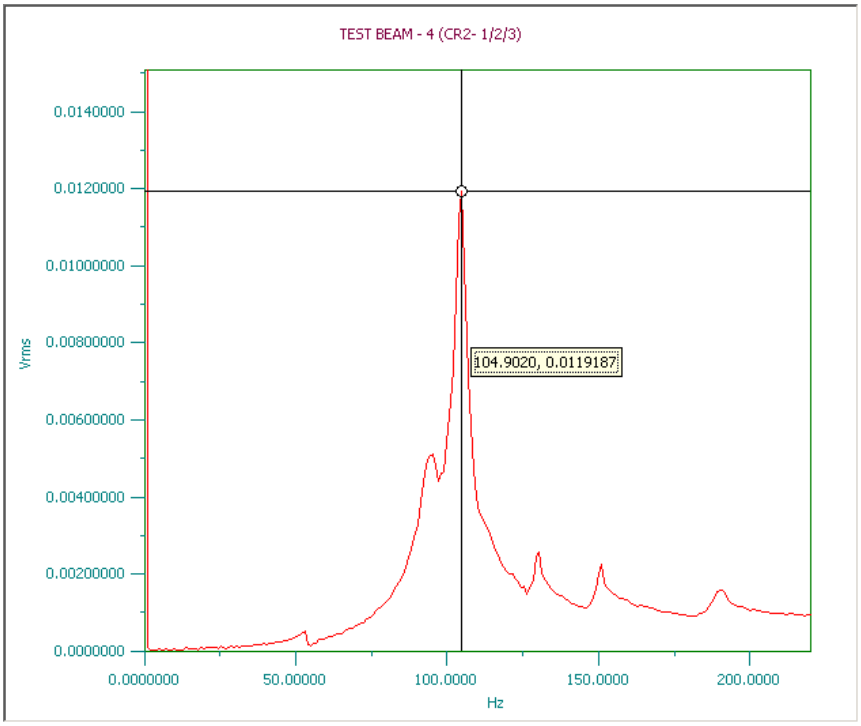

Figure E.48 Frequency for beam 4 at a load of 30.2 kN

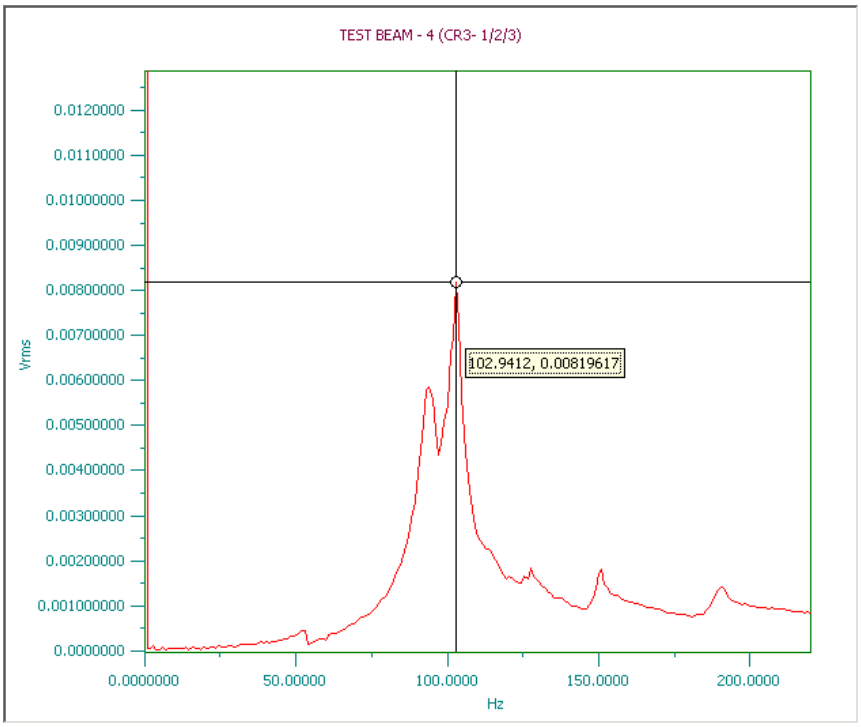

Figure E.49 Frequency for beam 4 at a load of 35.19 kN

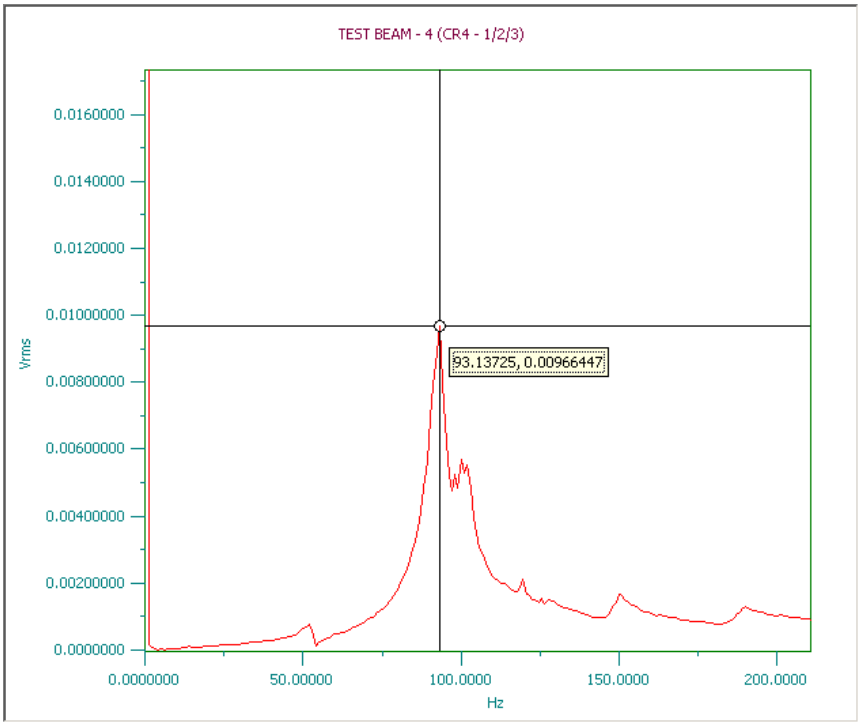

Figure E.50 Frequency for beam 4 at a load of 39.66 kN

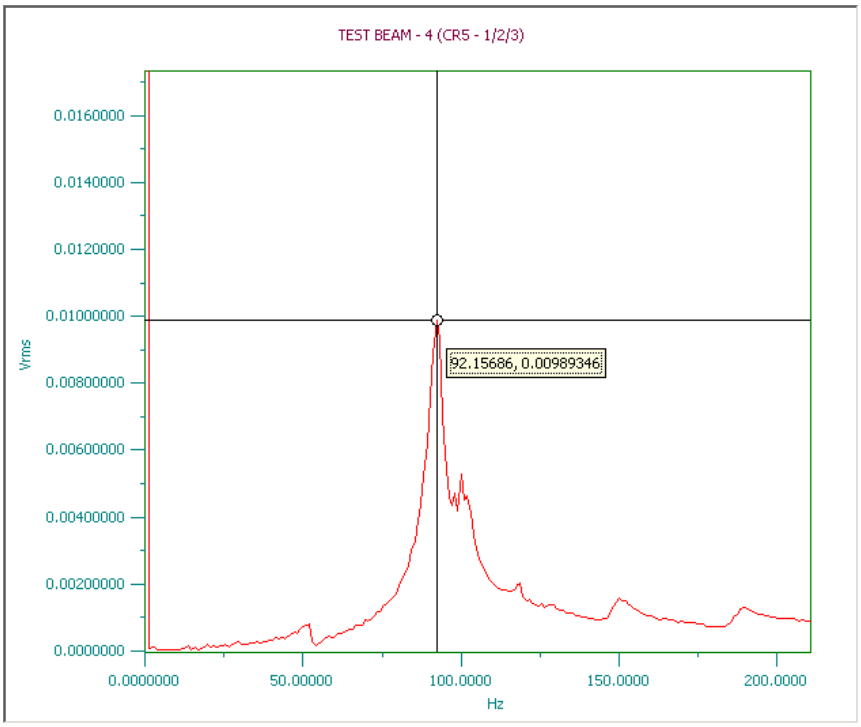

Figure E.51 Frequency for beam 4 at a load of 45.4 kN

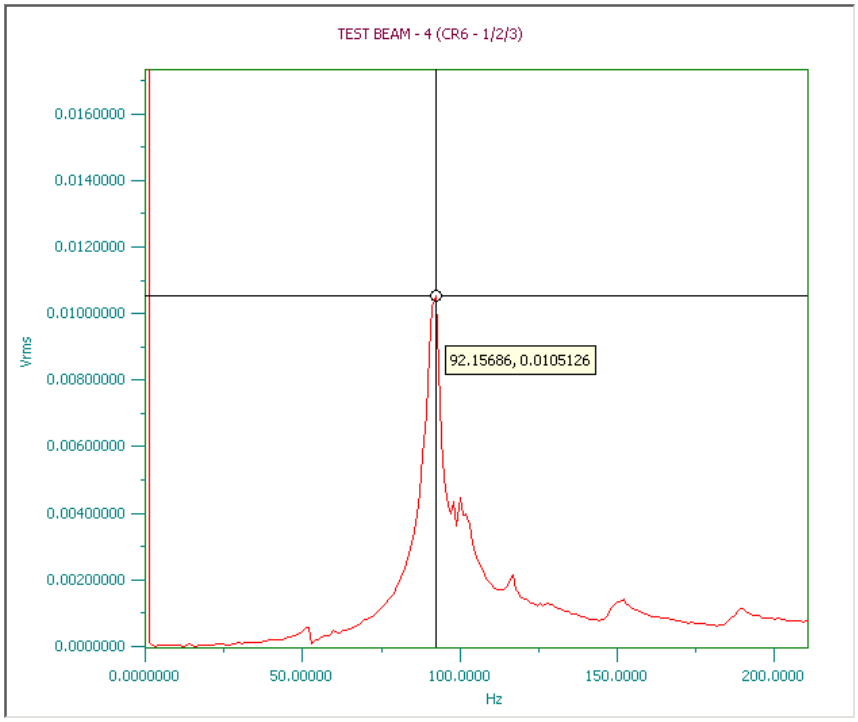

Figure E.52 Frequency for beam 4 at a load of 49.51 kN

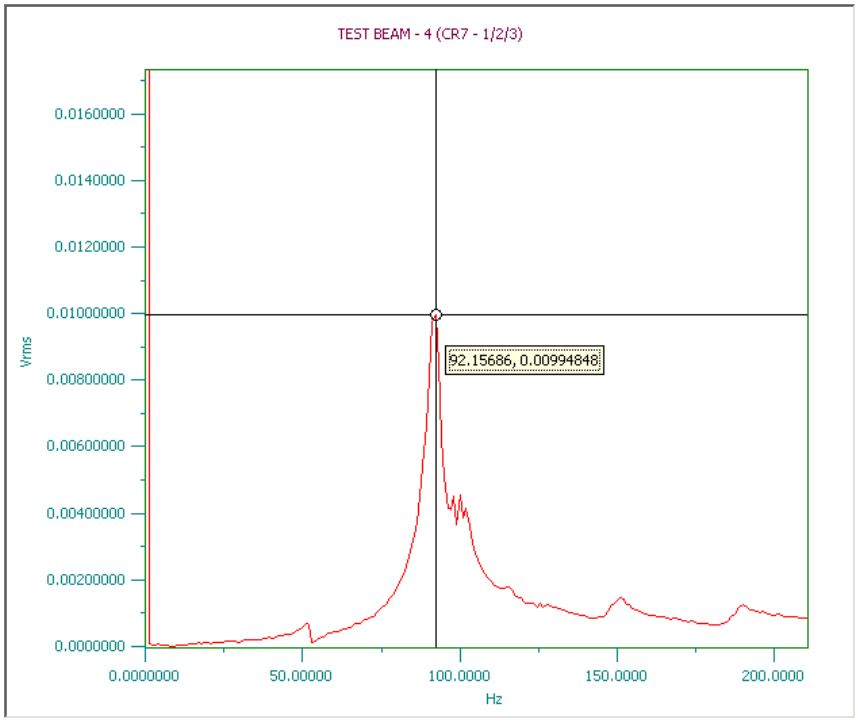

Figure E.53 Frequency for beam 4 at a load of 56.02 kN

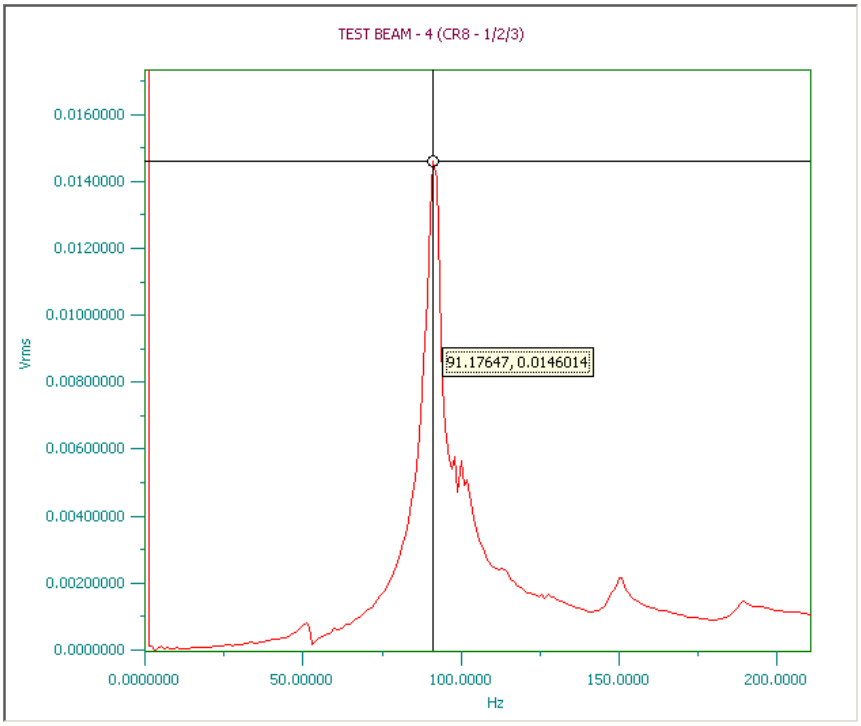

Figure E.54 Frequency for beam 4 at a load of 60.9 kN

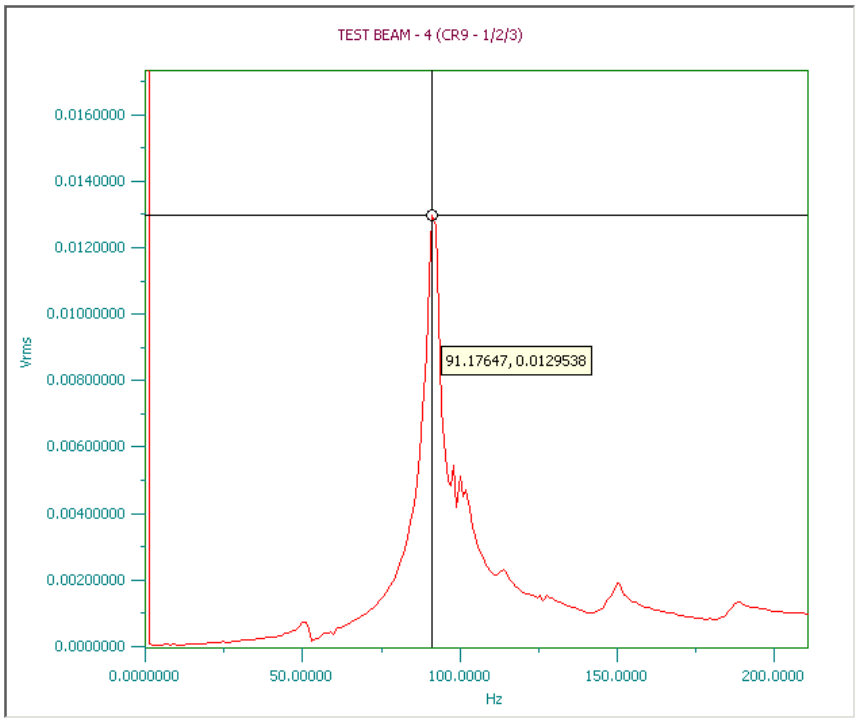

Figure E.55 Frequency for beam 4 at a load of 66.57 kN

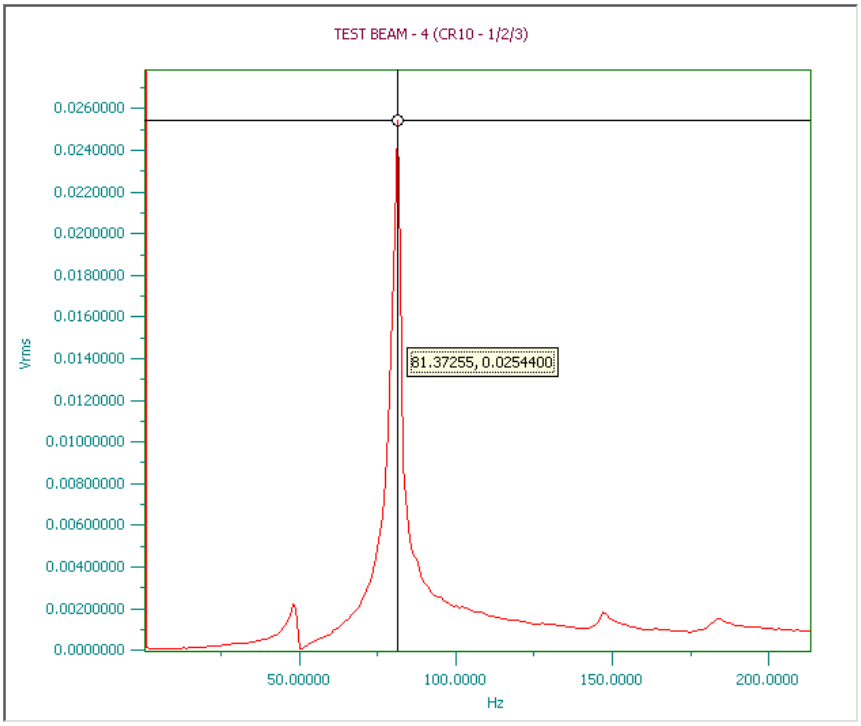

Figure E.56 Frequency for beam 4 at a load of 70.24 kN

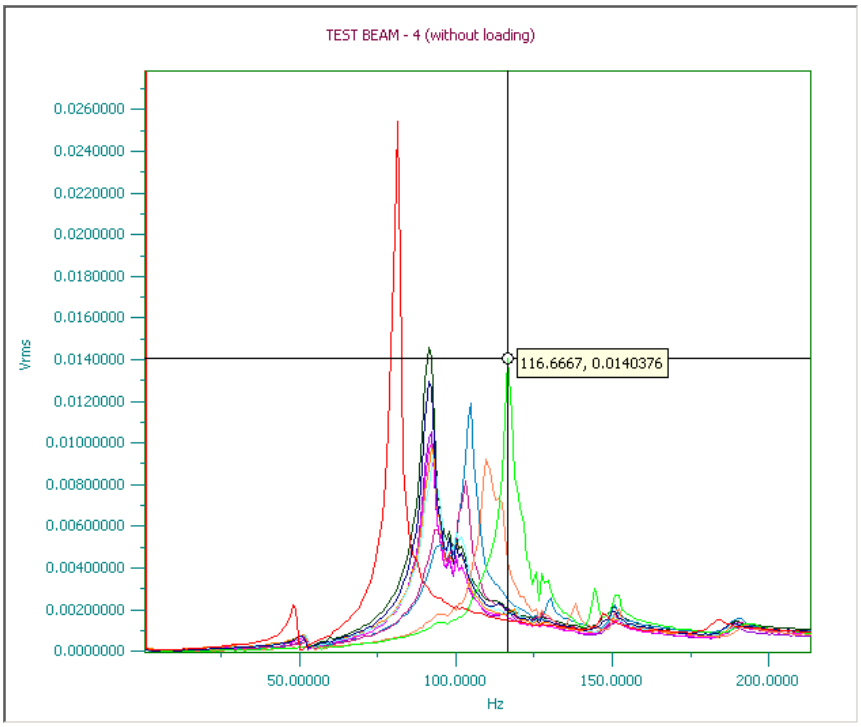

Figure E.57 Frequency for beam 4 at all load stages

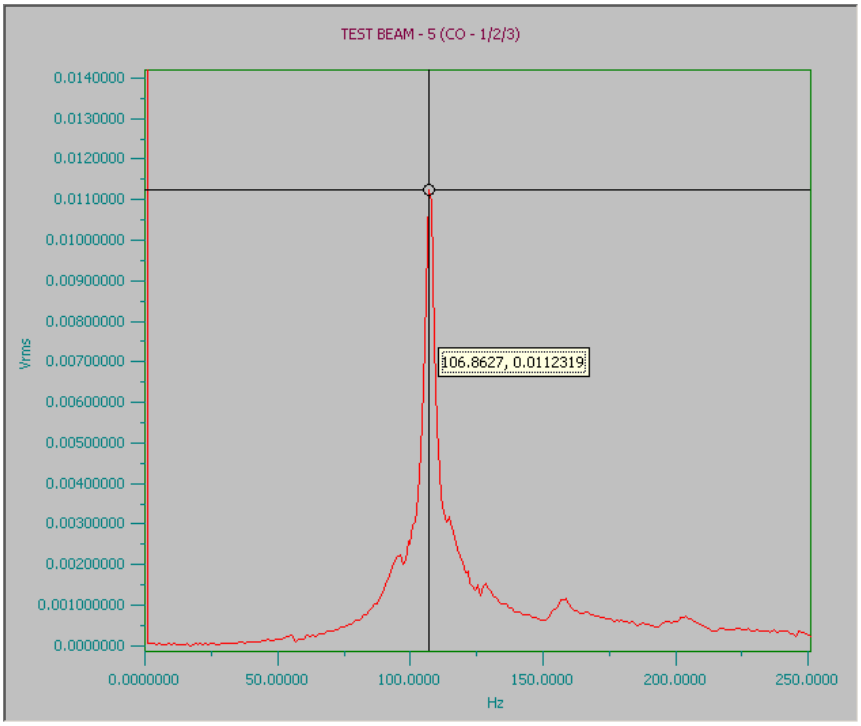

Figure E.58 Frequency for beam 5 at zero load

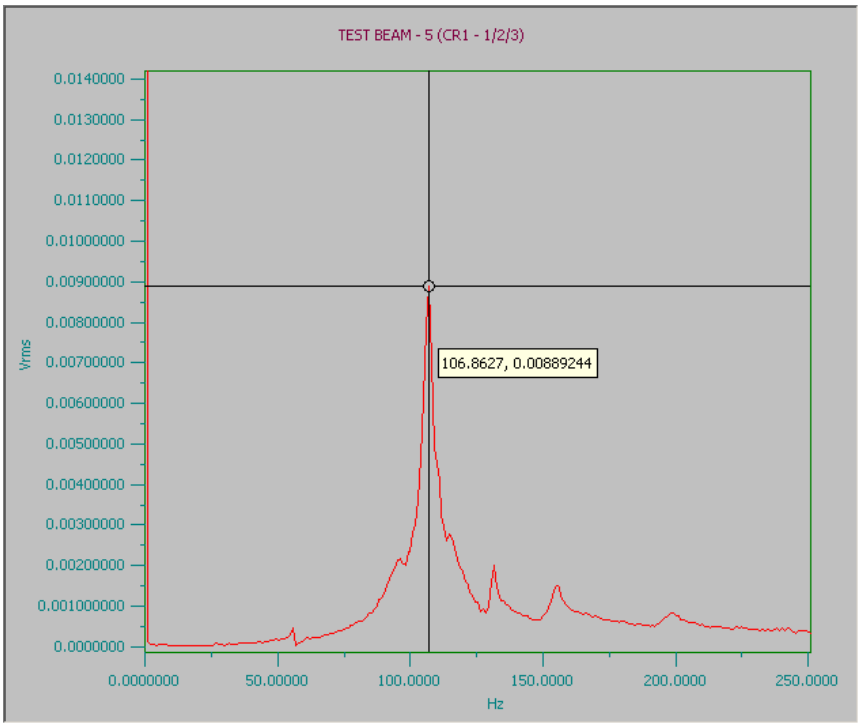

Figure E.59 Frequency for beam 5 at a load of 20.45 kN

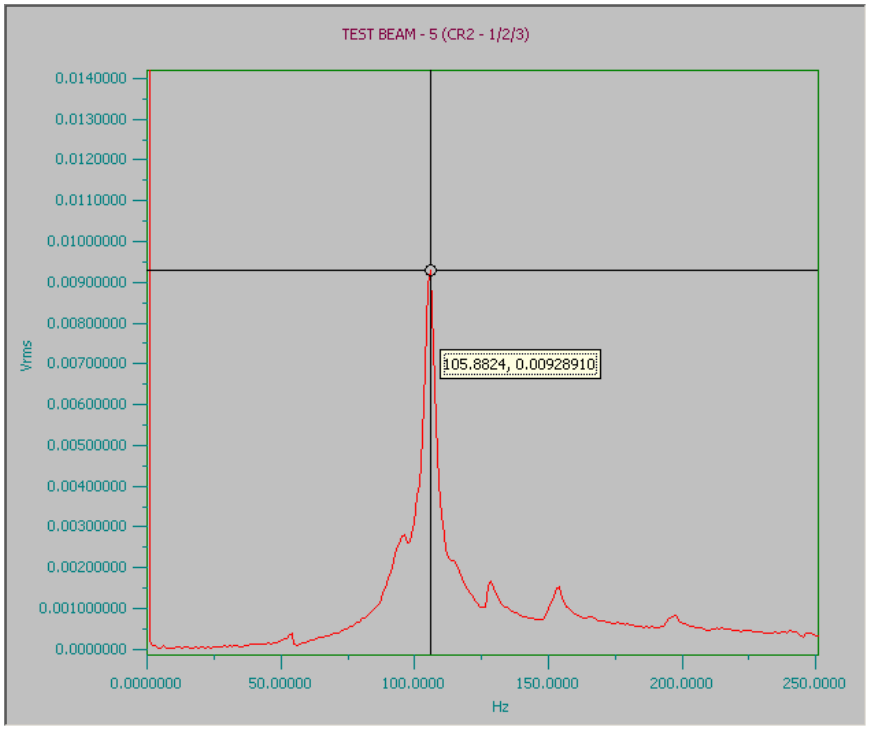

Figure E.60 Frequency for beam 5 at a load of 34.89 kN

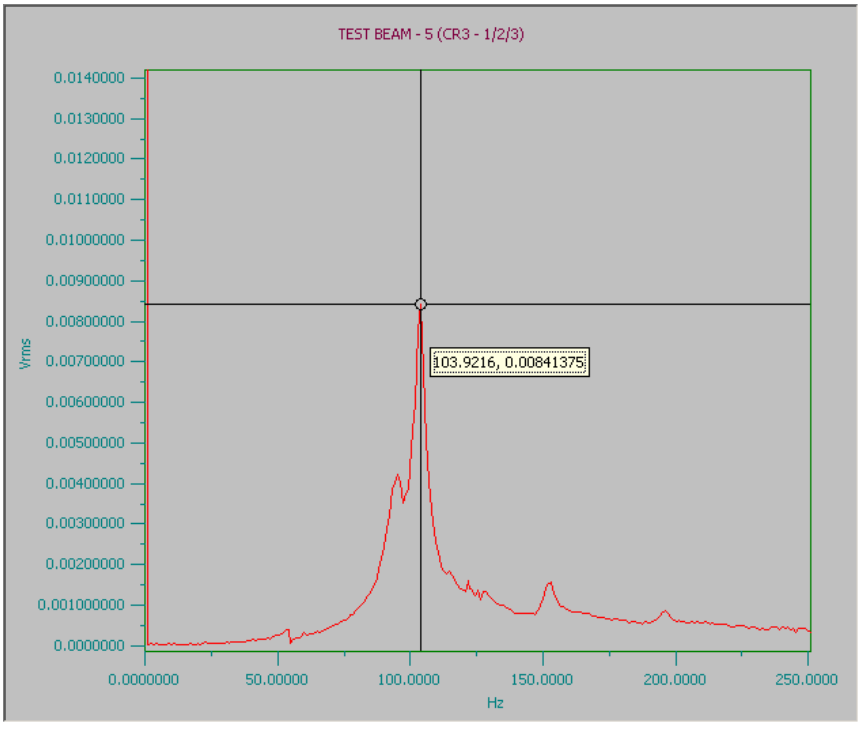

Figure E.61 Frequency for beam 5 at a load of 44.42 kN

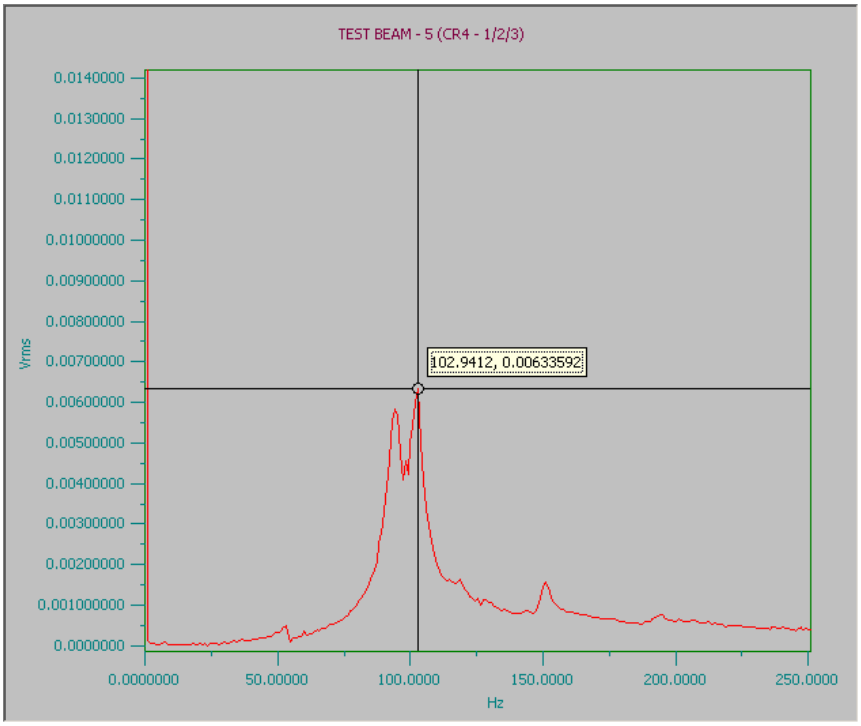

Figure E.62 Frequency for beam 5 at a load of 55.06 kN

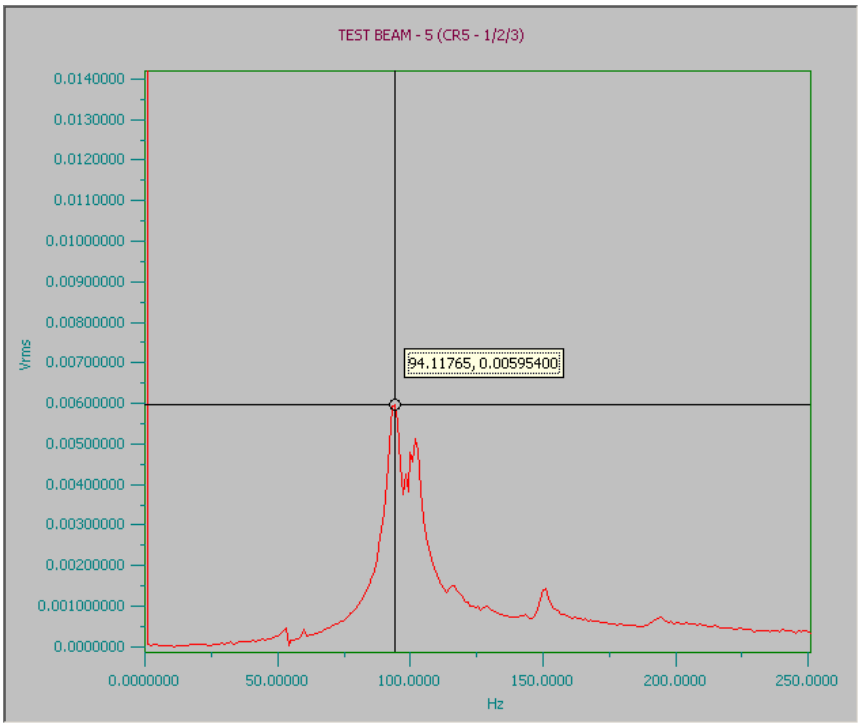

Figure E.63 Frequency for beam 5 at a load of 64.63 kN

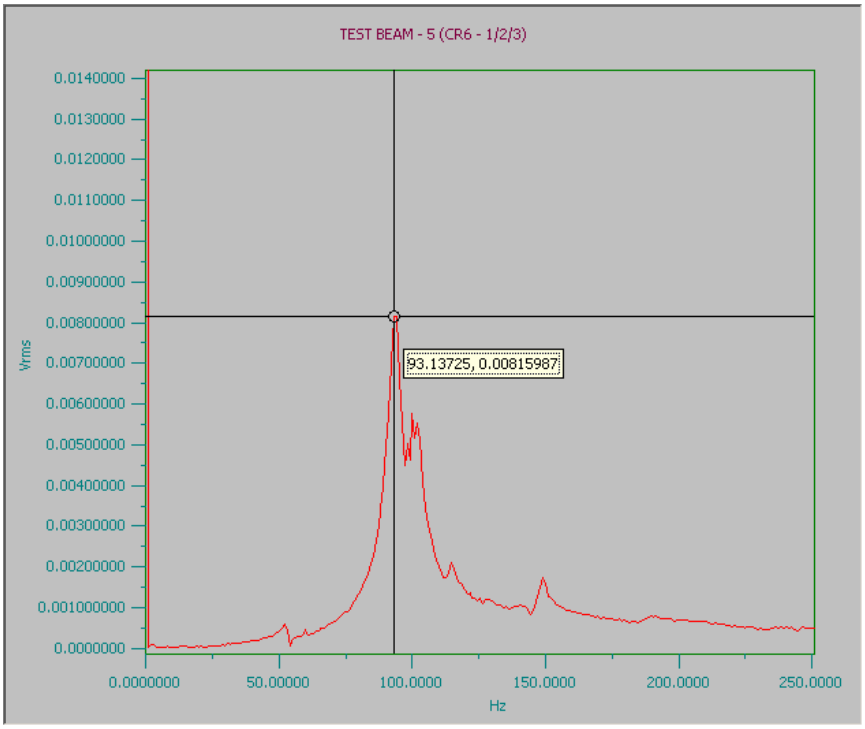

Figure E.64 Frequency for beam 5 at a load of 74.4 kN

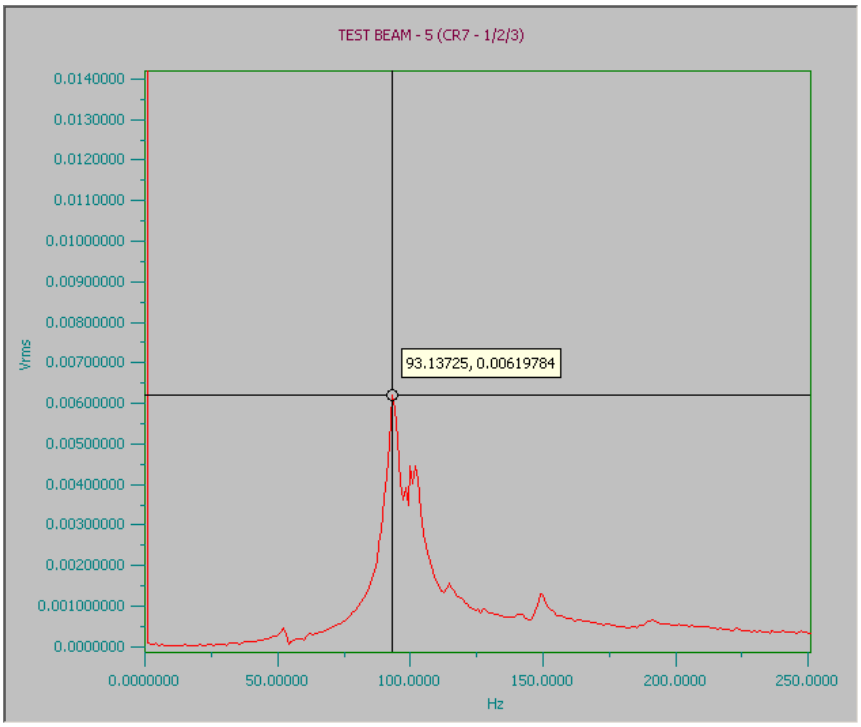

Figure E.65 Frequency for beam 5 at a load of 85.36 kN

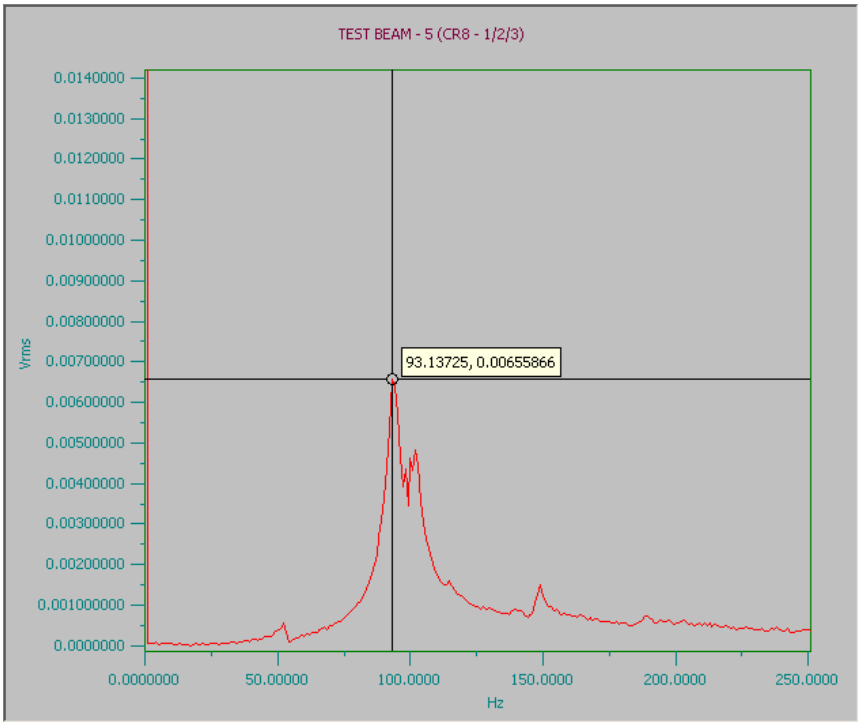

Figure E.66 Frequency for beam 5 at a load of 95.03 kN

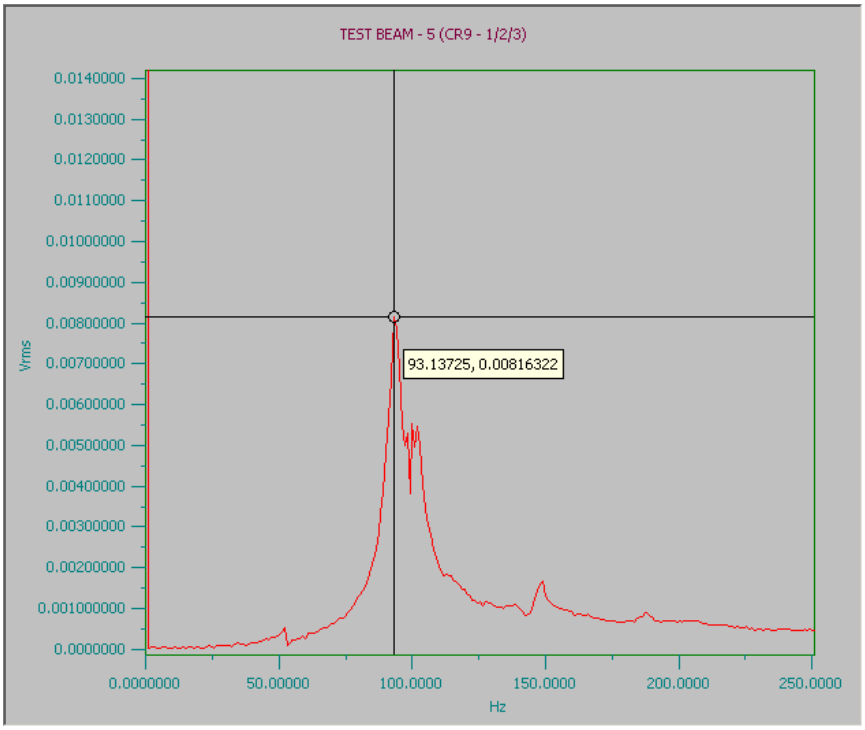

Figure E.67 Frequency for beam 5 at a load of 104.48 kN

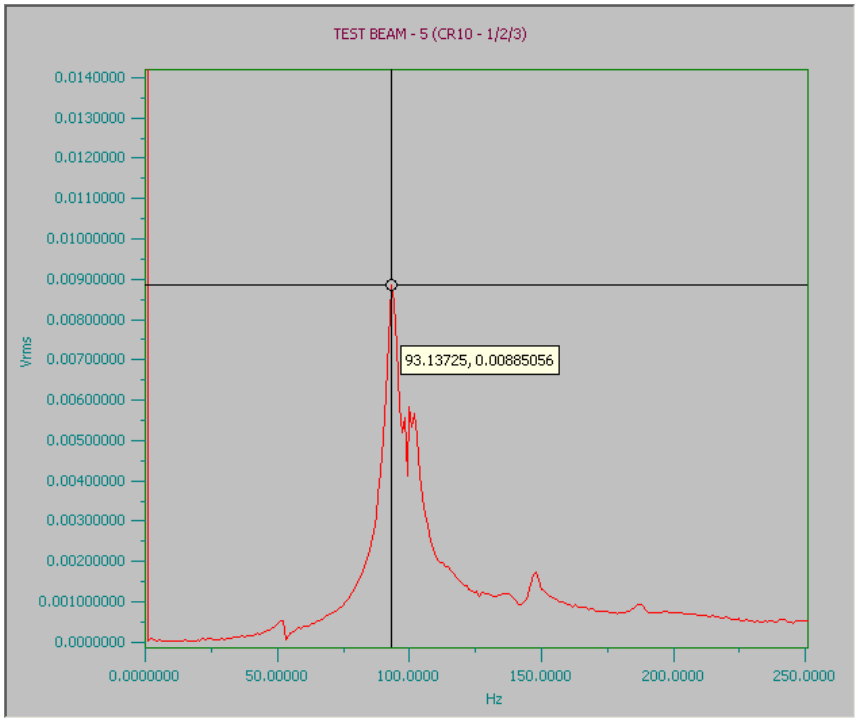

Figure E.68 Frequency for beam 5 at a load of 114.67 kN

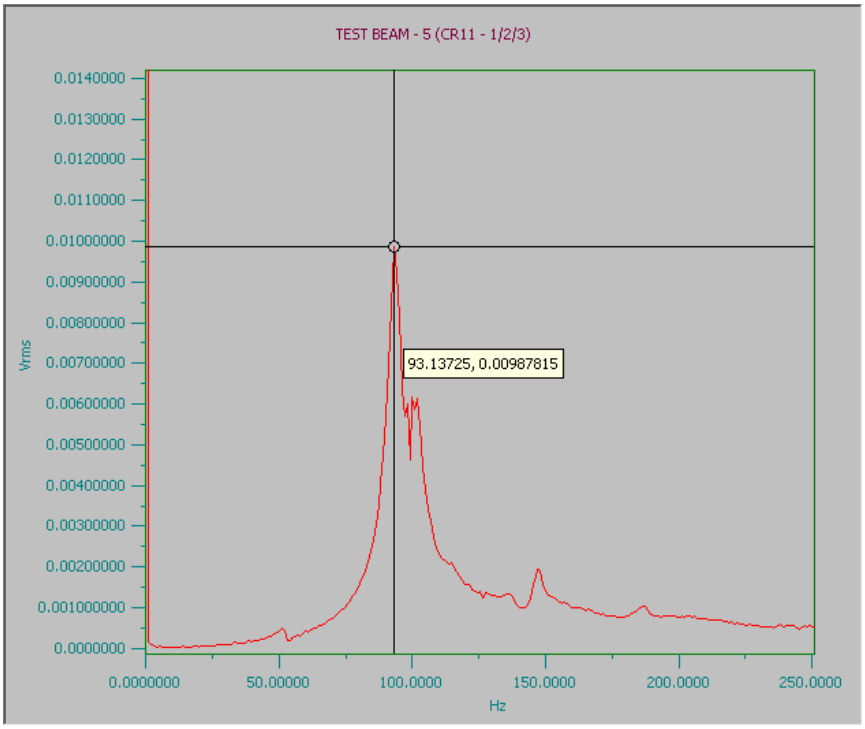

Figure E.69 Frequency for beam 5 at a load of 124.86 kN

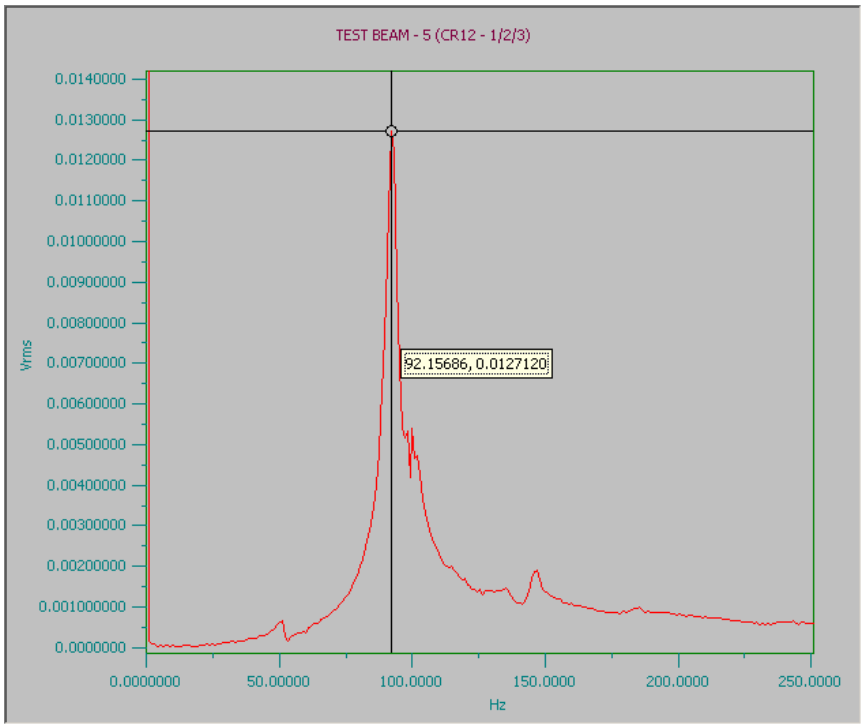

Figure E.70 Frequency for beam 5 at a load of 135.19 kN

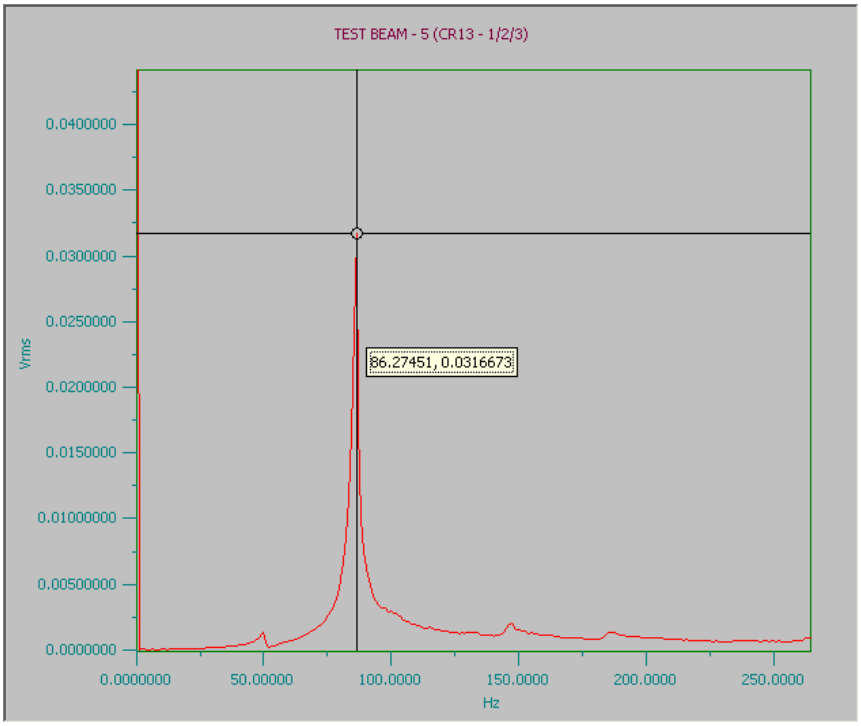

Figure E.71 Frequency for beam 5 at a load of 138.49 kN

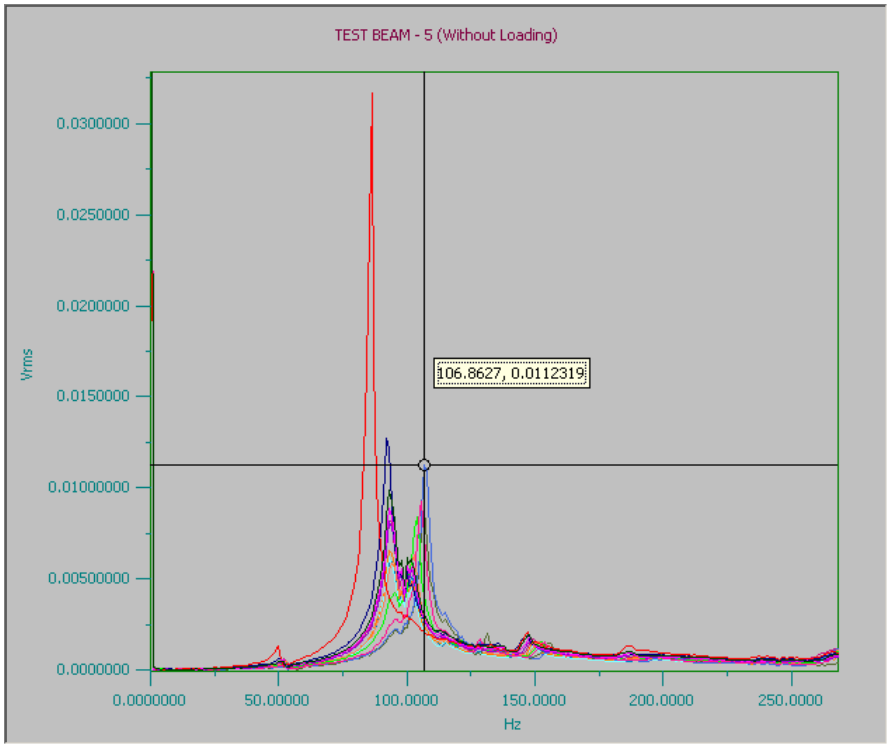

Figure E.72 Frequency for beam 5 at all load stages